THE NEUROGENIC POTENTIAL OF STEM CELLS IS ALTERED IN MUCOPOLYSACCHARIDOSIS TYPE IIIA

Rebecca Lehmann
BSc (Biomed), BSc (Hons)

Matrix Biology Unit
SA Pathology

Thesis submitted for the degree of
Doctor of Philosophy

in

Department of Molecular and Biomedical Science
School of Biological Sciences
Faculty of Science
The University of Adelaide

July 2019

Table of Contents

Abstract ..... **vii**

Declaration ..... **ix**

Acknowledgements ..... **x**

Abbreviations ..... **xii**

Chapter One: Introduction **1**

1.1 The Mucopolysaccharidoses **2**

1.1.1 Mucopolysaccharidosis Type IIIA **2**

1.1.1.1 Central Nervous System Pathology 5

1.1.1.2 Somatic Pathology 6

1.1.2 Mechanisms of Disease in MPS IIIA **8**

1.2 Glycosaminoglycans and Proteoglycans **11**

1.2.1 Heparan Sulphate **12**

1.2.1.1 Heparan Sulphate Synthesis 12

1.2.1.2 Heparan Sulphate Catabolism 13

1.2.2 Heparan Sulphate in MPS IIIA **15**

1.3 Neurogenesis **17**

1.3.1 Heparan Sulphate in Neurogenesis **19**

1.3.1.1 Fibroblast Growth Factor Signalling 20

1.3.1.2 Wnt Signalling 23

1.3.1.3 Bone Morphogenetic Protein Signalling 25

1.3.1.4 Hedgehog Signalling 27

1.3.2 Neurogenesis in MPS **29**

1.4 Modelling Neurological Disease **30**

1.4.1 Animal Models **30**

1.4.2 Modelling MPS IIIA neurogenesis *in vitro* **31**

1.4.2.1 Mesenchymal Stem Cells 31

1.4.2.2 Induced Pluripotent Stem Cells 35

1.5 Significance, Hypothesis and Aims **39**

Chapter Two: Materials and Methods **41**

2.1 Materials **42**

2.2 MPS GAG isolation **42**

2.2.1 GAG quantification....42
2.3 Human MSC *in vitro* studies....42
2.3.1 Human MSC cell culture....42
2.3.2 Human MSC neurogenic differentiation....43
2.3.2.1 Neural priming and maturation method....43
2.3.2.2 Maturation only method....44
2.3.3 Human MSC mesodermal differentiation assays....44
2.3.3.1 Human MSC osteogenic differentiation....44
2.3.3.2 Human MSC chondrogenic differentiation....45
2.3.3.3 Human MSC adipogenic differentiation....45
2.4 Animal husbandry and genotyping....46
2.5 Murine MSC *in vitro* studies....47
2.5.1 Murine MSC isolation....47
2.5.2 Murine MSC cell culture....48
2.5.3 Colony forming unit assay....48
2.5.4 Murine MSC neurogenic differentiation....49
2.5.4.1 Neural priming only method....50
2.5.4.2 Maturation only method....50
2.5.4.3 Neural priming and maturation method....50
2.6 Human iPSC *in vitro* studies....51
2.6.1 Fibroblast culture....51
2.6.2 Fibroblast reprogramming to iPSCs....52
2.6.2.1 Feeder-dependent iPSC culture....52
2.6.2.1.1 Conditioned media....53
2.6.2.2 Feeder-free iPSC culture....53
2.6.2.3 Karyotype analysis....54
2.6.3 iPSC differentiation to NPCs....54
2.6.4 iPSC-derived NPC neurogenic differentiation....56
2.7 Biochemical assays....56
2.7.1 Sulphamidase enzyme assay....56
2.7.2 Protein assays....57
2.7.2.1 BCA assay....57
2.7.2.2 QuanitPro BCA assay....57
2.8 CyQuant Proliferation assay....57
2.8.1 MPS IIIA MSC proliferation assay....57
2.8.1.1 MPS IIIA MSC rescue proliferation assay....58
2.8.2 MPS IIIA iPSC-NPC proliferation and rescue assay....58
2.9 Sulphamidase production....59

2.10 Gene expression 59
2.10.1 Reverse transcription 59
2.10.2 Real-time PCR 59
2.11 Immunofluorescence 60
2.12 Statistics 60

Chapter Three: Gene expression during neurogenic differentiation of human and murine mesenchymal stem cells 63
3.1 Introduction 64
3.2 Results 67
3.2.1 Transfer of the human MSC neural induction method to murine MSCs 67
3.2.2 Timecourse of neural gene expression during human MSC neurogenesis 69
3.2.3 Optimising methodology for neural induction of murine MSCs 71
3.2.3.1 Initial timecourse of gene expression throughout murine MSC neural induction 71
3.2.3.2 Timecourse of gene expression throughout the first 48 hours of murine MSC neural induction 74
3.3 Discussion 76
3.3.1 Human MSC neural induction 78
3.3.1.1 Human MSC-derived neurons are unable to survive in long-term culture conditions 79
3.3.2 Murine MSC neural induction 80
3.3.2.1 Murine MSC neurogenesis is accelerated compared to human MSCs 80
3.3.2.2 Previous murine MSC neural induction protocols and timeframes 81
3.3.2.3 The NP method increases neural gene expression above that of the M only method 83
3.3.3 Chapter conclusions and future directions 84

Chapter Four: The effect of extrinsic Mucopolysaccharidosis type IIIA glycosaminoglycans on mesenchymal stem cell differentiation 86
4.1 Introduction 87
4.2 Results 88
4.2.1 The effect of extrinsic MPS IIIA GAG on neurogenesis 88
4.2.2 The effect of extrinsic MPS IIIA GAG on traditional MSC lineages 90
4.2.2.1 Osteogenesis 90
4.2.2.2 Chondrogenesis 95
4.2.2.3 Adipogenesis 95
4.3 Discussion 99
4.3.1 Neurogenesis 99
4.3.1.1 Commercial full-length HS and heparin promote neurogenesis by promoting neural progenitor survival and proliferation 99

4.3.1.2 MPS IIIA GAG disrupts neurogenesis 101
4.3.1.3 GAGs from different MPS types have diverse effects on neurogenesis 105
4.3.2 Traditional mesodermal lineage differentiation 109
4.3.2.1 Commercial HS and MPS IIIA GAG have converse effects on MSC differentiation 109
4.3.2.2 A mechanism for MPS IIIA skeletal pathology 112
4.3.3 Chapter conclusions 113

Chapter Five: MPS IIIA stem cells: generation, proliferation and neurodifferentiation 115

5.1 Introduction 116
5.2 Results 118
5.2.1 Generation and neurogenic differentiation potential of MPS IIIA MSCs 118
5.2.1.1 CFU assay 118
5.2.1.2 Sulphamidase activity 119
5.2.1.3 Proliferation 119
5.2.1.4 Neural differentiation of MPS IIIA murine MSCs 121
5.2.2 Generation of MPS IIIA human iPSC lines 123
5.2.2.1 Fibroblasts 125
5.2.2.1.1 Sulphamidase activity 126
5.2.2.2 MPS IIIA iPSC lines 128
5.2.2.2.1 Pluripotency 128
5.2.2.2.2 Sulphamidase activity 130
5.2.3 Generation of MPS IIIA human iPSC-derived NPCs 130
5.2.3.1 Proliferation 132
5.2.4 Neural differentiation of human iPSC-derived NPCs 134
5.3 Discussion 140
5.3.1 MPS IIIA MSCs and iPSCs recapitulate the molecular hallmarks of disease 140
5.3.2 MSC and iPSC-NPC proliferation is decreased in MPS IIIA 143
5.3.3 MSC and iPSC neurogenesis is disrupted in MPS IIIA 146
5.3.4 Chapter conclusions 150

Chapter Six: Discussion and Conclusions 151

6.1 Disrupted stem cell proliferation and neurogenesis are likely contributors towards CNS pathology in MPS IIIA 152

6.2 Dysfunctions in stem cell proliferation and differentiation in MPS IIIA are likely a result of alterations in growth factor signalling 154

6.3 Potential uses of MPS IIIA stem cell models 157

6.3.1 Mechanisms of pathology 157
6.3.1.1 Further investigation into the effects of MPS IIIA HS on neurogenesis 157
6.3.1.2 Contribution of the MPS IIIA CNS environment to neurological pathology 159
6.3.1.3 Modelling MPS IIIA mesodermal lineage differentiation 159
6.3.1.4 Identifying contributing factors to previously unsuccessful therapies 160
6.3.2 Potential treatments 160
6.4 Conclusions 162

Appendices 164
Appendix A: Material List 165
Appendix B: Glycosaminoglycan Abbreviations 170
Appendix C: Publications 171

References 172

Abstract

Mucopolysaccharidosis type IIIA (MPS IIIA) is one of a series of 11 genetically inherited metabolic disorders and results from a deficiency in the lysosomal enzyme sulphamidase, leading to intracellular and extracellular accumulation of the glycosaminoglycan (GAG) heparan sulphate (HS). MPS IIIA is characterised by a profound neurological phenotype and mild skeletal pathology. Currently, the mechanisms leading to disease pathology are poorly understood in MPS IIIA. It has been suggested that the excess amount and aberrant structure of MPS IIIA HS compared to normal HS contributes to disease pathology, due to the vital role of HS in many developmental signalling pathways. GAG accumulation commences prenatally in MPS IIIA, with GAG storage present in the developing CNS *in utero*, indicating that alterations in CNS development processes may contribute to the neurological pathology of MPS IIIA patients.

This thesis aimed to determine the effects of aberrant MPS IIIA HS on one of the earliest processes in CNS development, neurogenesis, through the development of a range of *in vitro* models of MPS IIIA. Extrinsic, extracellular MPS IIIA HS was found to impair neurogenesis, providing a mechanism of pathology for the severe central nervous system (CNS) pathology prominent in patients. GAGs from a range of other MPS subtypes were found to have diverse effects on neurogenesis, indicating that MPS IIIA HS was distinctly pathogenic. Osteogenesis was similarly impaired by MPS IIIA HS, providing a molecular basis for the mild skeletal pathology observed in patients. To further investigate the effects of MPS IIIA on neurogenesis, two neurogenic MPS IIIA stem cell lines were developed. Mesenchymal stem cells (MSCs) isolated from a mouse model of MPS IIIA and induced pluripotent stem cells (iPSCs) derived from MPS IIIA patient fibroblasts were used to model MPS IIIA neurogenesis *in vitro*. MPS IIIA murine MSCs and neural progenitor cells derived from MPS

IIIA human iPSCs (iPSC-NPCs) displayed decreased proliferative capacity compared to normal cells, indicating a dysfunction in the processes required for stem cell proliferation, many of which are also involved in stem cell differentiation. Both cell lines were then induced along the neural lineage. A significant reduction in the expression of neural marker genes was seen in MPS IIIA murine MSCs when compared to normal murine MSCs, indicating a dysfunction in neurogenesis in MPS IIIA. Similarly, iPSC-derived NSCs induced to form neurons displayed less overt neuronal morphology and a significant decrease in the expression of neuron marker genes. It was hypothesised that alterations in stem cell proliferation and differentiation was a result of MPS IIIA HS disrupting the many HS-dependent signalling pathways involved in stem cell proliferation and differentiation.

Overall, through the development of stem cell models with neurogenic properties, this thesis has demonstrated that the MPS IIIA HS impairs neural progenitor proliferation, survival and maturation, likely via alterations in HS-dependent signalling pathways integral to stem cell proliferation and differentiation. Disrupted stem cell proliferation and neurogenesis was identified as a potential mechanism of pathology for the severe neurological pathology prominent in MPS IIIA patients.

Declaration

I certify that this work contains no material which has been accepted for the award of any other degree or diploma in my name in any university or other tertiary institution and, to the best of my knowledge and belief, contains no material previously published or written by another person, except where due reference has been made in the text. In addition, I certify that no part of this work will, in the future, be used in a submission in my name for any other degree or diploma in any university or other tertiary institution without the prior approval of the University of Adelaide and where applicable, any partner institution responsible for the joint award of this degree.

I give permission for the digital version of my thesis to be made available on the web, via the University's digital research repository, the Library Search and also through web search engines, unless permission has been granted by the University to restrict access for a period of time.

I acknowledge the support I have received for my research through the provision of an Australian Government Research Training Program Scholarship.

Rebecca Lehmann

Bachelor of Science (Honours)

Student Number : a1212579

***DATE** .15../..7../.2019..*

Acknowledgements

There are so many people I need to thank from throughout my PhD, without whom this thesis would not have been completed. First and foremost, to my supervisor Dr. Sharon Byers, for her advice and guidance throughout my PhD. Thanks must also go to my other supervisors; Dr. Ainslie Derrick Roberts, who has provided endless support and advice, despite having two babies throughout the course of my PhD, and Dr. Lachlan Jolly, for his expertise in iPSCs and neurobiology and a unique ability to calm me down when at my most stressed.

Thanks must go to all members of the Matrix Biology Lab at the Women's and Children's Hospital, past and present; Zhirui, Wan Ling, Matilda, Nathan, Srimayee, Daniel and Neimal. Thank you for your support and friendship over the last four years. Special thanks to Srimayee who assisted with my MSC mesodermal differentiation and to Nathan for reading through thesis chapter drafts. Thank you as well to all the staff in the Women's and Children's Animal House for your excellent care of the mice used in this study. I also need to thank everyone from the Gecz/Shoubridge group at the AHMS for welcoming me so warmly in all the time I spent there. Enormous thanks must go to Brett Johnson, who suffered through six months of iPSC reprogramming and culture with me, and to Claire Homan and Deb Sanders, for teaching me everything I know about iPSCs. Extra thanks to my lab girls, Karagh and Monika, for distracting me from PhD stress with Bachelor viewing nights.

I also need to thank my friends and family, who have endured many years of science talk, stress and last-minute cancellations due to my time-consuming cells. To my parents and sisters, thank you for all your support, assistance and understanding, especially when I have had to miss family celebrations due to PhD work. Finally, to Mark, thank you for your never-

ending support, care, advice and endless cups of tea, without which this thesis would not have been written.

Abbreviations

2S	2-*O*-sulphate
6S	6-*O*-sulphate
APC	Adenomatous polyposis coli
BCA	Bicinchoninic Acid
BDNF	Brain-derived neurotrophic factor
BMD	Bone mineral density
BMP	Bone morphogenetic protein
BSA	Bovine serum albumin
cDNA	Complementary DNA
CK1α	Casein kinase 1 alpha
CNS	Central nervous system
CRISPR	Clustered regularly interspaced short palindromic repeats
CS	Chondroitin sulphate
CS/DSPGs	Chondroitin sulphate/dermatan sulphate proteoglycans
DMEM	Dulbecco's Modified Eagle Medium
DS	Dermatan sulphate
Dvl	Dishevelled
EB	Embryoid body
ECM	Extracellular matrix
EGF	Epidermal growth factor
ESC	Embryonic stem cell
FCS	Foetal calf serum
FGF	Fibroblast growth factor
FGFR	Fibroblast growth factor receptor

FRS2α	FGFR substrate 2 alpha
FZD	Frizzled
GAG	Glycosaminoglycan
GDP	Guanosine diphosphate
GlcA	Glucuronic acid
GlcN	Glucosamine
GlcNA	*N*-acetylated glucosamine
GlcNA(6S)	6-*O*-suphated *N*-acetylated glucosamine
GlcNS	*N*-sulphated glucosamine
GlcNS(6S)	6-*O*-suphated *N*-sulphated glucosamine
GRB2	Growth factor receptor-bound 2
GSK3	Glycogen synthase kinase 3
GTP	Guanosine triphosphate
HA	Hyaluronan
hBM	Human bone marrow
HCl	Hydrochloric acid
hDP	Human dental pulp
HexA	Glucuronic acid or Iduronic acid
HexA(2S)	2-*O*-sulphated glucuronic acid or 2-*O*-sulphated iduronic acid
Hh	Hedgehog
HS	Heparan sulphate
HSC	Haematopoietic stem cell
HSPG	Heparan sulphate proteoglycan
IBMX	3-Isobutyl-1-methylxanthin
IdoA	Iduronic acid
IdoA(2S)	2-*O*-sulphated iduronic acid

IF	Intermediate filament
iPSC	Induced pluripotent stem cell
iPSC-NPC	iPSC-derived neural progenitor cell
KH2PO4	Potassium phosphate
Klf4	Kruppel-like factor 4
KS	Keratan sulphate
LRP5/6	Low-density lipoprotein receptor-related protein 5/6
LSDs	Lysosomal storage disorders
M only	Maturation only
M6PR	Mannose 6-phosphate receptor
MACS	Magnetic activated cell sorting
MAP2	Microtubule associated protein 2
MAPC	Multipotent adult proogenitor cell
MAPK	Mitogen activated protein kinase
MAPKK	Mitogen activated protein kinase kinase
MEFs	Mouse embryonic fibroblasts
MPS	Mucopolysaccharidosis
MPS I	Mucopolysaccharidosis type I
MPS II	Mucopolysaccharidosis type II
MPS III	Mucopolysaccharidosis type III
MPS IIIA	Mucopolysaccharidosis type IIIA
MPS IIIB	Mucopolysaccharidosis type IIIB
MPS IIIC	Mucopolysaccharidosis type IIIC
MPS VI	Mucopolysaccharidosis type VI
MPS VII	Mucopolysaccharidosis type VII
MRI	Magnetic resonance imaging

MSC	Mesenchymal stem cell
NA	*N*-acetylated
$Na_2EDTA.2H_2O$	Ethylenediaminetetraacetic acid disodium salt dihydrate
NAGLU	*α*-*N*-acetylglucosaminidase
NaOH	Sodium hydroxide
NCAM	Neural cell adhesion molecule
NDST	*N*-deacetyl-*N*-sulphotransferase
NE	Neuroepithelial
NeuroD1	Neurogenic differentiation 1
NF-H	Neurofilament heavy
NF-L	Neurofilament light
NF-M	Neurofilament medium
NMM	Neural maintenance media
NP	Neural priming
NP+M	NP and mutauration method
NPC	Neural progenitor cell
NS	*N*-sulphated
NSC	Neural stem cell
NSE	Neuron specific enolase
Oct3/4	Octamer-binding transcription factor 3/4
OST	*O*-sulphotransferase
PAGE	Polyacrylamide gel electrophoresis
Pax6	Paired box protein 6
PBS	Phosphate buffered solution
PCR	Polymerase chain reaction
PFA	paraformaldehyde

PG	Proteoglycan
PI3K	Phosphatidylinositol-4,5-bisphosphate 3-kinase
PKC	Protein kinase C
PLCγ1	Phospholipase C gamma 1
PP2A	Protein phosphotase 2A
Ptch	Patched
RA	Retinoic acid
RAF	Rapidly accelerated fibrosarcoma
RAR	Retinoic acid receptor
RARE	Retinoic acid response element
RAS	Rat sarcoma
RG	Radial glial
Ror-2	Receptor tyrosine kinase-like orphan receptor-2
Runx2	Runt related transcription factor 2
RXR	Retinoic X receptor
SDS	Sodium dodecyl sulfate
SEM	Standard area of the mean
SGZ	Subgranular zone
Shh	Sonic hedgehog
Smo	Smoothened
SOS	son of sevenless
Sox2	SRY (sex determining region-Y) box 2
SVZ	Subventricular zone
TGFβ	Trasforming growth factor beta
α	Alpha
α-MEM	Alpha-minimum essential medium

β	Beta
βIII-tubulin	Class III β-tubulin

Chapter One: Introduction

1.1 The Mucopolysaccharidoses

The Mucopolysaccharidoses (MPS) are a series of 11 genetically inherited lysosomal storage disorders (LSDs) which result from a deficiency in one of the enzymes required for glycosaminoglycan (GAG) degradation (Table 1.1). Catabolism of the GAGs dermatan sulphate (DS), heparan sulphate (HS), keratan sulphate (KS), chondroitin sulphate (CS) or hyaluronan (HA) are affected in MPS, either singularly or in combination (Neufeld & Muenzer, 2001). The resulting lysosomal accumulation of partially degraded GAGs leads to significant cellular, tissue and organ dysfunction in affected individuals (Muenzer, 2011). Clinical features common to more than one of the MPS types include organomegaly, corneal clouding, dysostosis multiplex, abnormal facies and neurological deterioration. Joint immobility or hypermobility, airway and cardiovascular dysfunction and impaired hearing also often present as clinical features. Profound central nervous system (CNS) involvement is present in the severe form of MPS I, MPS II, all subtypes of MPS III and MPS VII (Neufeld & Muenzer, 2001).

1.1.1 Mucopolysaccharidosis Type IIIA

MPS IIIA is one of the most common MPS disorders, with a prevalence in Australian children of 1 in 114 000 births (Meikle et al., 1999). MPS IIIA has an autosomal recessive inheritance and results from mutations in the *SGSH* gene, which encodes the lysosomal enzyme heparan *N*-sulphatase, commonly known as sulphamidase (Yogalingam & Hopwood, 2001). Currently, 148 unique mutations have been identified which have the ability to reduce or eliminate sulphamidase activity in humans (HGMD, 2018). Sulphamidase is one of a complex of enzymes required for the step-wise degradation of the GAG HS, cleaving glucosamine-*N*-sulphate bonds at the non-reducing end of HS (Figure 1.1). Its diminished activity results in lysosomal accumulation of partially degraded HS (Neufeld & Muenzer, 2001). Increased extracellular HS is also apparent, with elevated levels in the circulation, excreted in urine and

MPS Type	OMIM #	Enzyme Deficiency	Stored GAG	Primary Clinical Manifestations
MPS I	607014 (H) 607015 (H/S) 607016 (S)	α-*L*-Iduronidase	HS DS	CNS, skeletal and somatic pathology
MPS II	309900	Iduronate-2-sulphatase	HS DS	CNS, skeletal and somatic pathology
MPS IIIA	252900	Heparan *N*-sulphatase	HS	CNS and somatic pathology
MPS IIIB	252920	α-*N*-Acetyl-glucosaminidase	HS	CNS and somatic pathology
MPS IIIC	252930	Acetyl CoA:α-glucosaminide N-acetyltransferase	HS	CNS and somatic pathology
MPS IIID	252940	*N*-Acetylglucosamine 6-sulphatase	HS	CNS and somatic pathology
MPS IVA	253000	Galactose 6-sulphatase	KS CS	Skeletal and somatic pathology
MPS IVB	253010	β-Galactosidase	KS	Skeletal and somatic pathology
MPS VI	253200	*N*-Acetylgalatosamine 4-sulphatase	DS CS	Skeletal and somatic pathology
MPS VII	253220	β-Glucuronidase	HS DS CS	CNS, skeletal and somatic pathology
MPS IX	601492	Hyaluronidase	HA	Skeletal and somatic pathology

Table 1.1 Classification of the MPS disorders

Each MPS disorder results from a deficiency in a different lysosomal enzyme, leading to accumulation of the GAGs DS, HS, KS, CS or HA, either singularly or combination. H, Hurler Syndrome (severe MPS I); H/S, Hurler-Scheie Syndrome (moderate MPS I); S, Scheie Syndrome (mild MPS I). Adapted from Neufeld and Muenzer (2001).

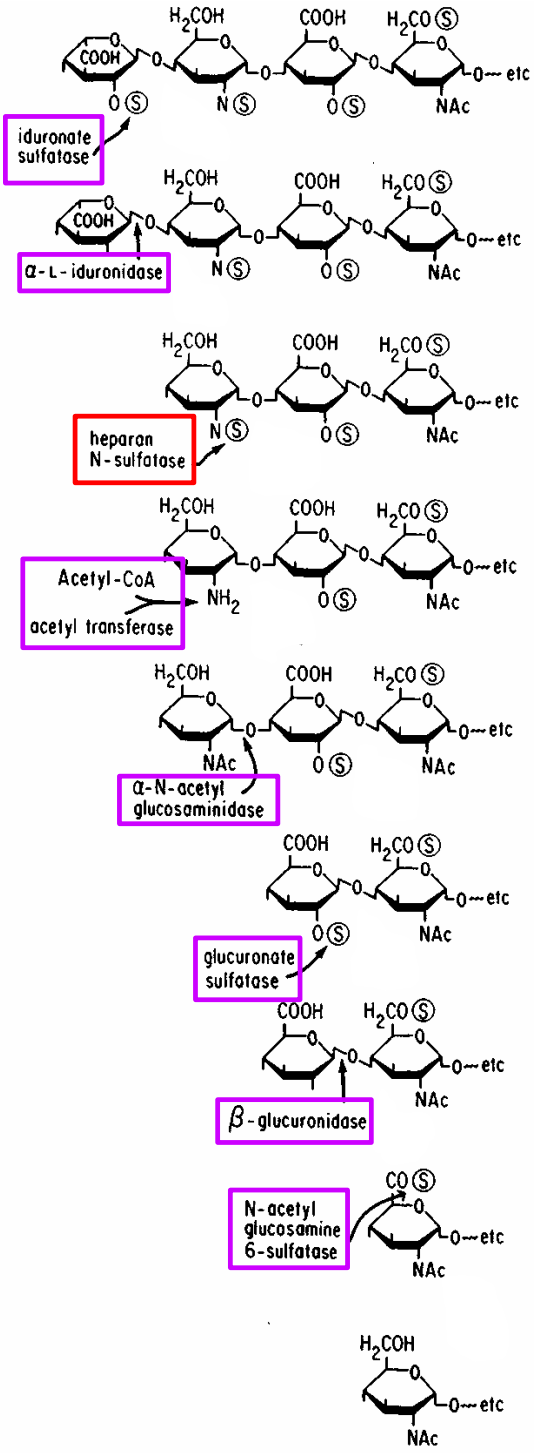

Figure 1.1: The stepwise degradation of HS

Heparan *N*-sulphatase (sulphamidase) is one of a series of enzymes required for the catabolism of HS. The enzymes required for HS degradation are highlighted in purple accompanied by the MPS type which results from their deficiency. Sulphamidase is deficient in MPS IIIA (highlighted in red) and thus, due to the strict sequence in which HS is degraded, HS degradation stops when an *N*-sulphated *N*-acetylglucosamine residue is present at the non-reducing terminus of the HS chain. Adapted from Hochuli et al. (2013).

present within the ECM (Holley et al., 2011; Meikle et al., 2004; Neufeld & Muenzer, 2001; Tomatsu et al., 2005). Individuals with MPS IIIA generally develop normally until approximately two years of age, with the first onset of symptoms between two and six years of age. These can include delayed development, poor sleep and hyperactive behaviour. Severe neurological deterioration often occurs between six and ten years of age and is associated with increasingly aggressive behaviour. Death commonly occurs due to inanition in the second or third decade of life (Neufeld & Muenzer, 2001).

1.1.1.1 Central Nervous System Pathology

MPS IIIA is characterised by a severe neurological phenotype. There is significant heterogeneity between patients; however, all forms of MPS III present with some form of neurological involvement. Due to neurological disease progression and the regressive phenotype prevalent in later life, many patients eventually enter a vegetative state (Muenzer, 2011). Consistent with the predominant neurological pathology seen in patients, HS storage occurs primarily within the CNS, with content significantly increased in the brain of MPS IIIA patients compared to normal (Constantopoulos et al., 1976). GAG storage begins prenatally, with inclusion bodies present in neurons of affected foetuses from the second trimester (Ceuterick et al., 1980). Significant increases in HS storage is similarly seen within the brain of the MPS IIIA mouse model, with storage primarily located within lysosomes of neurons and microglia of the amygdala, septal nucleus, piriform cortex and cerebral cortex (Figure 1.2A) (McGlynn et al., 2004; Wilkinson et al., 2012). An increase in glypican-1, a protein commonly associated with HS chains (refer section 1.2 for further details), is also seen in the hippocampus, an adult neural stem cell (NSC) niche, in MPS IIIA mice (Ohmi et al., 2011). Furthermore, the HS that accumulates in the murine model of MPS IIIA has a different structure to normal, with a distinctly modified sulfation pattern (Wilkinson et al., 2012). Secondary lipid storage is evident, with G_{M2} and G_{M3} gangliosides elevated in the

patient MPS IIIA brain. G_{M2} and G_{M3} ganglioside levels are similarly elevated in MPS IIIA mice, localised to the piriform and retrosplenial cortices, amygdala and neocortex (Constantopoulos & Dekaban, 1978; McGlynn et al., 2004; Wilkinson et al., 2012). Increased levels of unesterified cholesterol is also evident in the basal area of pyramidal neurons of the cortex, retrosplenial cortex and amygdala in MPS IIIA (Figure 1.2B) (McGlynn et al., 2004). Mild to moderate cortical atrophy is evident at the commencement of neurological deterioration in patients and progresses to severe cortical atrophy at later stages of disease (Jardim et al., 2010; Neufeld & Muenzer, 2001). Chronic neuroinflammation is prevalent in MPS IIIA, with astrocyte and microglia activation significantly higher in the MPS IIIA mouse brain compared to normal mice (Figure 1.2C and 1.2D) (Wilkinson et al., 2012). Neuroinflammation is widespread across the MPS IIIA brain, with global microglial activation, in contrast to the microglial niches found in normal mice (Wilkinson et al., 2012).

1.1.1.2 Somatic Pathology

In contrast to the severe neurological phenotype observed in MPS IIIA patients, somatic pathology is relatively mild. Clinically, hirsutism, coarse hair and hepatosplenomegaly are present in some cases of MPS IIIA; however, there is much heterogeneity and many patients do not present with these phenotypes. Recurrent and severe diarrhoea is not uncommon in young children with MPS IIIA, although this generally improves with age. In contrast to many of the other MPS types, coarse facial features are not widespread (Neufeld & Muenzer, 2001). Somatic pathology is also evident in the MPS IIIA mouse model, with increased HS storage within the liver and kidneys and to a lesser extent the spleen (Bhaumik et al., 1999; Crawley et al., 2006).

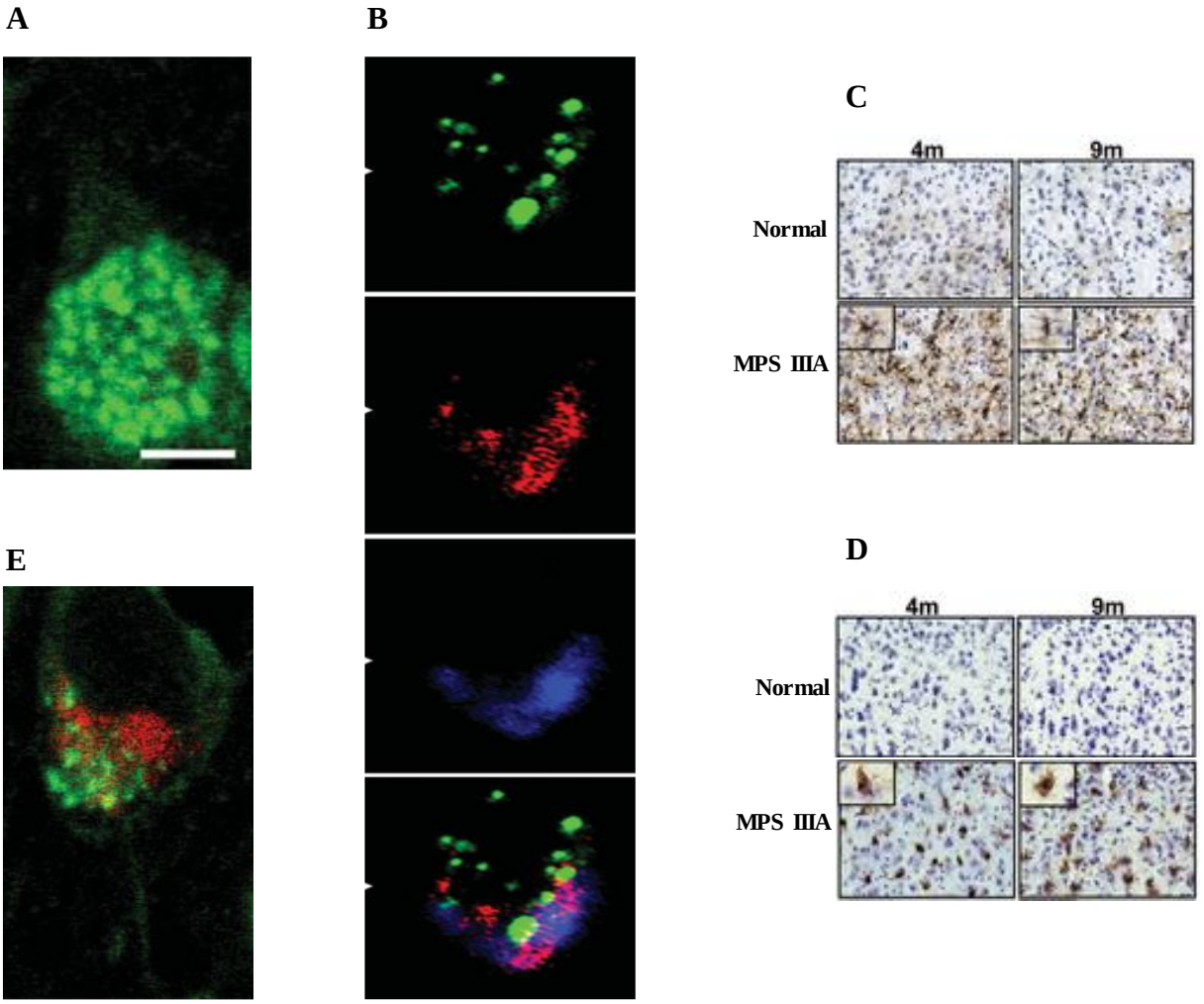

Figure 1.2: CNS cell pathology of MPS IIIA

A: Partially degraded HS (green) accumulates in lysosomes in MPS IIIA. **B:** Secondary storage of G_{M2} (green), G_{M3} (red) and unesterified cholesterol (blue) is evident within the MPS IIIA brain. Gangliosides rarely co-localise, indicating that they are stored in separate vesicles. **C:** A significant increase in positive GFAP staining (brown) indicates an increase in astrocyte activation across the MPS IIIA mouse brain at four and nine months of age. Boxed insert shows an enlarged single positively stained cell. **D:** A significant increase in positive Isolectin B4 staining (brown) indicates an increase in microglia activation across the MPS IIIA mouse brain at four and nine months of age. Boxed insert shows an enlarged single positively stained cell. **E:** HS (green) and G_{M3} gangliosides (red) are stored in separate vesicles within neurons. Figures A, B and E adapted from McGlynn et al. (2004). Figures C and D adapted from Wilkinson et al. (2012).

Skeletal disease is a prominent component of many of the MPS types but is limited in MPS IIIA. Hip deformities and scoliosis on a lesser scale to other MPS types have been reported in children with MPS IIIA, as have minor dysostosis multiplex and minimal joint stiffness (Neufeld & Muenzer, 2001; Valstar et al., 2010; White et al., 2011). Osteonecrosis of the femoral head leading to epiphyseal dysplasia has been reported and is associated with increased hip pain in patients (de Ruijter et al., 2013b; White et al., 2011). Osteopenia is the most prominent skeletal deformity identified in MPS IIIA patients, with decreased bone mineral density (BMD) identified in a number of patients (Nur et al., 2016; Rigante & Caradonna, 2004). It has been hypothesised that decreased BMD is a result of bone loss, a consequence of decreased mobility, as patients commonly become wheelchair bound from their early teens due to deterioration in neurological function (Rigante & Caradonna, 2004; White et al., 2011).

1.1.2 Mechanisms of Disease in MPS IIIA

The mechanisms that lead from mutation to disease in MPS IIIA are poorly understood. A wide spectrum of disease pathology is present amongst MPS IIIA patients; however, specific genotype-phenotype correlations have been difficult to establish. Whilst mutational analysis has identified mutations which commonly give rise to specific disease phenotypes, identical *SGSH* mutations have been shown to result in varied enzyme activities and disease severity, indicating that environmental and epigenetic factors may contribute to disease progression (McDowell et al., 1993; Piotrowska et al., 2009; Valstar et al., 2010). Correlations between sulphamidase activity and phenotype severity exist to a certain extent, with patients with higher sulphamidase activities often displaying an attenuated phenotype, whilst patients with below detectable enzyme activities generally exhibit a severe form of the disease (Perkins et al., 2001; Piotrowska et al., 2009). However, pathology severity is more directly affected by the accumulation of HS. Increased HS accumulation correlates with increased disease

severity, both amongst the MPS types and between mild and severe forms of the same subtype (Coppa et al., 2015; de Ruijter et al., 2013a; Hochuli et al., 2003). Pathology is often more severe in patients with a high rate of GAG synthesis compared to those with a low to average rate, indicating that the rate of HS turnover contributes towards disease severity (Piotrowska et al., 2009).

The different structure of MPS IIIA HS compared to normal HS is likely to contribute to its severe neurological phenotype. A distinct sulphation pattern with increased sulphate content was seen in HS isolated from MPS IIIA patient urine compared to HS from MPS I and II patient urine (Hochuli et al., 2003). Similarly, HS chains isolated from murine brain tissue were found to be more highly sulphated in MPS IIIA and MPS IIIB mice compared to MPS I mice (Wilkinson et al., 2012). It has been suggested that the increased sulphation of HS in MPS IIIA is at least partially responsible for the more severe pathology seen in this MPS type compared to the other HS-storing MPS disorders (Hochuli et al., 2003; Wilkinson et al., 2012). Furthermore, MPS IIIA patients with a more severe phenotype have been found to store HS fragments with a higher proportion of sulphated monosaccharides and disaccharides than those with an attenuated phenotype (Hochuli et al., 2003). Integral to cell membranes and the extracellular matrix (ECM), HS is an essential component of many signalling pathways during development and adulthood (Bernfield et al., 1999; Habuchi et al., 2004). This increased sulphation is likely to affect the ability of HS to bind to molecules involved in these signalling pathways, as sulphation patterns are crucial to this mechanism (Habuchi et al., 2004; Rong et al., 2001; Rusnati et al., 1994). HS accumulation begins prenatally and thus disruption of these signalling pathways during development could be contributing to the severe CNS pathology of MPS IIIA (Ceuterick et al., 1980; Greenwood et al., 1978; Harper et al., 1974; Martin & Ceuterick, 1983).

Although MPS IIIA is characterised by the accumulation of partially degraded HS, the secondary lipid storage of G_{M2} and G_{M3} gangliosides and unesterified cholesterol is another defining feature (McGlynn et al., 2004; Wilkinson et al., 2012). Ganglioside storage was originally hypothesised to be the result of lysosomal hydrolase dysfunction due to GAG accumulation; however, the mechanisms responsible for ganglioside accumulation are now thought to be more complex, due to the lack of consistent GAG and ganglioside co-localisation in the MPS IIIA mouse brain (Figure 1.2E) (McGlynn et al., 2004). It has been hypothesised that GAG accumulation may contribute to ganglioside storage through regulation of genes involved in ganglioside biosynthesis and degradation (Baumkotter & Cantz, 1983; Kreutz et al., 2013; Walkley, 2004). In addition, G_{M2} and G_{M3} gangliosides accumulate in separate vesicles to one another, suggesting their sequestration also occurs through independent mechanisms (Figure 1.2B) (McGlynn et al., 2004). Ganglioside and cholesterol storage are now believed to contribute directly towards disease pathology, although a clear connection is yet to be established. G_{M2} accumulation has been linked with ectopic dendritogenesis in MPS I and other LSDs, providing a possible mechanism of pathology (Purpura & Suzuki, 1976; Siegel & Walkley, 1994). Cholesterol also accumulates intracellularly in MPS IIIA; however, evidence suggests that the sequestration is the result of changes in cholesterol distribution across the cell rather than absolute increases in concentration (Karten et al., 2002; McGlynn et al., 2004). Elevated perikaryal cholesterol levels and concomitant decreases in axonal cholesterol levels have been seen in Niemann-Pick C neurons, which could have significant consequences for correct neuronal function (Karten et al., 2002). However, cholesterol accumulation may be regulated by a different mechanism in MPS IIIA (Davidson et al., 2009). As gangliosides and cholesterol do not necessarily co-localise within affected cells, or with HS, it is likely that their storage has independent effects on cellular function (Figure 1.2B) (McGlynn et al., 2004).

Chronic neuroinflammation is another prominent component of MPS IIIA pathology. MPS III mouse models exhibit chronic neuroinflammation, with increased astrocyte and microglial activation present in MPS IIIA and MPS IIIB brains at four and nine months of age (Figure 1.2C and 1.2D). Neuroinflammation progresses with time and was found to be more pronounced in the MPS III mouse models compared to the MPS I mouse model (Wilkinson et al., 2012). HS is an important factor in inflammation, influencing cytokine/chemokine production, leukocyte recruitment and inflammatory cell maturation, often serving as a molecular signal of injury in the absence of an exogenous pathogen (Taylor & Gallo, 2006; Wang et al., 2005). The elevated HS in MPS IIIA may therefore be directly responsible for the chronic neuroinflammation of the disease. Although a prominent component of MPS IIIA neuropathology, the extent to which neuroinflammation actually contributes to disease is disputed; MPS IIIB mice deficient in toll-like receptor 4 have shown that severe neurodegeneration occurs even without microglial activation by HS (Ausseil et al., 2008). However, administration of the anti-inflammatory drug aspirin to MPS IIIA mice has resulted in reduced CNS pathology (Arfi et al., 2011). Although originally thought to result solely from HS accumulation, it is now most likely that MPS IIIA pathogenesis results from a complex interplay between all neurological dysfunctions within the CNS.

1.2 Glycosaminoglycans and Proteoglycans

Glycosaminoglycans (GAGs) are long, unbranched polysaccharides involved in many cellular processes integral for growth and development (Lin, 2004; Mizuguchi et al., 2003; Perrimon & Bernfield, 2000). GAG chain length and post-translational sulphation patterns are thought to influence GAG function and specificity (Allen & Rapraeger, 2003; Nakato & Kimata, 2002). GAGs are considered post-translational modifications of selected core proteins which contain GAG attachment consensus sequences, such as the well-known SGD sequence; the addition of one or more GAG chains to a core protein results in formation of a proteoglycan

(PG) (Iozzo & Schaefer, 2015). PGs can be found intracellularly (reviewed in Kolset et al., 2004); however, PGs are primarily located within the extracellular matrix (ECM) or else integrated into the cell membrane (Bandtlow & Zimmermann, 2000; Lamoureux et al., 2007). PGs are vital during histogenesis, increasing morphogen binding efficacy by acting as co-receptors, or increasing morphogen concentrations at the cell surface through formation of a morphogen gradient (Bandtlow & Zimmermann, 2000; Yamaguchi, 2001).

1.2.1 Heparan Sulphate

HS is composed of repeating disaccharide units of *D*-glucuronic or *L*-iduronic acid and *N*-acetylglucosamine residues. Glucuronic and iduronic acids may be sulphated, whilst glucosamine is either sulphated or acetylated on the amino group, leading to a wide variety of possible sulphation patterns (Kjellen & Lindahl, 1991). HS largely functions as a PG, with HS chains bound to perlecan, agrin and collagen XVII found in the basement membranes of the ECM. However, HS chains bind primarily to glypicans and syndecans, the two major cell surface heparan sulphate proteoglycan (HSPG) families (Filmus & Selleck, 2001; Iozzo, 1998; Zimmermann & David, 1999). The HS chains bound to glypicans and syndecans are located close to the cell membrane, suggesting a role for HS in mediating PG interactions with signalling molecules, primarily fibroblast growth factors (FGFs), Wnts, bone morphogenic proteins (BMPs) and Hedgehogs (Hhs) (Esko et al., 2009; Guo & Wang, 2009; Kim et al., 2011; Song et al., 2005; Tkachenko et al., 2005; Topczewski et al., 2001; Veugelers et al., 1999; Xian et al., 2012; Yan & Lin, 2007).

1.2.1.1 Heparan Sulphate Synthesis

HS synthesis is initiated by the addition of an *N*-acetylglucosamine to a xylose-galactose-galactose-glucuronic acid tetrasaccharide linker, itself attached to the PG core protein by *O*-

glycosylation of a serine residue. Alternating units of glucuronic acid and *N*-acetylglucosamine are then added under the action of the EXT enzymes, assembling an unbranched polysaccharide chain (Esko & Selleck, 2002; Hacker et al., 2005). Concomitant with chain elongation, post-translational modifications occur in the Golgi apparatus, specifically sulphation and epimerisation (Figure 1.3).

HS chain modifications do not necessarily occur in the linear order seen in Figure 1.3; furthermore, modifications are not evenly distributed across the GAG chain, instead occurring in defined loci generating distinct domains that have biological significance (Hacker et al., 2005). Iduronic acid residues and sulphated *N*-acetylglucosamines cluster in regions known as *N*-sulphated (NS) domains, interspersed by regions containing unsulphated monosaccharides known as *N*-acetylated (NA) domains. NS and NA domains are separated by regions containing alternating *N*-acetyl and *N*-sulpho glucosamines, known as NA/NS domains (Hacker et al., 2005; Maccarana et al., 1996; Murphy et al., 2004). Therefore, the post-translational modification of HS results in chains with a wide range of possible sulphation patterns (Hacker et al., 2005).

1.2.1.2 Heparan Sulphate Catabolism

HS degradation is initiated by the extracellular enzyme heparanase, which cleaves HS chains from the proteoglycan core protein (Bame, 2001; Vlodavsky et al., 2007). These partially cleaved HS chains are then translocated to the lysosomes for further degradation by a complex of eight lysosomal enzymes (Figure 1.1). These enzymes act in a stepwise manner to remove monosaccharides from the non-reducing terminus of the GAG chain; however, prior to the removal of monosaccharides, all sulphate moieties must be removed. Four sulphatases achieve the removal of sulphate groups, whilst three glycosidases hydrolyse glycosidic bonds

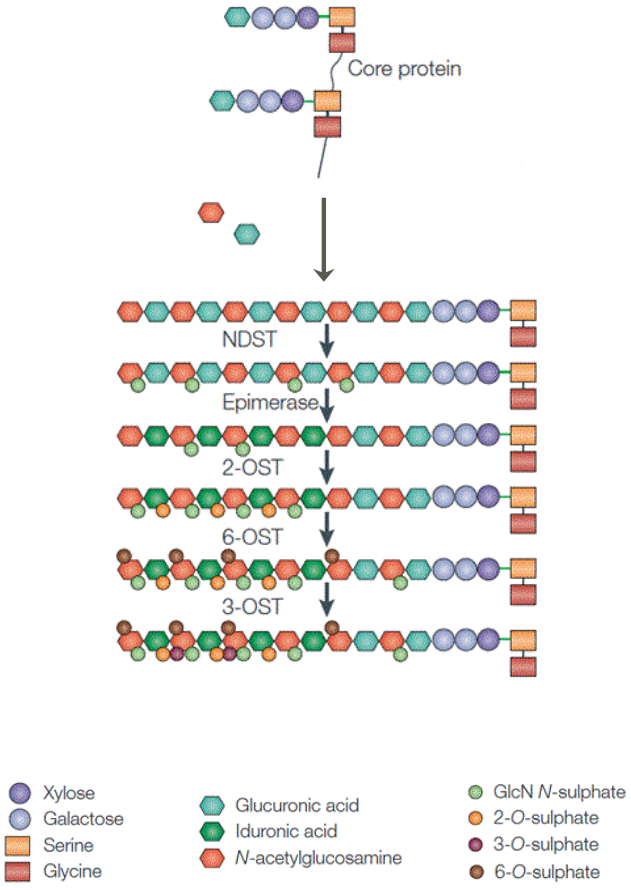

Figure 1.3: Heparan sulphate synthesis

HS chains are composed of alternating units of glucuronic acid and *N*-acetylglucosamine, which undergo a series of modifications to form a mature chain. NDST, *N*- deacetylase-*N*-sulphotransferase; OST, *O*-sulphotransferase. Adapted from Hacker et al. (2005).

between saccharides (Figure 1.1) (Neufeld & Muenzer, 2001). A single acetyltransferase acetylates glucosamine (GlcN) amino groups exposed by the removal of a sulphate group by heparan-*N*-sulphatase, allowing the glucosamine to later be cleaved by α-*N*-acetylglucosaminidase (Figure 1.1) (Neufeld & Muenzer, 2001).

1.2.2 Heparan Sulphate in MPS IIIA

A number of disease states are known to alter HS structure, often resulting in altered binding properties that exacerbate the existing disease (Blackhall et al., 2001; Kjellen & Lindahl, 1991; Osterholm et al., 2009). There has been increasing interest regarding the altered structure of GAGs in the MPS disorders and their possible effects on disease. HS sulphation patterns vary between the HS-storing MPS types. Different non-reducing terminal residues are characteristic of an individual MPS type; furthermore, the levels of sulphation across the HS backbone differ between MPS types (Figure 1.4) (Byers et al., 1998; Neufeld & Muenzer, 2001).

Whilst all patients with HS-storing MPS types excrete urinary HS with increased sulphate compositions compared to normal patients, patients with MPS IIIA have the highest proportion of the highly sulphated NS domains when compared to the HS from MPS I and MPS II patients (Hochuli et al., 2003). Similarly, HS isolated from MPS IIIA and MPS IIIB murine brain tissue was found to be more highly sulphated along its length than HS isolated from MPS I murine brain tissue. Specifically, an increase in tri- and di-sulphated disaccharide domains, HexA(2S)–GlcNS(6S) (where HexA is either glucuronic acid or iduronic acid) and HexA(2S)–GlcNS (see Appendix B for abbreviations), was seen in murine MPS IIIA and MPS IIIB brains (Wilkinson et al., 2012). The increased sulphation of HS in the MPS III

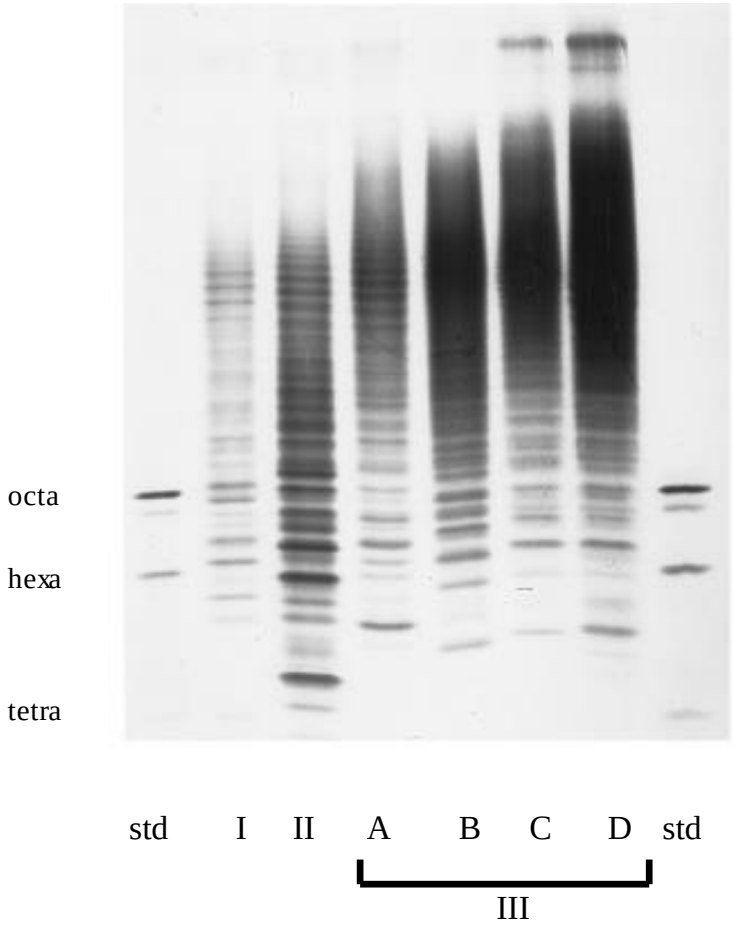

Figure 1.4: Gradient PAGE of MPS heparan sulphate

Gradient PAGE of HS isolated from urine of patients with MPS I (lane 2), MPS II (lane 3) and MPS IIIA-D (lanes 4-7). Octosaccharide, hexasaccharide and tetrasaccharide HS standards were included as controls (lanes 1 and 8). Distinct banding patterns are present for each MPS type. Adapted from Byers et al. (1998).

types has been hypothesised to contribute to the more severe neurological phenotype of the disease (Hochuli et al., 2003; Wilkinson et al., 2012).

1.3 Neurogenesis

Neurogenesis, the production of new neurons in the CNS, is a highly regulated process. Neurogenesis primarily occurs during development, but also continues into adulthood in the subgranular zone (SGZ) in the dentate gyrus of the hippocampus and the subventricular zone (SVZ) of the lateral ventricles (Cameron et al., 1993; Garcia-Verdugo et al., 1998). The primordial cell types of the developing embryonic brain are called neural stem or neural progenitor cells, which balance both proliferation and differentiation into mature, post-mitotic cells of the mature brain. Initially, they favour a proliferative state during an expansive phase required to increase overall brain size. They then switch into increasingly more differentiative states, firstly undergoing a neurogenic phase to produce the neuronal cells and subsequently gliogenic phases to produce glia and then oligodendrocytes. At the conclusion of these processes (early postnatally), the vast majority of NSCs become exhausted and persist only in a few specialised 'adult neurogenic niches', supplying new neurons to the olfactory and hippocampal structures (Figure 1.5A) (Martynoga et al., 2012; Panchision & McKay, 2002).

Neurogenesis is a production of neurons arising from the division of neural progenitor cells (NPCs), and is thus linked to their decision to self-renew (produce more progenitor cells) or differentiate (produce neurons). CNS development is driven by differing types of NPC cell divisions, classified as being either symmetric or asymmetric (Horvitz & Herskowitz, 1992; Rakic, 1995). During the expansive phase early in CNS development, NPCs (with neuroepithelial (NE) identity), favour symmetric cell divisions and divide to produce two more NPCs, driving NPC expansion. During the later neurogenic phase, NPCs switch to an

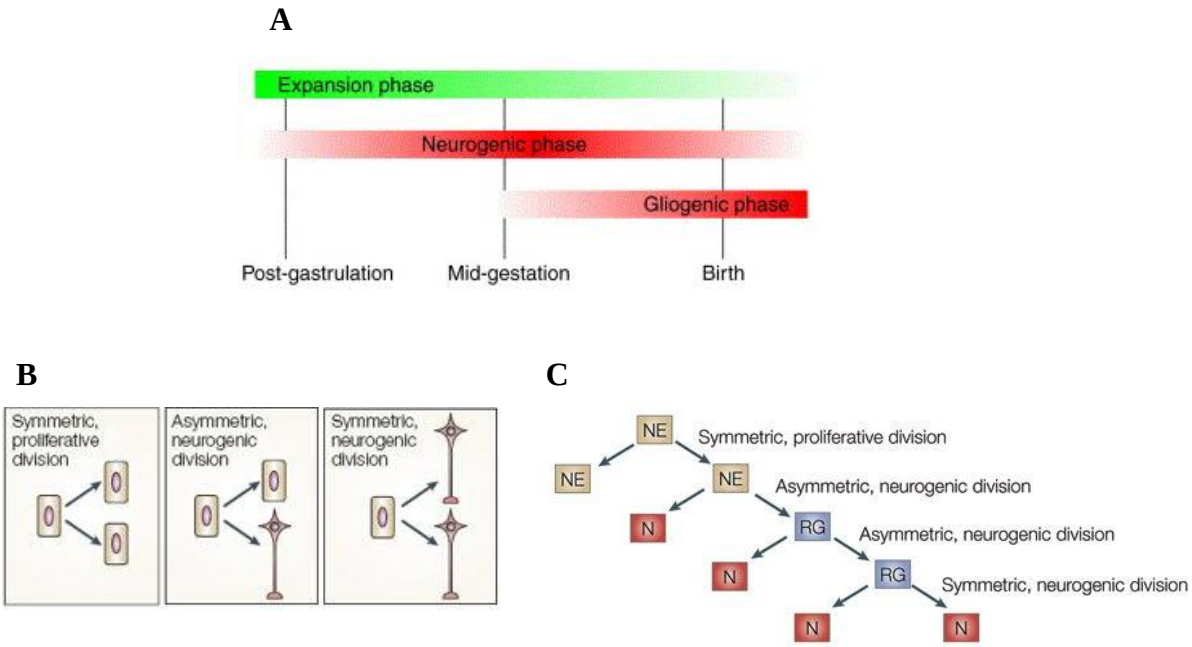

Figure 1.5: Cell division in neurogenesis

A: CNS development occurs in three phases; the expansion phase, the neurogenic phase and the gliogenic phase. **B:** Neurogenesis is dependent on symmetric and asymmetric cell divisions to maintain progenitor proliferation and neuron formation. **C:** Developmental neurogenesis involves the symmetric and asymmetric divisions of NPCs (which include neuroepithelial cells (NE) and radial glial cells (RG)) to produce neurons (N). Figure A adapted from Panchision and McKay (2002). Figures B and C adapted from Gotz and Huttner (2005).

asymmetric type of division, dividing to produce one NPC (with radial glial (RG) cell identity) and one neuron (Gotz & Huttner, 2005; Huttner & Brand, 1997; Kriegstein & Gotz, 2003). The RG population is able to expand through asymmetric divisions, producing one identical NPC (with RG cell identity) and one neuron (Gotz, 2003). At the conclusion of developmental neurogenesis, NPCs can undergo symmetric, neurogenic divisions, producing two mature neurons (Figure 1.5B and 1.5C). Through this last type of division, NPCs become exhausted, and very few NPCs exist beyond developmental stages (Huttner & Kosodo, 2005; Saito et al., 2003). RG NPCs are only maintained in two discrete neurogenic niches in the adult brain, driving adult neurogenesis in the hippocampus and olfactory systems (Bonfanti & Peretto, 2007).

1.3.1 Heparan Sulphate in Neurogenesis

HSPGs play a vital role in both embryonic and adult neurogenesis (Urban & Guillemot, 2014). Several morphogens and growth factors involved in neurogenesis require interactions with the HS chains of HSPGs, resulting in HS-dependent signalling regulation and ligand stability. HS binding capacity is dependent on the fine structure of the chain, specifically the sulphation patterns of the NS regions (Habuchi et al., 2004). HS chains generally modulate neurogenesis by enhancing receptor activation at low ligand concentrations. Low affinity interactions between HS and morphogens increase ligand concentration at the cell surface, enabling presentation of the ligand to its signalling receptor. As an additional mechanism, HSPGs can also form morphogen gradients to increase morphogen concentration at the cell membrane (Okolicsanyi et al., 2014). In some cases, HS chains act as co-receptors for morphogens, forming vital complexes integral for neurogenesis (Chang et al., 2000; Krufka et al., 1996).

1.3.1.1 Fibroblast Growth Factor Signalling

The FGF family of morphogens are dependent on HSPGs for function. Comprising of 22 members in mammals, the FGF family has an important role in development, with many FGFs required for CNS development. FGF signalling is initiated following ligand binding to the FGF receptor (FGFR). Whilst HSPGs also act to bind and protect FGFs within the ECM and accrue a reservoir of FGF at the cell surface, HS chains primarily act as co-receptors for FGF, resulting in formation of the FGF:FGFR:HS complex necessary for FGF signalling (Chang et al., 2000; Lin et al., 1999). FGFs bind to specific HS sulphation patterns; the tetrasaccharide GlcNS(6S)-IdoA(2S)-GlcNS(6S)-IdoA(2S) has been identified as the minimum FGF-2 binding motif (Guglier et al., 2008; Raman et al., 2003). MPS IIIA HS fragments have been shown to display increases in HexA(2S)-GlcNS(6S) disaccharides, where HexA represents either GlcA or IdoA (see Appendix B for abbreviations), indicating a potential increase in the proportion of the minimum FGF-2 binding motif compared to normal HS, albeit dependent on the specific tetrasaccharide formations (Wilkinson et al., 2012). The conformation of the binding motif varies between FGFs; for example, FGF-2 binds only to the 2-*O* and *N* sulphate groups of the binding motif, leaving the 6-*O* sulphate exposed (Ashikari-Hada et al., 2004; Guglier et al., 2008). However, 6-*O* sulphation of HS is required for bridging interactions between FGF-2 and the FGFR, forming the FGF:FGFR:HS complex (Pye et al., 2000; Pye et al., 1998). Formation of this complex induces dimerization of the FGFR intracellular tyrosine kinase domains, changing their orientation and increasing their proximity. This enables transphosphorylation of the tyrosine kinase domains, resulting in their activation. The activated tyrosine kinases are then able to phosphorylate, and thus activate, their intracellular substrates, most commonly FGFR substrate 2α (FRS2α) and phospholipase Cγ1 (PLCγ1). FRS2α activation is able to initiate downstream activation of the mitogen activated protein kinase (MAPK) or PI3K/AKT cascades, whilst PLCγ1 activation results in calcium signalling and activation of protein kinase C (PKC). Of these downstream pathways, the MAPK signalling pathway has been most implicated in neurogenesis due to its activation

of transcription factors involved in cell proliferation, differentiation and migration (Figure 1.6) (Chen et al., 2010).

As FGFs are involved in the upregulation of cell proliferation and differentiation-related genes, it is unsurprising that they play an important role in neurogenesis. In particular, FGF-2 is an established and well-studied neurogenic factor; high levels are present during development from the initiation of neurulation and its temporospatial expression in the developing CNS corresponds with neurogenesis in specific brain regions (Murphy et al., 1994; Powell et al., 1991). During development, FGF-2 is primarily involved in stimulating neural progenitor proliferation and maintaining stem cells in the cell cycle; however, FGF-2 has also been implicated in regulating neural differentiation (Chen et al., 2010; Israsena et al., 2004; Qian et al., 1997). In adults, FGF-2 expression is found in the neurogenic niches, the SGZ and the SVZ, and is thus implicated in the regulation of adult neurogenesis (Rai et al., 2007; Werner et al., 2011).

Defects in FGF signalling highlight the family's vital role in neurogenesis. Deletion of FGF receptors dramatically reduced progenitor proliferation during early development, resulting in reduced postnatal size of particular brain regions (Ohkubo et al., 2004; Rash et al., 2011). FGF-2 knockout mice display impairments in neuronal proliferation and differentiation, demonstrating the mitogenic role of FGF-2 (Raballo et al., 2000; Werner et al., 2011). Additionally, disruption of FGF-10 during development delays differentiation along the neural lineage by prolonging the proliferation of NE cells (Sahara & O'Leary, 2009).

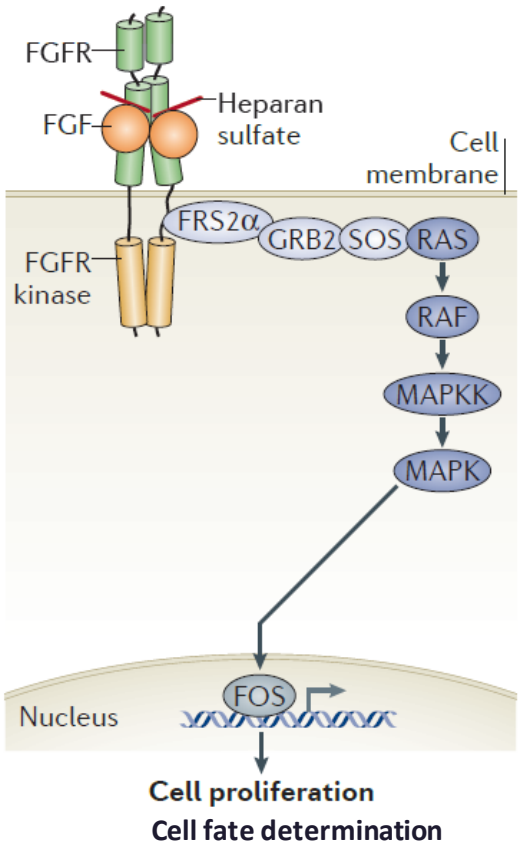

Figure 1.6: The FGF signalling pathway

Formation of the FGF:FGFR:HS complex induces FGFR dimerization, which juxtaposes the intracellular tyrosine kinase domains, allowing them to transphosphorylate one another. Activated FGFR tyrosine kinases activate the FGFR substrate 2α (FRS2α) by phosphorylation, which can in turn activate growth factor receptor-bound 2 (GRB2), an adaptor protein. GBR2 then recruits a guanine exchange factor, son of sevenless (SOS), which acts upon a GTP-ase, rat sarcoma (RAS), forcing the release of its GDP nucleotide and enabling it to instead bind GTP. Activated RAS is then able to phosphorylate and activate the rapidly accelerated fibrosarcoma (RAF) kinase, which in turn phosphorylates and activates mitogen activated protein kinase kinase (MAPKK). Activated MAPKK is then able to act upon mitogen activated protein kinase (MAPK); once activated, MAPK translocates from the cytoplasm to the nucleus where it activates target genes. Adapted from Goetz and Mohammadi (2013).

1.3.1.2 Wnt Signalling

Wnt signalling is also dependent on HSPGs for function. HSPGs act to increase Wnt concentration at the cell surface through the creation of morphogen gradients and ligand solubility maintenance, and to stabilise interactions between the Wnt and Frizzled (FZD) protein receptors (Figure 1.7) (Capurro et al., 2014; Capurro et al., 2005; Fuerer et al., 2010). Wnts bind to specific regions of HS chains, with HS binding domains identified in a number of Wnts (Cardin & Weintraub, 1989; Tran et al., 2012). Wnt binding is also dependent on the sulphation of the HS chain, with 6-*O*-sulphation, enriched in MPS IIIA HS, the most implicated (Ai et al., 2003; Wilkinson et al., 2012). Binding of Wnt ligands to FZD receptors results in activation of either the canonical or non-canonical signalling cascade (Gordon & Nusse, 2006; Prud'homme et al., 2002). Pathway activation is determined by the ability of Wnt ligands to bind to co-receptors during signalling initiation, with the LRP5/6 co-receptor associated with canonical Wnt signalling and the Ror-2 co-receptor associated with non-canonical Wnt signalling (Grumolato et al., 2010). The majority of HS binding domains exist on canonical Wnts; the canonical Wnt signalling pathway has been closely linked with neurogenesis in both the developing and adult brain (Hirabayashi et al., 2004; Lie et al., 2005; Tran et al., 2012).

Throughout neurogenesis, Wnt signalling has been found to regulate self-renewal, maintenance and differentiation of neural progenitors (Chenn & Walsh, 2002; Hirabayashi et al., 2004). β-catenin levels regulated by canonical Wnt signalling regulate the switch between proliferation and differentiation during developmental neurogenesis; early in development, increased canonical Wnt signalling is associated with increases in proliferation whilst decreased canonical Wnt signalling increases differentiation along the neural lineage; later in development, increased Wnt/β-catenin results in reduced proliferation and increased

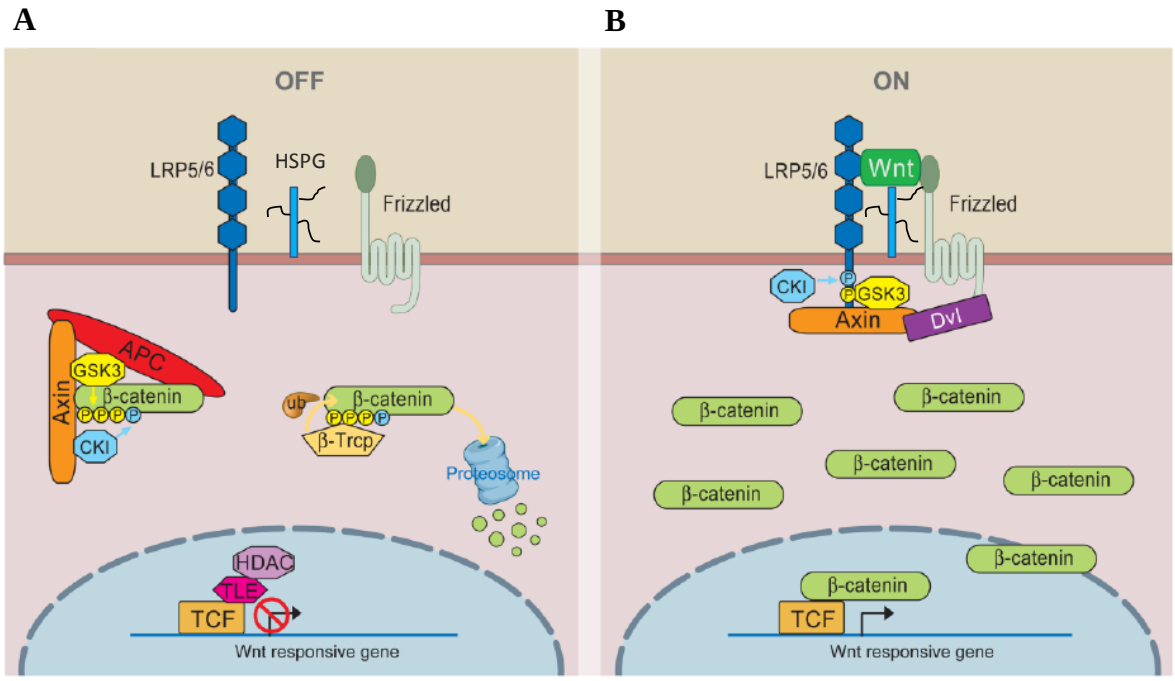

Figure 1.7: The canonical Wnt signalling pathway

A: In the absence of Wnt binding to frizzled (FZD), the destruction complex composed of axin, adenomatous polyposis coli (APC), protein phosphatase 2A (PP2A), glycogen synthase kinase 3 (GSK3) and casein kinase 1α (CK1α) is able to form. β-catenin is phosphorylated by GSK3, which is targeted for degradation by the ubiquitin ligase β-Trcp, and therefore unable to translocate to the nucleus. **B:** Binding of Wnt to the FZD (facilitated by the HS chains of HSPGs) and the LRP5/6 co-receptor results in activation of the dishevelled (Dvl) protein, binding it to FZD. This results in recruitment of the axin protein to the Wnt-LRP-FRD complex at the cell membrane. Recruitment of axin prevents the correct formation of the destruction complex, preventing GSK3 from phosphorylating β-catenin. β-catenin therefore accumulates within the cytoplasm before translocating to the nucleus, where it is able to interact with TCF transcription factors to upregulate target genes. Adapted from MacDonald et al. (2009).

differentiation (Chenn & Walsh, 2002; Hirabayashi et al., 2004; Mutch et al., 2010; Wrobel et al., 2007). Wnt signalling is also involved in adult neurogenesis, with increased canonical Wnt signalling promoting both cell proliferation and differentiation in the adult dentate gyrus (Lie et al., 2005). Wnt signalling regulates both developmental and adult neurogenesis through its regulation of genes involved in the cell cycle (e.g. cyclin D1) and neural differentiation (e.g. neurogenin-1 and -2). These genes are upregulated by the TCF/LEF transcription factors activated during canonical Wnt signalling (Qu et al., 2013). Aberrations in Wnt signalling have been found in many neurological disorders, highlighting their important role in neural development and maintenance (Durak et al., 2015; Lovestone et al., 2007; Pei et al., 1999; Voleti & Duman, 2012).

1.3.1.3 Bone Morphogenetic Protein Signalling

Cell-surface HSPGs are required for BMP signalling, with the removal of cell-surface HS preventing BMP binding and inhibiting Smad1/5/8 phosphorylation (Irie et al., 2003). HS is also believed to increase the bioavailability of BMP morphogens, preventing their degradation within the ECM and disrupting interactions between BMP and its antagonist, noggin (Figure 1.8) (Murali et al., 2013; Zhao et al., 2006). It has also been suggested that HS acts to enhance type II receptor recruitment following BMP binding, promoting formation of the heterotetrameric signalling complex, mediating BMP morphogen internalisation (Hu et al., 2009; Kuo et al., 2010). Similarly to the FGF and Wnt pathways, specific HS sulphation patterns are required for BMP binding; for example, *N*-sulphation and 6-*O*-sulphation have been identified as integral for HS:BMP-7 interactions, both of which are enriched in MPS IIIA HS (Irie et al., 2003; Wilkinson et al., 2012).

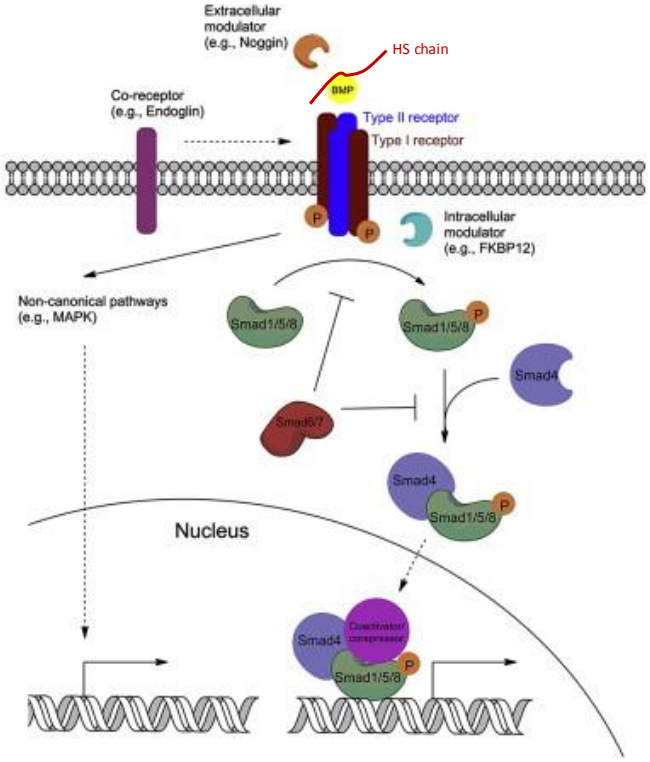

Figure 1.8: The canonical BMP signalling pathway

HS interactions with BMP ligands prevent their degradation within the ECM and disrupt interactions with the BMP antagonist, noggin, increasing ligand bioavailability at the cell surface. BMPs bind to type I and type II serine/threonine kinase receptors, forming a heterotetrameric complex. Formation of this complex enables the type II receptor to transphospohorylate the type I receptor, enabling the type I receptor to in turn phosphorylate Smad1/5/8. Phosphorylated Smad1/5/8 is able to bind Smad4, following which the complex is translocated to the nucleus. The Smad complex then associates with coactivators or corepressors to modulate expression of target genes. Adapted from Wang et al. (2014).

In contrast to many other HS-dependent signalling pathways, BMP acts as an inhibitory modulator of neural induction. During embryonic development of the ectoderm, BMP morphogens are known to promote formation of the epidermis, concurrently suppressing neural formation (Furuta et al., 1997; Hawley et al., 1995). Increases in BMP signalling also corresponded with decreased progenitor proliferation and increased apoptosis (Furuta et al., 1997; Graham et al., 1994). BMP expression increases with age and is associated with a reduction in hippocampal neural progenitor proliferation and neurogenesis; inhibition of BMP signalling increases neurogenesis and has been shown to restore cognitive defects in aging mice (Meyers et al., 2016; Yousef et al., 2015).

1.3.1.4 Hedgehog Signalling

HSPGs are also involved in Hh signalling. Hydrophobic Hhs are secreted and transported to the cell surface of cells expressing the Patched (Ptch) receptor (Panakova et al., 2005). Whilst lipidated proteins normally remain bound to the cell surface, Hhs must be released from the cell surface in order to bind to the Ptch receptor and initiate signal transduction (Ohlig et al., 2011; Tukachinsky et al., 2012; Zeng et al., 2001). HS chains are believed to regulate the release of Hh from the cell surface, indicating a positive regulatory role of HS (Figure 1.9) (Dierker et al., 2009; Jakobs et al., 2014; Lin, 2004; Ortmann et al., 2015). Indeed, mutant Hhs unable to bind to heparin display reduced Hh signalling *in vitro* (Chang et al., 2011). It has also been hypothesised that HSPGs may stabilise hydrophobic Hh morphogens following their release from the cell surface, preventing degradation, or act as a co-receptors for Hh interactions with its receptor, Ptch, as is seen in FGF signalling (Lin, 2004; Ohlig et al., 2011).

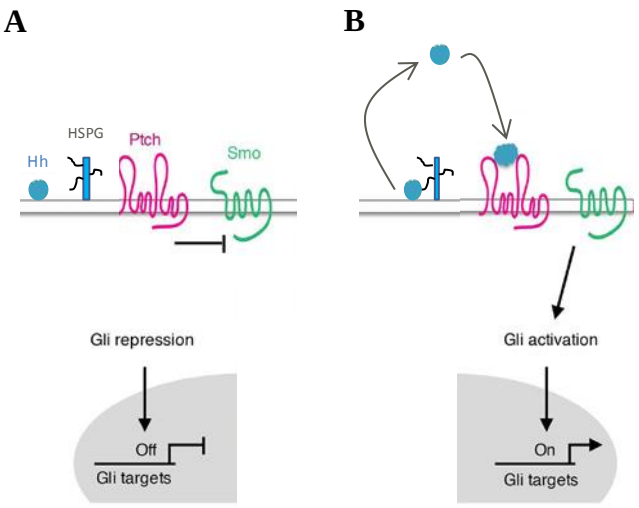

Figure 1.9: The Hh signalling pathway

A: In the absence of Hh, the Patched (Ptch) receptor inactivates the action of the Smoothened (Smo) receptor. This prevents the activation of the Gli transcription factor and results in repression of Gli target genes. **B:** Hh morphogens are released from the cell surface by HS chains and bind to the Ptch receptor, resulting in its inactivation and subsequent activation of Smo. Smo is able to activate the Gli transcription factor, allowing for transcription of Gli target genes. Adapted from Yao et al. (2016).

Hh is known to be vital for embryonic patterning during development (Fuccillo et al., 2004). Sonic hedgehog (Shh) controls the patterning of neural progenitors during development, and is believed to play a role in hippocampal neural plasticity (Komada et al., 2008; Machold et al., 2003). Activation of Shh signalling has been found to accelerate axon outgrowth and increase synaptic function (Mitchell et al., 2012; Yao et al., 2015), whilst disruptions in Shh signalling is believed to contribute to the pathology of several developmental and adult-onset neurological disorders (Blassberg et al., 2016; Boyd et al., 2015; Filges et al., 2011; Roper et al., 2006).

1.3.2 Neurogenesis in MPS

Studies which have examined the effects of the MPS disease state on neurogenesis have encountered dysregulation of the FGF signalling pathway. FGF-1, FGF-2 and FGFR mRNA expression was reduced within the brain in MPS IIIB mice compared to normal, with a concomitant reduction in proliferation in both the developing and adult brain of the MPS IIIB mouse model (Li et al., 2002). The FGF pathway was also disrupted in MPS I, where MPS I HS was found to interfere with FGF-2:FGFR interactions (Pan et al., 2005).

A reduction in stem cell proliferation and differentiation capacity has also been seen in MPS. Induced pluripotent stem cells (iPSCs) generated from MPS IIIB patient skin fibroblasts were unable to proliferate without an exogenous supply of the missing MPS IIIB enzyme, α-*N*-acetylglucosaminidase (NAGLU). The authors hypothesised, but did not confirm, that the iPSCs' inability to proliferate was a result of deficient FGF signalling due to aberrant HS (Lemonnier et al., 2011). Proliferation of NPCs isolated from MPS II mice was unaffected; however, mature neuron survival appeared to be reduced compared to normal NPCs (Fusar Poli et al., 2013).

1.4 Modelling Neurological Disease

Neurological disorders have proven to be difficult to model, primarily due to the difficulties in accessing human CNS tissue. Animal models and stem cells derived from somatic tissues are an alternative for investigating mechanisms of pathology and possible treatments for CNS disease.

1.4.1 Animal Models

Animal models have proven utility in investigating neurological diseases. Currently, two naturally occurring animal models of MPS IIIA exist; canine and murine (Bhaumik et al., 1999; Fischer et al., 1998). The MPS IIIA dog results from a c.737_739del (p.T246del) mutation whilst the MPS IIIA mouse carries a missense mutation of c.91 G>A (p.D31N) (Aronovich et al., 2000; Bhattacharyya et al., 2001). Sulphamidase activity is approximately 2% and 3% of wildtype in the canine and murine models respectively, resulting in intracellular HS accumulation and increased urinary excretion (Bhaumik et al., 1999; Fischer et al., 1998). The first clinical symptoms are seen at three years of age in MPS IIIA dogs, with the development of progressive ataxia and proprioceptive defects, leading to severe cerebellar ataxia and tremors at six years of age. However, no change in neurological function has been noted (Fischer et al., 1998; Jolly et al., 2007). The disease phenotype of the MPS IIIA mouse model closely mirrors the human disease. Mice appear normal at birth, with the first symptoms developing from 7-8 weeks of age. As the disease progresses mice become less active, developing a “scruffy” appearance and exhibiting a hunched posture and abdominal distension compared to normal littermates (Bhaumik et al., 1999). Functional neurological pathology is evident, with MPS IIIA mice consistently performing poorly in a range of behaviour tests (Crawley et al., 2006; Hemsley et al., 2007; Hemsley et al., 2009; McIntyre et al., 2010; Roberts et al., 2007). Due to its close mirroring of the human disease, the MPS IIIA murine model has been used extensively.

1.4.2 Modelling MPS IIIA neurogenesis *in vitro*

Although animal models are invaluable for research into neurological disorders, they have their limitations. In MPS IIIA, the microenvironment of the brain is complex; *in vitro* models of disease allow the contribution of a single component of the disease phenotype, such as GAG storage, towards overall neurological pathology to be determined. Stem cells with neurogenic properties have previously been isolated from MPS animal models, with murine-derived embryonic stem cells (ESCs) and NPCs used to model various MPS types (Fusar Poli et al., 2013; Heuer et al., 2001; Walton & Wolfe, 2007). Human *in vitro* models of disease provide an advantage over animal-derived cells, eliminating the confounding differences in development, lifespan and cellular pathways seen between species. Whilst CNS-derived human cell lines are difficult to obtain, the availability of cells from more readily available somatic tissues that are either able to be induced, or else inherently capable, of transdifferentiation into cells of the CNS provide an opportunity to model MPS IIIA neurogenesis *in vitro*.

1.4.2.1 Mesenchymal Stem Cells

Mesenchymal stem cells (MSC) were first described by Friedenstein et al. (1974). Fibroblast-like, spindle-shaped clonogenic cells were isolated from the bone marrow and defined as colony-forming unit fibroblasts capable of differentiating into adipocytes, osteocytes and chondrocytes of the mesodermal lineage (Friedenstein et al., 1974; Pittenger et al., 1999). MSCs were later found to exhibit transdifferentiation properties, producing cells of unrelated germline lineages under specific culture conditions (Figure 1.10) (Arthur et al., 2008; Azizi et al., 1998; Hermann et al., 2004; Kopen et al., 1999; Pereira et al., 1995; Pereira et al., 1998). The neurogenic properties of human MSCs were of particular interest and were identified upon culture with EGF, FGF-2 or retinoic acid, exposure to chemical compounds such as β-mercaptoethanol, co-culturing with neural lineage cells or increasing cyclic AMP levels

(Arthur et al., 2008; Bossolasco et al., 2005; Deng et al., 2001; Farzi-Molan et al., 2018; Gonmanee et al., 2018; Hermann et al., 2004; Mukai et al., 2016; Sanchez-Ramos et al., 2000; Woodbury et al., 2000).

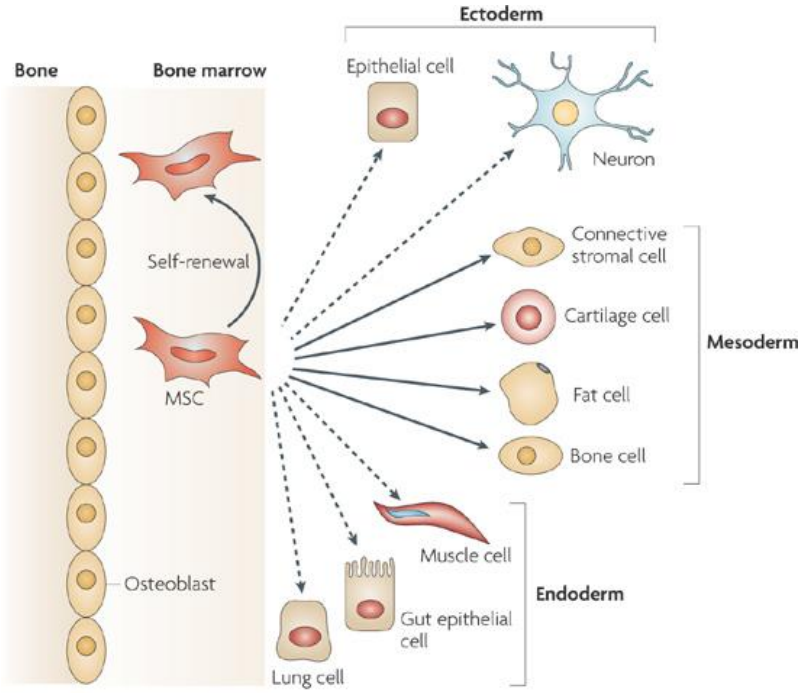

Figure 1.10: Transdifferentiation of MSCs

In addition to generating cells from their own mesodermal germline, MSCs can also differentiate into cells from the other two unrelated germline lineages. Adapted from Uccelli et al. (2008).

Due to their neurogenic properties, MSCs have been proposed as therapeutic agents to treat CNS disorders. Haematopoietic stem cells (HSCs), another bone marrow-derived cell type, are currently used to treat MPS I, MPS VI and MPS VII (Hobbs et al., 1981; Krivit et al., 1984; Yamada et al., 1998). Allogenic HSC transplants targeting the CNS rely on the ability of HSCs to cross the blood brain barrier and secrete the deficient enzyme into the CNS, where it can be taken up into neighbouring cells by mannose-6-phosphate receptors, targeting the enzyme to the lysosomes and decreasing GAG storage (Krivit et al., 1995). Unfortunately, HSC transplants carry significant risks, including the development of graft vs host disease, resulting in significant morbidity and mortality (Wang et al., 2016). MSCs have been proposed as an alternative to HSC transplants for MPS, their immunomodulatory effects hypothesised to reduce the risk of immune reactions from allogenic transplants. Furthermore, their ability to differentiate into neurons, as opposed to forming a component of the microglial cell system, provides a distinct advantage (Bartholomew et al., 2002; Di Nicola et al., 2002; Jackson et al., 2015; Krivit et al., 1995). Administration of MSCs was found to reduce GAG content and improve corneal defects in MPS VII mice and improve behavioural deficits in MPS I mice (Coulson-Thomas et al., 2013; da Silva et al., 2012; Meyerrose et al., 2008). Both HSCs and MSCs have been proposed for use in stem cell gene therapy. Following transfection with lentivirus encoding enzymes deficient in multiple MPS disorders, MSCs expressed higher levels of the deficient enzyme compared to transfected HSCs. Vector transduction efficiency was also higher in MSCs compared to HSCs. (Jackson et al., 2015). MSCs isolated from MPS I patients successfully overexpressed the enzyme deficient in MPS I, IDUA, following transfection with retrovirus encoding the *IDUA* gene. The ability of the secreted enzyme to correct human MPS I fibroblast pathology indicated their potential use for autologous MSC transplants (Baxter et al., 2002). MSCs have been used successfully in stem cell gene therapy to overexpress MPS enzymes *in vivo* (da Silva et al., 2012; Meyerrose et al., 2008).

Due to their multi-lineage potential, MSCs are an excellent candidate for modelling MPS IIIA *in vitro*, as they are able to model both the neurological and skeletal pathology typical of the disease. Our lab has recently determined that application of GAGs isolated from MPS I, MPS II and MPS VI patients to human MSCs from healthy human donors significantly delayed osteoblast differentiation and mineralisation and reduced osteoblast calcium deposition (Rout-Pitt et al., unpublished data). Similar methods can be used to examine the effect of HS isolated from MPS IIIA patients on neurogenesis. *In vitro* analysis with human MSCs is ideal; unlike cells of the CNS, MSCs are readily available from healthy donors and GAGs can be isolated from MPS IIIA patient or mouse urine, enabling the individual effect of MPS IIIA GAGs on neurogenesis to be directly determined in a human model.

To model the effects of intracellular GAG accumulation on neurogenesis, MSCs would need to be isolated from MPS patients; previously, MSCs have been isolated from MPS I patients to examine osteoclast formation (Gatto et al., 2012). Unfortunately, MSCs are difficult to procure from MPS IIIA patients due to the invasive nature of an MSC harvest. Murine models of MPS IIIA provide an alternate source of disease MSCs, due to their close mirroring of the MPS IIIA phenotype (section 1.4.1). Isolation and neurodifferentiation of MSCs isolated from the MPS IIIA mouse model would enable the development of an *in vitro* model of MPS IIIA neurogenesis. MSCs have previously been isolated from murine compact bone, bone marrow, dental pulp and umbilical cord and successfully differentiated along the neural lineage (Boregowda et al., 2016; Guimaraes et al., 2011; Sanchez-Ramos et al., 2000; Zhang et al., 2018; Zhao et al., 2016; Zhu et al., 2010). However, to date MSCs have not been isolated from murine models of any of the MPS disorders. It should be noted that the CNS is more directly accessible in mice than in humans and thus cells from the CNS, such as NSCs, could be isolated from the MPS IIIA mouse model, as has been achieved MPS II (Fusar Poli et al., 2013). MPS IIIA murine NSCs would be an alternate option to model neurogenesis *in vitro*

and would be of interest to examine further. However, for direct comparison to human MSC experiments examining the effects of extrinsic MPS IIIA GAG on neural differentiation (discussed previously), an MPS IIIA MSC model is advantageous to maintain consistency, due to the inherent differences between MSCs and NSCs and their neural differentiation (Ahmed et al., 2011; Lepski et al., 2010; New et al., 2015; Rossignol et al., 2014). However, due to the confounding differences between species, validation with a human source of cells with neurogenic properties would be advantageous. Induced pluripotent stem cells (iPSCs) are an example of one such cell type.

1.4.2.2 Induced Pluripotent Stem Cells

iPSCs have many advantages for disease modelling. They are by definition pluripotent and thus able to differentiate into cells of all three germline lineages; this is particularly useful for generating cells such as cardiomyocytes and neurons which are difficult to procure from humans (Figure 1.11) (Takahashi et al., 2007). They can be generated from easily accessible somatic cells, enabling modelling of disease without the ethical consideration plaguing ESC research. Indeed, even excluding the ethical considerations, it can be argued that iPSCs provide additional advantages over ESCs, as they provide a theoretically infinite source of pluripotent cells and enable disease modelling of a wide range of disorders (Bayart & Cohen-Haguenauer, 2013).

iPSCs were first generated from mouse embryonic fibroblasts and adult mouse tail-tip fibroblasts by Takahashi and Yamanaka (2006). Of the 24 candidate genes for maintaining pluripotency selected, four transcription factors were identified which, following retroviral-mediated transfer, successfully produced cells exhibiting the morphology and growth properties of ESCs; *Oct3/4, Sox2, c-Myc* and *Klf4* (Takahashi & Yamanaka, 2006). The

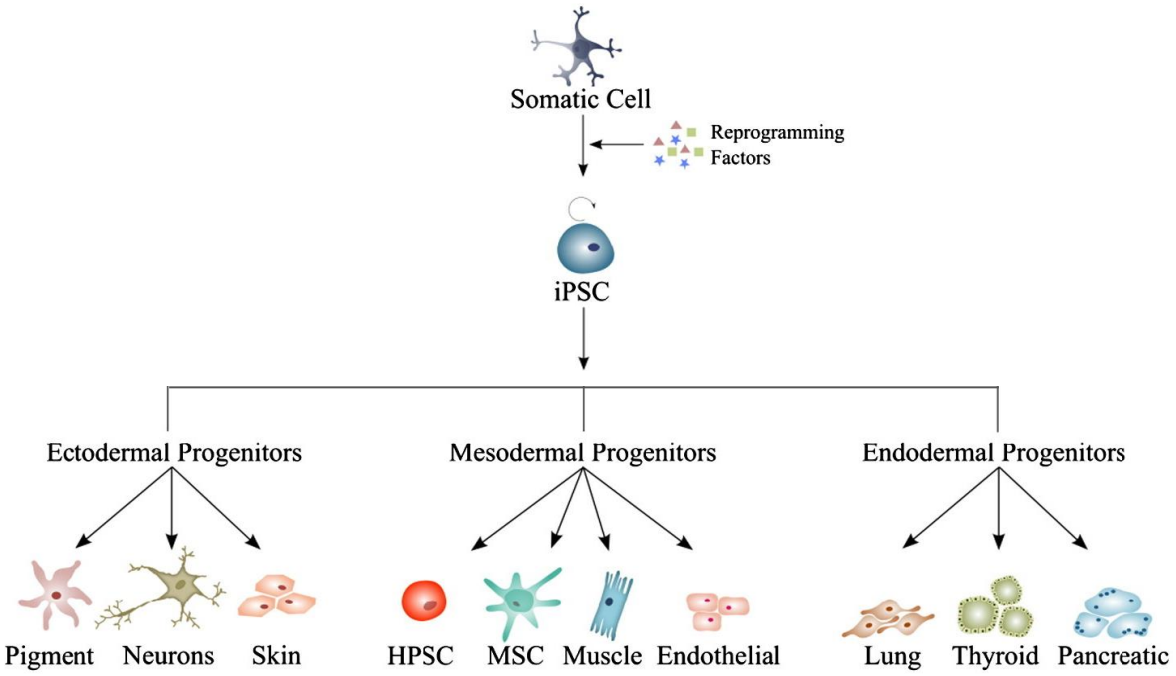

Figure 1.11: Generation and differentiation of iPSCs

Adult somatic cells such as skin fibroblasts can be reprogrammed into iPSCs through exposure to a cocktail of reprogramming growth factors. The pluripotency of iPSCs enables their differentiation down the three germline lineages. Adapted from Kaebisch et al. (2015).

ESC-like cells generated were found to be pluripotent, expressing ESC marker genes and contributing to mouse embryonic development following injection into blastocysts, and were subsequently designated iPSCs (Takahashi & Yamanaka, 2006). iPSCs were later successfully generated from adult human fibroblasts using the same methods (Takahashi et al., 2007). Whilst the original "Yamanaka" factors are the most frequently used, iPSCs have also been generated using the reprogramming factor combination of *Oct4*, *Sox2*, *Nanog* and *Lin28* (Yu et al., 2007). Permutations of these two common reprogramming factor cocktails using polycistronic vectors encoding up to six reprogramming factors have also successfully

established iPSC lines (Buecker et al., 2010; Kamata et al., 2010; Lee et al., 2010; Liao et al., 2008; Maherali et al., 2008).

Various delivery methods for the required growth factors have been established. Non-integrating delivery systems are the method of choice, due to the risks associated with insertional mutagenesis (Hacein-Bey-Abina et al., 2008; Hacein-Bey-Abina et al., 2003; Hennemann et al., 2000; Howe et al., 2008; Hu et al., 2011). The non-integrating Sendai virus, which exists in the cytoplasm as single stranded RNA, is commonly used as a delivery system due to their transient expression and efficient transduction efficiency (Fusaki et al., 2009; Ono et al., 2012; Seki et al., 2012).

iPSCs are an excellent candidate for modelling neurological disease in the MPS disorders. Skin fibroblasts are the most common somatic cell type used to generate iPSCs and are available from many MPS patients, as skin fibroblasts are commonly required for disease diagnosis (Lehman et al., 2011). iPSCs have been successfully generated from somatic cells of patients with MPS I, MPS II, MPS IIIB, MPS IIIC and MPS VII, in addition to a murine model of MPS VII (Bayo-Puxan et al., 2018; Canals et al., 2015; Griffin et al., 2015; Lemonnier et al., 2011; Meng et al., 2010; Rybova et al., 2018; Swaroop et al., 2018; Tolar et al., 2011; Vallejo-Diez et al., 2018; Varga et al., 2016a; Varga et al., 2016b, 2016c). An iPSC line has also been developed from an unaffected carrier of MPS II (Varga et al., 2016d). All MPS iPSCs were characterised as pluripotent, expressing ESC marker genes and demonstrating the ability to differentiate along all three germlines lineages. Vitally, the MPS iPSCs maintained key molecular hallmarks of the disease phenotype, exhibiting a significant reduction in activity of the relevant enzyme and an increase in stored GAG (Bayo-Puxan et al., 2018; Canals et al., 2015; Griffin et al., 2015; Lemonnier et al., 2011; Meng et al., 2010;

Swaroop et al., 2018; Tolar et al., 2011; Vallejo-Diez et al., 2018; Varga et al., 2016a; Varga et al., 2016b, 2016c).

A dysfunction in proliferation has been noted in some MPS iPSC lines. Murine MPS VII iPSCs displayed reduced proliferation compared to normal iPSCs; it was hypothesised that stored hyaluronan influenced E-cadherin expression, a regulator of cell-cell adhesions which in turn influence proliferation (Meng et al., 2010; Park et al., 2017; Stockinger et al., 2001). Embryoid body (EB) formation was subsequently significantly impaired in MPS VII iPSCs, with fewer, smaller EBs forming compared to control iPSCs. Treatment with β-glucuronidase, the enzyme deficient in MPS VII, successfully rescued the phenotype (Meng et al., 2010). EB growth was similarly decreased in MPS II iPSCs compared to normal (Rybova et al., 2018). Human MPS IIIB iPSCs required supplementation with the deficient NAGLU enzyme to circumvent impaired cell proliferation. Once cells had expanded sufficiently, they were successfully differentiated down the neural lineage in the absence of NAGLU (Lemonnier et al., 2011). In contrast, human MPS I, MPS II, MPS IIIC, and MPS VII iPSCs and iPSC-derived NPCs expanded normally in culture without exogenous supplementation of the deficient enzyme (Bayo-Puxan et al., 2018; Canals et al., 2015; Griffin et al., 2015; Swaroop et al., 2018; Tolar et al., 2011; Vallejo-Diez et al., 2018; Varga et al., 2016a; Varga et al., 2016b, 2016c).

Few of these studies generating MPS iPSC lines have directly compared control and MPS iPSC neural differentiation, instead simply demonstrating the ability of MPS iPSC lines to generate cells of the neuronal lineage as part of their pluripotency characterisation, without quantitative comparison to controls. Bayo-Puxan et al. (2018) examined *βIII-tubulin* expression in control and MPS VII iPSCs throughout neural induction, with no disparities

identified. A decrease in synaptotrophin was observed, indicating synaptic dysfunction in MPS VII iPSC-derived neurons. A decrease in GABAergic inhibitory neurons and neuronal activity was also noted. Synaptic activity was similarly decreased in MPS IIIC iPSC-derived neurons, with reduced spontaneous neuronal activity compared to normal iPSC-derived neurons. Lentiviral mediated gene correction of the *HGSNAT* gene rescued the phenotype (Canals et al., 2015). Migration and neural differentiation were examined following the administration of normal and MPS VII iPSC-derived NSCs to the striatum of normal mice; however, no discrepancies were identified (Griffin et al., 2015).

1.5 Significance, Hypothesis and Aims

MPS IIIA is caused by a deficiency in the enzyme sulphamidase, leading to accumulation of aberrantly structured HS. Patients with MPS IIIA exhibit severe CNS pathology, leading to a poor quality of life and early death. There is currently no effective treatment for MPS IIIA patients. To develop more effective therapies, the mechanisms of disease in MPS IIIA need to be elucidated; however, the contribution of the MPS IIIA HS towards the severe neurological disease characteristic of MPS IIIA is currently poorly understood. MPS-derived GAGs have previously been found by our lab to affect MSC osteoblast differentiation potential (Rout-Pitt et al., unpublished data), indicating an ability to disrupt developmental processes, and thus we hypothesise that these aberrant GAGs may similarly affect neural development. MPS IIIA GAGs are present throughout development in MPS IIIA, with GAG storage present in the developing CNS *in utero*, supporting a role for them in altering neurogenesis in MPS IIIA (Ceuterick et al., 1980; Greenwood et al., 1978; Harper et al., 1974; Martin & Ceuterick, 1983). To date, few studies have examined the early stages of neural development in MPS IIIA; to our knowledge, neurogenesis has not been examined. Therefore, this study aims to determine if altered CNS development contributes to the neurological pathology of MPS IIIA

patients, by exploiting the neurogenic capacity of stem cells to the model one of the earliest processes of CNS development, neurogenesis.

Hypothesis: The neurogenic potential of stem cells is altered in MPS IIIA

Aim 1: To characterise the timecourse of neural gene expression in human and murine MSC neural induction for use in Aims 2 and 3.

Aim 2: To determine the effect of extrinsic MPS IIIA GAGs on MSC differentiation.

Aim 3: To develop *in vitro* models of MPS IIIA to identify alterations in stem cell proliferation and neurogenesis

Chapter Two: Materials and Methods

2.1 Materials

Materials are listed in Appendix A.

2.2 MPS GAG isolation

MPS IIIA mice were placed in metabolic cages (Hatteras Instruments) for eight hours to collect urine. GAGs were isolated from urine as per Byers et al. (1998). MPS I, MPS II and MPS VI GAGs were previously isolated from patient urine and donated by Dr. Sharon Byers.

2.2.1 GAG quantification

Uronic acid content was determined as per Blumenkrantz and Asboe-Hansen (1973).

2.3 Human MSC *in vitro* studies

2.3.1 Human MSC cell culture

Human MSCs were sourced from bone marrow (hBM) and dental pulp (hDP) of healthy human donors as previously described (Gronthos et al., 2000; Gronthos et al., 2003). Human MSCs were cultured in human MSC basal growth media consisting of α-MEM (+ nucleosides) supplemented with 10% (v/v) foetal calf serum (FCS), 2mM L-glutamine, 100μM L-ascorbate-2-phosphate, 1mM sodium pyruvate, 50U/mL penicillin and 50μg/mL streptomycin. Cells were maintained at 37°C in 5% CO_2 and 90% humidity, with media changed twice weekly. At 90% confluency, cells were passaged by washing two times in phosphate buffered saline (PBS) followed by incubation with 10% (v/v) trypsin-EDTA for five minutes. The cell suspension was centrifuged at 390 x *g* for five minutes and the pellet resuspended in human MSC basal growth media. Cells were split at a 1:3 ratio.

2.3.2 Human MSC neurogenic differentiation

6-well or 12-well plates were coated with 10μg/mL poly-L-ornithine overnight at room temperature. Wells were washed twice with sterile water and coated with 5μg/mL laminin overnight at 37°C. Wells were washed once with PBS and once with human MSC basal growth media. hDP MSCs were harvested between passages seven to eight as per section 2.3.1 and plated at 1.6 x 10^4 cells per cm^2 onto poly-L-ornithine/laminin-coated plates in human MSC basal growth media. Cells were setup in triplicate for each timepoint and incubated at 37°C for three days before transfer into either neural priming (NP) or maturation (M) media. Basal media control samples were setup in triplicate and maintained in human MSC basal growth media.

2.3.2.1 Neural priming and maturation method

hDP MSCs plated on poly-L-ornithine/laminin-coated plates were transferred into NP media, consisting of Neurobasal A supplemented with 1X B27, 20 ng/mL EGF (ProSpec), 40 ng/mL FGF-2 (ProSpec), 50 U/mL penicillin and 50 μg/mL streptomycin for seven days. Cells were then transferred into M media consisting of a 1:1 ratio of DMEM (high glucose) and Ham's F-12 supplemented with 1x ITS+ premix stock, 40ng/mL FGF-2 (ProSpec), 0.5μM retinoic acid, 50 U/mL penicillin and 50 μg/mL streptomycin for a maximum of 21 days. For extrinsic GAG experiments (Chapter Four), GAGs were added to the neurogenic media at a concentration of 2μg/mL. Basal media control samples were maintained in human MSC basal growth media and RNA collected as below after 24 hours. Cells were fed with NP media or M media every two days. For timecourse experiments (Chapter Three), RNA was isolated with the PureLink™ RNA Micro Kit (Life Technologies) as per the manufacturer's instructions 1, 3, 5, 7, 8, 10, 12, 14, 16, 18, 20, 22, 24, 26 and 28 days post-induction. For extrinsic GAG experiments (Chapter Four), RNA was isolated with TRIzol (Life Technologies) followed by RNA clean-up with the RNeasy Mini Kit (Qiagen) as per the manufacturer's instructions 14

and 21 days post-induction. Expression of neural marker genes was determined by real-time PCR (section 2.10).

2.3.2.2 Maturation only method

hDP MSCs plated on poly-L-ornithine/laminin-coated plates were transferred into M media as per 2.3.2.1 for a maximum of 28 days. Basal media control samples were maintained in human MSC basal growth media and RNA collected as below after 24 hours. Cells were fed with M media every two days. For timecourse experiments (Chapter Three), RNA was isolated with the PureLink™ RNA Micro Kit (Life Technologies) as per the manufacturer's instructions 1, 3, 5, 7, 8, 10, 12, 14, 16, 18, 20, 22, 24, 26 and 28 days post-induction. Expression of neural marker genes was determined by real-time PCR (section 2.10).

2.3.3 Human MSC mesodermal differentiation assays

2.3.3.1 Human MSC osteogenic differentiation

hBM MSCs were harvested at passage seven as per section 2.3.1 and plated at 2.5 x 10^4 cells per cm^2 into 96-well plates in human MSC basal growth media. Cells were setup in triplicate for von Kossa staining and calcium quantification at each timepoint and condition. Cells were incubated at 37°C for overnight before transfer into osteogenic media consisting of α-MEM (+ nucleosides) supplemented with 5% (v/v) FCS, 2mM L-glutamine, 1mM sodium pyruvate, 100µM L-ascorbate-2-phosphate, 0.1µM dexamethasone, 10mM HEPES, 1.8mM potassium phosphate (KH_2PO_4), 50U/mL penicillin and 50µg/mL streptomycin. For extrinsic GAG experiments (Chapter Four), GAGs were added to the osteogenic media at a concentration of 3µg/mL. Basal media controls were maintained in human MSC basal growth media. Cells were fed with osteogenic media or human MSC basal growth media twice weekly. Cells were fixed with 1% (v/v) formaldehyde in PBS for 30 minutes at 4°C for von Kossa staining or

collected in 0.6M HCl for 48 hours at 4°C for calcium quantification one, two, three and four weeks post-induction. von Kossa staining was undertaken as per Bills et al. (1971). Calcium content was determined using the Calcium Assay Kit (Cayman Chemicals) as per the manufacturer's instructions. Following calcium extraction, CelLytic-M (Sigma Aldrich) was added to the cells and incubated overnight at 4°C to extract protein. Total protein was determined using the QuantiPro BCA Assay Kit (Sigma Aldrich) (section 2.7.2.2) and calcium content was normalised to protein content.

2.3.3.2 Human MSC chondrogenic differentiation

hBM MSCs were harvested at passage seven as per section 2.3.1 and 2 x 10^5 cells were transferred to V-bottomed 96-well plates in chondrogenic media consisting of DMEM (high glucose) supplemented with 1x ITS+ premix stock, 2mM L-glutamine, 1mM sodium pyruvate, 100µM L-ascorbate-2-phosphate, 0.1µM dexamethasone, 10ng/mL TGFβ, 50U/mL penicillin and 50µg/mL streptomycin. Cells were setup in triplicate for each timepoint and condition. For extrinsic GAG experiments (Chapter Four), GAGs were added to the chondrogenic media at a concentration of 5µg/mL. Basal media controls were maintained in human MSC basal growth media. Cells were centrifuged for 30 minutes at 300 x *g* to pellet cells. Cells were fed with chondrogenic media or human MSC basal growth media every other day. Cell pellets were collected for GAG synthesis analysis six days post-induction. GAG synthesis was determined by $^{35}SO_4$ incorporation as per Roberts et al. (2006).

2.3.3.3 Human MSC adipogenic differentiation

hBM MSCs were harvested at passage seven as per section 2.3.1 and plated at 2.5 x 10^4 cells per cm^2 into 96-well plates in human MSC basal growth media in triplicate for each timepoint and condition. Cells were incubated at 37°C for overnight before transfer into adipogenic

media consisting of α-MEM (+ nucleosides) supplemented with 5% (v/v) FCS, 2mM L-glutamine, 1mM sodium pyruvate, 100μM L-ascorbate-2-phosphate, 0.5nM isobutylmethylxanthine, 0.5μM hydrocortisone, 60μM indomethacin, 50U/mL penicillin and 50μg/mL streptomycin. For extrinsic GAG experiments (Chapter Four), GAGs were added to the adipogenic media at a concentration of 5μg/mL. Basal media controls were maintained in human MSC basal growth media. Cells were fed with adipogenic media or human MSC basal growth media twice weekly. Cells were fixed with 3.7% (v/v) formaldehyde in water for two minutes at room temperature for oil red O staining one, two, three, four and five weeks post-induction. Oil red O staining to identify adipocytes was undertaken as per Tang et al. (2003).

2.4 Animal husbandry and genotyping

All experimental procedures were approved by the Women's and Children's Health Network and The University of Adelaide animal ethics committees. Normal and MPS IIIA mice were bred from a colony maintained by the Matrix Biology Unit and housed at the Women's and Children's Hospital. Mice were housed in same sex groups on a 14/10 hour light/dark cycle at 22°C. Food and water available *ad libitum* and cages were cleaned weekly. Pups were tattooed for identification and a tail clip taken for genotype determination on day ten and weaned at three weeks of age. Tissue lysate was generated from toe clippings with lysis buffer (Viagen Biotech) containing 0.4 mg/mL Proteinase K as per the manufacturer's instructions. Tissue lysate was used in a polymerase chain reaction (PCR) based-genotyping protocol as per Roberts et al. (2009).

2.5 Murine MSC *in vitro* studies

2.5.1 Murine MSC isolation

MSCs were isolated from compact bone of wild-type and MPS IIIA mice. The MiniMACS™ separation system (Miltenyi Biotec) was used to remove haematopoietic stem cells (CD45.2 depletion) before selection of the remaining stem cells (Sca.1 selection). For each MSC preparation, four mice of the same sex and genotype were humanely killed at two months of age by isoflurane asphyxiation followed by cervical dislocation. Femurs and tibia were removed and cleaned of surrounding connective tissue. Bones were crushed into small fragments using a mortar and pestle, and then flushed repeatedly with 2% (v/v) FCS to remove bone marrow and red blood cells. Bone fragments were incubated with 3mg/mL collagenase type I for five minutes at 37°C. Bone fragments were then cut into smaller fragments and incubated with 3mg/mL collagenase type I for 60 minutes with shaking at 37°C. Bone fragments were washed with 2% (v/v) FCS and the suspension passed through a 70μM sieve. The suspension was centrifuged at 390 x *g* and the pellet resuspended in 2mL of murine MSC basal growth media, consisting of α-MEM (+ nucleosides) supplemented with 10% (v/v) FCS, 50U/mL penicillin and 50μg/mL streptomycin. Cell number was determined using trypan blue exclusion on a Countess™ automated cell counter (Life Technologies). Cells were transferred to a 10mL centrifuge tube and 8mL of 2% (v/v) FCS was added. The cell suspension was centrifuged at 390 x *g* for five minutes. Cells were resuspended in blocking solution consisting of 3% (w/v) bovine serum albumin (BSA) in PBS (refer Table 2.1 for volumes) and incubated on ice for 10 minutes. 1.5mL MACS buffer, consisting of 0.5% BSA (w/v) in 2mM $Na_2EDTA.2H_2O$ (PBS), was added to the tube and centrifuged at 390 x *g* for five minutes. The pellet was resuspended in anti-CD45.2-biotin antibodies (Miltenyi Biotec) at a 1/11 dilution in MACS buffer (refer Table 2.1 for volumes) and incubated on ice for 10 minutes. CD45.2 depletion was undertaken using anti-biotin microbeads in the MiniMACS™ separation system (Miltenyi Biotec) as per the manufacturer's instructions. The elute was retained in a new 10mL centrifuge tube and

centrifuged at 390 x *g* for five minutes. The pellet was resuspended in anti-Sca.1-biotin antibodies (Miltenyi Biotec) at a 1/11 dilution in MACS buffer (refer Table 2.1 for volumes) and incubated on ice for 10 minutes. Sca.1 selection was undertaken using anti-biotin microbeads in the MiniMACS™ separation system (Miltenyi Biotec) as per the manufacturer's instructions. The elute was discarded and the bound cells were recovered. The cell suspension was centrifuged at 390 x *g* for five minutes and the pellet resuspended in murine MSC basal growth media. All cells were transferred to a single well of a 24-well plate. After 24 hours, the well was washed three times with murine MSC basal growth media to remove floating cells and then maintained as per section 2.5.2.

2.5.2 Murine MSC cell culture

Murine MSCs were cultured in murine MSC basal growth media, consisting of α-MEM (+ nucleosides) supplemented with 10% (v/v) FCS, 50U/mL penicillin and 50μg/mL streptomycin. Cells were maintained at 37°C in 5% O_2, 10% CO_2 and 90% humidity, with media changed three times weekly. At 80% confluency, cells were passaged by washing two times in PBS followed by incubation with neat trypsin-EDTA for four minutes. The cell suspension was centrifuged at 390 x *g* for five minutes and the pellet resuspended in murine MSC basal growth media. Normal and MPS IIIA murine MSCs were split at 1:3 and 1:2 ratios respectively. To maintain proliferation, MPS IIIA murine MSCs were cultured in murine MSC basal growth media as above supplemented with 5ng/mL FGF-2 (ProSpec) from passage five.

2.5.3 Colony forming unit assay

Murine MSCs were harvested at passage five as per section 2.5.2 and plated at three different cell densities in murine MSC basal growth media: 8.0 x 10^1 cells per cm^2, 1.0 x 10^2 cells per cm^2 and 1.2 x 10^2 cells per cm^2 into 6-well plates. Cells were setup in triplicate for each

Solution	Dilution	Volume reagent per 10^7 cell (µL)	Volume MACS buffer per 10^7 cells (µL)
Blocking solution	-	110	-
Anti-CD45.2-biotin	1/11	10	100
Anti-Sca.1-biotin	1/11	10	100
Anti-biotin microbeads	1/4.5	20	70

Table 2.1: Dilutions and volumes for murine MSC isolation reagents

Volumes of reagents and MACS buffer is for up to 10^7 total cells immediately following isolation from compact bone. For higher cell numbers, volumes were increased proportionally.

timepoint. Cell were fed with murine MSC basal growth media three times weekly. Cells were fixed with 10% (v/v) formaldehyde in water for ten minutes at room temperature for crystal violet staining one and two weeks post-seeding. Cells were washed twice with water and then stained with 3% (w/v) crystal violet in water for 30 minutes at room temperature. Cells were washed twice with water and stored in water for colony counts. Colony width was measured using Olympus analySIS® LS Research Olympus Soft Imaging Solutions version 3.1 (Olympus Australia Pty. Ltd). Colonies were excluded if less than 2mm in width.

2.5.4 Murine MSC neurogenic differentiation

12-well plates were coated with 10µg/mL poly-L-ornithine overnight at room temperature. Wells were washed twice with sterile water and coated in 5µg/mL laminin overnight at 37°C. Wells were washed once with PBS and once with murine MSC basal growth media. Murine MSCs were harvested at passage eight as per section 2.5.2 and plated at 1.6 x 10^4 cells per cm^2 onto poly-L-ornithine/laminin-coated plates in murine MSC basal growth media. Cells

were setup in triplicate for each timepoint and incubated at 37°C for three days before transfer into either NP or M media. Basal media control samples were setup in triplicate and maintained in murine MSC basal growth media.

2.5.4.1 Neural priming only method

Murine MSCs plated on poly-L-ornithine/laminin-coated plates were transferred into NP media as per section 2.3.2.1 for a maximum of 48 hours. Basal media control samples were maintained in murine MSC basal growth media and RNA collected as below after four hours. RNA was isolated with the PureLink™ RNA Micro Kit (Life Technologies) as per the manufacturer's instructions 4, 8, 12, 16, 24, 36 and 48 hours post-induction. Expression of neural marker genes was determined by real-time PCR (section 2.10).

2.5.4.2 Maturation only method

Murine MSCs plated on poly-L-ornithine/laminin-coated plates were transferred into M media as per section 2.3.2.2 for a maximum of 48 hours. Basal media control samples were maintained in murine MSC basal growth media and RNA collected as below after four hours. RNA was isolated with the PureLink™ RNA Micro Kit (Life Technologies) as per the manufacturer's instructions 4, 8, 12, 16, 24, 36 and 48 hours post-induction. Expression of neural marker genes was determined by real-time PCR (section 2.10).

2.5.4.3 Neural priming and maturation method

Murine MSCs plated on poly-L-ornithine/laminin-coated plates were transferred into NP media as per section 2.3.2.1 for seven days. Cells were then transferred into M media as per section 2.3.2.1 for a maximum of 14 days. Basal media control samples were maintained in murine MSC basal growth media. Cells were fed with NP media, M media or murine MSC

basal growth media every two days. RNA was isolated with the PureLink™ RNA Micro Kit (Life Technologies) as per the manufacturer's instructions 1, 3, 5, 7, 8, 10, 12, 14, 16, 18 and 20 days post-induction. Expression of neural marker genes was determined by real-time PCR (section 2.10).

2.6 Human iPSC *in vitro* studies

2.6.1 Fibroblast culture

Human MPS IIIA fibroblasts were sourced from the National Referral Laboratory at the Women's and Children's Hospital, SA, Australia. Control fibroblasts were purchased from the Coriell Institute, USA. Fibroblasts were cultured in fibroblast basal growth media, consisting of DMEM (high glucose) supplemented with 10% (v/v) foetal calf serum (FCS), 50U/mL penicillin and 50µg/mL streptomycin. Cells were maintained at 37°C in 5% CO_2 and 90% humidity, with media changed twice weekly. At 90% confluency, cells were passaged by washing two times in PBS followed by incubation with 20% (v/v) trypsin-EDTA for five minutes. The cell suspension was centrifuged at 170 x *g* for five minutes and the pellet resuspended in fibroblast basal growth media. Cells were split at a 1:3 ratio.

For gene expression analysis, fibroblasts were plated at 2.0 x 10^4 cells per cm^2 in triplicate in 6-well plates in fibroblast basal growth media. RNA was isolated with TRIzol (Life Technologies) followed by RNA clean-up with the RNeasy Mini Kit (Qiagen) as per the manufacturer's instructions. Expression of pluripotency genes was determined by real-time PCR (section 2.10).

2.6.2 Fibroblast reprogramming to iPSCs

Human fibroblasts were reprogrammed to iPSCs via transduction with Sendai virus vectors expressing the Yamanaka factors, Oct3/4, Sox2, Klf2 and c-Myc (Takahashi & Yamanaka, 2006) using the CytoTune™-iPS 2.0 Sendai Reprogramming Kit (Life Technologies) as per the manufacturer's instructions. Three weeks post-transduction, single colonies with ESC-like morphology were manually picked and transferred to irradiated mouse embryonic fibroblast (MEF) coated 6-well plates, with one colony per well. MEF plates were prepared as per 2.6.2.1. A minimum of 11 colonies were picked per fibroblast cell line.

2.6.2.1 Feeder-dependent iPSC culture

Feeder-dependent iPSCs were cultured on MEFs (StemCore). MEF plates were prepared by coating 6-well plates with 0.1% (w/v) gelatin solution for two hours to overnight at 37°C. Gelatin was aspirated and plates dried for one hour at room temperature. MEFs were plated on dried gelatin-coated plates at 1.9 x 10^4 cells per cm^2 in DMEM (high glucose) supplemented with 10% (v/v) FCS, 100µM non-essential amino acids, 50U/mL penicillin and 50µg/mL streptomycin. Cells were incubated overnight at 37°C. MEF plates were washed once with PBS immediately before use.

iPSCs were cultured in DMEM/F-12 (+ GlutaMAX) supplemented with 20% (v/v) KnockOut ™ Serum Replacement, 100µM non-essential amino acids, 55µM β-mercaptoethanol, 20ng/mL FGF-2 (Life Technologies), 50U/mL penicillin and 50µg/mL streptomycin. Cells were maintained at 37°C in 5% CO_2 and 90% humidity, with media changed daily. Cells were passaged manually approximately every five days onto fresh MEF plates. MEFs were only able to condition the iPSCs media for six days; on day six, any iPSCs remaining on MEFs

were transferred into conditioned media as prepared in section 2.6.2.1.1 supplemented with 20ng/mL FGF-2 (Life Technologies) and 55µM β-mercaptoethanol.

2.6.2.1.1 Conditioned media

A T175 flask was coated with 0.1% (w/v) gelatin for two hours to overnight at 37°C. Gelatin was aspirated and the flask dried for one hour at room temperature. MEFs were plated on the dried gelatin-coated T175 flask at 6.0 x 10^4 cells per cm^2 in DMEM (high glucose) supplemented with 10% (v/v) FCS, 100µM non-essential amino acids, 50U/mL penicillin and 50µg/mL streptomycin. Cells were incubated overnight at 37°C and then transferred into 70mL DMEM/F-12 (+ GlutaMAX) supplemented with 20% (v/v) KnockOut ™ Serum Replacement, 100µM non-essential amino acids, 50U/mL penicillin and 50µg/mL streptomycin. Cells were maintained at 37°C in 5% CO_2 and 90% humidity. After 24 hours the media was collected and stored at 4°C, and 70mL fresh media was added to the T175 flask. Media was collected and stored at 4°C for a total of six days. The combined media was filtered through a 0.22µM filter and stored at -80°C. Conditioned media was thawed at 4°C overnight as required.

2.6.2.2 Feeder-free iPSC culture

For feeder-free culture, iPSCs were transferred from MEF plates to vitronectin-coated plates. 6-well plates were coated with 10µg/mL vitronectin in CellAdhere Dilution Buffer (StemCell Technologies) for one hour at room temperature. Wells were washed once with CellAdhere Dilution Buffer, following which 2mL TeSR-E8 media (StemCell Technologies), prepared as per the manufacturer's instructions, was added to each well. iPSCs were manually passaged from MEF plates to prepared vitronectin-coated plates and incubated overnight at 37°C. Feeder-free iPSCs were maintained at 37°C in 5% CO_2 and 90% humidity, with TeSR-E8

media changed daily. Feeder-free iPSCs were passaged approximately every five days with Gentle Cell Dissociation Reagent (StemCell Technologies) onto fresh vitronectin-coated plates as per the manufacturer's instructions.

For gene expression analysis, iPSCs were plated in triplicate in vitronectin-coated 6-well plates in TeSR-E8 media. RNA was isolated with TRIzol (Life Technologies) followed by RNA clean-up with the RNeasy Mini Kit (Qiagen) as per the manufacturer's instructions. Expression of pluripotency and neural marker genes was determined by real-time PCR (section 2.10). For immunofluorescence, iPSCs were plated in triplicate in vitronectin-coated NUNC 35mm dishes in TeSR-E8 media. Cells were fixed in 4% (w/v) PFA for 15 minutes at room temperature and washed three times in PBS before being stored at 4°C in PBS for immunofluorescence staining (section 2.11).

2.6.2.3 Karyotype analysis

G-band chromosome analysis of iPSCs was performed by SA Health (Cytogenetics, Women's and Children's Hospital, Adelaide).

2.6.3 iPSC differentiation to NPCs

iPSCs maintained in feeder-free conditions were differentiated to NPCs as per the cortical neural differentiation protocol established by Shi et al. (2012a) and optimised by Homan et al. (2018). Following dissociation with Accutase (StemCell Technologies) as per step 43 in Shi et al. (2012a), cells were plated on ECM-coated NUNC 6-well plates or flasks in neural expansion media consisting of a 1:1 ratio of Neurobasal and DMEM/F-12 (+ GlutaMAX) supplemented with 20ng/mL FGF-2 (Life Technologies), 1x B27 supplement, 1x N2 supplement, 5µg/mL insulin, 100µM non-essential amino acids, 100µM β-mercaptoethanol,

1mM L-glutamine, 50U/mL penicillin and 50µg/mL streptomycin. To prepare ECM-coated 6-well plates and flasks, ECM was diluted 1:100 in cold DMEM/F-12 (+ GlutaMAX), added to 6-well plates or flasks and incubated for two hours to overnight at 37°C. Wells and flasks were washed once with PBS immediately prior to use. Cells were plated at 2.1 x 10^5 cells per cm^2 and incubated at 37°C. Cells were maintained at 37°C in 5% CO_2 and 90% humidity, with media changed every two days.

At 90-100% confluency, iPSC-NPCs were passaged by washing once with PBS followed by incubation with 70µL per cm^2 pre-warmed Accutase (StemCell Technologies) per well/flask for up to ten minutes or until cells were forming single cells and detaching from the surface. An equal volume of neural expansion media was added to neutralise the Accutase (StemCell Technologies). Cells were centrifuged at 120 x *g* for three minutes and resuspended in neural expansion media. Cells were plated at 2.1 x 10^5 cells per cm^2 on ECM-coated plates and flasks (as prepared in section 2.6.3) for further expansion.

For gene expression analysis, iPSC-NPCs were plated at 2.1 x 10^5 cells per cm^2 in triplicate in ECM-coated 6-well plates in neural expansion media. RNA was isolated with TRIzol (Life Technologies) followed by RNA clean-up with the RNeasy Mini Kit (Qiagen) as per the manufacturer's instructions. Expression of neural marker genes was determined by real-time PCR (section 2.10). For immunofluorescence, iPSC-NPCs were plated in triplicate at 5.0 x 10^4 cells per cm^2 on ECM-coated coverslips in 12-well plates. Cells were fixed in 4% (w/v) PFA for 15 minutes at room temperature and washed three times in PBS before being stored at 4°C in PBS for immunofluorescence staining (section 2.11).

2.6.4 iPSC-derived NPC neurogenic differentiation

NUNC 6-well plates were coated with 100µg/mL poly-L-ornithine for four hours at 37°C. Wells were washed twice with PBS and coated in 20µg/mL laminin overnight at 37°C. Wells were washed once with Neurobasal media immediately prior to use. iPSC-NPCs were harvested at passage six with Accutase (StemCell Technologies) as per section 2.6.3 and plated at 5.0 x 10^4 cells per cm^2 onto poly-L-ornithine/laminin-coated plates in neural expansion media. Cells were setup in triplicate each timepoint and incubated at 37°C overnight before transfer into neural maintenance media consisting of a 1:1 ratio of Neurobasal and DMEM/F-12 (+ GlutaMAX) supplemented with 1x B27 supplement, 1x N2 supplement, 5µg/mL insulin, 100µM non-essential amino acids, 100µM β-mercaptoethanol, 1mM L-glutamine, 50U/mL penicillin and 50µg/mL streptomycin. Cells were fed with neural maintenance media 3, 5, 7 and 10 days post-seeding. From 13 days post-seeding, cells were fed every three days by removing 1mL old neural maintenance media and gently feeding with 1mL fresh neural maintenance media. For gene expression analysis, RNA was isolated 14, 21 and 28 days post-induction with TRIzol (Life Technologies) followed by RNA clean-up with the RNeasy Mini Kit (Qiagen) as per the manufacturer's instructions and expression of neural marker genes was determined by real-time PCR (section 2.10).

2.7 Biochemical assays

2.7.1 Sulphamidase enzyme assay

Sulphamidase activity was determined on cell lysates of murine MSCs, human fibroblasts and iPSCs. MSCs and fibroblasts were plated in triplicate at 1.05 x 10^4 cells per cm^2 into 6-well plates. iPSC colonies were plated at high confluency into vitronectin-coated 6-well plates. Cells were lysed in 0.1% Triton X-100 (v/v) in PBS at room temperature for 10 minutes, removed by scraping and transferred to 1.5mL centrifuge tube and frozen at -20°C. Enzyme activity was determined on 5µL samples as per Karpova et al. (1996), with the first incubation

decreased from 17 hours to 4.5 hours. Total protein was determined using the Bicinchoninic Acid (BCA) Assay Kit (Sigma Aldrich) (section 2.7.2.1) and enzyme activity was normalised to protein content.

2.7.2 Protein assays

2.7.2.1 BCA assay

Total protein was determined on cell lysates using the BCA Assay Kit (Sigma Aldrich) as per the manufacturer's instructions.

2.7.2.2 QuanitPro BCA assay

Samples with a lower protein content had protein determined using the QuantiPro BCA Assay Kit (Sigma Aldrich) as per the manufacturer's instructions.

2.8 CyQuant Proliferation assay

2.8.1 MPS IIIA MSC proliferation assay

Normal and MPS IIIA murine MSCs were seeded immediately post-isolation from compact bone (section 2.5.1) in four wells of a 24-well plate in murine MSC basal growth media (components listed in section 2.5.2). Cells were maintained at 37°C in 5% O_2, 10% CO_2 and 90% humidity. Wells were washed three times with media after 24 hours, following which media was changed every two days. Proliferation was determined using the CyQuant® Direct Cell Proliferation Assay kit (Life Technologies) as per the manufacturer's instructions 2, 9, 12 and 15 days post-seeding.

2.8.1.1 MPS IIIA MSC rescue proliferation assay

MPS IIIA murine MSCs were harvested at passage six as per section 2.5.2 and plated at 9.4 x 10^3 cells per cm^2 into 96-well plates in murine MSC basal growth media (components listed in section 2.5.2). Exogenous sulphamidase was produced through lentiviral-mediated overexpression of sulphamidase in CHOK1 cells (section 2.9) and added to the murine MSC basal growth media at concentrations of 0.1, 0.3 and 1.0 pmol/min as required. FGF-2 (ProSpec) was added to the culture media at concentrations of 1ng/mL, 3ng/mL and 5ng/mL as required. MPS IIIA murine MSCs were maintained in murine MSC basal growth media as controls. Cells were maintained at 37°C in 5% O_2, 10% CO_2 and 90% humidity, with media changed every two days. Proliferation was determined using the CyQuant® Direct Cell Proliferation Assay kit (Life Technologies) as per the manufacturer's instructions one hour post-seeding and then each day for a total of three days.

2.8.2 MPS IIIA iPSC-NPC proliferation and rescue assay

ECM-coated plates were prepared as per section 2.6.3. Normal and MPS IIIA human iPSC-NPCs were harvested at passage five as per section 2.6.3 and plated at 9.4 x 10^3 cells per cm^2 into 96-well plates in neural expansion media (components listed in section 2.6.3). Exogenous sulphamidase was produced through lentiviral-mediated overexpression of sulphamidase in CHOK1 cells (section 2.9) and added to the neural expansion media of MPS IIIA human iPSC-NPCs at concentrations of 0.1, 0.3 and 1.0 pmol/min as required. Normal and MPS IIIA human iPSC-NPCs were maintained in neural expansion media as controls. Cells were maintained at 37°C in 5% CO_2 and 90% humidity, with media changed every two days. Proliferation was determined using the CyQuant ® Direct Cell Proliferation Assay kit (Life Technologies) as per the manufacturer's instructions one hour post-seeding and then each day for a total of three days.

2.9 Sulphamidase production

A lentiviral vector encoding sulphamidase (pHIV-EF1αmmCOS) was produced as per Jackson et al. (2015). CHO-K1 cells were seeded 5.0 x 10^4 cells per cm^2 in Ham's F-12 supplemented with 10% (v/v) FCS and incubated at 37°C. After three hours, CHOK1 cells were transferred into Ham's F-12 supplemented with 8µg/mL polybrene, 100µg/mL gentamycin and 1.5µg of p24 protein of pHIV-EF1αmmCOS lentivirus and incubated at 37°C. After 24 hours, the media was removed and replaced with Ham's F-12 supplemented with 2mM L-glutamine, 50U/mL penicillin and 50µg/mL streptomycin and incubated at 37°C. After 48 hours, the media was collected and stored at 4°C. Sulphamidase activity was determined using the sulphamidase enzyme assay (section 2.7.1).

2.10 Gene expression

2.10.1 Reverse transcription

RNA was isolated from cell layers with either the PureLink™ RNA Micro Kit (Life Technologies) or with TRIzol (Life Technologies) followed by RNA clean-up with the RNeasy Mini Kit (Qiagen) as per the manufacturer's instructions. RNA concentration was determined using a nanodrop spectrophotometer (Thermo Scientific, USA). Between 100ng and 500ng of RNA was reverse transcribed to cDNA using the QuantiTect Reverse Transcriptase Kit (Qiagen) as per the manufacturer's instructions.

2.10.2 Real-time PCR

Real-time PCR was performed to determine gene expression. Exon-exon boundary gene specific primers were designed for all human and murine neural marker genes. Primers for pluripotency markers *Oct-4*, *Nanog* and *Sox-2* were designed as previously described (Homan et al., 2018). Cyclophilin A was included as a housekeeping gene. See Table 2.2 for primer sequences. Each 25µL real-time PCR reaction included 1µL cDNA, 1x SYBR™ Green PCR

Mastermix (Life Technologies), 0.45µM forward primer and 0.45µM reverse primer. Real-time reactions were carried out on an ABI 7300 thermocycler (Applied Biosystems) with initial steps of one cycle for two minutes at 50°C and one cycle for ten minutes at 95°. cDNA amplification consisted of 40 cycles of 15 seconds at 95°C and one minute at 60°C. A dissociation step of one cycle for 15 seconds at 95°C, 30 seconds at 60°C and 15 seconds at 95°C was added after the amplification step. The $2^{-\Delta\Delta Ct}$ method was used to determine the fold change in gene expression as per Livak and Schmittgen (2001). The relative expression method was used to determine mean normalised gene expression as per Pfaffl (2001) for iPSC-NPC gene expression.

2.11 Immunofluorescence

Immunofluorescent detection of Oct-4 and SSEA4 on 4% (w/v) PFA-fixed iPSCs was undertaken using the PSC 4-Marker Immunocytochemistry Kit (Life Technologies) as per the manufacturer's instructions (Lot# 1913522). Immunofluorescent detection of Pax6 and Nestin on 4% (w/v) PFA-fixed iPSC-NPSs was undertaken as per Homan et al. (2018). See Tables 2.3 and 2.4 for antibody specifications.

2.12 Statistics

The statistical significance of differences between means was determined using a Student's t-test, a one sample t-test or a one-way analysis of variance (ANOVA) followed by Tukey's HSD post-hoc test as appropriate in GraphPad Prism Version 7.03 for Windows (GraphPad Software., USA).

Gene	Species	Forward primer	Reverse primer	Published
Oct-4	Human	GACAGGGGGAGGGGAG GAGCTAGG	CTTCCCTCCAACCAGTT GCCCCAAAC	Homan et al., 2018
Nanog	Human	AGTCCCAAAGGCAAACA ACCCACTTC	TGCTGGAGGCTGAGGT ATTTCTGTCTC	Homan et al., 2018
Sox2	Human	GGGAAATGGGAGGGGT GCAAAAGAGG	TTGCGTGAGTGTGGAT GGGATTGGTG	Homan et al., 2018
Pax6	Human	CCAGGGCAACCTACGCA A	CTGAATCTTCTCCGTTG GAACT	
Nestin	Human	CGCACCTCAAGATGTCCC TC	CAGCTTGGGGTCCTGAA AGC	
Nestin	Murine	CTCAGATCCTGGAAGGT GGG	GCAGAGTCCTGTATGT AGCCA	
NCAM	Human	GTTACAGGCGAGGATGG CA	TCACACACAATCACGGC ATC	
NCAM	Murine	CGGAACATCAGCAGTGA AGAAA	CAAGGAGGACACACGA GCAT	
NeuroD1	Human	ACTACATCTGGGCTCTG TCGG	TTGGTGGTGGGTTGGG ATAAG	
βIII-tubulin	Human	GGGCCAAGTTCTGGGAA GTC	ATCCGCTCCAGCTGCAA GT	Jackson et al., 2015
βIII-tubulin	Murine	ATGGACAGTGTTCGGTC TGG	AGCACCACTCTGACCA AAGAT	
NF-M	Human	GACGGCGCTGAAGGAAA TC	CTCTTCGCCCTGGTGCA TAT	Jackson et al., 2015
NF-M	Murine	CGGGGAACCAAGTGGGA AAT	CCCCCTCTAGGAGTTTC CTGT	
NF-H	Human	GGACCTGCTCAATGTCAA GATG	GCCAAAGCCAATCCGA CAC	
MAP2	Human	GGAACCAACTCTCTCTG GATTT	GCATTCTCTCTTCAGCC TTCT	
MAP2	Murine	TAAGCGGAAAACCACAG CAG	CGTTTCTCTGGGCTCTT GCT	
NSE	Human	GGGCACTCTACCAGGAC TTTG	CCCTACATTGGCTGTGA ACT	
NSE	Murine	GCGGCTTTGCCCCCAAT A	TCACCATCTTTTCCGTG TAGC	
Cyclophilin A	Human	TCCTAAAGCATACGGGT CCT	CTTGCCATCCAACCACT CA	
Cyclophilin A	Murine	AGCATACAGGTCCTGGC ATC	TTCACCTTCCCAAAGAC CAC	

Table 2.2: Real-time PCR Primers

Target	Host Species	Type	Dilution	Concentration used	Catalogue Number	Company
Oct-4	Rabbit	Withheld by supplier	1:100	Withheld by supplier	A24867 (PSC 4-Marker Immunocytochemistry Kit)	Life Technologies
SSEA4	Mouse IgG3	Withheld by supplier	1:100	Withheld by supplier	A24866 (PSC 4-Marker Immunocytochemistry Kit)	Life Technologies
Pax6	Rabbit	Polyclonal	1:500	4µg/mL	901301	BioLegend
Nestin	Mouse	Monoclonal	1:300	3.33µg/mL	MAB5326	Millipore

Table 2.3: Primary Antibodies

Antibody	Conjugate	Type	Dilution	Concentration used	Catalogue Number	Company
Rabbit IgG	Alexa Fluor® 555	Withheld by supplier	1:250	Withheld by supplier	A24869 (PSC 4-Marker Immunocytochemistry Kit)	Life Technologies
Mouse IgG3	Alexa Fluor® 488	Withheld by supplier	1:250	Withheld by supplier	A24877 (PSC 4-Marker Immunocytochemistry Kit)	Life Technologies
Rabbit IgG	Alexa Fluor® 488	Polyclonal	1:700	2.86µg/mL	A21206	Life Technologies
Mouse IgG	Alexa Fluor® 555	Polyclonal	1:700	2.86µg/mL	A31570	Life Technologies

Table 2.4: Secondary Antibodies

Chapter Three: Gene expression during neurogenic differentiation of human and murine mesenchymal stem cells

3.1 Introduction

Neural induction is well established in human MSCs, with multiple factors used to induce neurogenesis *in vitro* (section 1.4.2.1). In contrast, significantly less is available in the literature on the neural induction of murine MSCs. Similarly to human, murine MSC neural induction protocols use a variety of culture conditions, with growth factors such as EGF and FGF-2, neurotrophic factors, retinoic acid, chemical compounds such as β-mercaptoethanol and co-culturing with foetal midbrain cells all previously used, either singularly or in combination (Locatelli et al., 2003; Sanchez-Ramos et al., 2000; Taha & Hedayati, 2010). In addition to reagent variability, timeframes vary greatly in murine MSC neural induction, with protocols ranging from 34 hours to three weeks in length (Mohammad et al., 2016; Taha & Hedayati, 2010). Long-term neural induction protocols are dominant in murine MSCs, with changes in neural gene expression not examined until many days following the initiation of neurogenesis (Abdullah et al., 2016; Chudickova et al., 2015; Liu et al., 2011; Locatelli et al., 2003; Parivar et al., 2015; Rezaei et al., 2011; Sanchez-Ramos et al., 2000; Taha & Hedayati, 2010; Tropel et al., 2006). As a result, these studies risk missing any alterations occurring at earlier stages of neural induction. Studies which have investigated the earlier stages of murine MSC neurogenesis have identified morphological changes from six hours post-induction and increases in the expression of neural marker genes *nestin*, *MAP2* and *NF-L* from 24 hours post-induction (Fujimura et al., 2005; Mohammad et al., 2016). However, none of these studies continued their analysis of murine MSC neurogenesis after 34 hours of neural induction. As a result, the current studies do not provide an extensive analysis of neural marker gene expression throughout the entire course of murine MSC neural induction.

This chapter aimed to characterise the timecourse of neural gene expression for human and murine MSC neural induction, to determine the most appropriate culture conditions for use in Chapters Four and Five. An established human neural induction protocol consisting of neural

priming followed by neuronal maturation (Jackson et al., 2015) was used for the neural induction of MSCs isolated from wildtype mice, to determine if the method could be directly transferred between species. Further studies were then undertaken to determine if neural priming was required for neural differentiation of human and murine MSCs. The stages of neurogenesis were tracked by determining changes in the expression of a number of genes which are tightly regulated throughout CNS development (Figure 3.1). This allowed, for the first time, the development of a comprehensive timeline of neural differentiation from human and murine MSCs, enabling easy identification of the optimal protocol for both human and murine MSC neural induction.

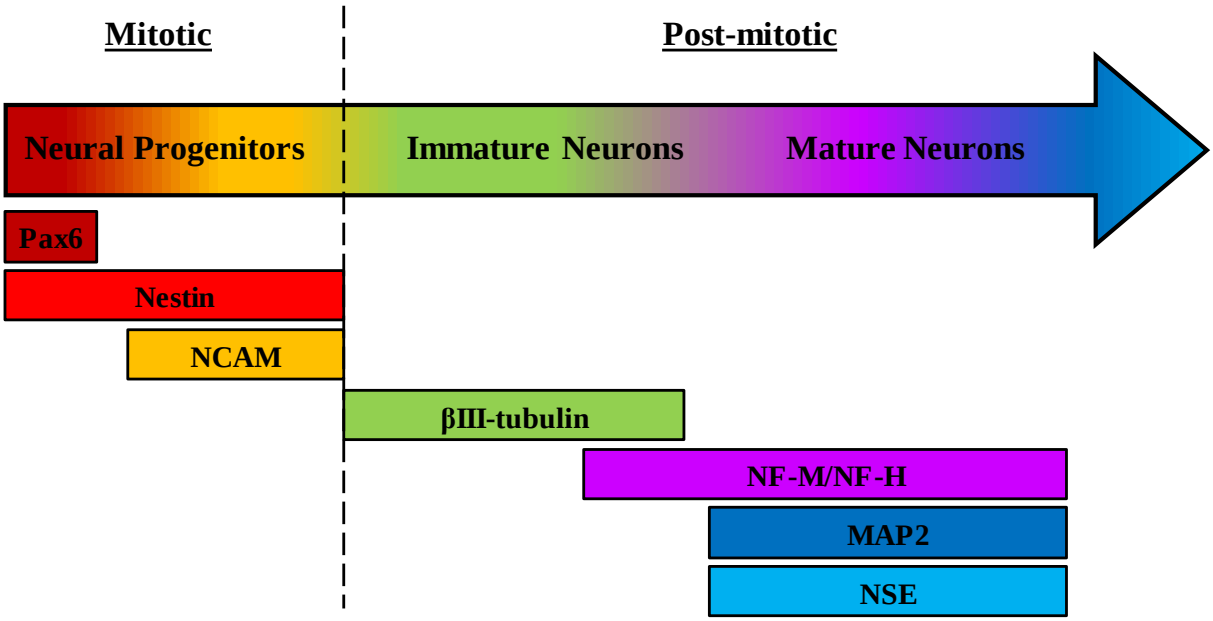

Figure 3.1: The stages of neurogenesis can be identified through the analysis of neural marker gene expression

Neural marker gene expression was used to identify the different stages of neurogenesis. *Pax6*, *nestin* and *NCAM* recognised neural progenitors; *pax6* is a paired homeobox transcription factor expressed in early human NE and RG cells. *Nestin* encodes an intermediate filament protein and is highly expressed in neural progenitors within the CNS (Lendahl et al., 1990; Thakurela et al., 2016; Zhang et al., 2010). *NCAM* promotes neural progenitor proliferation and migration and is considered a marker of late-stage neural progenitors (Guan et al., 2015; Kolkova et al., 2000; Quartu et al., 2008). *βIII-tubulin* is a marker of immature, post-mitotic neurons, as it is known to be expressed in neurons that have recently exited the cell cycle (Lee et al., 1990; Menezes & Luskin, 1994). *MAP2, NF-M, NF-H* and *NSE* are markers of mature neurons. *MAP2, NF-M* and *NF-H* are all associated with cytoskeletal formation whilst *NSE* encodes an enzyme only expressed at the later stages of neurogenesis (Carpenter & Ip, 1996; Harada et al., 2002; Hoffman et al., 1987; Isgro et al., 2015; Zhang et al., 2002).

3.2 Results

3.2.1 Transfer of the human MSC neural induction method to murine MSCs

Human and murine MSCs were differentiated along the neural lineage using the previously established neural priming and maturation method (NP+M) (detailed in section 2.3.2.1) (Arthur et al., 2008; Jackson et al., 2015). The expression of neural marker genes relative to undifferentiated MSCs maintained in MSC basal growth media (basal media controls) was analysed 14 days and 21 days post-neural induction. As expected, human MSCs were successfully induced along the neural lineage. *Nestin*, a marker of neural progenitors, was upregulated with an increase of 4.66 ± 0.53 fold at 14 days post-induction and significantly increased by 9.16 ± 3.17 fold 21 days post-induction. Expression of *βIII-tubulin*, a marker of immature post-mitotic neurons, was unchanged compared to basal media controls. *NF-M*, a marker of late-stage neurogenesis, was upregulated 9.32 ±3.59 fold compared to basal media controls 14 days post-induction respectively, suggesting the presence of post-mitotic neurons; however, this difference did not reach significance. Expression had decreased to only a 2.97 ± 0.68 fold increase compared to basal media controls 21 days post-induction (Figure 3.2A). When transferred to murine MSCs, this protocol was successful in inducing murine MSCs along the neural lineage, as evidenced by upregulation of all tested neural marker genes (Figure 3.2B). *βIII-tubulin* expression was significantly elevated both 14 and 21 days post-induction, with 20.58 ± 4.28 and 30.48 ± 5.16 fold increases respectively. *NF-M* expression was also significantly elevated, with a 17.26 ± 1.75 fold increase 21 days post-induction, indicating the formation of post-mitotic neurons (Figure 3.2B). Thus, in comparison to human MSC neural differentiation, murine MSC neural differentiation appeared to be accelerated, with earlier and significantly higher expression of *βIII-tubulin* and *NF-M*.

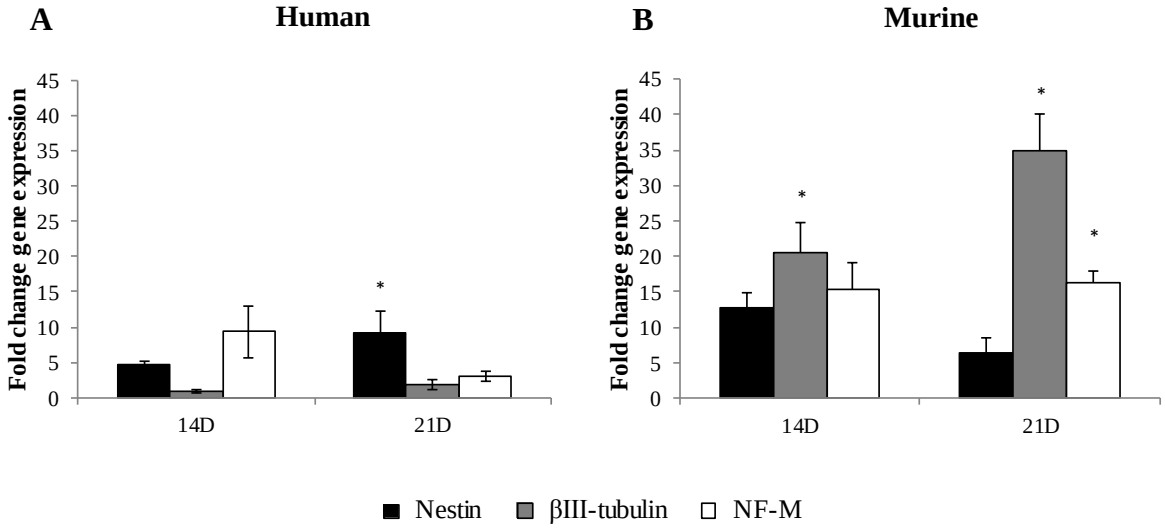

Figure 3.2: Transfer of the human MSC neural induction protocol to murine MSCs

Expression of neural genes in human (A) and murine (B) MSCs grown in NP+M media 14 and 21 days post-neural induction. Gene expression was normalised to cyclophilin A and the fold change relative to MSCs maintained in MSC basal growth media for 24 hours (basal media controls) was calculated using the ΔΔCt method. Results are expressed as mean ± SEM (n=3). * indicates significant difference between neuronal and basal media controls ($p<0.05$; one-way ANOVA, Tukey's HSD).

3.2.2 Timecourse of neural gene expression during human MSC neurogenesis

Our previously established method examined neural marker gene expression 14 and 21 days post-induction; however, gene expression was not examined at any other timepoints, either here or in previous publications using this method (Arthur et al., 2008; Jackson et al., 2015). Therefore, the timecourse of neural gene expression throughout human MSC neural induction was established. To determine if neural priming was required for neural induction, human MSCs were cultured in neural priming media followed by maturation media (NP+M) or in maturation media alone (M). The NP media used EGF and FGF-2 as neurogenic factors, whilst the M only media contained FGF-2 and RA (detailed in section 2.3.2.1).

Both the NP+M and M only methods successfully induced human MSCs along the neural lineage, with significant increases in multiple neural marker genes. The NP+M method significantly increased *nestin* and *NCAM* expression above that of basal media controls from 14 days-post induction, remaining elevated throughout neural induction, indicating the presence of neural progenitors (Figure 3.3A). Both early markers were also elevated when using the M only method; however, expression was lower than that of MSCs cultured using the NP+M method, with significant upregulation of *nestin* and *NCAM* not evident until 16 and 20 days post-induction respectively, indicating a delay in neural progenitor formation (Figure 3.3B). Expression of *pax6*, another early marker of neurogenesis, was unchanged throughout neural induction in both methods (Figure 3.3A and 3.3B). No expression of *NeuroD1*, a marker of early to intermediate neurogenesis, was observed at any time in either method (data not shown).

Both methods successfully formed post-mitotic neurons; increases in *βIII-tubulin* expression were evident from 16 days post-induction, with 8.65 ± 0.59 and 7.58 ± 0.95 fold increases

relative to basal media controls when using the NP+M and M only methods respectively (Figures 3.3C and 3.3D). Increases reached significance on days 16 and 24 of the NP+M method and day 24 of the M only method. *NF-M* was expressed at very low levels during the early stages of neurogenesis using both methods. Expression peaked in cells cultured in the NP+M media at 24 days post-induction, with a 16.26 ± 4.90 fold increase; however, this difference did not reach significance (Figure 3.3C). In contrast, human MSCs cultured using the M only method displayed a clear upregulation of *NF-M*, with a statistically significant 26.97 ± 9.75 fold increase in *NF-M* expression 24 days-post induction. Expression was maintained and peaked at 28 days post-induction, with a significant 41.01 ± 8.34 fold increase in expression compared to basal media controls (Figure 3.3D). Furthermore, *NF-M* expression at 28 days-post-induction was significantly elevated in MSCs cultured in the M only media compared to those cultured in the NP+M media (Figure 3.3C and 3.3D). In both methods, expression of *NF-H*, a marker of mature neurons, was significantly elevated 12 days post-induction; however, expression then dropped before increasing to reach significance once again at 18 days post-induction. *NF-H* was significantly upregulated from 18 days post-induction, with 32.30 ± 3.05 and 34.15 ± 3.57 fold increases at day 18 when using the NP+M and the M only methods respectively. *NF-H* remained elevated for the remainder of the neural induction protocol for both methods; however, gene expression was generally higher in the M only method, with statistically significant increases in *NF-H* compared to those cultured in the NP+M method at 22 and 24 days post-induction (Figure 3.3C and 3.3D). *NSE*, which encodes an enzyme expressed only by mature neurons, was significantly elevated compared to basal media controls media between 16 and 22 days post-induction when using the NP+M method (Figure 3.3C). A similar trend was seen for the M only method; however, *NSE* expression was significantly higher 16 days post-induction for human MSCs cultured in the M only media compared to those in the NP+M media (Figure 3.3C and 3.3D). From 24 days post-induction, *NSE* expression dropped to below significance in both neural induction methods (Figure 3.3C and 3.3D). *MAP2*, another marker of mature neurons, was not expressed over the course of

neural induction for either method (data not shown). Thus, both methods successfully induced human MSCs along the neural lineage, forming neural progenitors and post-mitotic neurons from 14-16 days post-induction. However, the original NP+M method significantly improved the formation of neural progenitors, whilst the M only method enhanced neuronal maturation.

3.2.3 Optimising methodology for neural induction of murine MSCs

3.2.3.1 Initial timecourse of gene expression throughout murine MSC neural induction

A similar timecourse was setup to analyse neural gene expression throughout murine MSC neural induction in NP+M media (detailed in section 2.5.4.3). *Nestin* (Figure 3.4A) and *NF-M* (Figure 3.4B) expression was significantly elevated within 24 hours of transfer into neural priming media, with 2.72 ± 0.12 and 10.52 ± 1.90 fold increases in gene expression respectively. *NF-M* expression remained elevated until five days post-induction, peaking at five days with a 17.53 ± 2.77 fold increase compared to basal media controls (Figure 3.4B). *βIII-tubulin* was elevated from 24 hours post-induction; however, this increase did not reach significance until five days post-induction where a 10.64 ± 3.61 fold increase compared to basal media controls was evident (Figure 3.4B). Expression of neural marker genes was downregulated compared to basal media control expression levels by seven days post-induction; however, secondary elevations in some genes were seen following the addition of the maturation media. *Nestin* and *NF-M* were both significantly elevated eight days post-induction, with *NF-M* expression also significantly upregulated at 12 days post-induction (Figure 3.4A and 3.4B). *Nestin* and *NF-M* expression returned to basal media control expression levels for the remainder of the protocol. No significant increase in *NCAM*, *MAP2* or *NSE* expression was evident over the course of neural induction (Figure 3.4A and 3.4B). This data confirmed the previous conclusion (section 3.2.1) that murine MSC neural induction was accelerated compared to human, with significant increases in neural gene expression within 24 hours of neural induction.

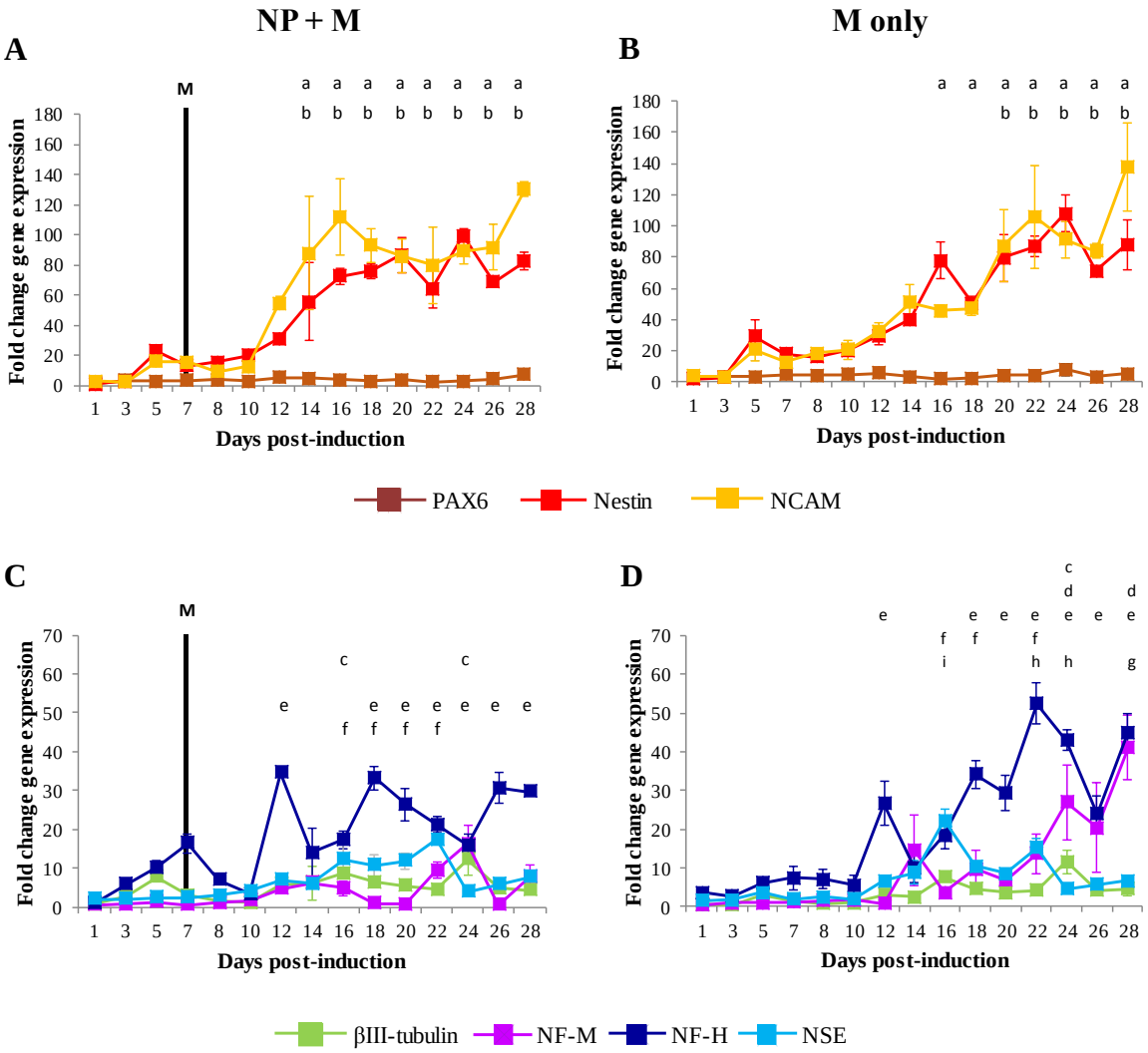

Figure 3.3: Timecourse of neural gene expression throughout human MSC neurogenesis

Expression of early (A, B) and late (C,D) neural marker genes in human MSCs grown in NP+M (A, C) and M only (B, D) media. Gene expression was normalised to cyclophilin A and the fold change relative to MSCs maintained in human MSC basal growth media for 24 hours (basal media controls) was calculated using the ΔΔCt method. Black line denotes transfer from NP media to M media (M). Results are expressed as mean ± SEM (n=3). Letters a-f indicate significant difference between neuronal and basal media controls: a = *nestin*, b = *NCAM*, c = *βIII-tubulin*, d = *NF-M*, e = *HF-H*, f = *NSE*. Letters g-i indicate significant difference between NP+M media and M only media at the same timepoint: g = *NF-M*, h = *NF-H*, i = *NSE* ($p<0.05$; one-way ANOVA, Tukey's HSD).

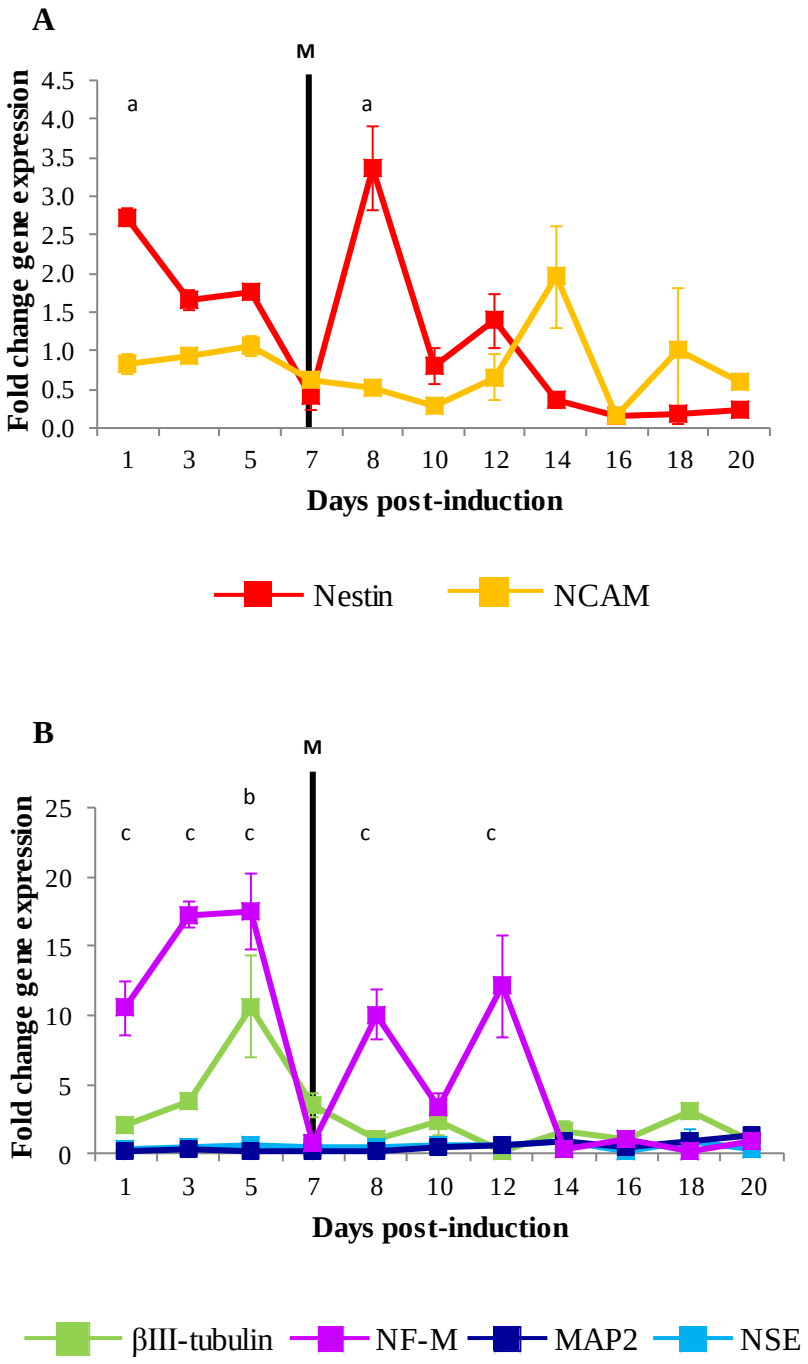

Figure 3.4 Timecourse of neural gene expression throughout murine MSC neurogenesis in NP+M media

Expression of early (A) and late (B) neural marker genes in murine MSCs grown in NP+M media. Gene expression was normalised to cyclophilin A and the fold change relative to MSCs maintained in murine MSC basal growth media for 24 hours (basal media controls) was calculated using the ΔΔCt method. Black line denotes transfer from NP media to M media (M). Results are expressed as mean ± SEM (n=3). Letters indicate significant difference between neuronal and basal media controls: a = *nestin*, b = *βIII-tubulin*, c = *NF-M* ($p<0.05$; one-way ANOVA, Tukey's HSD).

3.2.3.2 Timecourse of gene expression throughout the first 48 hours of murine MSC neural induction

To further investigate the accelerated nature of murine MSC neurogenesis, a timecourse of gene expression over the first 48 hours of neural induction was undertaken. Murine MSCs were cultured in either the NP media, with the maturation step excluded due to the reduced timeframe, or the M only media, to determine the optimum method for murine MSC neural induction. Morphological changes were evident within four hours of neural induction when using both the NP only (Figure 3.5B) and M only methods (Figure 3.5C) compared to basal media controls (Figure 3.5A). However, further changes in morphology manifested earlier in the NP only method, with cell elongation evident 12 hours post-induction (Figure 3.5D). Similar morphology was not seen in the M only method until 16 hours post-induction (Figure 3.5G). No morphological changes were evident in basal media controls over the first 24 hours of neural induction (Figure 3.5A and 3.5H).

Early markers *nestin* and *NCAM* were expressed in murine MSCs induced along the neural lineage using both induction methods; however, expression was never significantly elevated above basal media controls (Figure 3.6A and 3.6B). *βIII-tubulin* expression was increased when using the NP only method from four hours post-induction and remained elevated over the 48 hour protocol, with expression fluctuating between 1.73 ± 0.29 and 2.87 ± 0.47 fold higher than basal media controls (Figure 3.6C), indicating the formation of immature, post-mitotic neurons. In contrast, *βIII-tubulin* expression was never elevated above basal media controls when using the M only method; indeed, *βIII-tubulin* was significantly lower in murine MSCs cultured in the M only media than those in the NP only media at multiple timepoints over the 48 hour protocol (Figure 3.6C and 3.6D). *NF-M* expression was significantly higher than basal media controls from eight hours post-induction when using the NP only method, indicating the presence of a more mature neuron population (Figure 3.6C).

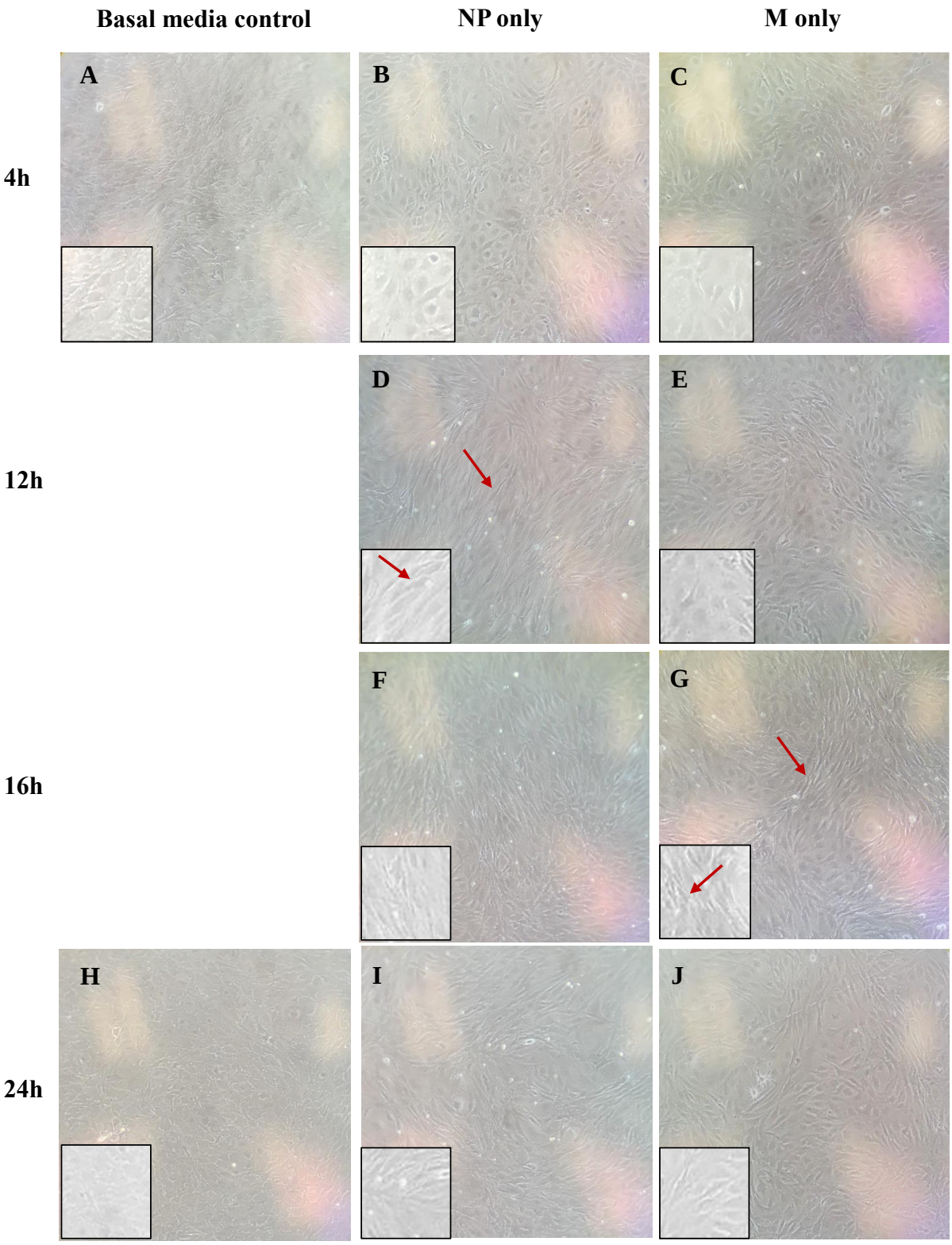

Figure 3.5 Murine MSC morphology throughout neural induction

Images of murine MSCs maintained in murine MSC basal growth media (basal media controls) (A, H), NP media (B, D, F, I) and M only media (C, E, G, J) over the course of neural induction. Red arrows indicate an elongated cell. Boxed insert shows an enlarged region. Images taken on an iPhone 7.0 at 10x magnification.

In contrast, *NF-M* expression was never significantly elevated above basal media controls when using the M only method; expression was also significantly lower than that of murine MSCs cultured in the NP only media (Figure 3.6C and 3.6D). Overall, increased neural gene expression was evident within four hours of neural induction when using the NP only method, with neurons formed within eight hours. In comparison, whilst the M only method induced neurogenesis, it was decreased and delayed in comparison to the NP only method.

3.3 Discussion

MSCs were first identified to have neurogenic properties *in vitro* by Woodbury et al. (2000) and Sanchez-Ramos et al. (2000), with human, rat and mouse MSCs able to differentiate into neurons in the presence of β-mercaptoethanol or EGF and BDNF respectively. Brazelton et al. (2000) were the first to demonstrate the neural plasticity of MSCs *in vivo*, with bone-marrow derived cells expressing neural markers visible in the brains of mice administered intravenously with MSCs. The neural properties of MSCs are believed to originate from their basal expression of several neural marker genes; a previous study found MSCs cultured in basal growth media expressed multiple neural markers, with 100% of cells expressing *nestin*, 12% expressing *βIII-tubulin* and 13.2% expressing *NF-M (*Deng et al., 2006). Low levels of *NSE*, *NeuN*, *MAP2* and *GFAP* expression have also been identified in undifferentiated MSCs (Sanchez-Ramos et al., 2000; Tondreau et al., 2004; Woodbury et al., 2000). These basal expression levels have been hypothesised to prime MSCs for neural differentiation, with expression subsequently significantly upregulated following transfer into neural induction conditions. Due to these neurogenic properties, MSCs have been identified as an ideal candidate for modelling disease neurogenesis *in vitro*. In comparison to ESCs, iPSCs and NSCs, MSCs are easily accessible and require only basic culture conditions. MSCs can be isolated from a wide range of species, including both humans and mice. Whilst human MSCs

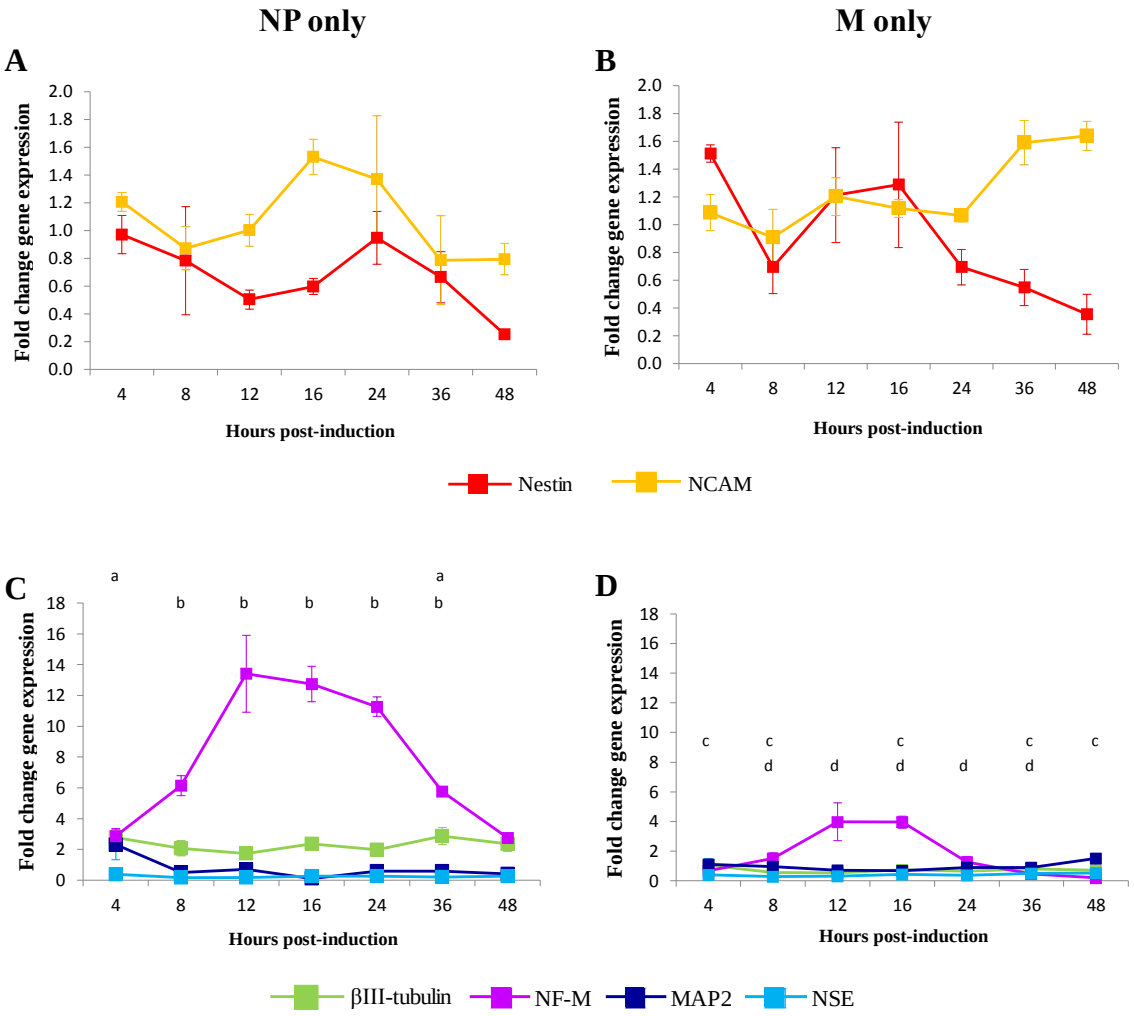

Figure 3.6: Timecourse of neural gene expression throughout the early stages of murine MSC neurogenesis

Expression of early (A, B) and late (C,D) neural marker genes in murine MSCs grown in NP only (A, C) and M only (B, D) media. Gene expression was normalised to cyclophilin A and the fold change relative to MSCs maintained in murine MSC basal growth media for four hours (basal media controls) was calculated using the ΔΔCt method. Results are expressed as mean ± SEM (n=3). Letters a-b indicate significant difference between neuronal and basal media controls: a = *βIII-tubulin*, b = *NF-M* ($p<0.05$; one-way ANOVA, Tukey's HSD). Letters c-d indicate significant difference between NP+M and M only medias at same timepoint: c = *βIII-tubulin*, d = *NF-M* ($p<0.05$; one-way ANOVA, Tukey's HSD.

are preferred when modelling human neurogenesis *in vitro*, murine disease models provide an ideal source of MSCs when they are unavailable from patients.

3.3.1 Human MSC neural induction

This study used well-established neurogenic factors for MSC neural induction, namely EGF, FGF-2 and RA. EGF is commonly used for early stages of *in vitro* neurogenesis, due to its role as a promoter of proliferation and differentiation during development, inducing neural progenitor proliferation and promoting neural crest cell neurogenesis *in vitro* (Garcez et al., 2009; Reynolds et al., 1992). FGF-2 is an established and well-studied neurogenic factor, and is commonly used for neural induction of multiple cells types (Arthur et al., 2008; Chudickova et al., 2015; Locatelli et al., 2003; Palmer et al., 1999; Shi et al., 2012a). During development, high levels are present from the initiation of neurulation, with its temporo-spatial expression in the developing CNS corresponding with neurogenesis in specific brain regions (Murphy et al., 1994; Powell et al., 1991). Despite the vital roles of EGF and FGF-2 in early neural development, this study found that priming with these growth factors was not required for promoting neurogenesis in human MSCs, with significant increases in the expression of *nestin* and *NSE*, markers of neural progenitors and mature neurons respectively, occurring concurrently 16 days post-induction when using the M only method. However, neural priming appeared to increase the neural progenitor population, evidenced by significant increases in the expression of early neural marker genes *nestin* and *NCAM* from 14 days post-induction when using the NP+M method. In contrast, significant increases in *nestin* and *NCAM* expression were not seen until 16 and 20 days post-induction, respectively, when using the M only method. This is in line with previous data which found that EGF and FGF-2 promoted the expansion of human neural progenitors (Vescovi et al., 1999).

Whilst RA is often associated with neuronal maturation, RA is also implicated in early neurogenesis (Jackson et al., 2015; Jones-Villeneuve et al., 1982; Okada et al., 2004; Tan et al., 2015). A reduction in RG proliferation and decreased formation of intermediate neural progenitors is evident in RA-deficient mice (Haushalter et al., 2017). Similarly, RA depletion resulted in a decrease of newborn neural progenitors in the early stages of adult neurogenesis (Jacobs et al., 2006). It is subsequently unsurprising that M only conditions successfully induced neurogenesis and generated neural progenitors. However, it should be noted that neuronal maturation appeared to be favoured when using the M only method, with *NF-M*, *NF-H* and *NSE* expression significantly upregulated in MSCs cultured in the M only method compared to those in the NP+M media. It is therefore likely that whilst the M only conditions are amenable to neural progenitor formation, differentiation to neurons is promoted. This appeared to deplete the early neural progenitor population. The neural progenitor population appeared to recover when using the M only method over the timecourse, with early neural marker gene expression reaching the levels seen when using the NP+M method by day 20 of the protocol.

3.3.1.1 Human MSC-derived neurons are unable to survive in long-term culture conditions

Whilst both the NP+M and M only methods successfully induced neurogenesis in human MSCs, neither method allowed for long-term survival *in vitro*. The significant decreases in *βIII-tubulin* and *NF-M* from 26 days post-induction in the NP+M method suggested cytoskeletal alterations, which have previously been associated with increased neuronal death (Bursch et al., 2000; Hoffman, 1989; reviewed in McMurray, 2000; Nixon & Logvinenko, 1986; Paris et al., 2010). Intermediate filaments (IF) are formed by tetrapolymers containing, amongst others, a combination of NF-L, NF-M and NF-H. IF formation does not require all neurofilament subunits; for example, NF-L and NF-H are able to form IFs in the absence of

NF-M (Beaulieu et al., 1999; Carpenter & Ip, 1996; Carter et al., 1998). The maintained expression of *NF-H* indicates that IFs are still present during neural induction; however, when coupled with the decreased expression of *NF-M* at 26 days post-induction, it is likely the number decreases in the later stages of the protocol. Furthermore, IFs function best when composed of all three neurofilament subunits; it is likely that these cytoskeletal alterations resulting from downregulated *NF-M* have an adverse effect on neuron function (Carpenter & Ip, 1996). This hypothesis is supported by the decreased expression of *NSE* in the NP+M method, as *NSE* is only expressed by functional mature neurons. In the M only method, *NF-M* expression remains elevated, indicating that neurofilament production is unaffected; however the decreases in *βIII-tubulin* and *NSE* suggest a decreased survival of neurons. Therefore, it is likely that neuron survival is higher in the M only conditions; however, neither method is conducive to long-term survival of human MSC-derived neurons *in vitro*. In contrast, the continued expression of *nestin* and *NCAM* throughout neural induction indicated that neural progenitor survival was unaffected by long-term culture in either the NP+M or M only conditions.

3.3.2 Murine MSC neural induction

3.3.2.1 Murine MSC neurogenesis is accelerated compared to human MSCs

Transfer of the human MSC neural induction protocol to murine MSCs quickly demonstrated the accelerated nature of murine MSC neurogenesis compared to human. Initial investigations determined that neural gene expression was elevated 24 hours post-induction, in line with previous studies (Fujimura et al., 2005; Mohammad et al., 2016; Safford et al., 2002). Further analysis determined that the NP protocol resulted in upregulation of *βIII-tubulin* four hours post-induction, indicating the formation of immature neurons. Upregulation of *NF-M* eight hours post-induction indicated that neuronal maturation had commenced. Therefore, the first 48 hours of neural induction were identified as the critical period for murine MSC

neurogenesis; in contrast, increases in neural markers were not evident until 14 days post-induction in human MSCs. The rapid neural induction of murine MSCs compared to human MSCs *in vitro* mirrored the shorter developmental timeframe of mice *in utero*. The murine gestational period is on average 21 days, in contrast to 280 days for humans; cortical neurogenesis is similarly accelerated, being a 6 day process in mice compared to 100 days in humans (Caviness et al., 1995; Takahashi et al., 1996). Similarly to MSCs, other stem cell types display accelerated neurogenesis in murine-derived cells compared to human. Mouse ESC neural differentiation protocols are generally between 6 days and 18 days in length (Bain et al., 1995; Chen et al., 2013; Fraichard et al., 1995; Jing et al., 2011; Kim et al., 2009; Mohamad et al., 2013; Strubing et al., 1995), whereas human methods can take anywhere from 28 days to 82 days (Espuny-Camacho et al., 2013; Gaspard et al., 2008; Li et al., 2009; Shi et al., 2012b). Likewise, iPSC neural induction timeframes are extended for human-derived cells, with murine-derived iPSC neural induction protocols commonly requiring two weeks (Chen et al., 2013; Mohamad et al., 2013), in comparison to human-derived iPSC neural induction protocols which can be as long as 90 days (Gunhanlar et al., 2018; Shi et al., 2012a; Shi et al., 2012b). Thus, the accelerated nature of murine MSC neural induction is likely a result of the shorter developmental timeframe of mice compared to humans.

3.3.2.2 Previous murine MSC neural induction protocols and timeframes

Previous studies have noted the accelerated nature of murine MSC neural induction; Fujimura et al. (2005) found an increase in nestin positive cells six hours post-induction, with MAP2 and NF-L staining increased 24 hours post-induction. However, the method of induction used in this study varied greatly from our protocols, with neurogenesis promoted through culture with insulin, indomethacin and IBMX. These factors are commonly used to induce neurogenesis *in vitro*; insulin and insulin-like growth factors are highly involved in neurogenesis *in vivo*, being tightly regulated throughout neural development, whilst

indomethacin is a known anti-inflammatory, preventing the formation of microglia whilst promoting the formation of neurons (Lopes et al., 2016; McGuiness et al., 2017; Pimentel et al., 1996). IBMX is commonly used to elevate cAMP levels, resulting in activation of the proteinase K pathway, which is known to be integral for MSC neurogenesis (Deng et al., 2001; Kim et al., 2002; Mayr & Montminy, 2001; Wang et al., 2007). However, the use of chemical factors for *in vitro* neural induction is disputed, due to the cellular stress and toxicity created by their use (Lu et al., 2004; Neuhuber et al., 2004; Tropel et al., 2006). Mohammad et al. (2016) similarly noted increased *nestin* expression six hours post-induction, with increases in expression of *NF-L* from 12 hours post-induction and *MAP2* 24 hours post-induction. However, neurogenesis was induced using β-mercaptoethanol; it has been suggested that neuron-like morphological changes and increases in neural gene expression in the presence of β-mercaptoethanol are likely to be the result of cellular stress and toxicity, with cellular shrinkage and cytoskeleton changes responsible as opposed to neural differentiation (Lu et al., 2004).

Other studies have used methods for murine MSC neural induction which more closely mirror our own, which attempt to replicate the brain microenvironment to induce neurogenesis; however, none have examined the early stages of neurogenesis. In our protocol, EGF and FGF-2 successfully induced murine MSCs along the neural lineage. Locatelli et al. (2003) previously found that *nestin* and *βIII-tubulin* expression was upregulated 7 days post-induction with EGF and FGF-2, followed by upregulation of *βIII-tubulin, NF-L* and *NSE* expression 14 days post-induction. Similar results were seen in studies by Liu et al. (2011) and Rezaei et al. (2011) in response to EGF and FGF-2. FGF-2 has also been used alone to induce neurogenesis, with increases in neural gene expression evident from four days post-induction (Parivar et al., 2015; Tropel et al., 2006). RA was the major component of our M only media and has previously been used in conjunction with foetal midbrain cells and brain-

derived neurotrophic factor (BDNF) to induce murine MSC neurogenesis, with an increase in NeuN positively stained cells seen seven days post-induction (Sanchez-Ramos et al., 2000). Culture conditions such as these which replicate the brain microenvironment are generally considered superior to those reliant on a response to chemicals (discussed previously). In line with previous studies of chemical-induced neurogenesis, Deng et al. (2006) found that neuron-like morphology following culture with IBMX *in vitro* was likely to be a response to cellular stress, as no increase in neural marker genes was evident. In contrast, MSCs implanted into the brain responded to environmental cues, differentiating into neurons and astrocytes. Therefore, this chapter presents the first study in which neural gene expression is examined within the first 24 hours of murine MSC neural induction, where neurogenesis was incited by replicating the brain environment *in vitro*.

3.3.2.3 The NP method increases neural gene expression above that of the M only method

A direct comparison between the NP and M only methods determined that murine MSC neuronal maturation was not dependent on RA; indeed, whilst both methods were able to increase the expression of neural marker genes, these increases only reached significance in murine MSCs cultured in under NP conditions. Furthermore, mature neural marker gene expression was consistently significantly higher in murine MSCs cultured in NP media than those cultured in M only media. The presence of EGF and RA were the primary differences between the NP and M only methods, with EGF included in the NP media and RA in the M only media; FGF-2 was present in both. EGF has previously been found to be effective in forming mature neurons in murine-derived cells and acts by binding to the EGF receptor, activating pathways capable of upregulating neural genes (Kelly et al., 2005; Reynolds et al., 1992). Furthermore, the combination of EGF and FGF-2 successfully promotes neural differentiation of ESCs, with combination culture increasing the proportion of neurons

compared to their singular use (Garcez et al., 2009). RA regulates neurogenesis by binding to a transcription complex heterodimer in the nucleus, comprising of the retinoic acid receptor (RAR) and retinoic X receptor (RXR), which then binds to the retinoic acid response elements (RARE) DNA sequence. This enables the upregulation of a number of target genes, many of which promote neurogenesis (reviwed in Maden, 2007). Whilst RA is commonly implicated in both the early and later stages of neurogenesis both *in vitro* and *in vivo* (section 3.3.1), a previous study by Haushalter et al. (2017) noted that radial glial progenitor maturation occurred earlier in a mouse model displaying an RA deficiency, with increased *βIII-tubulin* expression, compared to wildtype mice. The combination of EGF and FGF-2, in addition to the absence of RA, are likely contributing to the increased neural gene expression in the NP method.

3.3.3 Chapter conclusions and future directions

This chapter aimed to determine the optimal culture conditions for the neural induction of human and murine MSCs, for use in Chapters Four and Five. In human MSCs, the original NP+M method previously used by our lab (Jackson et al., 2015) was found to be ideal, promoting neural progenitor formation and self-renewal in addition to differentiation to neurons. This contrasted with the M only method, which appeared to favour progenitor differentiation to neurons, potentially depleting the early neural progenitor pool. A method capable of forming distinct neural progenitor and neuron populations is advantageous; if used to model disease neurogenesis, changes in either cell population can then be easily identified. Our previous timepoints (Jackson et al., 2015) of 14 and 21 days post-induction appeared to be appropriate for monitoring the progress of neurogenesis, with the first upregulation of neural marker genes seen 14 days post-induction and downregulation of mature markers evident at 24 days post-induction, indicating a loss in neuron survival from this time.

The NP method appeared to be optimal for murine MSC neural induction, promoting a significant increase in neural marker gene expression above both growth controls and MSCs cultured under M only conditions. Furthermore, due to the accelerated nature of murine MSC neurogenesis compared to human MSCs, the first 48 hours were determined to be the most vital. The NP only conditions were found to be sufficient for neuronal maturation of murine MSCs, with no requirement for further culture in M only media.

This study supports previous findings that both human and murine MSCs are capable of neural differentiation and are therefore appropriate for modelling neurogenesis *in vitro*. This study has been the first to develop a timecourse of neural gene expression throughout MSC neurogenesis for both human and murine-derived cells; notably, this is the first study to examine gene expression in murine MSCs over the first 48 hours of neural induction. Both human and murine-derived MSCs have their own advantages. MSCs of human origin are likely to more closely model the human disease phenotype, which is of especial benefit when considering MSCs as a potential therapy. However, the easy availability of MSCs from murine models of neurological disorders provides a distinct advantage when modelling disease neurogenesis *in vitro*. Furthermore, the accelerated nature of murine MSC neurogenesis enables succinct experiments in comparison to human MSCs. Therefore, depending on the application, both human and murine MSCs can be used to great effect for *in vitro* modelling of neurogenesis.

Chapter Four: The effect of extrinsic Mucopolysaccharidosis type IIIA glycosaminoglycans on mesenchymal stem cell differentiation

4.1 Introduction

In addition to intracellular accumulation of HS, MPS IIIA is also characterised by increased extracellular HS, with elevated levels in circulation, excreted in urine and within the ECM (Holley et al., 2011; Meikle et al., 2004; Neufeld & Muenzer, 2001; Tomatsu et al., 2005). HS is hypothesised to be released from cells by several mechanisms, including exocytosis, microglial phagocytosis and apoptosis (Fedele, 2015; Huang et al., 1997; Martins et al., 2015; McGlynn et al., 2004; Wada et al., 2000). In contrast to normal HS, the HS released in MPS IIIA exists as partially degraded fragments and display significant increases in sulphation (Wilkinson et al., 2012). Extracellular HS is required for many signalling pathways involved in development, including the FGF, Wnt, Hh and TGFβ pathways. HS acts to modulate interactions between the morphogen and its receptor, or to increase ligand concentration at the cell surface (section 1.3.1) (Baeg et al., 2001; Chang et al., 2000; Hacker et al., 1997; Lin et al., 1999; Pfeiffer et al., 2002). The ability of HS to bind to morphogens and initiate signal transduction is determined by the patterns of sulphation across the length of the chain (reviewed in Hacker et al., 2005). Thus, the GAGs found in MPS IIIA are likely to affect HS-dependant signalling pathways; indeed, mutations in HSPG synthesis have been shown to reduce FGF signal transduction and downregulate Wnt signalling (Hacker et al., 1997; Venero Galanternik et al., 2015). Due to their vital role in development, changes in HS-dependent signalling pathways are likely to have downstream effects on stem cell differentiation, which could provide a potential mechanism of pathology for MPS IIIA.

In this chapter, the effect of MPS IIIA GAG on stem cell differentiation was examined for the first time. MSCs from healthy human donors were induced along the neural lineage using the NP+M method established in Chapter Three, in the presence of MPS IIIA GAG and commercially available HS, to compare the effects of these different structures on neurogenesis. The effect of commercially available DS and heparin, and MPS I, MPS II and

MPS VI GAGs on neurogenesis was also examined, to determine if any changes in neurogenesis as a result of MPS IIIA GAG were unique. In addition, MSCs were induced along the traditional mesodermal lineages (Friedenstein et al., 1974; Pittenger et al., 1999), to determine if MPS IIIA GAG resulted in any other alterations in stem cell development.

4.2 Results

4.2.1 The effect of extrinsic MPS IIIA GAG on neurogenesis

In accordance with the human MSC neural differentiation method established in Chapter Three, MSCs isolated from healthy human donors were initially induced along the neural lineage in the absence of GAG (0 GAG controls). As expected, the data was in line with the results presented in Chapter Three, with significant elevations in the expression of several neural marker genes 14 and 21 days post-induction (data not shown). All neural gene expression presented in this chapter will be determined relative to this 0 GAG control data.

To determine their effect on neurogenesis, commercially available HS and heparin were added to the culture media throughout the course of neural induction. Commercial HS increased the expression of several neural marker genes, with 3.66 ± 1.54, 2.22 ±0.72 and 3.06 ±0.46 fold increases in *nestin, NCAM* and *βIII-tubulin,* respectively, 14 days post-induction, indicating an increase in the formation of neural progenitors and immature post-mitotic neurons (Figure 4.1A). By 21 days post-induction, all gene expression had returned to baseline levels (Figure 4.1C). The addition of heparin also upregulated neural gene expression, with significant increases of 7.08 ± 0.85, 3.58 ±0.40 and 2.90 ± 0.29 in *nestin, NCAM* and *βIII-tubulin* respectively at 14 days post-induction (Figure 4.1A). Heparin also increased expression of *NSE,* a marker of mature neurons, 3.48 ± 1.13 fold 21 days post-induction; however, this did not reach significance (Figure 4.1C). In contrast to the

commercially available GAGs, the addition of MPS IIIA GAG had little effect on neurogenesis 14 days post-induction, with no significant change in gene expression (Figure 4.1A). However, at 21 days post-induction, *NCAM* and *βIII-tubulin* expression was significantly downregulated, indicating a decrease in neural progenitors and immature neurons (Figure 4.1C). Thus, HS was able to promote the early stages of neurogenesis, with the more highly sulphated heparin (Kjellen & Lindahl, 1991) promoting both the early and late stages of neurogenesis; in contrast, HS-containing MPS IIIA GAG was found to disrupt neurogenesis.

Other neuropathic forms of MPS store DS in addition to HS. Thus, as a comparison to MPS IIIA HS-containing GAGs, GAGs from MPS I and MPS II were added to the culture media to determine their effects on neurogenesis. As a comparison, GAG from MPS VI, a DS/CS-storing non-neuropathic form of MPS, was also added to the neural induction media, in addition to commercially available DS. In contrast to commercial HS and heparin, commercial DS had little effect on neurogenesis, with no change in neural marker gene expression 14-days post-induction (Figure 4.1B). A small but significant increase of 1.73 ± 0.13 fold in *βIII-tubulin* expression was evident 21 days post-induction (Figure 4.1D). MPS I GAG, containing aberrant HS and DS, had little effect on neurogenesis, aside from a 1.87 ± 0.22 fold decrease in *NCAM* expression 21 days post-induction (Figure 4.1D). In contrast, MPS II GAG mirrored the results seen for MPS IIIA GAG, with significant reductions of 4.13 ± 0.85 and 5.0 ± 1.36 fold in *NCAM* and *βIII-tubulin* expression, respectively, 21 days post-induction, despite storing the same GAGs as MPS I (Figure 4.1D). GAG from MPS VI, a DS/CS-storing MPS type, was found to promote early neurogenesis; *nestin* and *NCAM* expression was significantly increased 14 days post-induction, with a small but significant increase in *nestin* expression remaining 21 days post-induction (Figure 4.1B and D). Therefore, of the HS-storing MPS types, MPS II GAG was found to disrupt neurogenesis in a

similar manner to MPS IIIA GAG, whilst MPS I had little effect. In contrast, MPS VI GAG promoted the early stages of neurogenesis.

4.2.2 The effect of extrinsic MPS IIIA GAG on traditional MSC lineages

The primary focus of this study was to determine the effect of MPS IIIA GAG on neurogenesis, due to the severe neurological pathology of MPS IIIA. However, the effects of MPS IIIA GAG on MSC differentiation along traditional mesodermal lineages was also of interest. Skeletal pathology is less pronounced in MPS IIIA compared to many other MPS types; however, mild pathology has been reported in a number of MPS IIIA patients (Chen et al., 1996; de Ruijter et al., 2013b; Neufeld & Muenzer, 2001; Nur et al., 2016; Rigante & Caradonna, 2004; Scaramuzzo et al., 2012; White et al., 2011). No studies have examined the molecular mechanisms underlying this pathology in MPS IIIA. By examining the effects of MPS IIIA GAG on MSC differentiation along other lineages, we can determine if MPS IIIA GAG directly impairs neurogenesis, as opposed to a global inhibition of MSC differentiation.

4.2.2.1 Osteogenesis

MSCs isolated from healthy human donors were successfully differentiated along the osteogenic lineage in the absence of GAG (0 GAG controls), as demonstrated by calcium levels of 4.60 ± 0.85µg/µg protein one week post-induction compared to 0.53 ± 0.06µg/µg protein in undifferentiated MSCs maintained in human MSC basal growth media (basal media controls) (Figure 4.2). Calcium content continued to increase in 0 GAG controls over the four weeks of osteogenic induction, with 12.48 ± 0.91 µg/µg protein four weeks post-induction (Figure 4.2). Positive von Kossa staining was evident within one week of osteogenic induction, indicating an increase in mineral formation (Figure 4.3). The addition of

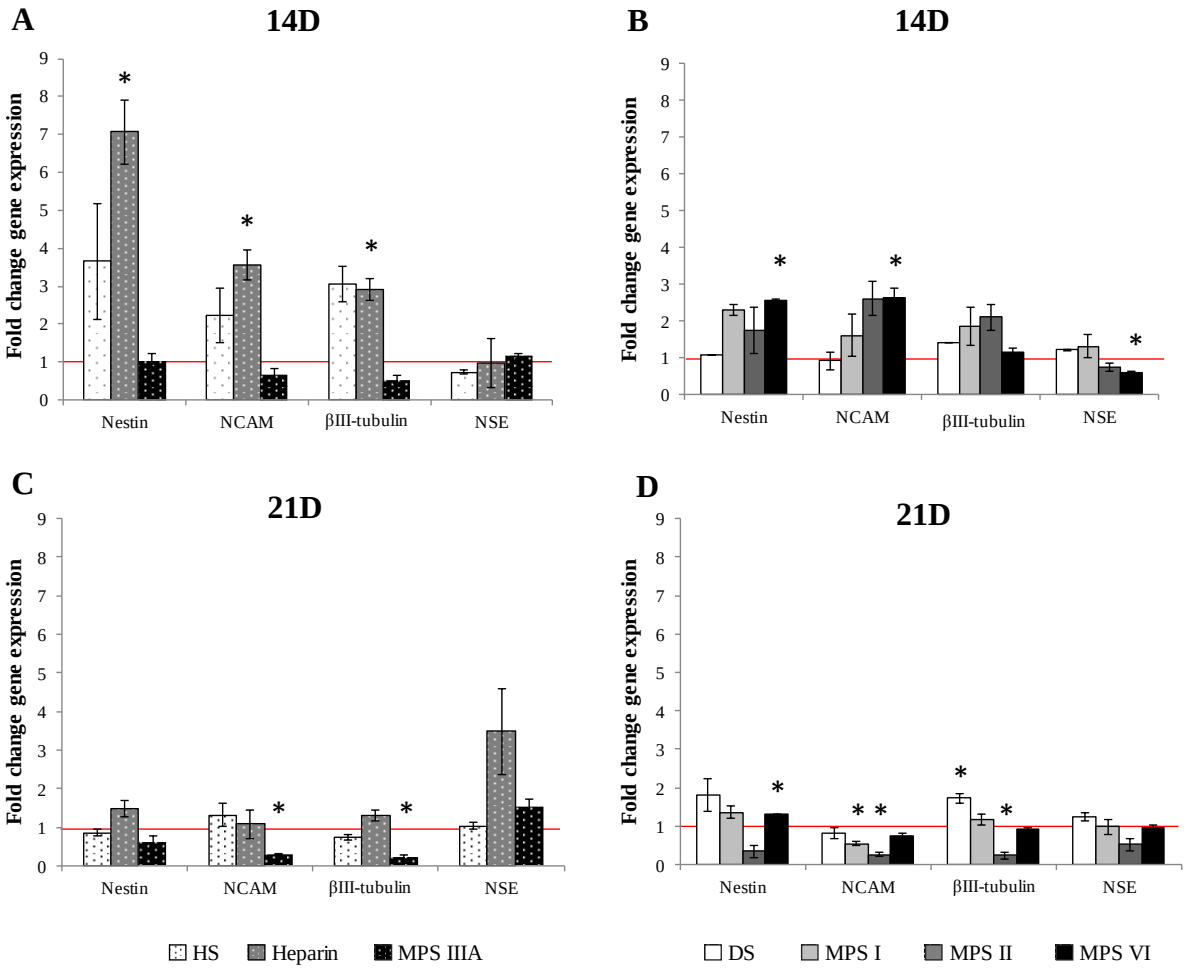

Figure 4.1: The effect of commercially available and MPS GAGs on neurogenesis of human MSCs

Expression of neural genes in the presence of commercially available and MPS GAGs 14 (A-B) and 21 (C-D) days post-neural induction. Gene expression was normalised to cyclophilin A and the fold change relative to MSCs induced along the neural lineage in the absence of GAG (0 GAG controls) was calculated using the ΔΔCt method. Red line denotes baseline 0 GAG gene expression. Results are expressed as mean ± SEM (n=3). * indicates significant difference compared to 0 GAG controls ($p<0.05$; one sample t-test).

commercial HS had little effect on the early stages of osteogenesis, with calcium levels in line with 0 GAG controls. Further mineralisation appeared to be delayed in the presence of HS, with calcium content at 4.65 ± 0.80 µg/µg protein three weeks post-induction, significantly lower than 0 GAG controls (Figure 4.2). However, calcium content remained increased compared to basal media controls (0.99 ± 0.38µg/µg protein) and von Kossa staining continued to be evident (Figure 4.2 and 4.3). Calcium content reached 0 GAG control levels in the presence of HS by four weeks post-induction (Figure 4.2). Commercial heparin had little effect on osteogenesis, aside from a small decrease in calcium content one week post-induction in comparison to 0 GAG controls; however, this difference did not reach significance (Figure 4.2). Positive von Kossa staining was evident throughout osteogenesis in the presence of commercial heparin (Figure 4.3).

In contrast to the commercially available GAGs, the addition of MPS IIIA GAG to the osteogenic media reduced osteogenesis, with calcium levels of only 0.78 ± 0.25µg/µg protein and 0.54 ± 0.17µg/µg protein one and two weeks post-induction respectively. In contrast, 0 GAG controls had calcium levels of 4.60 ± 0.85µg/µg protein and 5.06 ± 0.99µg/µg protein respectively (Figure 4.2). Calcium levels remained low in the presence of MPS IIIA GAG for the remainder of osteogenesis, with significant reductions in calcium compared to 0 GAG controls three and four weeks post-induction (Figure 4.2). Furthermore, von Kossa staining was not visible in the presence of MPS IIIA GAG (Figure 4.3), thereby indicating that, in contrast to commercial HS and heparin, MPS IIIA GAG inhibited osteogenesis.

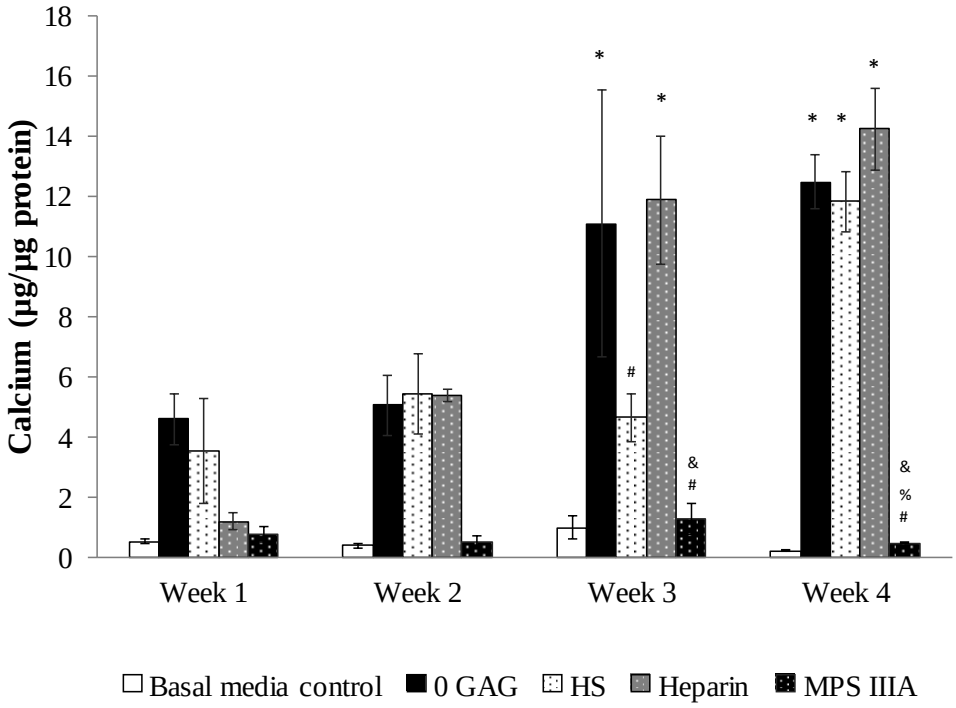

Figure 4.2: The effect of commercially available and MPS GAGs on osteogenesis of human MSCs

Calcium content in human MSCs induced along the osteogenic lineage for four weeks in the presence of HS, heparin and MPS IIIA GAG. Results are expressed as mean ± SEM (n=3). * indicates significant difference compared to basal media control at same timepoint; # indicates significant difference compared to 0 GAG control at same timepoint; % indicates significant difference compared to HS at the same timepoint; & indicates significant difference compared to heparin at the same timepoint ($p<0.05$; one-way ANOVA, Tukey's HSD).

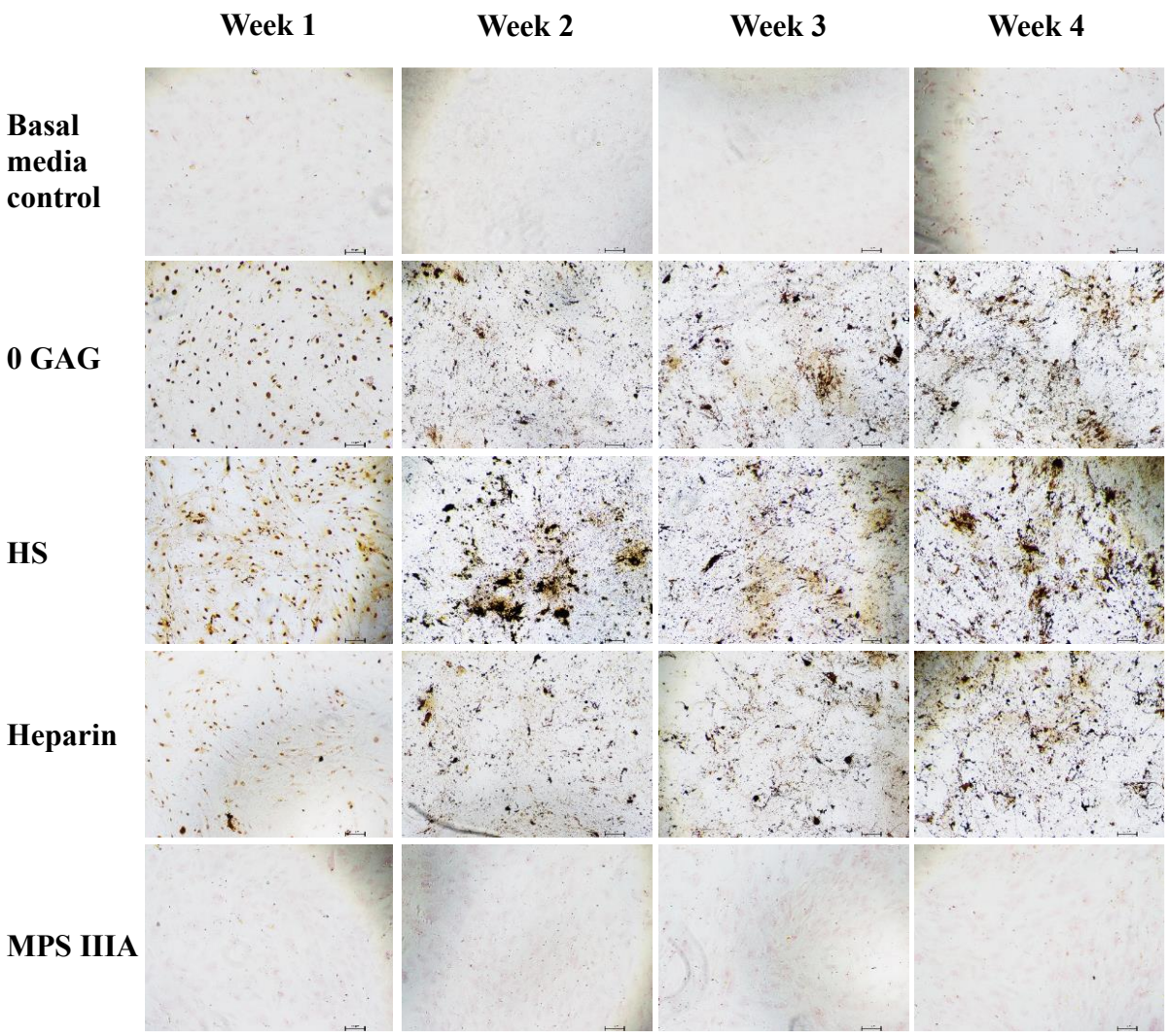

Figure 4.3: von Kossa staining for human MSC osteogenesis

von Kossa staining in human MSCs induced along the osteogenic lineage for four weeks in the presence of HS, heparin and MPS IIIA GAG. Images taken on a Nikon Eclipse TS2 at 10x magnification. Scale bar represents 100µm.

4.2.2.2 Chondrogenesis

MSCs were successfully differentiated along the chondrogenic lineage in the presence of normal and MPS GAGs, as evidenced by increases in $^{35}SO_4$ incorporation into proteoglycans. The addition of commercially available HS and heparin significantly decreased chondrogenesis compared to 0 GAG controls, being at 51.13 ± 1.93% and 76.11 ± 2.97% of 0 GAG controls respectively (Figure 4.4). In contrast, MPS IIIA GAG had no significant effect on chondrogenesis compared to 0 GAG controls (Figure 4.4). Commercial HS had the greatest effect on chondrogenesis, being significantly reduced compared to both heparin and MPS IIIA GAG (Figure 4.4).

4.2.2.3 Adipogenesis

MSCs isolated from healthy human donors were successfully differentiated along the adipogenic lineage in the absence of GAG (0 GAG control). Adipogenesis was obvious from three weeks post-induction, with a cell count of 27 ± 4 oil red O positive cells. In contrast, undifferentiated MSCs maintained in human MSC basal growth media (basal media controls) had no positive oil red O stained cells at any timepoint (Figure 4.5).

The addition of commercially available HS to the adipogenic induction media had little effect on MSC adipogenesis until four weeks post-induction, where a significant increase in adipocyte counts was seen, with counts of 137.5 ± 17.5 compared to 19 ± 2 for 0 GAG controls. HS continued to promote adipogenesis, with cell counts again significantly higher than 0 GAG control five weeks post-induction (Figure 4.5). Similarly to commercial HS, the more highly sulphated heparin had little effect on adipogenesis until four weeks post-induction; here, adipocyte counts increased to 80.5 ± 9.5, significantly higher than 0 GAG controls. However, heparin did not promote adipogenesis to the same degree as HS, with

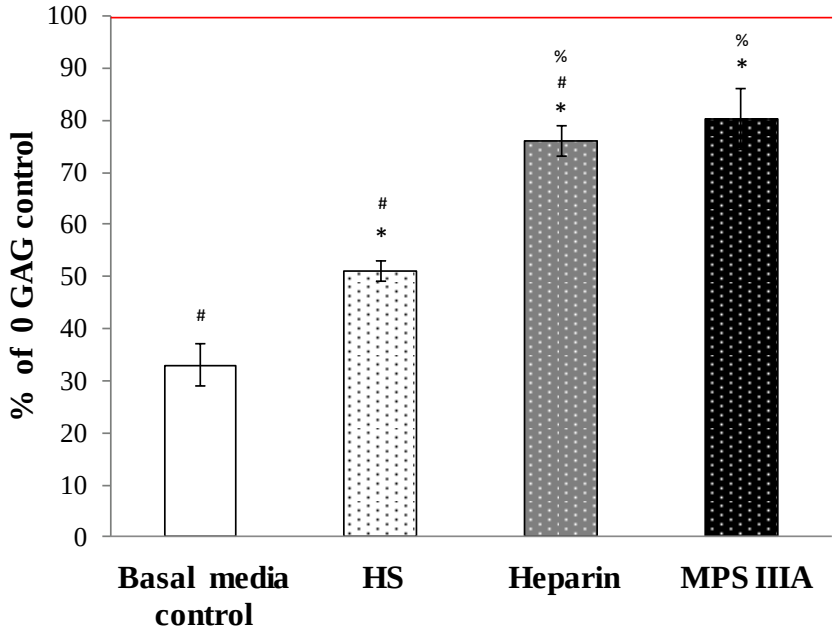

Figure 4.4: The effect of commercially available and MPS GAGs on chondrogenesis of human MSCs

$^{35}SO_4$ incorporation into proteoglycans in human MSCs induced along the chondrogenic lineage for six days in the presence of HS, heparin and MPS IIIA GAG. Results are shown as a percentage of the values for 0 GAG controls. Red line denotes 0 GAG levels (100%). Results are expressed as mean ± SEM (n=3). * indicates significant difference compared to basal media control; # indicates significant difference compared to 0 GAG control; % indicates significant difference compared to HS ($p<0.05$; one-way ANOVA, Tukey's HSD).

adipocyte counts significantly lower in the presence of heparin compared to HS. This trend continued at five weeks post-induction, with adipocyte counts significantly higher in the presence of heparin compared to 0 GAG controls, but unable to reach the counts seen in the presence of HS (Figure 4.5). Therefore, whilst both HS and heparin increased adipocyte formation, HS was the most successful in promoting adipogenesis.

MPS IIIA GAG had a notably disparate effect on adipogenesis compared to the commercially available GAGs. Three weeks post-induction, adipocyte counts were only at 8 ± 2 in the presence of MPS IIIA GAG compared to 0 GAG controls, which had adipocyte counts of 27 ± 4 (Figure 4.5). Adipocyte counts continued to be lower in the presence of MPS IIIA GAG compared to 0 GAG controls four and five weeks post-induction; counts of 11.5 ± 3.5 were seen in the presence of MPS IIIA GAG compared to 19 ± 2 for 0 GAG controls four weeks post-induction, and counts of 18.5 ± 0.5 compared to 33 ± 1 in MPS IIIA GAG and 0 GAG controls respectively five weeks post-induction (Figure 4.5). However, whilst notable decreases, these differences did not reach significance. MPS IIIA GAG significantly reduced adipocyte counts compared to MSCs cultured with HS and heparin four and five weeks post-induction (Figure 4.5). Therefore, in contrast to commercial HS and heparin, MPS IIIA GAG was found to delay and decrease adipogenesis.

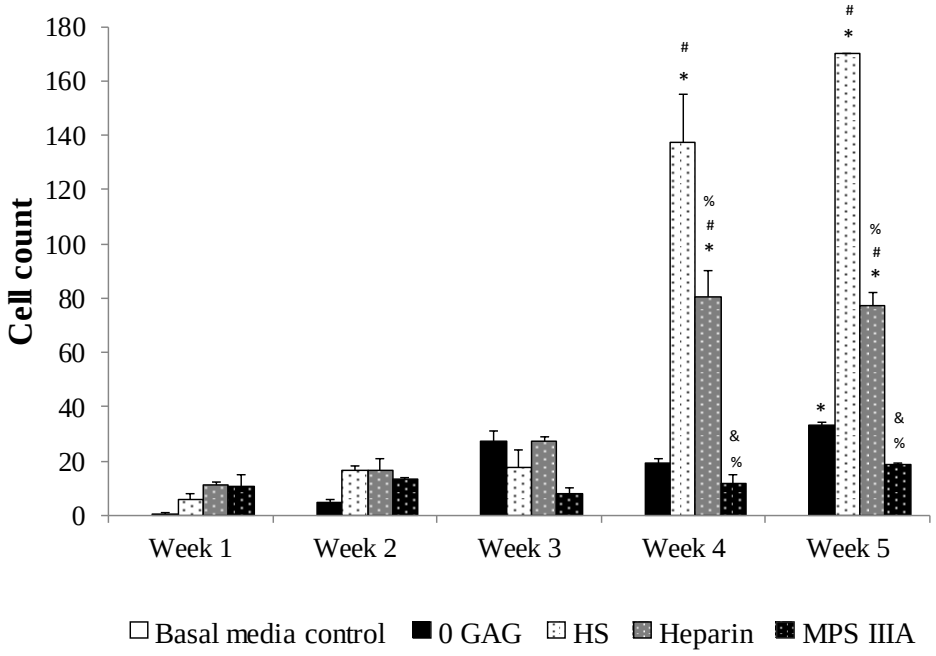

Figure 4.5: The effect of commercially available and MPS GAGs on adipogenesis of human MSCs

Positive oil red O cell counts in human MSCs induced along the adipogenic lineage for five weeks in the presence of HS, heparin and MPS IIIA GAG. Results are expressed as mean ± SEM (n=3). No oil red O positive cells were present in basal medical control samples (white bars). * indicates significant difference compared to basal media control at the same timepoint; # indicates significant difference compared to 0 GAG control at the same timepoint; % indicates significant difference compared to HS at the same timepoint; & indicates significant difference compared heparin at the same timepoint ($p<0.05$; one-way ANOVA, Tukey's HSD).

4.3 Discussion

4.3.1 Neurogenesis

4.3.1.1 Commercial full-length HS and heparin promote neurogenesis by promoting neural progenitor survival and proliferation

Commercially available full-length HS and heparin were both found to promote neurogenesis, with the more highly sulphated heparin having the greatest effect. Promotion of early neurogenesis was the most noticeable, with elevated expression of *nestin, NCAM* and *βIII-tubulin* 14 days post-induction, indicating increased neural progenitor proliferation and differentiation. HS chains are integral to several signalling pathways involved in proliferation and neurogenesis, stabilising morphogens and increasing their concentration at the cell surface or acting as co-receptors for signal transduction (section 1.3.1). The HS–dependent signalling pathways are involved in neurogenesis, with the Wnt, Hh and FGF pathways known to promote neural differentiation (Charytoniuk et al., 2002; Fuccillo et al., 2004; Hirabayashi et al., 2004; Machold et al., 2003; Munji et al., 2011). The FGF signalling pathway is one of the most central and highly studied pathways involved in neural progenitor proliferation and differentiation, and will be used here as an example. HS chains are required to modulate interactions between FGF and the FGFR via formation of the FGF:FGFR:HS complex (section 1.3.1.1). One pathway activated by formation of the FGF:FGFR:HS complex is the MAPK/ERK pathway, which upregulates a number of genes involved in CNS development, promoting neural progenitor proliferation and differentiation (Figure 4.6) (Hurtado & De Robertis, 2007; Jiang et al., 2015; Kuroda et al., 2005).

Activation of the MAPK pathway further promotes neurogenesis through inhibition of specific signalling pathways. One example is the BMP signalling pathway, which must be inhibited for neurogenesis. Similarly to FGF, HS chains are required for BMP signalling, with

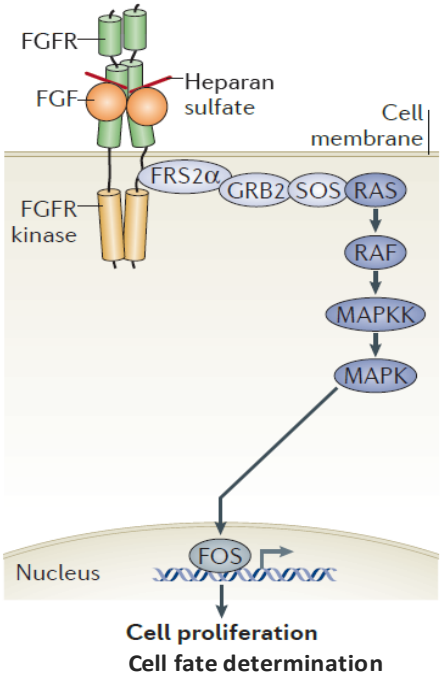

Figure 4.6: The FGF signalling pathway

HS chains are required for formation of the FGF:FGFR:HS complex, which activates the MAPK/ERK pathway, promoting proliferation and neurogenesis. Adapted from Goetz and Mohammadi (2013).

HS binding preventing BMP morphogen degradation and interaction with its antagonist, noggin (Irie et al., 2003; Kraushaar et al., 2012; Kuo et al., 2010; Murali et al., 2013; Zhao et al., 2006); however, activation of the MAPK pathway acts to inhibit downstream targets of BMP signalling via differential phosphorylation of Smad1 (Aubin et al., 2004; Kretzschmar et al., 1997; Lim et al., 2000; Pera et al., 2003; Rogers et al., 2011; Shou et al., 1999). In addition to its role in differentiation, attenuation of BMP signalling has also been shown to increase neural progenitor proliferation, with an increased population of neural progenitors in the hippocampus of aging mice following BMP inhibition (Yousef et al., 2015). Thus, in our

study, increased commercially available HS and heparin are likely increasing the concentration of FGF morphogens at the cell surface, promoting FGF-mediated MAPK signalling whilst concurrently inhibiting BMP signalling, thereby increasing neural progenitor survival and proliferation and promoting progenitor maturation.

4.3.1.2 MPS IIIA GAG disrupts neurogenesis

In contrast to commercially available HS and heparin, MPS IIIA GAG decreased neural gene expression. The most significant alterations in neural gene expression were seen 21 days post-induction, with significant reductions in *NCAM* and *βIII-tubulin* expression, markers of neural progenitors and immature neurons respectively, thus indicating a decrease in neural progenitor survival, proliferation and maturation. In contrast to the full length, typically sulphated HS and heparin used in this study, MPS IIIA GAG exists as partially degraded fragments, due to the sulphamidase deficiency distinctive of the disease (Neufeld & Muenzer, 2001). Distinct patterns of sulphation are integral for HS binding to signalling factors (section 1.3.1); however, MPS IIIA HS is known to be highly sulphated in comparison to normal HS, with significant increases in the tri-sulphated disaccharide HexA(2S)-GlcNS(6S) and the di-sulphated disaccharide HexA(2S)-GlcNS, and significant decreases in the mono-sulphated disaccharide HexA-GlcNS and the acetylated disaccharides HexA-GlcNA(6S) and HexA-GlcNA, where HexA represents either GlcA or IdoA (see Appendix B for abbreviations) (Table 4.1) (Hochuli et al., 2003; Wilkinson et al., 2012). Whilst the actual sequence of fragments is unknown, these changes in disaccharide composition of HS demonstrate an increase in sulphation and suggest alterations in the distinct patterns of sulphation involved in morphogen binding.

	HexA(2S)-GlcNS(6S) (% of total HS)	HexA-GlcNS(6S) (% of total HS)	HexA(2S)-GlcNS (% of total HS)	HexA-GlcNS (% of total HS)	HexA-GlcNA(6S) (% of total HS)	HexA-GlcNA (% of total HS)
Wildtype	9	8	15	18	9	50
MPS I	19 (*)	7	25 (*)	10 (*)	7	38 (*)
MPS II	31 (*)	3	32 (*)	10 (*)	9	20 (*)
MPS IIIA	22 (*)	5 (*)	30 (*)	8 (*)	6 (*)	30 (*)

Table 4.1 HS disaccharide composition

Disaccharide composition of HS from wildtype, MPS I, MPS II and MPS IIIA mouse brains. Values were estimated from figures in Wilkinson et al. (2012) and Gleitz et al. (2018). * denotes significance compared to wildtype disaccharide as determined in the literature.

As before (section 4.3.1.1), the well-studied FGF signalling pathway was selected as an example and examined in more detail, due to its integral role in neural progenitor proliferation and differentiation. Normal FGF signalling relies on a balance of binding affinities to form the FGF:FGFR:HS complex, with high affinity interactions between FGF and FGFRs (K_D = 10-500pM) and low affinity interactions between FGF and HS (K_D = 5-50nM) (reviewed in Gallagher & Turnbull, 1992). This balance enables HS to increase FGF concentration at the cell surface whilst allowing FGF:FGFR interactions, enabling the transfer of FGF from ECM-localised HSPGs to cell surface-bound FGFRs. However, the existence of MPS IIIA HS within the ECM may act to alter this balance. MPS IIIA HS exists as GAG fragments devoid of a PG core protein within the ECM, as opposed to normal HS, which exists primarily as cell surface-bound PGs (Filmus & Selleck, 2001; Iozzo, 1998; Zimmermann & David, 1999). These MPS IIIA HS fragments are extracellular soluble components, able to reside in and affect processes in the ECM in addition to the cell surface. MPS IIIA HS interferes with FGF

signalling by competing with normal HS; FGF bound to MPS IIIA HS is more likely to be located extracellularly, away from the cell surface HS and receptors. This has previously been shown in MPS I, where aberrant 2-*O*-sulphated HS inhibited CXCL12 binding to its cell surface receptor, due to MPS I HS sequestering of CXCL12 within the ECM (Watson et al., 2014). Similarly, masking the action of excess extracellular HS in MPS I and MPS IIIB fibroblasts restored FGF-2 signalling (De Pasquale et al., 2018). Therefore, excess, extracellular MPS IIIA HS is likely binding FGF, decreasing its concentration at the cell surface and reducing FGF signalling, thus impairing neural progenitor proliferation and neurogenesis.

Any changes in FGF proximity to cell surface receptors by MPS IIIA HS may be exacerbated by alterations in MPS IIIA HS morphogen binding capacity compared to normal HS. Due to the dependence of the FGF signalling pathway on HS chains, signalling is likely to be affected by alterations in HS sulphation within the NS regions of the HS chains. Of all the HS-dependent signalling pathways involved in neurogenesis, the distinct sulphation patterns required in the FGF pathway are the most well-established. FGF:HS interactions are dependent on *N*-sulphation and 2-*O*-sulphation, with 6-*O*-sulphation of HS instead involved in FGF:FGFR interactions (Ashikari-Hada et al., 2004; Guglier et al., 2008; Pye et al., 2000; Pye et al., 1998). MPS IIIA HS displays a significant increase in composition of all sulphate groups; however, the highest increases are seen in *N*-sulphation and 2-*O*-sulphation, with 2-*O* sulphation displaying the highest increase, with 52% of MPS IIIA HS disaccharides containing a 2-*O*-sulphate group, compared to 20% of disaccharides in normal HS (Wilkinson et al., 2012). HS chains with long stretches of *N*-sulphation and 2-*O* sulphation are known to have high affinity for FGF-2 (Turnbull et al., 1992). When specifically looking at the FGF-2 ligand, one of the most well-studied within the FGF family and highly implicated in CNS development, interactions between the FGF-2 morphogen and HS are dependent on the

distinct GlcNS(6S)-IdoA(2S)-GlcNS(6S)-IdoA(2S) tetrasaccharide (Guglier et al., 2008; Pye et al., 1998; Raman et al., 2003). MPS IIIA HS fragments have been shown to display increases in HexA(2S)-GlcNS(6S) disaccharides, where HexA represents either GlcA or IdoA (see Appendix B for abbreviations), following digestion with heparitinases (Table 4.1) (Wilkinson et al., 2012). Thus, if these two disaccharides appear in tandem, MPS IIIA HS will contain a higher proportion of the minimum FGF-2 binding motif compared to normal HS, increasing the likelihood of FGF-2 binding to MPS IIIA HS as opposed to normal HS; however, this is dependent on specific tetrasaccharide formations.

Altered sulphation patterns and the subsequent modified morphogen binding affinities have the potential to have significant effects on signalling pathways. Indeed, it could be that the altered and increased sulphation of MPS IIIA HS has a more significant effect on FGF signalling in MPS IIIA than the existence of excess GAG; if FGF-2 were to have a higher affinity for MPS IIIA HS than the FGFR, formation of the FGF:FGFR;HS complex would be prevented entirely, resulting in significant disruption of the FGF signalling pathway. However, significant research into the specific patterns of sulphation across the MPS IIIA HS backbone would be required to further investigate this hypothesis.

Therefore, this study has identified impaired stem cell proliferation and differentiation as a potential mechanism for the CNS pathology of MPS IIIA. It is likely that extracellular MPS IIIA HS binds FGF-2, creating a reservoir of FGF-2 within the ECM, decreasing FGF-2:FGFR interactions at the cell surface and subsequently reducing FGF-2 signalling and impairing both neural progenitor proliferation and neurogenesis. Alterations in the sulphation patterns of MPS IIIA HS compared to normal HS are likely exacerbating this effect by increasing the binding affinity of FGF-2 for MPS IIIA HS compared to normal HS; however,

further investigation into the precise arrangement of disaccharides within MPS IIIA HS should be considered to determine if this increase in implicated disaccharides translates to an increase in FGF-2 affinity.

4.3.1.3 GAGs from different MPS types have diverse effects on neurogenesis

MPS II GAG was found to have a similar effect on MSC neurogenesis as MPS IIIA GAG, with a significant decrease in multiple neural marker genes. MPS II and MPS IIIA both result from sulphatase deficiencies, resulting in significant increases in *N*-sulphation, 2-*O*-sulphation and 6-*O*-sulphation across the length of the HS chain compared to normal HS and similar disaccharide compositions, indicating similar sulphation patterns (Gleitz et al., 2018; Wilkinson et al., 2012). Further investigation into the precise arrangements of MPS II and MPS IIIA disaccharides would be required for confirmation; however, any similarities in the distinct patterns of sulphation across the HS backbone in MPS II and MPS IIIA HS would likely be responsible for the similar effects on neurogenesis, with both structures altering HS binding capacity and consequently the HS-dependent signalling pathways involved in neurogenesis.

In contrast to MPS II and MPS IIIA, MPS I GAG was found to have little effect on neurogenesis compared to 0 GAG controls. A significant decrease of 1.87 ± 0.22 fold *NCAM* expression compared to 0 GAG controls was seen 21 days post-induction; however, expression remained increased compared to MPS II and MPS IIIA GAG, which had 4.13 ± 0.85 and 3.33 ± 0.18 fold decreases in *NCAM* expression respectively. The disparate effect of MPS I GAG on neurogenesis compared to MPS II and MPS IIIA was unexpected, given the overlap in pathology between the disorders, with all storing HS and resulting in CNS disease. The different effects of MPS I and MPS II GAG was particularly surprising, given their

similarity in disease phenotype. Furthermore, both MPS I and MPS II store a combination of HS and DS. However, it has previously been found that the composition of individual HS and DS chains stored differs between the MPS types (Gleitz et al., 2018; Holley et al., 2011; Tomatsu et al., 2005; Wilkinson et al., 2012). MPS I results from an iduronidase deficiency, as opposed to the sulphatase deficiencies seen in MPS II and MPS IIIA. Therefore, the partially degraded HS fragments found in MPS I are enriched in unsulphated iduronic acid residues, in contrast to the sulphate residues seen in MPS II and MPS IIIA. Despite this, MPS I HS remains more highly sulphated than normal HS, with significant increases in *N*-sulphation, 2-*O*-sulphation and 6-*O*-sulphation compared to normal HS (Holley et al., 2011; Wilkinson et al., 2012). However, this increase in sulphation did not reach the levels seen in MPS IIIA HS, with the greatest difference seen in 2-*O*-sulphate composition, with a significant decrease in MPS I HS compared to MPS IIIA HS (Wilkinson et al., 2012). Specifically, a significant decrease in the di-sulphated disaccharide HexA(2S)-GlcNS was seen in MPS I compared to MPS IIIA, whilst comparable levels were seen between MPS II and MPS IIIA (Table 4.1) (Gleitz et al., 2018; Wilkinson et al., 2012). 2-*O*-sulphation is known to be integral for HS:FGF interactions (Turnbull et al., 1992). Thus, it is possible that this small decrease in HS sulphation in MPS I in comparison to MPS II and MPS IIIA HS is altering its FGF binding capacity. A reduction in the ability of ECM-localised MPS I HS to bind to FGF would enable FGF to reach the cell surface-anchored HS and FGFR, increasing FGF signalling and thus neurogenesis.

However, it should be noted that whilst MPS I HS is less sulphated than MPS IIIA HS, it still displays higher levels of sulphation than normal HS (Table 4.1), and has been previously shown to alter the ability of HS to bind to morphogens FGF-2 and BMP-4 and the chemokine CXCL12 (Khan et al., 2008; Pan et al., 2005; Watson et al., 2014). Thus, the limited effect of MPS I GAG on neurogenesis was unexpected. Whilst the sulphation patterns of MPS GAGs

play an important role in their function, GAG concentration is also likely to contribute. MPS I and MPS II both store HS and DS; however, the composition varies between the two types. MPS I GAG is known to have a higher ratio of DS compared to HS, in contrast to MPS II GAG, which has a higher composition of HS (Table 4.2) (Chuang et al., 2014; Langereis et al., 2015; Tomatsu et al., 2005). It is clear from the MPS IIIA data that increased extracellular HS impairs neurogenesis; in contrast, increased MPS VI GAG, largely composed of DS (Table 4.2) was able to promote early neurogenesis, supporting the concept that stored HS in the MPS disorders is the major contributor towards neurological pathology. Thus, the increased volume of extracellular HS in MPS II would result in more FGF being bound by HS in the ECM and prevented from reaching the FGFR to initiate signalling, thus impairing neurogenesis. A lesser amount of HS within the ECM in MPS I would decrease the amount of FGF being bound by HS in the ECM compared to MPS II, therefore allowing more to reach the cell surface and form the FGF:FGFR:HS complex required for FGF signalling. However, further study, preferably involving the analysis of the effects of MPS I and MPS II HS and DS individually on neurogenesis, would be required for confirmation.

MPS VI GAG did not impair neurogenesis; in contrast, early neurogenesis appeared to be promoted, with a significant increase in *nestin* and *NCAM* expression 14 days post-induction, indicating an increase in the progenitor population. This is likely a result of the absence of HS, as MPS VI stores only DS/CS (Table 4.2) (Neufeld & Muenzer, 2001). Similarly to HS, DS is known to be involved in neurogenesis and development, with chondroitin sulphate/dermatan sulphate proteoglycan (CS/DSPG) expression regulated throughout neural development (Bao et al., 2005; Ishii & Maeda, 2008; Mitsunaga et al., 2006; Shimazaki et al., 2005; Yamada et al., 2018). DSPGs have also been found to promote neuron survival and development *in vitro* (Faissner et al., 1994; Junghans et al., 1995; Kappler et al., 1997; Koops et al., 1996; Long et al., 2016). Thus, change in DS sulphation patterns may explain the

	HS (µg/mL)	DS (µg/mL)
Wildtype	3.88	1.68
MPS I	7.3	276.9
MPS II	824	164
MPS IIIA	8901	0.73
MPS VI	1.26	105.5

Table 4.2 HS and DS compositions

Total urinary HS and DS isolated from MPS I, MPS II, MPS IIIA and MPS VI patients and healthy controls (Chuang et al., 2014).

promoter effect of MPS VI GAG on neurogenesis, as changes in DS sulphation levels and patterning have previously been shown to alter downstream processes (Vicente et al., 2001). Similarly to HS, DS is able to bind to FGF-2; indeed, wound healing experiments have shown that DS stimulated FGF2-mediated proliferation to a greater extent than heparin (Penc et al., 1998). Due to the *N*-acetylgalactosamine 4-sulphatase deficiency of MPS VI, the stored DS has increased 4-*O*-sulphation compared to normal, MPS I and MPS II DS (Hochuli et al., 2003). Increases in 4-*O* sulphation of DS has previously been associated with an increase in FGF signalling, a known promoter of proliferation and neurogenesis (Taylor et al., 2005). An increase in FGF-mediated proliferation is likely to have a significant effect on the neural progenitor population, with increased survival and proliferation. Thus, the increase in neural gene expression in the presence of MPS VI GAG is likely a result of a combination of alterations in DS structure and an absence of excess, aberrant HS.

In summary, this study demonstrated that GAGs from different MPS types had varied effects on neurogenesis. This is likely due to the integral role of GAGs in many neurogenic signalling pathways, with changes in GAG concentration and sulphation patterns modifying morphogen binding, subsequently altering these signalling pathways.

4.3.2 Traditional mesodermal lineage differentiation

4.3.2.1 Commercial HS and MPS IIIA GAG have converse effects on MSC differentiation

No inhibitory effects were seen following the addition of commercial HS and heparin to the adipogenic and osteogenic culture media throughout differentiation along either lineage; osteogenesis was maintained, with calcium content and von Kossa staining in line with 0 GAG controls, whilst adipogenesis increased in the presence of commercial HS and heparin. In contrast, MPS IIIA GAG was found to disrupt both osteogenesis and adipogenesis, inhibiting calcium production and mineralisation, and reducing adipocyte formation. As with neurogenesis, a complex of HS-mediated signalling pathways are involved in mesodermal differentiation, requiring distinct patterns of sulphation for ligand binding (Allen et al., 2001; Behr et al., 2010; Brickman et al., 1998; Rodda & McMahon, 2006; Wang et al., 2004). Osteogenesis is particularly reliant on HS-dependent signalling pathways, with activation of the FGF, Wnt, Hh and TGBβ pathways required for bone development, promoting osteoblast activation, maturation and mineralisation, bone remodelling and trabecular bone formation (Chen & Long, 2013; Gazzerro et al., 2007; Hu et al., 2005; Mishina et al., 2004; Montero et al., 2000; Okamoto et al., 2006; Rodda & McMahon, 2006; Xiao et al., 2010). However, many of these pro-osteogenic pathways have also been identified as anti-adipogenic, such that induction along one lineage comes at the expense of the other (Bennett et al., 2002; Kawai et al., 2007; Suh et al., 2006; Xiao et al., 2010; Zehentner et al., 2000). One HS-dependent signalling pathway which is notable in promoting both osteogenesis and adipogenesis is the

BMP pathway, a member of the TGFβ superfamily (Mishina et al., 2004; Okamoto et al., 2006; Tang et al., 2004; Zehentner et al., 2000; zur Nieden et al., 2005). Binding of the BMP ligand to its receptor activates both the canonical Smad-dependent pathways and the non-canonical MAPK pathway, both of which upregulate expression of *Runx2* and *PPARγ*, the primary osteogenic and adipogenic genes respectively (James, 2013). Given the pro-osteogenic nature of many HS-dependent signalling pathways, the maintenance of osteogenesis observed in our study in the presence of normal HS and heparin was unsurprising; however, the significant increase in adipogenesis indicates that the BMP pathway is likely being promoted, thereby allowing for both osteogenic and adipogenic differentiation.

Both osteogenesis and adipogenesis were disrupted in the presence of MPS IIIA HS, likely a result of increased HS and altered sulphation patterns increasing the propensity of MPS IIIA HS to bind morphogens, creating a morphogen reservoir within the ECM and preventing interactions with receptors at the cell surface. Osteogenesis was the most severely affected, with complete inhibition of bone formation in the presence of MPS IIIA GAG; this is likely due to the integral role of multiple HS-dependent signalling pathways on osteogenesis. Supporting this, both FGF and BMP signalling have previously been shown to decrease in the presence of MPS I GAG (Khan et al., 2008; Pan et al., 2005). The concurrent decrease in differentiation along both lineages once again suggests the involvement of BMP signalling. A reduction in BMP signalling would subsequently decrease *PPARγ* expression; downregulation of this vital adipogenic gene is likely to compensate for any pro-adipogenic signals resulting from reduced osteogenesis. Thus, MPS IIIA HS-mediated morphogen binding is likely to be responsible for the disruption of the normal co-ordination of osteogenesis and adipogenesis, resulting in a decrease in both processes.

In contrast to osteogenesis and adipogenesis, commercial HS reduced chondrogenesis, with a significant reduction in $^{35}SO_4$ incorporation compared to 0 GAG controls. MPS IIIA GAG had little effect on chondrogenesis, with no significant decrease in $^{35}SO_4$ incorporation compared to 0 GAG controls. The effect of heparin on chondrogenesis appeared to fall between that of commercial HS and MPS IIIA GAG; $^{35}SO_4$ incorporation was significantly lower than 0 GAG controls, but significantly higher than when cultured in the presence of HS. The role of HS-dependent signalling pathways on chondrogenesis is complex; the FGF and Hh pathways have been shown to link chondrogenesis to osteogenesis, promoting cartilage formation, whilst the canonical Wnt pathway is a known inhibitor of MSC chondrogenic differentiation (Correa et al., 2015; Day et al., 2005; Hill et al., 2005; Huang et al., 2018; Im & Quan, 2010; Mundy et al., 2016; Schmidt et al., 2018; Steinert et al., 2012). Whilst BMP signalling is integral for osteogenesis and adipogenesis, its involvement in chondrogenesis is less well understood; BMP signalling is known to promote chondrogenesis (de Mara et al., 2013; Denker et al., 1999; Kramer et al., 2000; Majumdar et al., 2001); however, upregulation of a downstream gene target, *Runx2*, has been shown to inhibit chondrogenesis, with *Runx2*-deficient cells preferentially differentiating into chondrocytes instead of osteoblasts in the presence of BMP-2 (Armiento et al., 2017; Hinoi et al., 2006; Kobayashi et al., 2000; Lengner et al., 2005). Increased HS is likely promoting *Runx2* expression via an increase in the HS-mediated Wnt signalling pathway, preventing chondrogenic differentiation of MSCs. Thus, MPS IIIA HS-mediated morphogen binding, as discussed previously, would result in a subsequent decrease in *Runx2* expression, thereby allowing chondrogenesis.

Heparin appeared to disrupt chondrogenesis, but to a significantly lesser extent than commercial HS. Heparin is known to be a "promiscuous" binder, due to a significant increase in sulphation compared to HS; consisting largely of tri-sulphated disaccharide units, heparin will generally contain the combinations of sulphate groups required for morphogen

interactions (Loo et al., 2001; Pye et al., 1998). It is possible that this increase in sulphation results in extracellular heparin binding morphogens in a similar manner to MPS IIIA GAG, subsequently decreasing *Runx2* expression, as has been suggested by others (Irie et al., 2003). However, it would be unexpected for heparin and MPS IIIA GAG to bind morphogens in a similar manner, as heparin and MPS IIIA GAG have had converse effects in all other MSC differentiation pathways presented in this chapter. As an alternate hypothesis, heparin may be upregulating all HS-dependent pathways, due to its increased ability to bind and activate morphogens. Therefore, both chondrogenic pathways such as FGF and Hh and anti-chondrogenic pathways such as the Wnt pathway would be upregulated, potentially creating a compensatory relationship with chondrogenic upregulation rescuing anti-chondrogenic upregulation. Further investigation would be required to determine the exact mechanisms underlying heparin-mediated signalling in chondrogenesis. In brief, this data suggests that alterations in MSC differentiation in the presence of MPS IIIA GAG were a result of aberrant signalling of HS-dependent pathways, due to MPS IIIA HS-mediated morphogen binding.

4.3.2.2 A mechanism for MPS IIIA skeletal pathology

In contrast to all other MPS types, patients with MPS III have traditionally displayed only minimal skeletal pathology (Chen et al., 1996; Neufeld & Muenzer, 2001; Scaramuzzo et al., 2012). The dominance of the MPS IIIA neurological phenotype has limited investigation into the prevalence of skeletal pathology. However, recent studies have identified that orthopaedic abnormalities are more prevalent in MPS IIIA than previously thought, contributing to a poor quality of life in patients. Musculoskeletal manifestations have been reported in MPS IIIA patients, with hip deformities such as acetabular dysplasia and osteonecrosis of the femoral head common ailments (de Ruijter et al., 2013b; White et al., 2011). Epiphyseal dysplasia resulting from osteonecrosis of the femoral head has in particular been associated with increased hip pain in both ambulatory and non-ambulatory patients, due to the slow but

persistent resorption and fragmentation of the femoral head (White et al., 2011). Spinal deformities have also been reported, with vertebral body hypoplasia and scoliosis present in paediatric patients with MPS IIIA (White et al., 2011).

The primary osteogenic phenotype identified in MPS IIIA patients is osteopenia, which can lead to an increased risk of fractures in patients. Reduced bone mineral density (BMD) has been identified in a number of patients, with increased age, the use of anti-epileptic medication and reduced mobility identified as risk factors for decreasing BMD (Nur et al., 2016; Rigante & Caradonna, 2004). Rigante and Caradonna (2004) concluded that the skeletal pathology was likely a result of neurological pathology outcomes rather than an underlying molecular cause, concurring with long-standing assumptions that skeletal pathology in MPS III patients was a result of reduced mobility throughout their lifetime, resulting in disuse osteopenia. Patients commonly become non-ambulatory from their early teens (White et al., 2011). However, the effects of MPS IIIA GAG identified in this study, with MPS IIIA GAG inhibiting osteogenesis, provides a potential underlying, direct mechanism for skeletal disease in MPS, with extracellular MPS IIIA GAG likely binding morphogens and disrupting HS-mediated pro-osteogenic signalling pathways.

4.3.3 Chapter conclusions

This chapter aimed to determine the effects of excess, extracellular MPS IIIA GAG on MSC differentiation. Commercial HS and heparin were found to promote neurogenesis, osteogenesis and adipogenesis; in contrast, MPS IIIA GAG disrupted all three pathways, implicating disrupted neurogenesis and osteogenesis as contributors towards the severe neurological and mild skeletal pathology seen in MPS IIIA. It was hypothesised that extracellular MPS IIIA GAG binds to growth factors, creating reservoirs of growth factors

within the ECM, preventing growth factor binding to cell surface bound HS and receptors in several HS-dependent signalling pathways involved in stem cell proliferation and differentiation. Contributing to this was the increased sulphation of MPS IIIA HS compared to normal HS, with the sulphation patterns present on MPS IIIA HS associated with an increased likelihood of morphogen binding and thus increased growth factor sequestration. The effect of exogenous HS on chondrogenesis was unique, with commercial HS disrupting chondrogenesis and MPS IIIA GAG having little effect, supporting previous findings that cartilage and joint pathology have not been reported in MPS IIIA patients. This indicated that MPS IIIA GAG was disrupting specific signalling pathways and differentiation lineages, as opposed to a global inhibition of all MSC differentiation. This provides a potential mechanism for the severe neurological pathology evident in MPS IIIA patients, which may also contribute toward the skeletal pathology observed.

Chapter Five: MPS IIIA stem cells: generation, proliferation and neurodifferentiation

5.1 Introduction

MPS IIIA is characterised by the intracellular accumulation of the GAG HS (Neufeld & Muenzer, 2001). It has previously been demonstrated that HS accumulation commences prenatally, including within cells of the CNS, indicating that developmental pathways may be affected in MPS IIIA and thus contributing to the disease pathology (Ceuterick et al., 1980; Greenwood et al., 1978; Harper et al., 1974; Martin & Ceuterick, 1983). In particular, HS accumulation within foetal neurons (Ceuterick et al., 1980; Martin & Ceuterick, 1983) could disrupt neurodevelopmental pathways such as neurogenesis, indicating a thus far uninterrogated mechanism of pathology for the severe CNS disease of MPS IIIA. Using MSCs from healthy human donors, Chapter Four identified that extrinsic MPS IIIA GAG disrupted neurogenesis (refer section 4.2.1). For further investigation into neurogenesis in MPS IIIA, this chapter aimed to develop and characterise two neurogenic *in vitro* models of MPS IIIA, a murine MSC line and a human iPSC line.

The neurogenic properties of MSCs has identified them as a potential cell type for modelling disease neurogenesis *in vitro* (Sanchez-Ramos et al., 2000). MSCs from MPS patients would provide an excellent source of stem cells for modelling cell development *in vitro*. MSCs have previously been isolated from MPS I patients and exhibited increased osteoclast formation capacity compared to normal MSCs (Gatto et al., 2012). Unfortunately, MSCs are difficult to procure from MPS IIIA patients due to the invasive nature of a stem cell harvest. Due to its close mirroring of the human disease phenotype, the murine MPS IIIA mouse model has been suggested as an alternative source of MPS IIIA MSCs (Bhaumik et al., 1999; Crawley et al., 2006). For our study, murine MPS IIIA MSCs provide an additional advantage, allowing direct comparison to the human MSC experiments examining the effects of extrinsic MPS IIIA GAG on neural differentiation (Chapter Four). Previously, our lab has isolated MSCs exhibiting a $CD45.2^-$, $CD34^-$, $CD29^+$ and $Sca.1^+$ phenotype typical of murine MSCs from

normal mice by magnetic activated cell sorting (MACS) (Rostovskaya & Anastassiadis, 2012) (Matrix Biology Unit, unpublished data). However, MSCs have not been isolated from mouse models of any of the MPS subtypes.

iPSCs present as an ideal cell type of human origin for modelling MPS IIIA neurogenesis *in vitro.* Skin fibroblasts are commonly used for iPSC reprogramming and, in contrast to MSCs, are readily available from MPS IIIA patients due to their use in diagnostic procedures (Lehman et al., 2011). Furthermore, as a variety of mutations are available, iPSCs also allow for the assessment of genotype/phenotype correlations, which can be valuable for clinicians at diagnosis. iPSCs have previously been successfully generated from somatic cells of patients with MPS I, MPS II, MPS IIIB, MPS IIIC and MPS VII (Bayo-Puxan et al., 2018; Canals et al., 2015; Griffin et al., 2015; Lemonnier et al., 2011; Rybova et al., 2018; Swaroop et al., 2018; Tolar et al., 2011; Vallejo-Diez et al., 2018; Varga et al., 2016a; Varga et al., 2016b, 2016c). Neurogenesis was examined in MPS VII iPSCs by quantifying *βIII-tubulin* expression throughout neural induction; no disparities were identified between MPS VII and control iPSCs (Bayo-Puxan et al., 2018). MPS iPSCs have also been used previously to model synaptogenesis *in vitro*, identifying decreases in synaptic activity in MPS VII and MPS IIIC (Bayo-Puxan et al., 2018; Canals et al., 2015).

Overall, this chapter aimed to develop two neurogenic *in vitro* models of MPS IIIA; a murine MSC line and a human iPSC line. Following phenotypic characterisation, these cell lines were used to identify any alterations in stem cell proliferation or neurogenesis in MPS IIIA.

5.2 Results

5.2.1 Generation and neurogenic differentiation potential of MPS IIIA MSCs

The MPS IIIA mouse model provides a source of disease MSCs to examine MPS IIIA proliferation and neurogenesis *in vitro*. $CD45.2^-$, $CD34^-$, $CD29^+$ and $Sca.1^+$ cells were isolated from normal and MPS IIIA mouse long bones by MACS separation (section 2.5.1) and were identified as MSCs based on their fibroblast-like morphology and plastic adherent properties (data not shown).

5.2.1.1 CFU assay

The ability to form colonies following seeding at low density is an essential property of MSCs (Friedenstein, 1980; Friedenstein et al., 1974; Samsonraj et al., 2015). Therefore, a colony forming unit (CFU) assay was conducted as part of the characterisation of MPS IIIA MSCs. Following plating at the lowest seeding density of 800 cells/well, normal MSCs successfully formed colonies one week post-seeding, as was expected, with an average of 13.63 ± 3.61 colonies per well. The average number of colonies formed increased to 27.26 ± 11.16 and 47.70 ± 1.36 colonies per well following the plating of normal MSCs at the higher seeding densities of 1000 and 1200 cells/well respectively (Figure 5.1A). Colony number increased in normal MSCs two weeks post-seeding at all seeding densities; however, normal MSC colonies had increased in size and number such that colonies were overlapping, and it was therefore difficult to discern and count individual colonies (data not shown).

In contrast to normal MSCs, no distinct colonies were visible in MPS IIIA MSCs one week following plating at the lowest seeding density of 800 cells/well. Colonies successfully formed at the higher seeding densities, with an average of 1.36 ± 1.36 colonies and 8.18 ± 4.72 colonies formed one week post-seeding at 1000 and 1200 cells/well respectively.

However, colony number was significantly reduced compared to normal MSCs (Figure 5.1A). Thus, MPS IIIA MSCs were able to form colonies, a defining feature of MSCs; however, colony formation was significantly reduced compared to normal murine MSCs.

5.2.1.2 Sulphamidase activity

MPS IIIA MSCs were found to exhibit significantly reduced sulphamidase activity compared to normal MSCs, with sulphamidase activities of 0.41 ± 0.41 pmol/hr/mg protein and 79.04 ± 8.02 pmol/hr/mg protein respectively, with MPS IIIA MSC sulphamidase activity 0.52% of normal activity (Figure 5.1B). This recapitulated the sulphamidase deficiency typical of MPS IIIA disease (Neufeld & Muenzer, 2001).

5.2.1.3 Proliferation

The CFU assay (section 5.2.1.1) indicated the potential of a decrease in MPS IIIA MSC proliferation compared to normal MSCs. For confirmation, a proliferation assay was conducted on normal and MPS IIIA MSCs immediately after isolation from murine compact bone. MPS IIIA MSC cell number was 53.83 ± 14.71% of normal MSC cell number nine days post-isolation, indicating a reduction in MPS IIIA MSC proliferation compared to normal. MPS IIIA MSC proliferation declined over time; MPS IIIA cell number was significantly lower than normal MSCs 12 and 15 days post-isolation, with significant decreases to 49.34 ± 2.13% and 42.67 ± 5.08% of normal MSCs respectively (Figure 5.2A).

Decreased proliferation has been observed previously in MPS IIIB iPSCs. It was hypothesised to be due to impaired FGF-2 signalling resulting from interactions with excess MPS IIIB HS.; proliferation was rescued through supplementation with the deficient MPS IIIB enzyme, NAGLU (Lemonnier et al., 2011). Therefore, the ability of recombinant sulphamidase or

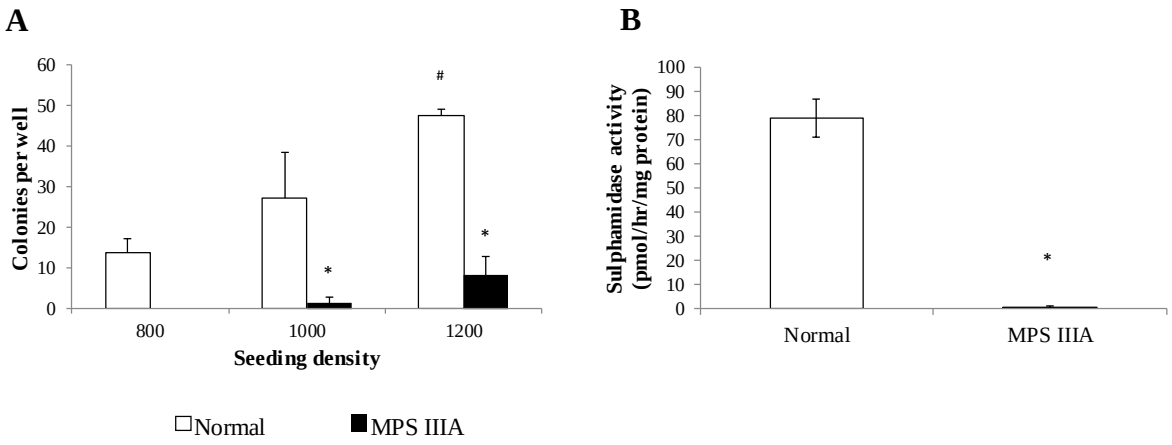

Figure 5.1: Characterisation of MPS IIIA murine MSCs

A: The number of colonies formed by normal (white bars) and MPS IIIA (black bars) MSCs one week post-seeding at different seeding densities. Results are expressed as mean ± SEM (n=3). * indicates significant difference compared to normal MSCs at same timepoint; # indicates significant difference compared to 800 seeding density of same genotype ($p<0.05$; one-way ANOVA, Tukey's HSD). **B:** Sulphamidase activity in cell layers of normal and MPS IIIA murine MSCs. Results are expressed as mean ± SEM (n=3). * indicates significant difference compared to normal MSCs ($p<0.05$; Student's t-test).

FGF-2 to rescue MPS IIIA MSC proliferation was determined by adding each to the MSC culture medium (section 2.8.1.1). Supplementation with sulphamidase resulted in a small but significant increase in cell number one day post-seeding to 137.5 ± 6.93% of untreated MPS IIIA MSCs in the presence of 0.3pmol/min sulphamidase (Figure 5.2B). However, this effect did not persist at subsequent timepoints. Additional concentrations of sulphamidase had no effect on MPS IIIA MSC cell number. In contrast, FGF-2 was found to have a dose-dependent response on cell number. The lowest concentration of 1ng/mL FGF-2 had little effect on MPS IIIA MSC proliferation, with no change in cell number compared to untreated MPS IIIA MSCs. The addition of 3ng/mL FGF-2 increased cell number, with a significant increase to 168 ± 5.67% of untreated MPS IIIA MSCs after two days. The highest FGF-2 concentration of 5ng/mL had the greatest effect, being significantly higher than untreated MPS IIIA MSCs at all timepoints (Figure 5.2C). Thus, whilst exogenous sulphamidase had limited effects in rescuing the impaired proliferation phenotype of MPS IIIA MSCs, exogenous FGF-2 was able to promote proliferation in a dose dependent manner.

5.2.1.4 Neural differentiation of MPS IIIA murine MSCs

Normal and MPS IIIA MSCs were induced along the neural lineage using the NP method previously established in Chapter Three. The expression of neural marker genes was determined relative to undifferentiated MSCs maintained in murine MSC basal growth media for four hours (basal media controls). Neural gene expression of normal MSCs induced along the neural lineage mirrored that seen in Chapter Three (section 3.2.3.2). Expression of *nestin*, a marker of progenitors, decreased over the 48 hour timecourse, indicating a decrease in the presence of cells with a neural progenitor-like phenotype; however, this difference did not reach significance and so should be interpreted with caution (Figure 5.3A). Significant increases in neuronal markers *βIII-tubulin* and *NF-M* expression were evident from four hours

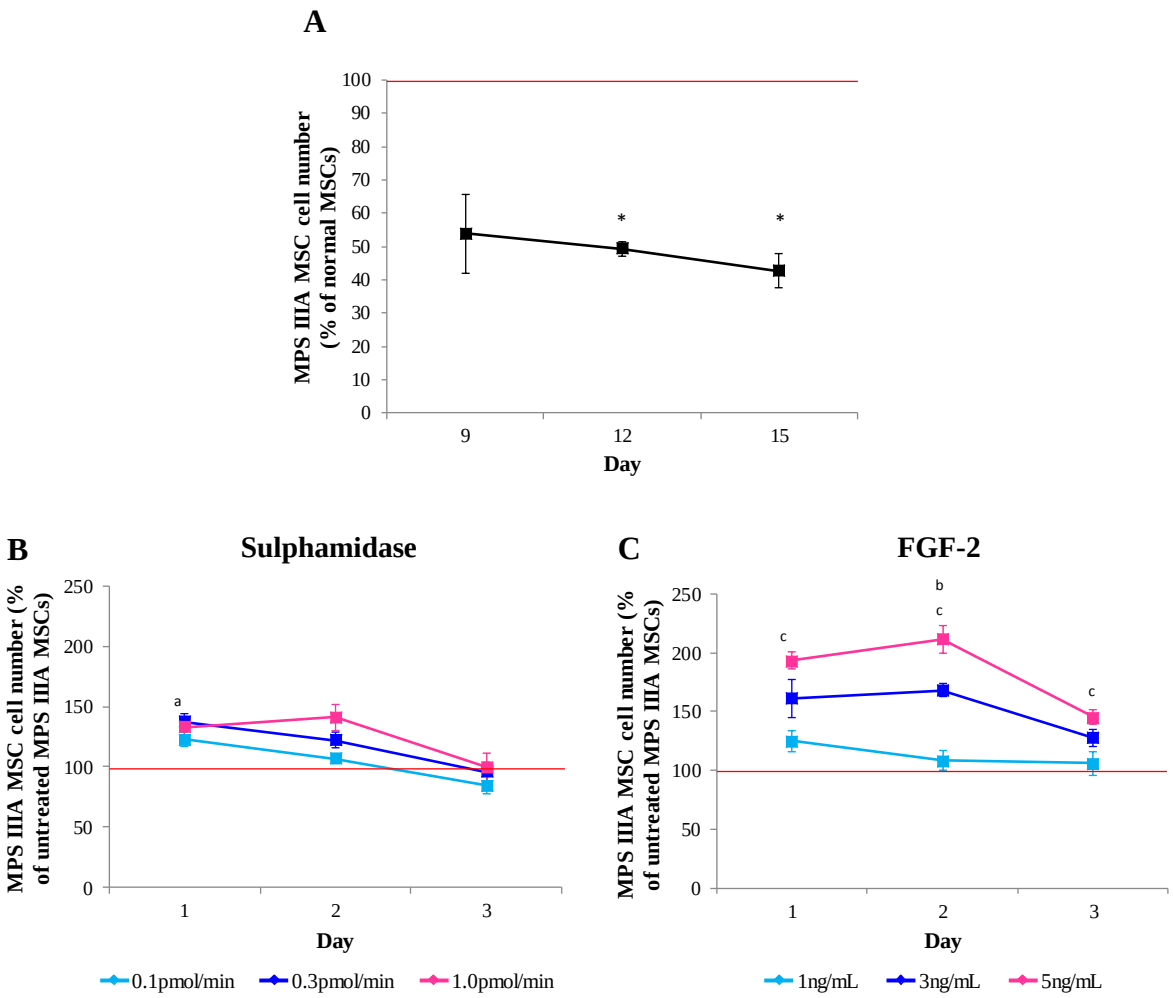

Figure 5.2: MPS IIIA murine MSC proliferation

A: Cell number of MPS IIIA murine MSCs as a percentage of normal murine MSC cell number. Red line denotes normal murine MSC cell number (100%). Results are expressed as mean ± SEM (n=3). * indicates significant difference compared to normal MSCs at the same timepoint ($p<0.05$; one sample t-test). **B-C:** Cell number of MPS IIIA murine MSCs treated with exogenous sulphamidase (B) or FGF-2 (C) as a percentage of untreated MPS IIIA murine MSC cell number. Red line denotes untreated MPS IIIA murine MSC cell number (100%). Results are expressed as mean ± SEM (n=3). Letters a-c indicate significant difference compared to untreated MPS IIIA MSCs at the same timepoint: a = 0.3 pmol/min sulphamidase, b = 3ng/mL FGF-2, c = 5ng/mL FGF-2 ($p<0.05$; one sample t-test).

and eight hours post-induction, respectively, compared to basal media controls, suggesting the formation of post-mitotic neurons from progenitor cells (Figure 5.3B-C).

Nestin expression decreased in MPS IIIA MSCs compared to basal media controls four hours post-induction, whilst *βIII-tubulin*, increased 4.32 ± 0.21 fold, indicating the formation of immature neurons (Figure 5.3 A-B). However, *βIII-tubulin* expression decreased steadily over the 48 hour timecourse, with expression significantly lower than that seen in normal MSCs 48 hours post-induction, with only a 1.35 ± 0.06 fold increase in *βIII-tubulin* expression compared to basal media controls. In contrast, normal MSC *βIII-tubulin* expression was 5.64 ± 0.72 hold higher than basal media controls 48 hours post-induction (Figure 5.3B). No significant change in expression of *NF-M*, a marker of mature post-mitotic neurons, was seen compared to basal media controls over the 48 hour timecourse in MPS IIIA MSCs, indicating that immature neurons were unable to survive and mature into post-mitotic neurons (Figure 5.3C).

5.2.2 Generation of MPS IIIA human iPSC lines

The MPS IIIA murine MSC model identified decreased stem cell proliferation and immature neuron survival and maturation as potential underlying mechanisms of pathology. Whilst murine MSCs are an easily accessible source of MPS IIIA stem cells with neurogenic properties, their non-human origin is a disadvantage, due to differences in development, lifespan and cellular pathways between species. Therefore, confirmation with a human-based cell model is advantageous. Unfortunately, MSCs are difficult to obtain from MPS IIIA patients; however, fibroblasts are easily accessible as they are required for disease diagnosis or confirmation. In addition, human iPSC lines allow for the analysis of various *SGSH* mutations and sulphamidase activities on disease phenotype. The pluripotent nature of iPSCs

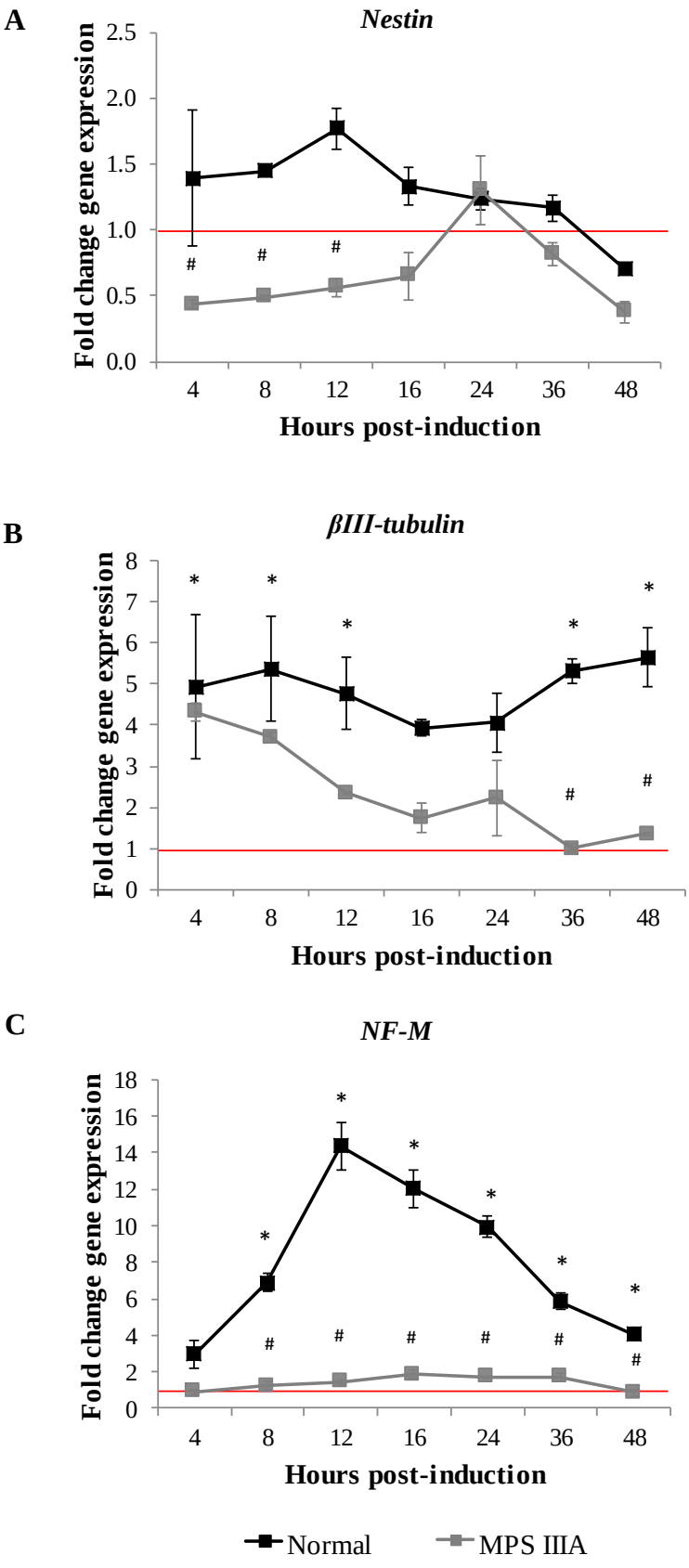
A
Nestin
Fold change gene expression
2.5
2.0
1.5
1.0
0.5
0.0
4
8
12
16
24
36
48
Hours post-induction
B
βIII-tubulin
Fold change gene expression
8
7
6
5
4
3
2
1
0
Hours post-induction
C
NF-M
Fold change gene expression
18
16
14
12
10
8
6
4
2
0
Hours post-induction
Normal
MPS IIIA

Figure 5.3: MPS IIIA murine MSC neural differentiation

Expression of *nestin* (A), *βIII-tubulin* (B) and *NF-M* (C) throughout neural differentiation of normal (black line) and MPS IIIA (grey line) murine MSCs. Gene expression was normalised to cyclophilin A and the fold change relative to MSCs maintained in murine MSC basal growth media for four hours (basal media controls) was calculated using the ΔΔCt method. Red line denotes basal media control baseline gene expression. Results are expressed as mean ± SEM (n=3). * indicates significant difference between neuronal MSC and basal media controls; # indicates significant difference between normal neuronal MSC and MPS IIIA neuronal MSC gene expression at the same timepoint ($p<0.05$; one-way ANOVA, Tukey's HSD).

enables *in vitro* modelling of neurogenesis; in addition, iPSCs can be differentiated along multiple neurogenic lineages as required, forming astrocytes and oligodendrocytes (Krencik & Zhang, 2011; Wang et al., 2013). To date, an MPS IIIA iPSC line has not been developed. This study aimed to develop iPSC lines from two MPS IIIA patients, and to use these models to identify any changes in neurogenesis as a result of the disease.

5.2.2.1 Fibroblasts

Fibroblasts were obtained from one unaffected donor and two MPS IIIA patients, designated Patient 1 and Patient 2. All fibroblast lines expanded easily in culture. The clinical records and mutational analysis of Patient 1 and Patient 2, provided by the National Referral Laboratory at the Women's and Children's Hospital, is summarised in Table 5.1. A review of the literature identified that the compound heterozygous missense mutations in Patient 1 have been previously published and are associated with an intermediate phenotype, in line with our

	Phenotype	Age of diagnosis	Mutation in *SGSH*
Patient 1	Intermediate	7	c.892 T>C (p.S298P) c.1828 G>A (p.R433Q)
Patient 2	Severe	2	c.672 C>A (p.Y224*)

Table 5.1: Patient fibroblast summary

Fibroblasts were obtained from MPS IIIA patients. Clinical information and *SGSH* mutation analysis were provided by the National Referral Laboratory at the Women's and Children's Hospital, SA, Australia.

patient's clinical records (Di Natale et al., 2003; Valstar et al., 2010). The homozygous nonsense mutation of Patient 2 has not been previously published.

5.2.2.1.1 Sulphamidase activity

Sulphamidase activity was significantly reduced in MPS IIIA fibroblasts compared to control fibroblasts. Control fibroblasts sulphamidase activity was at 116.1 ± 6.53 pmol/hr/mg protein, compared to Patient 1 fibroblasts which had sulphamidase activity of 16.4 ±7.75 pmol/hr/mg protein. Sulphamidase activity was further reduced in Patient 2 fibroblasts, with activity at 0.85 ±0.77 pmol/hr/mg protein; however, the difference between the two MPS IIIA fibroblast lines did not reach significance (Figure 5.4). Activity was below the detectable limit of the assay in many Patient 2 fibroblast samples. Thus, the MPS IIIA fibroblasts were found to mirror the enzyme deficiency phenotype of MPS IIIA, with decreased sulphamidase activity correlating with an increase in disease severity.

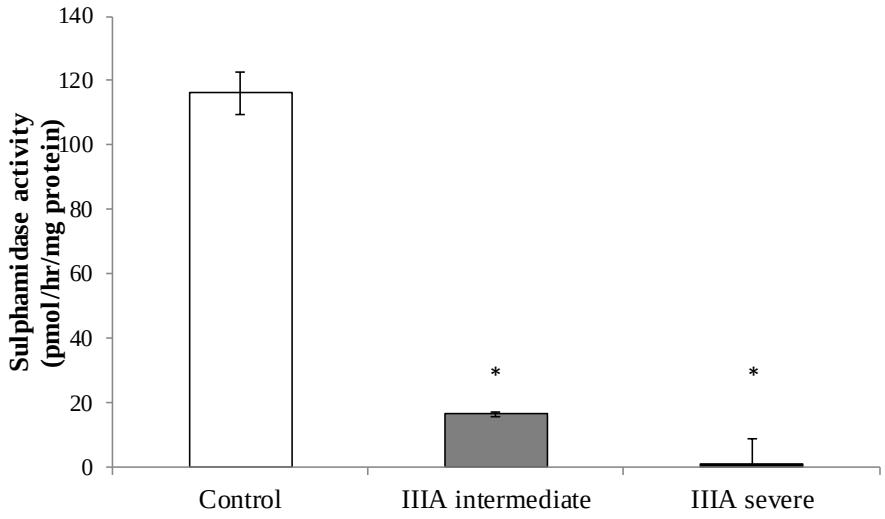

Figure 5.4: MPS IIIA fibroblast sulphamidase activity

Sulphamidase activity in cell layers of normal, Patient 1 (IIIA intermediate) and Patient 2 (IIIA severe) fibroblasts. Results are expressed as mean ± SEM (n=3). * indicates significant difference compared to normal fibroblasts ($p<0.05$; one-way ANOVA, Tukey's HSD).

5.2.2.2 MPS IIIA iPSC lines

Control, Patient 1 and Patient 2 fibroblasts were reprogrammed to iPSCs. Following reprogramming, a minimum of 11 clones with ESC-like morphology were selected per fibroblast cell line for continued passage. As expected, a number of clones did not survive multiple passages; by passage five, eight control, four Patient 1 and four Patient 2 clones remained. Both Patient 1 and Patient 2 iPSCs were able to expand easily in culture at a similar rate to control iPSCs. After a minimum of 13 passages, four control, two Patient 1 and three Patient 2 iPSC clones were sent for karyotype analysis. All control iPSC clones analysed were found to have normal karyotypes of 46, XY. One Patient 1 clone was found to display a normal karyotype of 46, XY, with the second exhibiting an abnormal karyotype of 46, XY, -21, t(5:21)(q12;p11.2). Two Patient 2 iPSC clones had normal karyotypes of 46, XX. The remaining clone had an abnormal karyotype of 46, XX, del(7)(q32). One karyotypically normal clone of each cell line was chosen for further analysis (Figure 5.5).

5.2.2.2.1 Pluripotency

Control, Patient 1 and Patient 2 iPSCs were identified as pluripotent, with significant increases in expression of *Oct-4*, *Sox2* and *Nanog* compared to the original fibroblasts from which the iPSCs were derived (Figure 5.6A). Positive Oct-4 and SSEA4 staining of colonies provided additional evidence of pluripotency (Figure 5.6B). No significant difference in iPSC morphology (Figure 5.5 D-F) or pluripotency profile (Figure 5.6 A-B) was seen between control, Patient 1 or Patient 2 iPSCs.

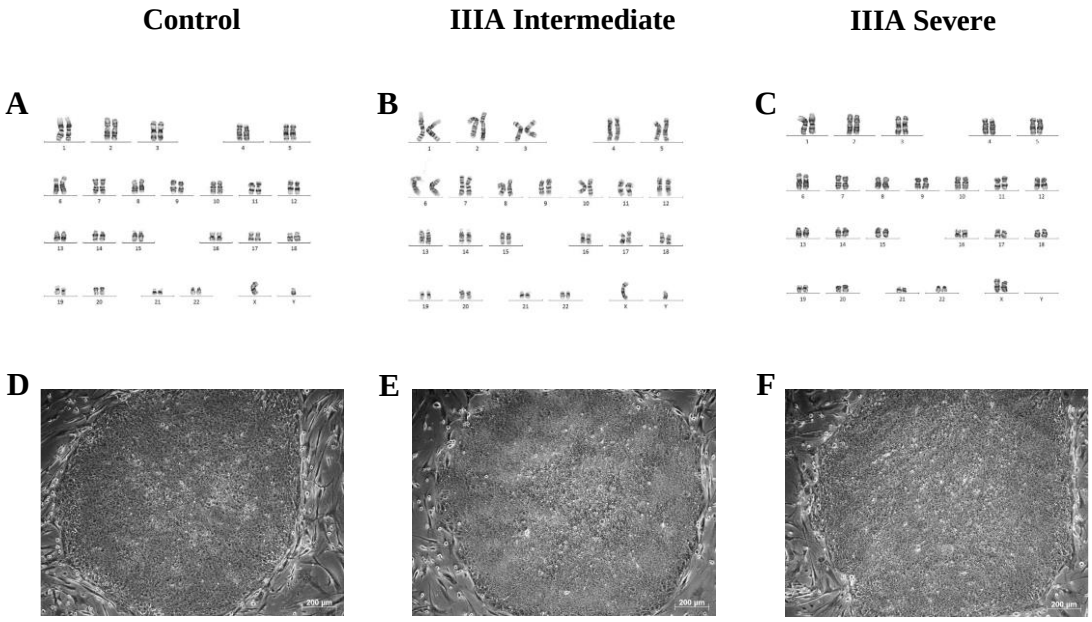

Figure 5.5: MPS IIIA iPSC karyotype and morphology

Karyogram (A-C) and morphology (D-F) of control, Patient 1 (IIIA intermediate) and Patient 2 (IIIA severe) iPSCs after a minimum of 13 passages. Morphology images taken on an AxioCam MRm high resolution camera at 5x magnification. Scale bar represents 200µm.

5.2.2.2.2 Sulphamidase activity

In a similar manner to the MPS IIIA fibroblasts (Figure 5.4), the reprogrammed MPS IIIA iPSC clones had reduced sulphamidase activity compared to control iPSC clones. Control iPSC sulphamidase activity was at 73.46 ± 7.36 pmol/hr/mg protein; in contrast, Patient 1 iPSC sulphamidase activity was significantly reduced to 29.43 ± 3.82 pmol/hr/mg protein. Sulphamidase activity was further reduced in Patient 2 iPSCs to 0.07 ± 0.07 pmol/hr/mg protein, significantly lower than both control and Patient 1 iPSCs (Figure 5.6C). Thus, MPS IIIA iPSCs appear to recapitulate the molecular hallmarks of the human disease, with reduced sulphamidase activity compared to normal iPSCs. These results also mirror those seen in fibroblasts (Figure 5.4), with decreased enzyme activity correlating with an increase in disease severity, indicating that the underlying biochemical deficit was maintained post-reprogramming.

5.2.3 Generation of MPS IIIA human iPSC-derived NPCs

Control and Patient 1 (MPS IIIA intermediate) iPSCs were differentiated along the neural lineage to form NPCs (section 2.6.3). Both control and MPS IIIA iPSCs successfully formed neural rosette structures, with no difference seen between the two lines, indicating that neural progenitor induction was not affected in MPS IIIA (data not shown). Neural progenitors were isolated from neural rosettes and cultured in the presence of FGF-2. After two passages, morphology typical of neural progenitors was evident in both control and Patient 1 cells (Figure 5.7A). The formation of neural progenitors was confirmed through immunofluorescent detection of Pax6 and nestin, two markers of neural progenitors. Positive staining was detected in both control and Patient 1 cells after six passages (Figure 5.7B). These cells were thus designated iPSC-derived NPCs (iPSC-NPCs). *Pax6* and *nestin* expression in iPSC-NPCs was confirmed by real-time PCR. Both control and MPS IIIA iPSC-NPCs exhibited significant expression of *pax6*; however, it was of note that *pax6* expression

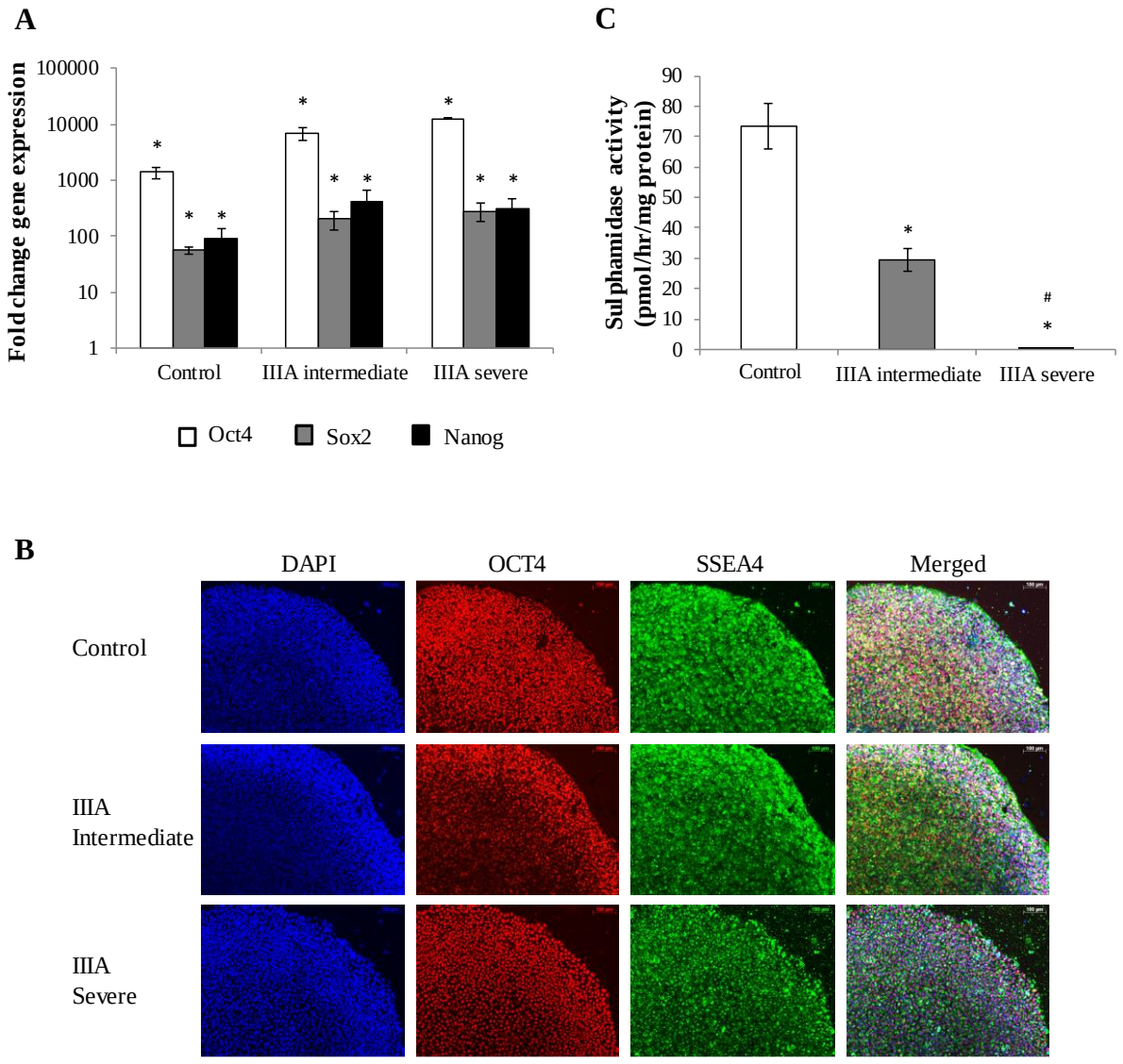

Figure 5.6: Characterisation of MPS IIIA iPSCs

A: Expression of pluripotency genes in control, Patient 1 (IIIA intermediate) and Patient 2 (IIIA severe) iPSCs. Gene expression was normalised to cyclophilin A and the fold change relative to the corresponding normal or patient fibroblasts calculated using the ΔΔCt method. Results are expressed as mean ± SEM (n=3). * indicates significant difference compared to fibroblasts ($p<0.05$; one-way ANOVA, Tukey's HSD). **B:** Immunofluorescence of control, Patient 1 (IIIA intermediate) and Patient 2 (IIIA severe) iPSCs. Images taken on an AxioCam MRm high resolution camera at 10x magnification. Scale bar represents 100µm. **C:** Sulphamidase activity of cell layers of control, Patient 1 (IIIA intermediate) and Patient 2 (IIIA severe) iPSCs. Results are expressed as mean ± SEM (n=3). * indicates significant difference compared to control iPSCs; # indicates significant difference compared to Patient 1 (IIIA intermediate) iPSCs ($p<0.05$; one-way ANOVA, Tukey's HSD).

was higher in MPS IIIA iPSC-NPC than in control iPSC-NPCs (Figure 5.7C). In line with positive immunofluorescent staining, both control and MPS IIIA iPSC-NPCs expressed *nestin*; however, expression levels were not significant (Figure 5.7C).

5.2.3.1 Proliferation

Due to the decreased proliferative capacity of MPS IIIA MSCs, proliferation was examined in MPS IIIA iPSC-NPCs. Similarly to MSCs, MPS IIIA iPSC-NPCs were found to exhibit an impaired proliferation phenotype. In control iPSC-NPCs, cell number increased to 263.9 ± 14.54% of the cell number seen one hour post-seeding (T0) after three days, significantly higher than at one day post-seeding. In contrast, MPS IIIA iPSC-NPC cell number did not significantly increase over the cell number seen one day post-seeding, with cell number only at 162.9 ± 31.7% of T0 cell number after three days (Figure 5.8A). Distinct differences were also evident when examining the slope of the line for the two iPSC-NPC cell lines, with a slope of 77.5%/day for control iPSC-NPCs and 45.3%/day for MPS IIIA iPSC-NPCs. Examination of the slope of the line only between days two and three further demonstrated the decreased proliferation of MPS IIIA iPSC-NPCs; the control iPSC-NPCs slope was 82.9%/day, whilst the MPS IIIA iPSC-NPC slope was only 9.4%/day (Figure 5.8A). In line with this finding, MPS IIIA iPSC-NPC cell number was significantly lower than control iPSC-NPCs three days post-seeding (Figure 5.8A).

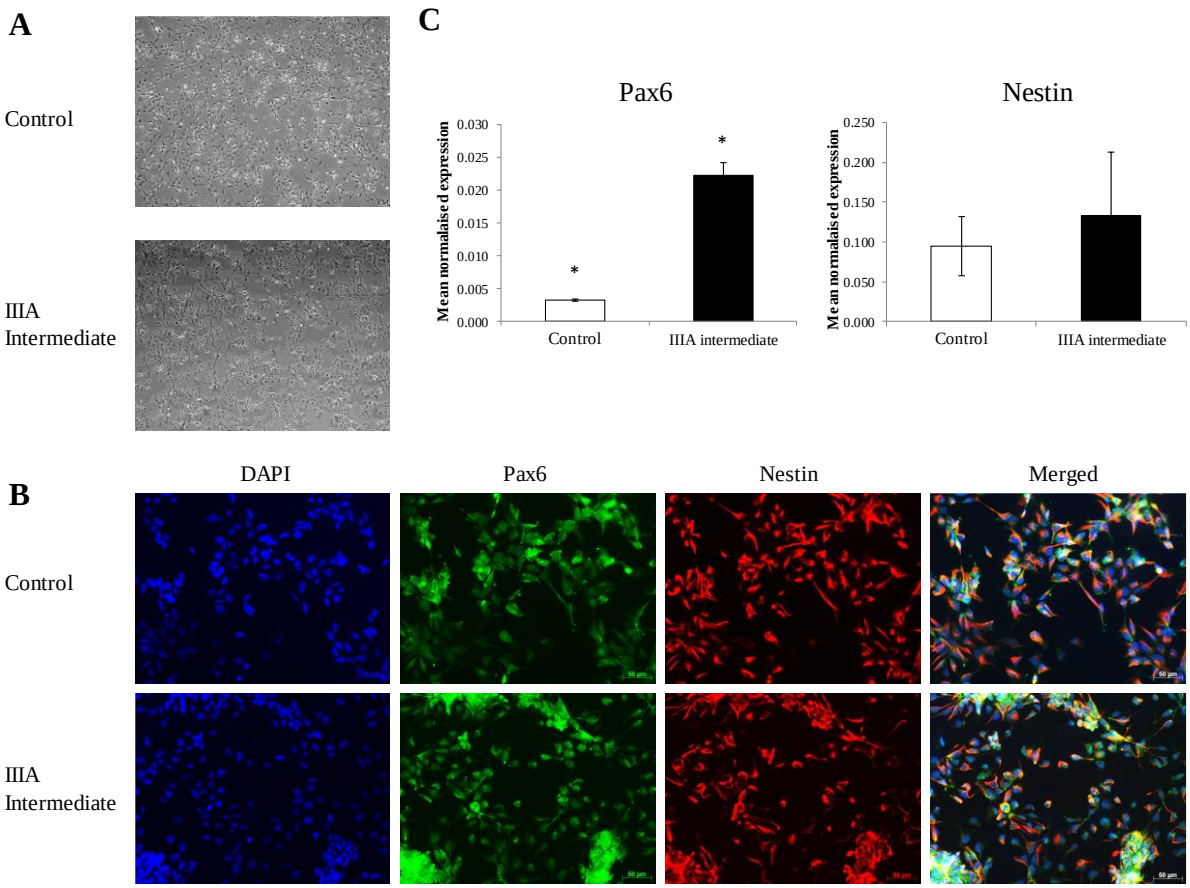

Figure 5.7: MPS IIIA iPSC-derived NPCs

A: Brightfield images of control and MPS IIIA iPSC-NPCs at passage two. Images were taken on an AxioCam MRm high resolution camera at 5x magnification. **B:** Immunofluorescence of control and Patient 1 (IIIA intermediate) iPSC-derived NPCs at passage six. Images taken on an AxioCam MRm high resolution camera at 20x magnification. Scale bar represents 50µm. **C:** Expression of neural marker genes in control and Patient 1 (IIIA intermediate) iPSC-NPCs at passage six. Mean normalised gene expression relative to cyclophilin A was calculated using the relative expression method as per Pfaffl (2001). Results are expressed as mean normalised expression ± SEM (n=3). * indicates significant difference compared to theoretical value of zero ($p<0.05$; one sample t-test).

Similar to murine MPS IIIA MSCs, exogenous sulphamidase was added to the culture media of MPS IIIA iPSC-NPCs to attempt to rescue the impaired proliferation phenotype. As iPSC-NPCs were cultured in neural expansion media containing 20ng/mL FGF-2, an FGF-2 based rescue assay was not conducted. The addition of exogenous sulphamidase had little effect on proliferation of MPS IIIA iPSC-NPCs, with no significant change in cell number (Figure 5.8B).

5.2.4 Neural differentiation of human iPSC-derived NPCs

Control and MPS IIIA iPSC-NPCs were induced to form neurons by withdrawing FGF-2 from the neural maintenance media for a total of four weeks (section 2.6.4). One day post-plating, prior to the removal of FGF-2, iPSC-NPCs maintained a neural progenitor-like morphology (Figure 5.9A and 5.9B). However, MPS IIIA iPSC-NPCs appeared to display more features characteristic of neurons, with a slightly more elongated morphology and neurite extensions visible (Figure 5.9B). iPSC-NPCs continued to proliferate in the first seven days of neural induction, with an increase in cell density evident. However, control iPSC-NPCs appeared more confluent than MPS IIIA iPSC-NPCs seven days post-induction, covering the entire surface of the well (Figure 5.9C and 5.9D). This supported the previously identified impaired proliferation phenotype of MPS IIIA iPSC-NPCs (Section 5.2.3.1). By day 10 of neural induction, a distinct neuron-like morphology was evident in control iPSC-NPCs cultures. Neuronal bodies were beginning to aggregate together and axon extensions were forming across the well (Figure 5.9E). Axon extensions were visible in MPS IIIA iPSC-NPCs; however, this was to a lesser extent that in control iPSC-NPCs. Aggregations of neuronal bodies were not evident in MPS IIIA iPSC-NPCs after 10 days of neural induction (Figure 5.9F).

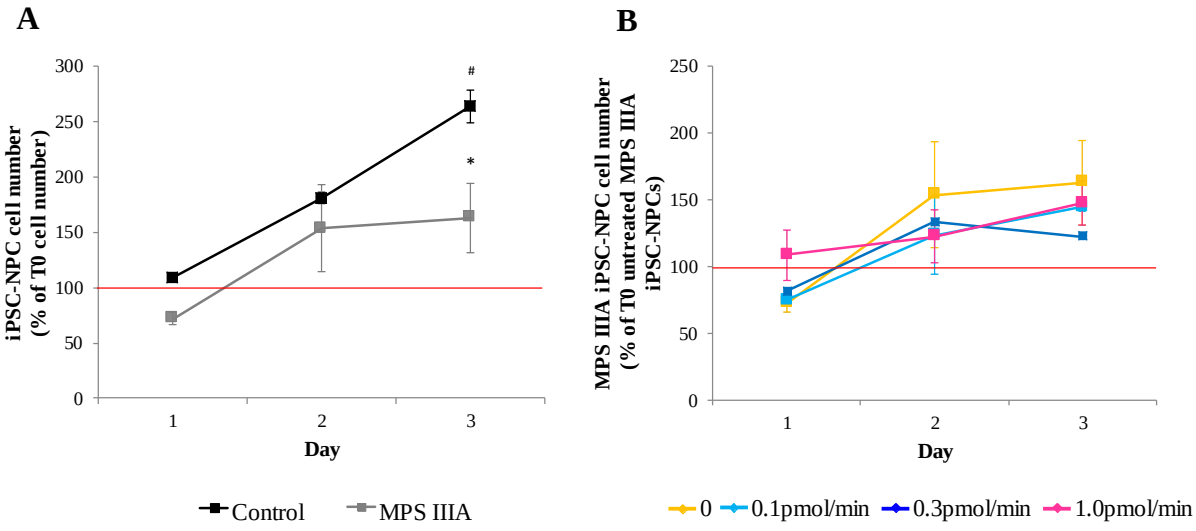

Figure 5.8: MPS IIIA iPSC-NPC proliferation

A: Cell number of iPSC-NPCs as a percentage of cell number one hour post-seeding (T0). Red line denotes T0 cell number (100%). Results are expressed as mean ± SEM (n=3). * indicates significant difference compared to control iPSC-NPCs at the same timepoint; # indicates significant difference compared to day one of the same genotype ($p<0.05$; one-way ANOVA, Tukey's HSD). **B:** Cell number of MPS IIIA iPSC-NPCs treated with exogenous sulphamidase as a percentage of untreated MPS IIIA iPSC-NPC cell number one hour post-seeding (T0). Red line denotes T0 cell number (100%). Results are expressed as mean ± SEM (n=3). No significance ($p<0.05$; one-way ANOVA, Tukey's HSD).

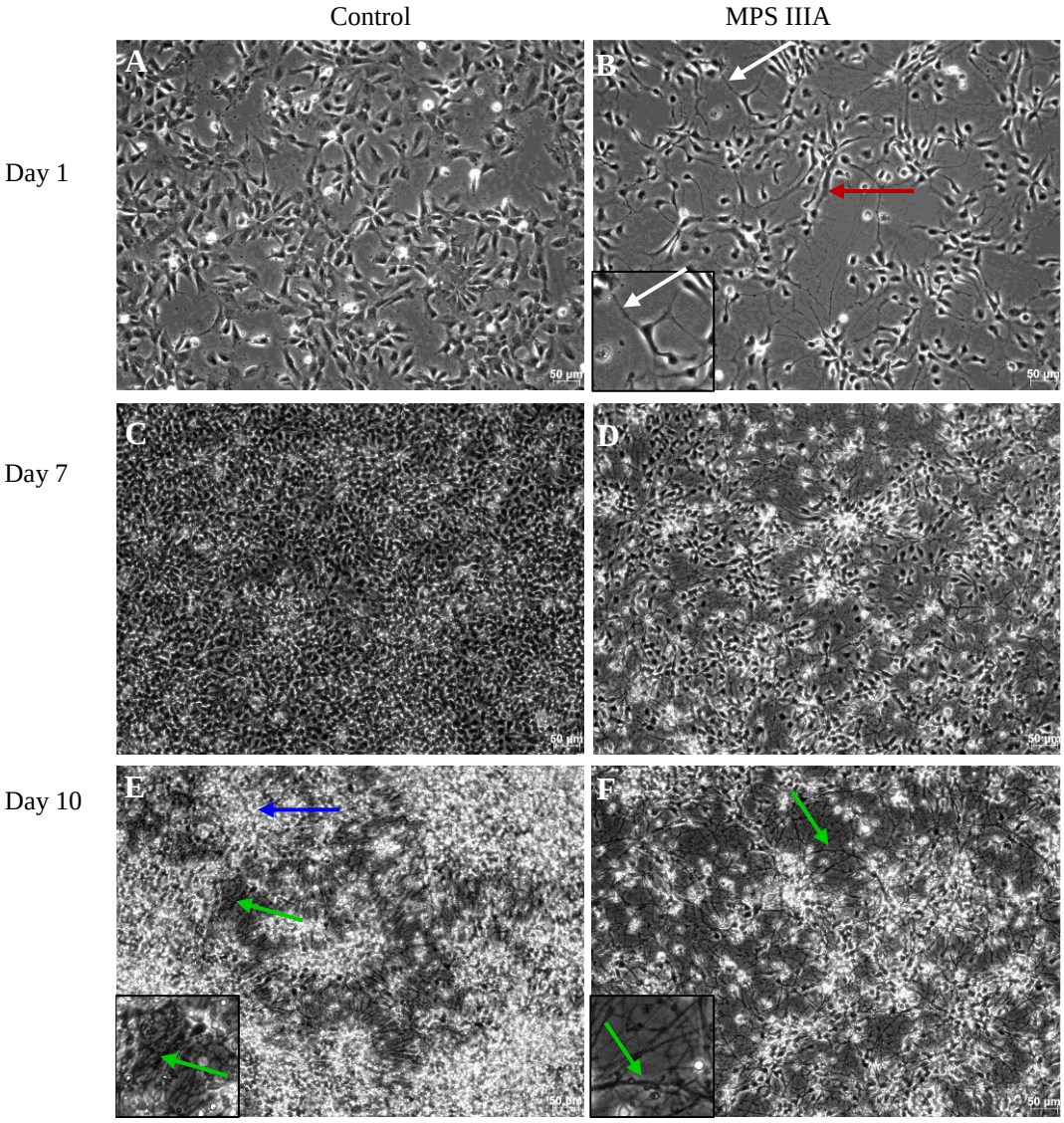

Figure 5.9: First 10 days of MPS IIIA iPSC-NPC neural differentiation

Brightfield images of control and MPS IIIA iPSC-NPCs one (A-B), seven (C-D) and ten (E-F) days post-induction. Arrows indicate an elongated cell (red), neurite extension (white), neuronal body aggregation (blue) and neurite extension (green). Boxed insert shows enlarged region of distinct morphology. Images were taken on an AxioCam MRm high resolution camera at 10x magnification. Scale bar represents 50µm.

Further changes in control iPSC-NPC morphology to that typical of neurons continued over the course of neural induction (Figures 5.10A, 5.10D and 5.10F). By day 28 of neural induction, large aggregations of neuronal bodies dominated the culture, connected by distinct axonal bundles (Figure 5.10F). This morphology was consistent across the wells in all replicates. Whilst neuron-like morphology was evident in MPS IIIA iPSC-NPCs 21 days post-induction, neuronal body aggregations were significantly smaller than what was seen in control iPSC-NPCs (Figure 5.10B). Indeed, cell body aggregates were still forming at day 21 of neural induction in MPS IIIA iPSC-NPCs, with characteristic morphology not seen in all aggregates (Figure 5.10C). By day 28 of neural induction, typical neuronal morphology was evident in MPS IIIA iPSC-NPCs, with clear aggregations of neuronal bodies and large axonal bundles extending across the culture (Figure 5.10G). However, neuronal body aggregates were much smaller in MPS IIIA iPSC-NPCs compared to control iPSC-NPCs at day 28 days of neural induction and axonal networks appeared less extensive (Figures 5.10F and 5.10G). Furthermore, neuron-like morphology was not consistent across the cultures. Confluent areas of cells without neuronal body aggregates were visible in MPS IIIA iPSC-NPCs 28 days post-induction (Figure 5.10H). Overall, both control and MPS IIIA iPSC-NPCs displayed morphological changes characteristic of various stages of neurogenesis over the course of neural induction; however, MPS IIIA iPSC-NPCs displayed a decrease in neuronal body aggregate and axonal bundle network formation compared to control iPSC-NPCs.

The expression of neural marker genes was examined to further investigate the observed morphological changes and quantify to any differences between control and MPS IIIA iPSC-NPC neurogenesis. Neural marker gene expression was determined relative to undifferentiated iPSC-NPCs cultured in neural expansion media containing FGF-2 (undifferentiated controls). Both control and MPS IIIA iPSC-NPCs expressed *nestin*, a marker of neural progenitors, throughout the course of neural induction. However, little change in expression was seen compared to undifferentiated controls, indicating that a neural

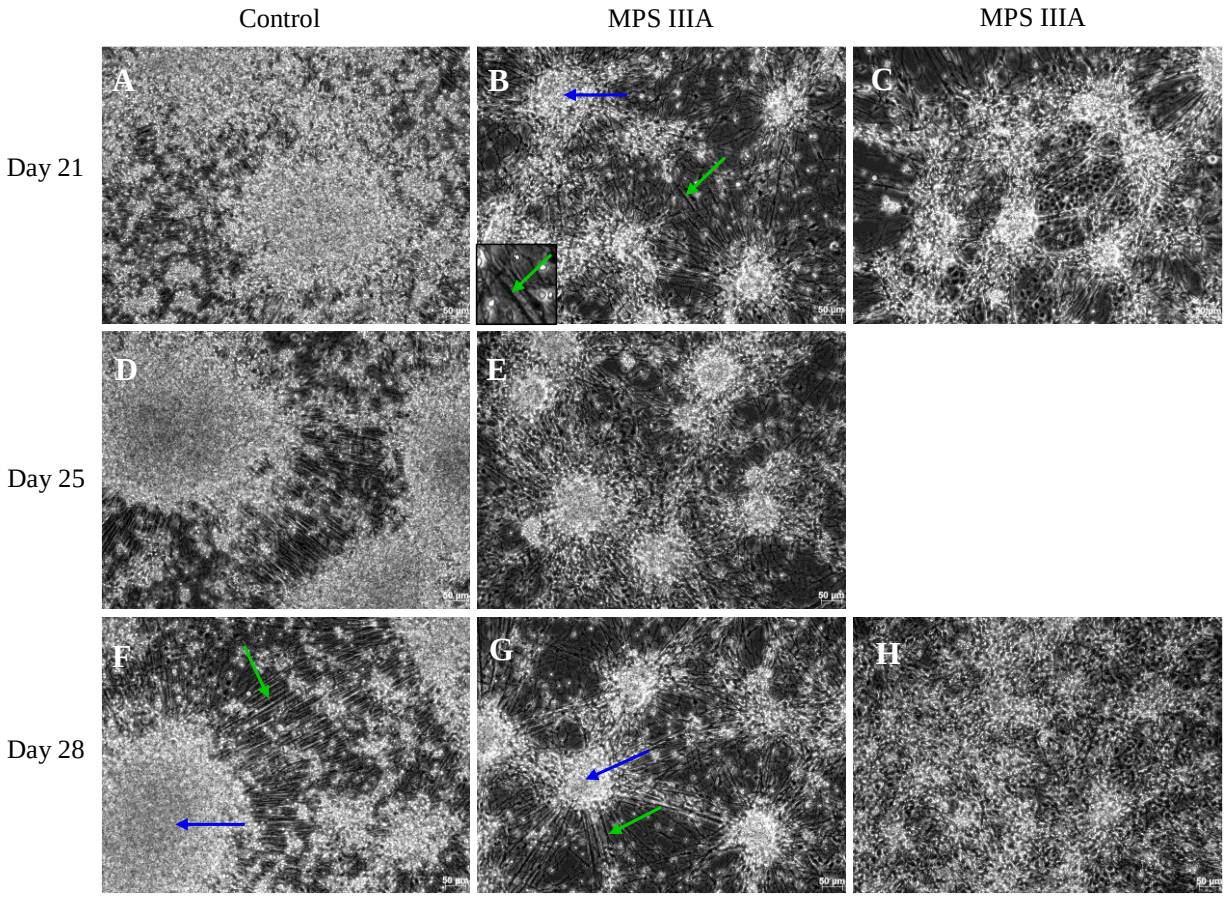

Figure 5.10: Final 8 days of MPS IIIA iPSC-NPC neural differentiation

Brightfield images of control and MPS IIIA iPSC-NPCs 21 (A-C), 25 (D-E) and 28 (F-H) days post-induction. Arrows indicates a neuronal body aggregation (blue) and axonal extension bundles (green). Boxed insert shows enlarged region of distinct morphology. Images were taken on an AxioCam MRm high resolution camera at 10x magnification. Scale bar represents 50µm.

progenitor population was maintained over the timecourse in both control and MPS IIIA iPSC-NPCs (Figure 5.11A). *βIII-tubulin* expression was increased in control iPSC-NPCs from 14 days post-induction, with 17.58 ± 7.10 and 23.94 ± 10.52 fold increases in expression 14 and 21 days post-induction compared to undifferentiated controls respectively, indicating the formation of immature neurons. Expression peaked 28 days post-induction with a significant 26.51 ± 6.31 fold increase compared to growth controls. *βIII-tubulin* expression was also upregulated in MPS IIIA iPSC-NPCs compared to undifferentiated controls following the initiation of neural induction; however, expression was consistently lower than in control iPSC-NPCs, with a 4.43 ± 2.59, 6.48 ± 5.65 and 1.76 ± 0.78 fold increase in *βIII-tubulin* expression compared to undifferentiated controls 14, 21 and 28 days post-induction respectively (Figure 5.11B).

Very little change in the expression of *NF-M*, a marker of mature neurons, was seen in either control or MPS IIIA iPSC-NPCs compared to undifferentiated controls following the initiation of neural differentiation. Expression appeared to decrease in MPS IIIA iPSC-NPCs, with 1.05 ± 0.54 fold and 7.77 ± 0.14 fold decreases in *NF-M* expression compared to undifferentiated controls 14 and 28 days post-induction respectively (Figure 5.11C). However, these differences did not reach significance. A distinct disruption in the expression of *NF-H* and *NSE*, additional markers of mature neurons, was seen in MPS IIIA iPSC-NPCs. *NF-H* expression increased steadily over the course of neural induction in control iPSC-NPCs, with significant increases of 2.01 ± 0.02 and 3.23 ± 0.27 fold compared to undifferentiated controls 21 and 28 days post-induction respectively. In contrast, no significant change in *NF-H* expression was seen in MPS IIIA iPSC-NPCs compared to undifferentiated controls, with expression significantly lower than control iPSC-NPCs 21 and 28 days post-induction, indicating a dysfunction in neuron formation (Figure 5.11D). This was supported by the decreased expression of *NSE* in MPS IIIA iPSC-NPCs compared to

control iPSC-NPCs. *NSE* expression was significantly increased in control iPSC-NPCs compared to undifferentiated controls at all timepoints, with expression peaking at 28 days post-induction with a 485.1 ± 26.87 fold increase in expression. *NSE* expression did increase in MPS iPSC-NPCs compared to undifferentiated controls, with the highest increase of 20.34 ± 15.68 fold seen 28 days post-induction, indicating the presence of neurons; however, expression was significantly lower than what was seen in control iPSC-NPCs throughout neural induction, indicating a comparative disruption in neuron formation or survival (Figure 5.11E).

5.3 Discussion

5.3.1 MPS IIIA MSCs and iPSCs recapitulate the molecular hallmarks of disease

This study has developed the first reported MPS IIIA murine MSC and human iPSC lines which recapitulate the disease phenotype seen in patients. Murine MPS IIIA MSCs and human MPS IIIA iPSCs were both found to display reduced sulphamidase activity compared to normal cells, recapitulating the disease phenotype and establishing *in vitro* models of MPS IIIA. This is in line with previously published MSC and iPSC-based models of other MPS subtypes. MSCs isolated from MPS I patients were found to recapitulate the MPS I disease phenotype, exhibiting less than 1% of normal IDUA activity, the enzyme deficient in MPS I. MPS I MSCs were used to model mesodermal differentiation *in vitro*, identifying increased osteoclastic capacity in MPS I MSCs compared to normal MSCs (Gatto et al., 2012). Human iPSC lines of MPS I, MPS II, MPS IIIB, MPS IIIC and MPS VII have been developed, all displaying decreased activity of their deficient enzyme (Bayo-Puxan et al., 2018; Canals et al., 2015; Griffin et al., 2015; Lemonnier et al., 2011; Rybova et al., 2018; Swaroop et al., 2018; Tolar et al., 2011; Vallejo-Diez et al., 2018; Varga et al., 2016a; Varga et al., 2016b, 2016c). Generating cells of the CNS is the most common use of MPS iPSCs, with MPS I,

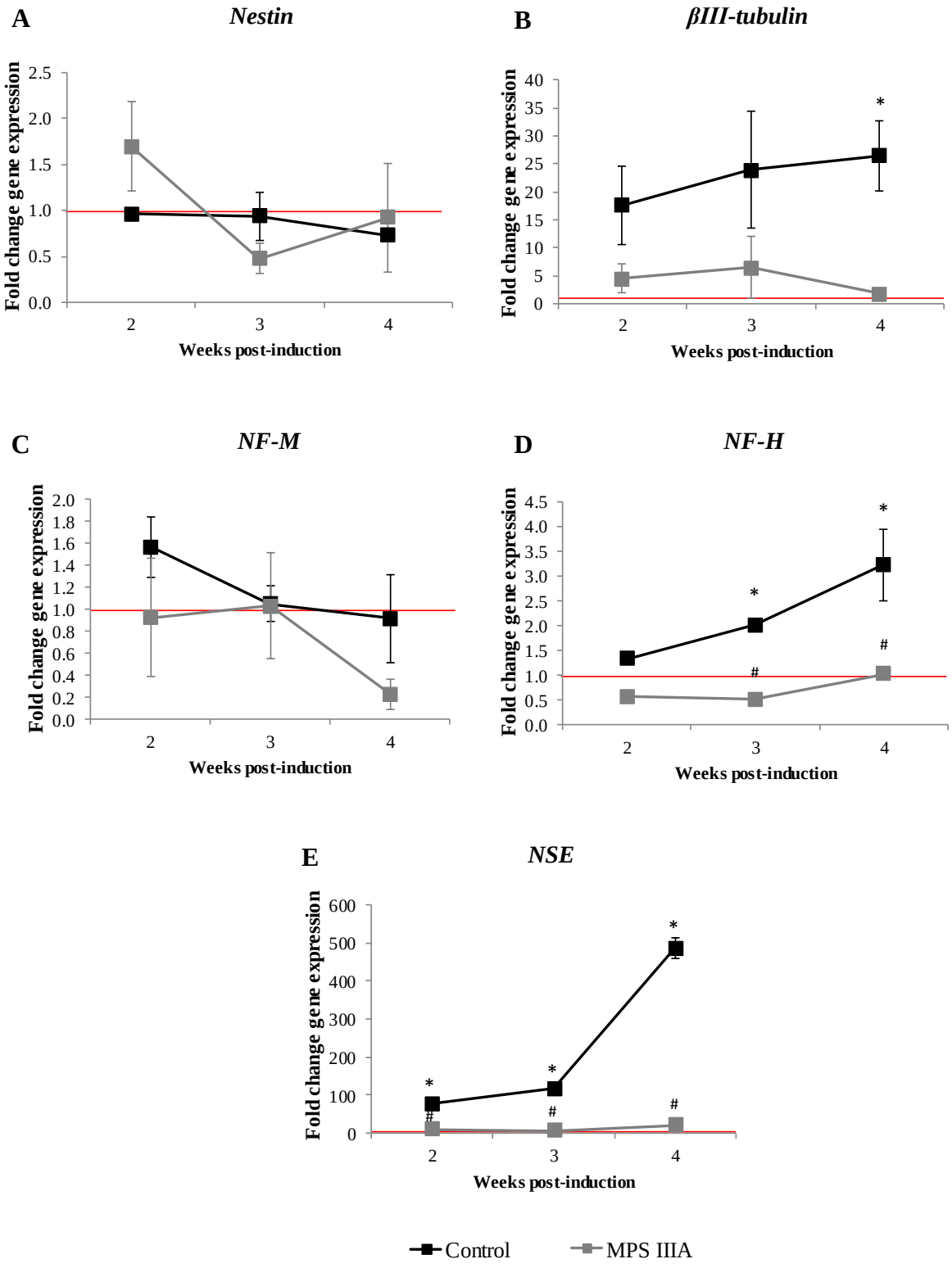
A
Nestin
Fold change gene expression
2.5
2.0
1.5
1.0
0.5
0.0
2
3
4
Weeks post-induction
B
βIII-tubulin
Fold change gene expression
40
35
30
25
20
15
10
5
0
*
2
3
4
Weeks post-induction
C
NF-M
Fold change gene expression
2.0
1.8
1.6
1.4
1.2
1.0
0.8
0.6
0.4
0.2
0.0
2
3
4
Weeks post-induction
D
NF-H
Fold change gene expression
4.5
4.0
3.5
3.0
2.5
2.0
1.5
1.0
0.5
0.0
*
*
#
#
2
3
4
Weeks post-induction
E
NSE
Fold change gene expression
600
500
400
300
200
100
0
*
*
*
#
#
#
2
3
4
Weeks post-induction
Control
MPS IIIA

Figure 5.11: MPS IIIA iPSC-NPC neural differentiation

Expression of *nestin* (A), *βIII-tubulin* (B), *NF-M* (C), *NF-H* (D) and *NSE* (E) expression throughout neural differentiation of control (black line) and MPS IIIA (grey line) iPSC-NPCs. Gene expression was normalised to cyclophilin A and the fold change relative to undifferentiated iPSC-NPCs cultured in neural expansion media (undifferentiated controls) was calculated using the ΔΔCt method. Red line denotes undifferentiated control baseline gene expression. Results are expressed as mean ± SEM (n=3). * indicates significant difference between neuronal iPSC-NPC and undifferentiated controls; # indicates significant difference between control neuronal iPSC-NPC and MPS IIIA neuronal iPSC-NPC gene expression at the same timepoint ($p<0.05$; one-way ANOVA, Tukey's HSD).

MPS II, MPS IIIB, MPS IIIC and MPS VII iPSCs all previously differentiated along the neural lineage. MPS IIIC and MPS VII iPSCs were used to model neuronal network formation and connectivity, identifying decreases in synaptic activity in MPS neurons compared to normal (Bayo-Puxan et al., 2018; Canals et al., 2015). MPS I iPSC-derived NPCs were used to identify alterations in the autosomal/lysosomal pathways, with upregulation of the autophagy pathways seen in MPS I compared to normal. MPS II and MPS IIIB iPSCs were induced to form neurons, identifying disorganised lysosomes and Golgi apparatus in affected cells (Lemonnier et al., 2011; Rybova et al., 2018; Swaroop et al., 2018). In addition to exploiting their neurogenic properties, MPS I iPSCs have also been used to model differentiation along the haematopoietic lineage in order to determine their efficacy as an alternative to HSC transplant (Tolar et al., 2011).

In this study, both the MPS IIIA MSC and iPSC lines were used for neural differentiation, allowing for *in vitro* modelling of MPS IIIA neurogenesis; however, in the future, these cell lines could be used to model differentiation along multiple lineages. Of particular interest would be the mesodermal lineages, due to the deleterious effect of MPS IIIA GAG on osteogenesis and adipogenesis identified in Chapter Four.

5.3.2 MSC and iPSC-NPC proliferation is decreased in MPS IIIA

Both MSC and iPSC-NPC proliferation was found to be impaired in MPS IIIA. Interestingly, the addition of exogenous sulphamidase was unable to rescue the phenotype. This is in contrast to MPS IIIB iPSCs, where decreased proliferation was rescued by the addition of the deficient enzyme, NAGLU (Lemonnier et al., 2011). Similarly, treatment with β-glucuronidase, the deficient enzyme in MPS VII, rescued the impaired embryoid body formation phenotype seen in murine MPS VII iPSCs (Meng et al., 2010). Lysosomal HS should be metabolised in the presence of sulphamidase; the maintenance of decreased proliferation suggests that either the amount added was insufficient to restore normal sulphamidase function or that sulphamidase was unable to reach the lysosomes. The amounts of sulphamidase used to promote proliferation in this study were based on previously successful cross-correction experiments, where exogenous sulphamidase was added to the culture media of MPS IIIA fibroblasts, to be taken up and delivered to the lysosomes and reduce GAG storage; however, the efficacy in MPS IIIA MSCs or iPSC-NPCs has not been previously examined. Interestingly, normal MSCs in this study displayed sulphamidase activity of 0.67 ± 0.07 pmol/min (presented as 79.04 ± 8.02 pmol/hr/mg protein when normalised to total protein content), well within the scope of the sulphamidase activities of 0.1, 0.3 and 1.0 pmol/min used in the proliferation rescue assay, indicating that the amount added should have been sufficient to restore normal sulphamidase function; however, MPS IIIA MSCs remained unable to proliferate. Measuring sulphamidase activity within the

lysosomes of MPS IIIA MSCs, and likewise iPSC-NPCs, would determine if exogenous sulphamidase was reaching the lysosomes following its addition to the culture media. Furthermore, due to the vital role of the cation independent mannose 6-phosphate receptors (CI-M6PR) in the trafficking of sulphamidase into the lysosomes in fibroblasts, it would be of interest to determine if sulphamidase uptake is similarly mediated by CI-M6PRs in MSCs and iPSC-NPCs. Determining CI-M6PR expression and turnover in MPS IIIA MSCs and iPSC-NPCs would be of interest, as any alterations would influence the ability of exogenous sulphamidase to reach the lysosomes and thus the concentration of sulphamidase required to restore normal sulphamidase function.

Exogenous FGF-2 was found to increase proliferation of MPS IIIA MSCs in a dose dependent manner, with cell number increasing as the FGF-2 concentration increased. The ability of exogenous FGF-2 to rescue the impaired proliferation seen in MPS IIIA MSCs suggests a role for FGF-2 signalling in the proliferation phenotype. FGF-2, reliant on HS chains for signalling, is a known promoter of proliferation, playing a vital role in formation of the CNS, with high levels present throughout neural development (refer section 1.3.1.1). One potential mechanism is that excess intrinsic MPS IIIA HS secreted from MSCs, displaying altered sulphation patterns compared to normal HS, is sequestering FGF-2, preventing FGF-2 signalling, as discussed at length in Chapter Four. This hypothesis is supported by the increase in proliferation seen in the presence of FGF-2, as this would allow more of the morphogen to reach the cell surface and initiate FGF-2 signalling. The dose dependent effect of FGF-2 on MPS IIIA MSC proliferation further supports this hypothesis. Indeed, MPS I HS has previously been shown to interfere with FGF-2:FGFR1:HS interactions, resulting in decreased FGF-2 mediated proliferation (Pan et al., 2005). However, due to the mitogenic effect of FGF-2, further investigation would be required for confirmation. This is the first report of MSC isolation from an MPS mouse model and thus it is unknown if other MPS

subtypes also display alterations in proliferation. MSCs isolated from MPS I patients were able to expand normally in culture, suggesting that the disrupted proliferation of MPS IIIA MSCs may be unique; however, further analysis would be required for confirmation.

An FGF-2 rescue assay was not conducted in MPS IIIA iPSC-NPCs as the cells were cultured in neural expansion media containing 20ng/mL FGF-2, a significantly higher concentration than the 5ng/mL used as the maximum concentration in the MPS IIIA MSC rescue assay. The disrupted proliferation of MPS IIIA iPSC-NPCs in the presence of such high concentrations of FGF-2 suggests that an alternate mechanism was impairing iPSC-NPC proliferation compared to MSC proliferation in MPS IIIA; other HS-dependant signalling pathways, such as the Wnt and Hh pathways, are also involved in proliferation and are therefore likely candidates (Chenn & Walsh, 2002; Hirabayashi et al., 2004; Plaisant et al., 2011). It would also be of interest to examine the effect of further increases in FGF-2 concentration in MPS IIIA iPSC-NPCs on proliferation; however, it should be noted that changes in FGF-2 concentration may influence the ability of iPSC-NPCs to maintain a neural progenitor state. To date, no other MPS iPSC-derived NPC cell lines have displayed reductions in proliferation and thus the phenotype present in MPS IIIA appears to be, thus far, unique to this MPS type.

In contrast to MSCs and iPSC-NPCs, MPS IIIA iPSCs did not appear to display disruptions in proliferation. However, it should be noted that iPSC proliferation was not quantified, due the propensity of iPSCs to grow as colonies rather than as single cells. However, colony size and density, in addition to the days between passages, was not notably different between control, Patient 1 and Patient 2 iPSCs. This contrasts with MPS IIIB and MPS VII iPSCs, which were observed, by eye, to have a clear, obvious reduction in growth (Lemonnier et al., 2011; Meng et al., 2010). Supplementation with their deficient enzymes was required to stimulate

proliferation. However, the proliferative capacity of previously derived MPS iPSCs has been variable, with all other MPS iPSC lines expanding easily in culture without exogenous enzyme supplementation (refer section 1.4.2.2). iPSC media consistently contains FGF-2 to maintain pluripotency; therefore, it is possible that disparities in FGF-2 concentration are contributing towards the varied proliferation phenotypes evident amongst MPS iPSC lines. Proliferation was only disrupted in MPS IIIB iPSCs grown under feeder-dependent conditions of 10ng/mL FGF-2; under feeder-free conditions, iPSCs were cultured in the presence of 100ng/mL FGF-2 and exhibited a normal proliferation phenotype (Lemonnier et al., 2011). For our studies, iPSCs were cultured in 100ng/mL FGF-2 under feeder-free conditions, a significant increase to the 20ng/mL used in iPSC-NPC culture and the 5ng/mL used for MSC rescue assays. This increase in FGF-2 concentration may have promoted MPS IIIA iPSC proliferation by rescuing any potential disruptions as a result of aberrant HS.

Overall, this study has identified that stem cell proliferation appears to be impaired in MPS IIIA MSCs and iPSC-NPCs, but not iPSCs, likely as a result of alterations in the FGF-2 signalling pathway by MPS IIIA HS. Further investigation into downstream processes of FGF-2 signalling, such as activation of the MAPK pathway, should be examined for confirmation. In addition, it would be of note to determine the contribution of other HS-dependent signalling pathways, such as the Wnt, BMP and Hh pathways, towards the impaired proliferation phenotype of MPS IIIA.

5.3.3 MSC and iPSC neurogenesis is disrupted in MPS IIIA

MPS IIIA appeared to disrupt neurogenesis, with significant decreases in neural gene expression in both MPS IIIA MSCs and iPSC-NPCs compared to control cells. In MPS IIIA MSCs, a rapid decrease in *βIII-tubulin* expression was seen over the course of neurogenesis and expression of *NF-M* was significantly decreased compared to normal MSCs from eight

hours post-induction, indicating a dysfunction in immature neuron survival and maturation into post-mitotic neurons.

When examining iPSC-derived neural induction, neural progenitor formation appeared unaffected in MPS IIIA, with formation of the integral neuroepithelial sheet and neural rosettes unchanged between control and Patient 1 (MPS IIIA intermediate) derived-iPSCs. Both control and MPS IIIA iPSC-NPCs displayed neural progenitor-like morphology and expressed markers of neural progenitors, *pax6* and *nestin*, indicating the successful formation of a neural progenitor population from patient-derived iPSCs. Expression of the generic NSC marker, *nestin*, was comparable between control and MPS IIIA iPSC-NPCs, indicating a similar global neural progenitor population and formation capacity. However, MPS IIIA iPSC-NPCs were found to express higher levels of the dorsal cortical progenitor marker, *pax6*, compared to control iPSC-NPCs, suggesting that the specific makeup of the heterogenous neural progenitor population may vary between the two lines (Zhang et al., 2010). Confirmation of the neural progenitor population in the two cell lines through analysis of additional generic neural progenitor markers such as *Sox1* (Venere et al., 2012) would be advantageous. Further investigation would be required to interrogate any underlying differences in the makeup of the control and MPS IIIA heterogenous neural progenitor populations

Similarly to MPS IIIA MSCs, neuronal differentiation was impacted in MPS IIIA iPSC-NPCs. MPS IIIA iPSC-NPC morphology appeared more “neuronal” immediately prior to neural induction, with neurite extensions and a more elongated morphology evident. However, upon differentiation, several lines of evidence suggested that MPS IIIA iPSC-NPC cultures had reduced numbers of neurons. MPS IIIA cultures did not display the same degree

of overt neuronal morphology, with delayed formation and reduced presence of neuronal body aggregates (ganglion-like structures) and less prominent axonal bundles. The expression of several post-mitotic neuron marker genes was decreased in MPS IIIA iPSC-NPCs compared to control iPSC-NPCs, with the difference becoming more prominent as neurogenesis progressed. In contrast, no significant change in *nestin* expression was seen between control and MPS IIIA iPSC-NPCs throughout neural induction, indicating that neural progenitor formation was unaffected in MPS IIIA iPSC-NPCs. Thus, this data indicated that MPS IIIA iPSCs were able to form neural progenitors; however, the formation or survival of neurons was disrupted.

FGF-2 was implicated in disrupting MSC proliferation (section 5.2.1.3); due to its integral role in CNS development (refer section 1.3.1.1), it was hypothesised that aberrant FGF-2 signalling may also contribute towards the disruptions in neurogenesis observed in MPS IIIA MSCs and iPSC-NPCs. Aberrations in neurogenesis in MPS IIIA iPSC-NPCs may result from intrinsic MPS IIIA HS-mediated sequestration of FGF-2 ligands, as discussed previously, as exogenous FGF-2 is withdrawn from iPSC-NPCs for neural differentiation, thus decreasing its bioavailability. However, murine MSC neural differentiation is promoted through supplementation with 40ng/mL FGF-2; the high bioavailability of FGF-2 throughout neural differentiation suggests that FGF-2 sequestration is an unlikely underlying mechanism for disrupted neural differentiation in MPS IIIA MSCs. Thus, a different mechanism may be involved in disrupted MSC neurogenesis compared to iPSC-NPC neurogenesis. It is likely that other HS-dependent signalling pathways are also affected by excess, aberrantly sulphated MPS IIIA HS and contribute towards disrupted neurogenesis. One likely pathway is the Wnt signalling pathway, which requires HS chains to function and is highly involved in neurogenesis (refer section 1.3.1.2). Canonical Wnt signalling is responsible for regulating the switch between proliferation and neurogenesis, with increases in Wnt signalling inhibiting

proliferation and promoting differentiation of neural progenitors. Inhibition of Wnt signalling was found to decrease neural differentiation (Hirabayashi et al., 2004). Therefore, a disruption of Wnt signalling, likely via sequestration of Wnt morphogens by intrinsic, aberrant MPS IIIA HS in the ECM, could potentially contribute towards the disruptions in neurogenesis seen in this study.

The contribution of the sulphamidase deficiency towards impaired neurogenesis was not directly examined in this study. Previous work has identified that an increase in activity of the deficient enzyme reversed or partially reversed aberrant pathology seen in MPS iPSCs or MPS iPSC-derived neural cells (Bayo-Puxan et al., 2018; Canals et al., 2015; Lemonnier et al., 2011; Meng et al., 2010). Therefore, it would be of interest to determine if supplementation with exogenous enzyme would be sufficient to restore the neural differentiation capacity of MPS IIIA MSCs or iPSC-NPCs. A further point of interest would be to examine any changes in neural differentiation between Patient 1 and Patient 2 iPSCs. Whilst sulphamidase activity was lower in both Patient 1 and Patient 2 fibroblasts and iPSCs compared to control cells, enzyme activity was lowest in the cells from Patient 2, who clinically displayed the most severe phenotype. Identifying a correlation between residual enzyme activity level and neural differentiation capacity could assist in identifying the contribution of sulphamidase activity towards the neurological pathology of MPS IIIA. A correlation between patient disease severity and iPSC phenotype (i.e. enzyme activity, GAG storage and lysosomal size) has recently been identified in MPS I (Swaroop et al., 2018). Neurogenesis was not examined; however, alterations in the expression of lysosomal and autosomal genes compared to normal were identified, with the most extensive changes seen in the severe Hurler syndrome subgroup and the least changes seen in the milder Scheie syndrome (Swaroop et al., 2018). Finally, CRISPR-mediated correction of the mutation in the

SGSH gene would be required to confirm the contribution of the *SGSH* mutation and subsequent reduction in sulphamidase activity towards impaired neurogenesis.

5.3.4 Chapter conclusions

This chapter aimed to develop MPS IIIA stem cell lines in order to model MPS IIIA neurogenesis *in vitro*. MSCs were isolated from an MPS IIIA mouse model and found to have significantly reduced sulphamidase activity compared to MSCs isolated from normal mice, modelling the human disease phenotype. Fibroblasts obtained from MPS IIIA patients similarly displayed significantly decreased sulphamidase activity compared to controls, with this reduced enzyme activity maintained following reprogramming to iPSCs. Both MSCs and iPSCs were used to model MPS IIIA neurogenesis *in vitro*, identifying a reduction in proliferation and a disruption in neurogenesis, primarily in neuron formation and survival, likely a result of alterations in HS-dependent signalling pathways due to the presence of excess, aberrantly sulphated MPS IIIA HS. The FGF and Wnt pathways are suggested as potentially affected pathways due to their roles in regulating neural progenitor proliferation and maturation. This supports the findings of Chapter Four and indicates that disruptions in neurodevelopmental pathways, including neural progenitor proliferation and neurogenesis, are a potential mechanism of pathology for the neurological disease of MPS IIIA.

Chapter Six: Discussion and Conclusions

6.1 Disrupted stem cell proliferation and neurogenesis are likely contributors towards CNS pathology in MPS IIIA

MPS IIIA results from a deficiency in the enzyme sulphamidase, leading to the accumulation of the GAG HS (Neufeld & Muenzer, 2001). Patients with MPS IIIA display severe neurological pathology and mild skeletal disease; however, the contribution of MPS IIIA HS accumulation to disease pathology is poorly understood. Currently, no treatments are available for MPS IIIA patients and thus determining the underlying mechanisms of pathology is integral for designing more effective therapies.

This study identified that MPS IIIA HS, in contrast to normally sulphated HS, impaired MSC differentiation along the neurogenic lineage following its addition to the culture media. Therefore, disrupted neurogenesis is likely an underlying mechanism contributing to the severe CNS pathology of MPS IIIA. Osteogenesis was similarly disrupted by MPS IIIA HS, indicating that impaired osteogenesis may be contributing towards the mild skeletal pathology seen in MPS IIIA patients.

Two *in vitro* cell models of MPS IIIA were developed to investigate the effects of MPS IIIA on neurogenesis. A reduction in cell proliferation was seen in MPS IIIA murine MSCs and human iPSC-NPCs compared to normal cells, indicating that decreased progenitor proliferation may contribute towards MPS IIIA disease pathology. Similarly to the results seen for extrinsic MPS IIIA HS, both models identified disruptions in neurogenesis in the MPS IIIA cell lines, supporting the original findings that MPS IIIA HS alters the neurogenic potential of stem cells. Therefore, disrupted stem cell proliferation and neurogenesis were identified as major contributors to CNS pathology in MPS IIIA.

The effects of HS accumulation (or reduced HS turnover) on CNS pathology are likely to commence during development, as increased HS content can be seen prenatally in MPS IIIA (Ceuterick et al., 1980; Greenwood et al., 1978; Harper et al., 1974; Martin & Ceuterick, 1983). Reduced proliferative capacity is likely to decrease the initial pool of neuroepithelial and radial glial (RG) cells; developmental neurogenesis is also likely to be disrupted, and thus potentially irreversible CNS damage may be occurring *in utero*. Indeed, stabilisation of CNS pathology, not improvement, is the best report from therapies currently at the clinical trial stage for MPS IIIA (Jones et al., 2016; Tardieu et al., 2014). The implication of neural progenitor expansion and neurogenesis as contributors to CNS pathology in MPS IIIA suggests that neurodevelopmental pathways are disrupted in MPS IIIA and contributing to the disease phenotype. This was surprising due to the neurodegenerative phenotype and classification of the disease. However, this supports a previous suggestion that the CNS pathology of MPS IIIA may have a neurodevelopmental component, likely due to the presence of excess, aberrant MPS IIIA HS, following the finding that excitatory postsynaptic structure and function is abnormal in the developing somatosensory cortex in the MPS IIIA mouse model (Dwyer et al., 2017). In patients, the delayed onset of symptoms and late diagnosis prevent examination for any potential changes in CNS phenotype at birth; earlier changes suggest aberrations in neurodevelopmental pathways compared to neurodegenerative. To our knowledge, CNS structure and potential brain malformations have not been investigated in MPS IIIA patients through Magnetic Resonance Imaging (MRI) imaging at birth. However, MRI has identified structural abnormalities, increased white matter lesions, a decrease in grey matter volume, cortical atrophy and hydrocephalus from between 12 months and 2 years of age, indicating that changes in the CNS are present from an early age, often before the onset of symptoms, suggesting that changes in neurodevelopmental neurogenesis may contribute to the CNS pathology of MPS IIIA (Reichert et al., 2016; Shapiro et al., 2016; Truxal et al., 2016).

Neurogenesis continues in the SGZ in the dentate gyrus of the hippocampus and the SVZ of the lateral ventricles in adult mammals; therefore, reduced adult neurogenesis may also contribute to the progressive, neurodegenerative nature of MPS IIIA CNS pathology (Cameron et al., 1993; Garcia-Verdugo et al., 1998). Whilst commencing prenatally, GAG storage increases over time, likely resulting in ongoing complications within the adult NSC niches. Indeed, due to the adult source of our stem cells, our neurogenesis studies may more closely model adult neurogenesis. Progressive deterioration of adult neurogenesis is linked with ageing in normal rodents and is prominent in other CNS disorders, including animal models of Alzheimer's disease and Parkinson's disease (Faure et al., 2011; Hoglinger et al., 2004; Wirths, 2017). Adult neurogenesis is particularly implicated in neural plasticity, the ability of the brain to adapt to new experiences and create new neural pathways (Ming & Song, 2005; Schmidt-Hieber et al., 2004; Toda & Gage, 2018). Neural plasticity is integral for memory and the ability to learn new skills, and thus a decrease in adult neurogenesis could underly the inability of MPS IIIA patients to learn and retain new information and skills as their disease progresses (Mangina & Sokolov, 2006; Neufeld & Muenzer, 2001; Schmidt-Hieber et al., 2004). Decreased adult neurogenesis could contribute towards the severe cortical atrophy seen in MPS IIIA patients at the later stages of the disease. It has been suggested that neuronal death may not be the sole underlying mechanism of this phenotype; thus, a reduction in adult neurogenesis, including RG survival and expansion, could provide an additional potential mechanism for this phenotype (Hassiotis et al., 2014; Jardim et al., 2010; Neufeld & Muenzer, 2001; Wilkinson et al., 2012).

6.2 Dysfunctions in stem cell proliferation and differentiation in MPS IIIA are likely a result of alterations in growth factor signalling

This study identified a potential mechanism for the severe neurological pathology of MPS IIIA, with MPS IIIA HS disrupting neural progenitor proliferation and maturation. However,

the specific means by which MPS IIIA HS disrupted stem cell development was not investigated in detail and was beyond the scope of this thesis. It was hypothesised that the HS which accumulates in MPS IIIA was disrupting signalling pathways integral to stem cell proliferation and differentiation, due to reliance of these pathways on HS chains to function. The data in this thesis suggested that a "morphogen sequestration" model may occur, whereby excess, partially degraded extracellular MPS IIIA HS secreted from the lysosomes is able to bind signalling molecules. Whilst the sequence of HS fragments that accumulate in MPS IIIA has not been determined, the altered patterns of sulphation along the HS backbone in partially degraded MPS IIIA GAG are likely to alter its ability to bind to morphogens. For example, MPS IIIA HS is known to be enriched for disaccharides contained within the GlcNS(6S)-IdoA(2S)-GlcNS(6S)-IdoA(2S) tetrasaccharide integral for interactions between HS and FGF-2, one of the most well-studied morphogens (refer section 4.3.1.2 for detailed discussion) (Guglier et al., 2008; Pye et al., 1998; Raman et al., 2003; Wilkinson et al., 2012). This is likely to result in a subsequent increase in FGF-2 binding to MPS IIIA HS compared to normal HS. However, this is dependent on specific tetrasaccharide formations. Therefore, the combination of high extracellular GAG concentrations and the presence of aberrant sulphation patterns may result in extracellular MPS IIIA HS binding morphogens, resulting in morphogen sequestration and preventing their binding to receptors located on the cell surface (Figure 6.1). This was supported by the observation that excess FGF-2 was able to rescue proliferation of MPS IIIA MSCs, likely a result of a higher amount of FGF-2 able to saturate the ECM located MPS IIIA HS and reach the cell-surface-bound receptors (section 5.2.1.3). Decreased morphogen-receptor interactions would result in a subsequent reduction in signalling activity in pathways such as the FGF, Wnt, BMP and Hh pathways, thus decreasing the expression of target genes involved in stem cell proliferation and differentiation.

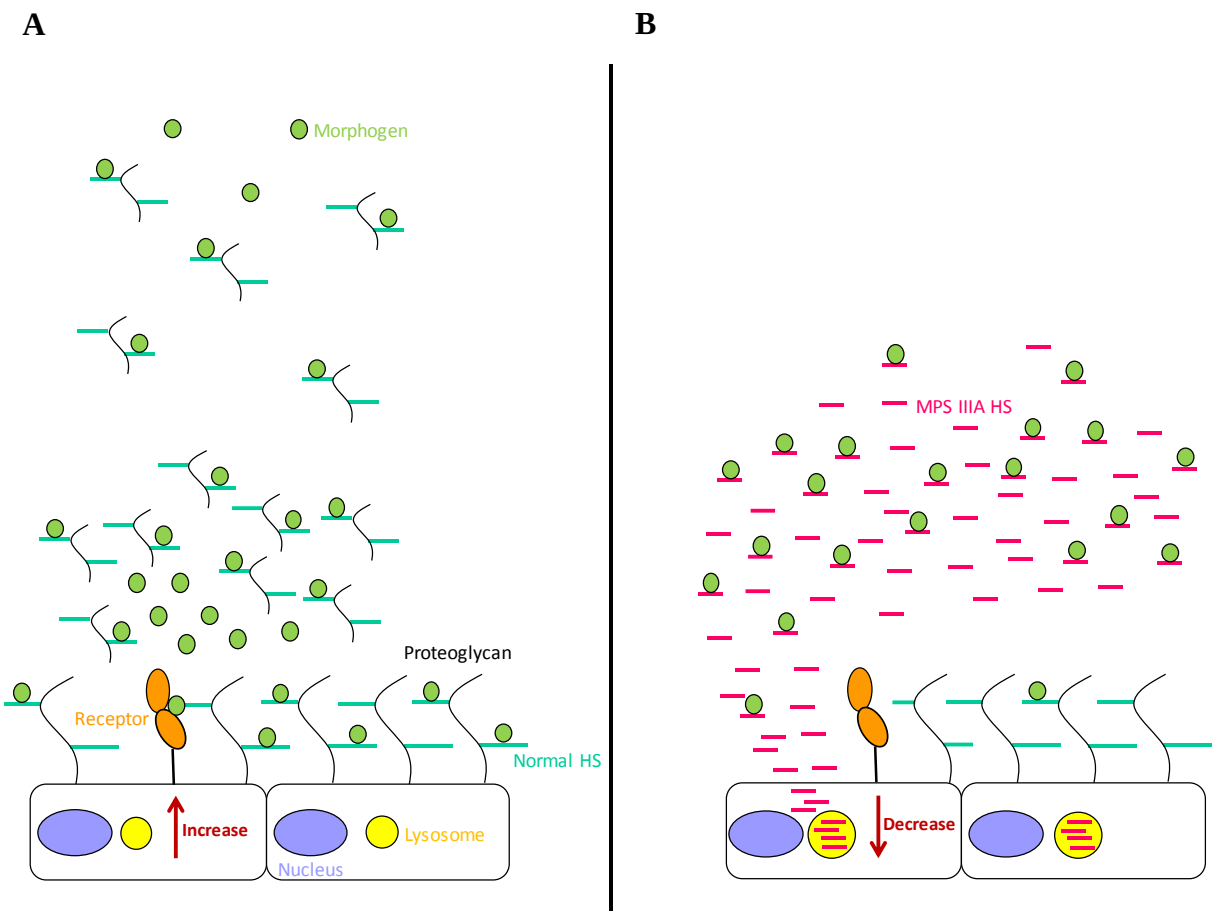

Figure 6.1: The proposed "morphogen sequestration" model

MPS IIIA HS may disrupt stem cell proliferation and differentiation by binding to morphogens and sequestering them within the ECM, away from their receptors at the cell surface. **A:** Under normal conditions, HS functions as a PG at the cell surface and within the ECM and is later metabolised within the lysosomes. Extracellular HS binds to morphogens through low affinity interactions, increasing morphogen concentration at the cell surface. Morphogens are released from ECM HS and instead bind to cell surface-bound receptors, mediated by cell surface-bound HS chains. Binding of morphogens to their receptors initiates the subsequent signalling pathway, resulting in upregulation of genes involved in stem cell proliferation and differentiation. **B:** In MPS IIIA, partially degraded HS accumulates within the lysosomes and is released into the ECM. High volumes of MPS IIIA HS within the ECM bind to morphogens. Morphogens remain bound to ECM MPS IIIA HS and are sequestered within the ECM, unable to reach cell surface-bound receptors and cell surface-bound HSPGs. As a result, signalling pathway is decreased, resulting in decreased expression of genes involved in stem cell proliferation and differentiation.

6.3 Potential uses of MPS IIIA stem cell models

6.3.1 Mechanisms of pathology

This study determined that MPS IIIA HS impairs stem cell proliferation and differentiation, with the dysfunction in neural progenitor proliferation and maturation likely contributing to the severe CNS pathology evident in patients. This was determined through the development of multiple *in vitro* models of MPS IIIA, allowing the effects of both extrinsic and intrinsic MPS IIIA HS to be determined. These models could now be used for further investigation of mechanisms of pathology in MPS IIIA.

6.3.1.1 Further investigation into the effects of MPS IIIA HS on neurogenesis

To continue the initial findings presented in this thesis, the cell models developed in these studies could be used to investigate the mechanisms underlying disrupted MPS IIIA neurogenesis. For example, the MPS IIIA cell lines developed in this thesis could be used to investigate and test the proposed "morphogen sequestration" model (Figure 6.1). Morphogen sequestration could be examined by investigating defects in the downstream HS-dependent signalling pathways, a functional outcome of the proposed model. Investigating specific pathways will also provide evidence of the precise growth factors involved. The FGF signalling pathway in particular has been discussed at length throughout this thesis; examining levels of downstream proteins in the MAPK pathways would be beneficial to confirm its role. However, examining levels of downstream proteins in the β-catenin, Gli and Smad pathways would allow the role of the Wnt, Hh and BMP pathways, respectively, to be elucidated.

Chapter Four demonstrated that extrinsic GAGs from different MPS types differed in their effects on neurogenesis. It would be of interest to compare the effects of intrinsic GAG accumulation in the different MPS subtypes on neurogenesis. The availability of mouse

models of MPS I, MPS II, MPS IIIA, MPS IIIB, MPS IIIC, MPS IIID and MPS VII would enable the isolation of MSCs from all MPS types with neurological pathology (Bhaumik et al., 1999; Birkenmeier et al., 1989; Clarke et al., 1997; Li et al., 1999; Marco et al., 2016; Muenzer et al., 2002; Roca et al., 2017; Tomatsu et al., 2002). iPSC lines have been established for MPS I, MPS II, MPS IIIB, MPS IIIC and MPS VII, providing cells of human origin to investigate if intrinsic MPS IIIA HS is uniquely pathogenic (Bayo-Puxan et al., 2018; Canals et al., 2015; Griffin et al., 2015; Lemonnier et al., 2011; Rybova et al., 2018; Swaroop et al., 2018; Tolar et al., 2011; Vallejo-Diez et al., 2018; Varga et al., 2016a; Varga et al., 2016b, 2016c). MPS VII iPSC lines have been used to study neurogenesis *in vitro* and *in vivo* in comparison to normal cells. *In vitro*, no change in *βIII-tubulin* expression was seen over the course of neural induction in MPS VII iPSCs compared to normal iPSCs, indicating that *GUSB* mutation and MPS VII GAG storage had no effect on immature neuron formation (Bayo-Puxan et al., 2018). Similarly, no difference in migration or neural differentiation was seen between normal and MPS VII iPSC-derived NSCs following their administration to normal mice, once again indicating that MPS VII GAG had little effect on neurogenesis (Griffin et al., 2015). In MPS IIIC, synaptic activity was reduced in MPS IIIC iPSC-derived neurons, indicating that *HGSTAT* mutation and MPS IIIC GAG disrupted synaptogenesis. No dysfunction in neuron formation was reported (Canals et al., 2015). Therefore, currently MPS IIIA is the only MPS disorder to report impaired neurogenesis as a potential underlying mechanism of pathology, as identified in this thesis.

In addition, to further investigate the effects of MPS IIIA HS on neurogenesis, these cell models could be used to determine any other dysfunctions in CNS development which could contribute to MPS IIIA disease pathology. In particular, the MPS IIIA iPSC line could be used to investigate alterations in synaptic activity compared to controls; MPS IIIC and MPS VII iPSCs have previously been used to model neuronal network formation and have identified

dysfunctions in neuronal activity and synaptic connectivity (Bayo-Puxan et al., 2018; Canals et al., 2015).

6.3.1.2 Contribution of the MPS IIIA CNS environment to neurological pathology

The addition of exogenous MPS IIIA GAG decreased neurogenesis in normal MSCs (section 4.2.1), indicating that, in additional to primary HS storage, the MPS IIIA microenvironment plays a role in CNS dysfunction. The microenvironment of the MPS IIIA brain is extremely complex, with increased ganglioside and cholesterol storage and significant neuroinflammation (Constantopoulos & Dekaban, 1978; McGlynn et al., 2004). Through the combination of the MPS IIIA mouse model and MPS IIIA iPSCs, the effect of the MPS IIIA brain microenvironment on neurogenesis could be determined. Administrations of MPS IIIA iPSCs to normal mice and normal iPSCs to MPS IIIA mice would allow direct comparison of the effects of the intrinsic cellular pathology and the external aberrant microenvironment on stem cell survival and proliferation. This would be integral for determining the efficacy of stem cell-based therapies, which will be discussed in section 6.3.2.

6.3.1.3 Modelling MPS IIIA mesodermal lineage differentiation

In addition to examining the effects of intrinsic MPS IIIA HS on neurogenesis, the MPS IIIA stem cell models developed in this thesis could be used to determine their effects on other lineages. Chapter Four identified a decrease in osteogenesis and adipogenesis of normal human MSCs in the presence of extrinsic MPS IIIA HS (section 4.2.2.1 and 4.2.2.3). Similarly to the work done for neurogenesis, as presented in this thesis, inducing the MPS IIIA MSC line along the mesodermal lineage would allow for *in vitro* modelling of MPS IIIA osteogenesis, chondrogenesis or adipogenesis. Methods are well established for differentiation of iPSCs along the mesodermal lineage to form MSCs (Hynes et al., 2016); differentiation of MPS IIIA iPSCs to MSCs is currently underway by our group, which will likewise allow for

analysis of MPS IIIA mesodermal differentiation in comparison to normal. In particular, identifying a disruption in osteogenesis in the MPS IIIA MSC or iPSC lines would provide confirmation that MPS IIIA HS affects the osteogenic capacity of stem cells, as identified in Chapter Four. This would provide further evidence for a potential molecular mechanism underlying the mild skeletal pathology of MPS IIIA.

6.3.1.4 Identifying contributing factors to previously unsuccessful therapies

Finally, these cell models could be used to investigate the mechanisms underlying previously proposed therapies which were unsuccessful in MPS IIIA. Of particular interest would be HSC transplants, which have only been successful in treating CNS disease in MPS I (Hoogerbrugge et al., 1995; Lange et al., 2006; Lau et al., 2010; Sivakumur & Wraith, 1999). Chapter Four demonstrated the different effects of MPS GAGs on MSC neural induction, with MPS IIIA GAG disrupting neurogenesis whilst MPS I GAG had little effect. In a similar manner, MPS GAGs could influence the HSC survival and treatment efficacy, with the MPS I environment potentially being more conducive for HSC survival. MPS II GAG had a similar effect to MPS IIIA GAG on MSC neurogenesis; interestingly, HSC transplants are also often unsuccessful in treating MPS II CNS pathology (Akiyama et al., 2014; Guffon et al., 2009; McKinnis et al., 1996; Shapiro et al., 1995; Vellodi et al., 1999). Thus, it is possible that MPS IIIA GAGs impair HSC survival and proliferation, reducing the efficacy of HSC transplants. Identifying factors which contributed to previously unsuccessful treatments is integral for the development of more effective therapies.

6.3.2 Potential treatments

The development of MPS IIIA cell lines could assist in the development of new therapies. Enzyme replacement therapy, bone marrow transplant, substrate deprivation therapy and gene

therapy have all been suggested as potential treatments for MPS IIIA. However, to date these treatments had limited efficacy or been highly invasive (de Ruijter et al., 2012; Delgadillo et al., 2011; Hemsley et al., 2007; Hoogerbrugge et al., 1995; Jones et al., 2016; Lange et al., 2006; Rozaklis et al., 2011; Tardieu et al., 2014). The MPS IIIA cell models developed in this study could be used to test the efficacy of new treatments *in vitro*, before transfer to an *in vivo* model. Due to the primary CNS disease in MPS IIIA, cell models with neurogenic potential provide a distinct advantage over the currently used somatic cells such as fibroblasts (Anson et al., 2007; Jackson et al., 2015; Roberts et al., 2006). The MPS IIIA cell lines developed in this thesis were used here to identify impaired neurogenesis as a potential contributor towards the severe neurological disease seen in MPS IIIA patients; in the future, these same cell lines could be used to test the efficacy of treatments designed to combat this phenotype.

In addition, the MPS IIIA cell lines developed in this thesis could themselves be used as a treatment for MPS IIIA. MSCs have previously been suggested as an alternative to the HSCs currently used in bone marrow transplants, with their immunomodulatory effects and neurogenic properties providing an advantage over the currently used HSCs (da Silva et al., 2012). iPSC-derived cells have been proposed by many as a potential therapeutic for untreatable genetic diseases (reviewed in Barral & Kurian, 2016; reviewed in Xie & Tang, 2016). Both MSCs isolated from MPS IIIA patients and iPSC-NPCs derived from patient somatic cells could be used for autologous stem cell therapy. Stem cells isolated from an MPS IIIA patient would undergo CRISPR modification to correct the *SGSH* gene, resulting in expression of cDNA with the correct nucleotide sequence and thus normal sulphamidase activity. Following the administration of cells to the original patients, the secreted enzyme would be able to cross-correct patient cells, resulting in HS degradation. Furthermore, the CRISPR-corrected cells could themselves differentiate into neurons, supplementing the affected patient neurons with new, unaffected cells. The use of autologous cells would provide

a distinct advantage, eliminating the need for HLA matched donors. The allogenic HSC transplants currently used to treat CNS pathology in MPS I patients carry significant risks, including the development of graft vs host disease, resulting in significant morbidity and mortality (Wang et al., 2016). However, the neurogenic capacity of CRISPR corrected patient MSCs and iPSCs would need to be investigated *in vitro,* to determine if CRISPR correction rescues the disruption in neurogenesis that was identified in this study, before further *in vivo* studies could be conducted.

6.4 Conclusions

This study aimed to examine a potential underlying mechanism for the severe neurological pathology seen in MPS IIIA patients; that the aberrant HS found in MPS IIIA affects the proliferative and neurogenic potential of stem cells. Following the identification of optimal methods for human and murine MSC neural differentiation, MSCs and iPSCs were used to model stem cell proliferation and differentiation in MPS IIIA. Overall, MPS IIIA HS was found to impair neural progenitor proliferation, survival and maturation, indicating that disrupted stem cell proliferation and neurogenesis contributes towards the severe CNS pathology in MPS IIIA. In addition, MPS IIIA HS was found to disrupt osteogenesis, providing a potential mechanism for the moderate skeletal disease in patients. It was hypothesised that stem cell proliferation and differentiation were disrupted due to the presence of excess, partially degraded MPS IIIA HS fragments enriched in sequences required for morphogen binding. In the proposed "morphogen sequestration" model, extracellular MPS IIIA HS binds to morphogens, reducing morphogen-receptor interactions at the cell surface and thus limiting the upregulation of genes involved in stem cell proliferation and differentiation. The MPS IIIA cell models developed in this thesis can be used to further investigate the underlying mechanisms of pathology contributing to the severe neurological phenotype, specifically the proposed "morphogen sequestration" method. Finally, the

identification of disrupted proliferation and neurogenesis as a mechanism contributing to MPS IIIA CNS pathology, as presented in this thesis, will assist in the development of more efficacious therapies for MPS IIIA patients.

Appendices

Appendix A: Material List

12-well plates	Corning Inc., USA
24-well plates	Corning Inc., USA
4-Methylumbelliferyl 2-deoxy-2-sulfamino -a-D-glucopyranoside sodium salt	Carbosynth, USA
6-well plates	Corning Inc., USA
96-well plates	Corning Inc., USA
Accutase	StemCell Technologies Pty.Ltd., VIC, Australia
anti-biotin antibody	Miltenyi Biotec Pty. Ltd., NSW, Australia
anti-CD45.2-biotin antibody	Miltenyi Biotec Pty. Ltd., NSW, Australia
anti-Sca.1-biotin antibody	Miltenyi Biotec Pty. Ltd., NSW, Australia
Ascorbate-2-phosphate	WAKO Chemicals, USA
B27 supplement (50x)	Life Technologies Pty. Ltd., VIC, Australia
Bicinchoninic Acid (BCA) Assay Kit (cat# BCA1-1KT)	Sigma-Aldrich Pty. Ltd., NSW, Australia
Bovine serum albumin	Sigma-Aldrich Pty. Ltd., NSW, Australia
Calcium Assay Kit (cat# 701220)	Cayman Chemical Company, USA
CellAdhere Dilution Buffer	StemCell Technologies Pty.Ltd., VIC, Australia
CELLSTAR 175cm^2 cell culture flask	Greiner Bio-One, Austria
CELLSTAR 25cm^2 cell culture flask	Greiner Bio-One, Austria
CELLSTAR 75cm^2 cell culture flask	Greiner Bio-One, Austria
CelLytic M	Sigma-Aldrich Pty. Ltd., NSW, Australia
Collagenase type I from *Clostridium histolyticum*	Sigma-Aldrich Pty. Ltd., NSW, Australia

CyQuant direct cell proliferation assay kit (cat# C35011)	Life Technologies Pty. Ltd., VIC, Australia
CytoTune™-iPS 2.0 Sendai Reprogramming Kit (cat# A16517)	Life Technologies Pty. Ltd., VIC, Australia
Dermatan Sulphate	Sigma-Aldrich Pty. Ltd., NSW, Australia
Dexamethasone	Sigma-Aldrich Pty. Ltd., NSW, Australia
DMEM (high glucose)	Life Technologies Pty. Ltd., VIC, Australia
DMEM/F-12	Life Technologies Pty. Ltd., VIC, Australia
DMEM/F-12 (GlutaMAX)	Life Technologies Pty. Ltd., VIC, Australia
ECM gel from Engelbreth-Holm-Swarm murine sarcoma	Sigma-Aldrich Pty. Ltd., NSW, Australia
EGF	Prospec-Tany TechnoGene Ltd., Israel
Fetal calf serum	Life Technologies Pty. Ltd., VIC, Australia
FGF-2 (iPSC studies)	Life Technologies Pty. Ltd., VIC, Australia
FGF-2 (MSC studies)	Prospec-Tany TechnoGene Ltd., Israel
Formaldehyde	ChemSupply, SA, Australia
Gelatin from bovine skin	Sigma-Aldrich Pty. Ltd., NSW, Australia
Gentamycin	Life Technologies Pty. Ltd., VIC, Australia
Gentle Cell Dissociation Reagent	StemCell Technologies Pty.Ltd., VIC, Australia
Glutamine	Sigma-Aldrich Pty. Ltd., NSW, Australia
Ham's F-12	Life Technologies Pty. Ltd., VIC, Australia
Heparan Sulphate (Bovine Kidney)	Sigma-Aldrich Pty. Ltd., NSW, Australia
Heparin (Porcine Intestinal Mucosa)	Sigma-Aldrich Pty. Ltd., NSW, Australia
HEPES	Sigma-Aldrich Pty. Ltd., NSW, Australia
Hydrocortisone	Sigma-Aldrich Pty. Ltd., NSW, Australia
Indomethacin	Sigma-Aldrich Pty. Ltd., NSW, Australia

Insulin	Sigma-Aldrich Pty. Ltd., NSW, Australia
Isobutylmethylxanthine	Sigma-Aldrich Pty. Ltd., NSW, Australia
Isopropanol	ChemSupply, SA, Australia
ITS Supplement	Sigma-Aldrich Pty. Ltd., NSW, Australia
KnockOut™ Serum Replacement	Life Technologies Pty. Ltd., VIC, Australia
Laminin from Engelbreth-Holm-Swarm murine sarcoma (α1β1γ1)	Life Technologies Pty. Ltd., VIC, Australia
MEFs	StemCore, QLD, Australia
Metabolic cages	Hatteras Instruments Inc., USA
Microfuge tubes	Eppendorf South Pacific Pty. Ltd, NSW, Australia
MiniMACS separator	Miltenyi Biotec Pty. Ltd., NSW, Australia
MS columns	Miltenyi Biotec Pty. Ltd., NSW, Australia
N2 Supplement (100x)	Life Technologies Pty. Ltd., VIC, Australia
$Na_2EDTA.2H_2O$	Sigma-Aldrich Pty. Ltd., NSW, Australia
NaOH	Sigma-Aldrich Pty. Ltd., NSW, Australia
Neurobasal	Life Technologies Pty. Ltd., VIC, Australia
Neurobasal A	Life Technologies Pty. Ltd., VIC, Australia
Neutral Red	ProSciTech, QLD, Australia
Non-essential amino acids	Life Technologies Pty. Ltd., VIC, Australia
NUNC 35mm dishes	Thermo Fischer Scientific Pty. Ltd., VIC, Australia
NUNC nunclon delta surface plates	Thermo Fischer Scientific Pty. Ltd., VIC, Australia
Oil Red O	ProSciTech, QLD, Australia
PBS	Life Technologies Pty. Ltd., VIC, Australia
Penicillin/Streptomycin	Sigma-Aldrich Pty. Ltd., NSW, Australia
Polybrene	Sigma-Aldrich Pty. Ltd., NSW, Australia
Poly-L-orthinine	Sigma-Aldrich Pty. Ltd., NSW, Australia

Proteinase K	Sigma-Aldrich Pty. Ltd., NSW, Australia
PSC 4-Marker Immunocytochemistry Kit (cat# A24881) (lot# 1913522)	Life Technologies Pty. Ltd., VIC, Australia
PureLink™ RNA Micro Kit (cat# 12183-016)	Life Technologies Pty. Ltd., VIC, Australia
QuantiPro BCA protein kit (cat# QPBCA-1KT)	Sigma-Aldrich Pty. Ltd., NSW, Australia
QuantiTect Reverse Transcription Kit (cat# 205311)	Qiagen Pty. Ltd, VIC, Australia
Retinoic acid	Sigma-Aldrich Pty. Ltd., NSW, Australia
RNeasy mini kit (cat# 74104)	Qiagen Pty. Ltd, VIC, Australia
Silver nitrate	Merck, VIC, Australia
Sodium pyruvate	Sigma-Aldrich Pty. Ltd., NSW, Australia
Sodium Thiosulphate	Thermo Fischer Scientific Pty. Ltd., VIC, Australia
SYBR™ Green PCR Mastermix (2x)	Life Technologies Pty. Ltd., VIC, Australia
TeSR-E8	StemCell Technologies Pty.Ltd., VIC, Australia
TGFβ	Prospec-Tany TechnoGene Ltd., Israel
Triton-X	Sigma-Aldrich Pty. Ltd., NSW, Australia
TRIzol	Life Technologies Pty. Ltd., VIC, Australia
Trypsin-EDTA	Sigma-Aldrich Pty. Ltd., NSW, Australia
V-botton 96 well plates	Corning Inc., USA
Viagen lysis buffer	Australian Biosearch Inc., WA, Australia
Vitronectin XF	StemCell Technologies Pty.Ltd., VIC, Australia
α-MEM (nucleosides)	Life Technologies Pty. Ltd., VIC, Australia
β-mercaptoethanol	Life Technologies Pty. Ltd., VIC, Australia

All other reagents used in this study were of analytical reagent grade and were obtained from:

Ajax Finechem Pty. Ltd., Seven Hills, NSW

BDH (VWR), Bio-Strategy Pty. Ltd., VIC, Australia

Sigma-Aldrich Pty. Ltd., NSW, Australia

Appendix B: Glycosaminoglycan Abbreviations

2S	2-*O*-sulphate
6S	6-*O*-sulphate
GlcA	Glucuronic acid
GlcN	Glucosamine
GlcNA	*N*-acetylated glucosamine
GlcNA(6S)	6-*O*-suphated *N*-acetylated glucosamine
GlcNS	*N*-sulphated glucosamine
GlcNS(6S)	6-*O*-suphated *N*-sulphated glucosamine
HexA	Glucuronic acid or Iduronic acid
HexA(2S)	2-*O*-sulphated glucuronic acid or 2-*O*-sulphated iduronic acid
IdoA	Iduronic acid
IdoA(2S)	2-*O*-sulphated iduronic acid
NA	*N*-acetylated
NS	*N*-sulphated

Appendix C: Publications

Published abstracts arising from this thesis:

Lehmann R, Selway C., Byers S., Derrick Roberts A. (2018). *Aberrant heparan sulphate impairs mesenchymal stem cell proliferation and neurogenesis in Mucopolysaccharidosis type IIIA.* Molecular Genetics and Metabolism. 123(2): S84.

Lehmann R, Derrick Roberts A, Byers S. (2016). *Accumulation of MPS GAG influences stem cell differentiation.* Molecular Genetics and Metabolism. 117(2): S72.

References

Abdullah, RH, Yaseen, NY, Salih, SM, Al-Juboory, AA, Hassan, A & Al-Shammari, AM 2016, 'Induction of mice adult bone marrow mesenchymal stem cells into functional motor neuron-like cells', *Journal of Chemical Neuroanatomy*, vol. 77, Nov, pp. 129-142.

Ahmed, AU, Tyler, MA, Thaci, B, Alexiades, NG, Han, Y, Ulasov, IV & Lesniak, MS 2011, 'A comparative study of neural and mesenchymal stem cell-based carriers for oncolytic adenovirus in a model of malignant glioma', *Molecular Pharmaceutics*, vol. 8, no. 5, Oct 3, pp. 1559-1572.

Ai, X, Do, AT, Lozynska, O, Kusche-Gullberg, M, Lindahl, U & Emerson, CP, Jr. 2003, 'QSulf1 remodels the 6-O sulfation states of cell surface heparan sulfate proteoglycans to promote Wnt signaling', *Journal of Cell Biology*, vol. 162, no. 2, Jul 21, pp. 341-351.

Akiyama, K, Shimada, Y, Higuchi, T, Ohtsu, M, Nakauchi, H, Kobayashi, H, Fukuda, T, Ida, H, Eto, Y, Crawford, BE, Brown, JR & Ohashi, T 2014, 'Enzyme augmentation therapy enhances the therapeutic efficacy of bone marrow transplantation in mucopolysaccharidosis type II mice', *Molecular Genetics and Metabolism*, vol. 111, no. 2, Feb, pp. 139-146.

Allen, BL, Filla, MS & Rapraeger, AC 2001, 'Role of heparan sulfate as a tissue-specific regulator of FGF-4 and FGF receptor recognition', *Journal of Cell Biology*, vol. 155, no. 5, Nov 26, pp. 845-858.

Allen, BL & Rapraeger, AC 2003, 'Spatial and temporal expression of heparan sulfate in mouse development regulates FGF and FGF receptor assembly', *Journal of Cell Biology*, vol. 163, no. 3, Nov 10, pp. 637-648.

Anson, DS, McIntyre, C, Thomas, B, Koldej, R, Ranieri, E, Roberts, A, Clements, PR, Dunning, K & Byers, S 2007, 'Lentiviral-mediated gene correction of mucopolysaccharidosis type IIIA', *Genetic Vaccines and Therapies*, vol. 5, p. 1.

Arfi, A, Richard, M, Gandolphe, C, Bonnefont-Rousselot, D, Therond, P & Scherman, D 2011, 'Neuroinflammatory and oxidative stress phenomena in MPS IIIA mouse model: the positive effect of long-term aspirin treatment', *Molecular Genetics and Metabolism*, vol. 103, no. 1, May, pp. 18-25.

Armiento, AR, Alini, M & Stoddart, MJ 2017, 'Investigating the interaction between Runx2 and PRB during in vitro chondrogenesis and osteogenesis of human mesenchymal stromal cells', *Osteoarthritis and Cartilage*, vol. 25, p. S166.

Aronovich, EL, Carmichael, KP, Morizono, H, Koutlas, IG, Deanching, M, Hoganson, G, Fischer, A & al, e 2000, 'Canine heparan sulfate sulfamidase and the molecular pathology underlying Sanfilippo syndrome type A in Dachshunds', *Genomics*, vol. 68, no. 1, Aug 15, pp. 80-84.

Arthur, A, Rychkov, G, Shi, S, Koblar, SA & Gronthos, S 2008, 'Adult human dental pulp stem cells differentiate toward functionally active neurons under appropriate environmental cues', *Stem Cells*, vol. 26, no. 7, Jul, pp. 1787-1795.

Ashikari-Hada, S, Habuchi, H, Kariya, Y, Itoh, N, Reddi, AH & Kimata, K 2004, 'Characterization of growth factor-binding structures in heparin/heparan sulfate using an octasaccharide library', *Journal of Biological Chemistry*, vol. 279, no. 13, Mar 26, pp. 12346-12354.

Aubin, J, Davy, A & Soriano, P 2004, 'In vivo convergence of BMP and MAPK signaling pathways: impact of differential Smad1 phosphorylation on development and homeostasis', *Genes & Development*, vol. 18, no. 12, Jun 15, pp. 1482-1494.

Ausseil, J, Desmaris, N, Bigou, S, Attali, R, Corbineau, S, Vitry, S, Parent, M, Cheillan, D, Fuller, M, Maire, I, Vanier, MT & Heard, JM 2008, 'Early neurodegeneration progresses independently of microglial activation by heparan sulfate in the brain of mucopolysaccharidosis IIIB mice', *PloS One*, vol. 3, no. 5, p. e2296.

Azizi, SA, Stokes, D, Augelli, BJ, DiGirolamo, C & Prockop, DJ 1998, 'Engraftment and migration of human bone marrow stromal cells implanted in the brains of albino rats--similarities to astrocyte grafts', *Proceedings of the National Academy of Sciences of the United States of America*, vol. 95, no. 7, Mar 31, pp. 3908-3913.

Baeg, GH, Lin, X, Khare, N, Baumgartner, S & Perrimon, N 2001, 'Heparan sulfate proteoglycans are critical for the organization of the extracellular distribution of Wingless', *Development*, vol. 128, no. 1, Jan, pp. 87-94.

Bain, G, Kitchens, D, Yao, M, Huettner, JE & Gottlieb, DI 1995, 'Embryonic stem cells express neuronal properties in vitro', *Developmental Biology*, vol. 168, no. 2, Apr, pp. 342-357.

Bame, KJ 2001, 'Heparanases: endoglycosidases that degrade heparan sulfate proteoglycans', *Glycobiology*, vol. 11, no. 6, Jun, pp. 91r-98r.

Bandtlow, CE & Zimmermann, DR 2000, 'Proteoglycans in the developing brain: new conceptual insights for old proteins', *Physiological Reviews*, vol. 80, no. 4, Oct, pp. 1267-1290.

Bao, X, Pavao, MS, Dos Santos, JC & Sugahara, K 2005, 'A functional dermatan sulfate epitope containing iduronate(2-O-sulfate)alpha1-3GalNAc(6-O-sulfate) disaccharide in the mouse brain: demonstration using a novel monoclonal antibody raised against dermatan sulfate of ascidian Ascidia nigra', *Journal of Biological Chemistry*, vol. 280, no. 24, Jun 17, pp. 23184-23193.

Barral, S & Kurian, MA 2016, 'Utility of Induced Pluripotent Stem Cells for the Study and Treatment of Genetic Diseases: Focus on Childhood Neurological Disorders', *Frontiers in Molecular Neuroscience*, vol. 9, p. 78.

Bartholomew, A, Sturgeon, C, Siatskas, M, Ferrer, K, McIntosh, K, Patil, S, Hardy, W, Devine, S, Ucker, D, Deans, R, Moseley, A & Hoffman, R 2002, 'Mesenchymal stem cells suppress lymphocyte proliferation in vitro and prolong skin graft survival in vivo', *Experimental Hematology*, vol. 30, no. 1, Jan, pp. 42-48.

Baumkotter, J & Cantz, M 1983, 'Decreased ganglioside neuraminidase activity in fibroblasts from mucopolysaccharidosis patients. Inhibition of the activity in vitro by sulfated glycosaminoglycans and other compounds', *Biochimica et Biophysica Acta (BBA) - Bioenergetics*, vol. 761, no. 2, Dec 13, pp. 163-170.

Baxter, MA, Wynn, RF, Deakin, JA, Bellantuono, I, Edington, KG, Cooper, A, Besley, GT, Church, HJ, Wraith, JE, Carr, TF & Fairbairn, LJ 2002, 'Retrovirally mediated correction of bone marrow-derived mesenchymal stem cells from patients with mucopolysaccharidosis type I', *Blood*, vol. 99, no. 5, Mar 1, pp. 1857-1859.

Bayart, E & Cohen-Haguenauer, O 2013, 'Technological overview of iPS induction from human adult somatic cells', *Current Gene Therapy*, vol. 13, no. 2, Apr, pp. 73-92.

Bayo-Puxan, N, Terrasso, AP, Creyssels, S, Simao, D, Begon-Pescia, C, Lavigne, M, Salinas, S, Bernex, F, Bosch, A, Kalatzis, V, Levade, T, Cuervo, AM, Lory, P, Consiglio, A, Brito, C & Kremer, EJ 2018, 'Lysosomal and network alterations in human mucopolysaccharidosis type VII iPSC-derived neurons', *Scientific Reports*, vol. 8, no. 1, Nov 9, p. 16644.

Beaulieu, JM, Robertson, J & Julien, JP 1999, 'Interactions between peripherin and neurofilaments in cultured cells: disruption of peripherin assembly by the NF-M and NF-H subunits', *Biochemistry and Cell Biology*, vol. 77, no. 1, pp. 41-45.

Behr, B, Panetta, NJ, Longaker, MT & Quarto, N 2010, 'Different endogenous threshold levels of Fibroblast Growth Factor-ligands determine the healing potential of frontal and parietal bones', *Bone*, vol. 47, no. 2, Aug, pp. 281-294.

Bennett, CN, Ross, SE, Longo, KA, Bajnok, L, Hemati, N, Johnson, KW, Harrison, SD & MacDougald, OA 2002, 'Regulation of Wnt signaling during adipogenesis', *Journal of Biological Chemistry*, vol. 277, no. 34, Aug 23, pp. 30998-31004.

Bernfield, M, Gotte, M, Park, PW, Reizes, O, Fitzgerald, ML, Lincecum, J & Zako, M 1999, 'Functions of cell surface heparan sulfate proteoglycans', *Annual Review of Biochemistry*, vol. 68, pp. 729-777.

Bhattacharyya, R, Gliddon, B, Beccari, T, Hopwood, JJ & Stanley, P 2001, 'A novel missense mutation in lysosomal sulfamidase is the basis of MPS III A in a spontaneous mouse mutant', *Glycobiology*, vol. 11, no. 1, Jan, pp. 99-103.

Bhaumik, M, Muller, VJ, Rozaklis, T, Johnson, L, Dobrenis, K, Bhattacharyya, R, Wurzelmann, S, Finamore, P, Hopwood, JJ, Walkley, SU & Stanley, P 1999, 'A mouse model for mucopolysaccharidosis type III A (Sanfilippo syndrome)', *Glycobiology*, vol. 9, no. 12, Dec, pp. 1389-1396.

Bills, CE, Eisenberg, H & Pallante, SL 1971, 'Complexes of organic acids with calcium phosphate: the von Kossa stain as a clue to the composition of bone mineral', *Johns Hopkins Medical Journal*, vol. 128, no. 4, Apr, pp. 194-207.

Birkenmeier, EH, Davisson, MT, Beamer, WG, Ganschow, RE, Vogler, CA, Gwynn, B, Lyford, KA, Maltais, LM & Wawrzyniak, CJ 1989, 'Murine mucopolysaccharidosis type VII. Characterization of a mouse with beta-glucuronidase deficiency', *Journal of Clinical Investigation*, vol. 83, no. 4, Apr, pp. 1258-1266.

Blackhall, FH, Merry, CL, Davies, EJ & Jayson, GC 2001, 'Heparan sulfate proteoglycans and cancer', *British Journal of Cancer*, vol. 85, no. 8, Oct 19, pp. 1094-1098.

Blassberg, R, Macrae, JI, Briscoe, J & Jacob, J 2016, 'Reduced cholesterol levels impair Smoothened activation in Smith-Lemli-Opitz syndrome', *Human Molecular Genetics*, vol. 25, no. 4, Feb 15, pp. 693-705.

Blumenkrantz, N & Asboe-Hansen, G 1973, 'New method for quantitative determination of uronic acids', *Analytical Biochemistry*, vol. 54, no. 2, Aug, pp. 484-489.

Bonfanti, L & Peretto, P 2007, 'Radial glial origin of the adult neural stem cells in the subventricular zone', *Progress in Neurobiology*, vol. 83, no. 1, Sep, pp. 24-36.

Boregowda, SV, Krishnappa, V & Phinney, DG 2016, 'Isolation of Mouse Bone Marrow Mesenchymal Stem Cells', *Methods in Molecular Biology*, vol. 1416, pp. 205-223.

Bossolasco, P, Cova, L, Calzarossa, C, Rimoldi, SG, Borsotti, C, Deliliers, GL, Silani, V, Soligo, D & Polli, E 2005, 'Neuro-glial differentiation of human bone marrow stem cells in vitro', *Experimental Neurology*, vol. 193, no. 2, Jun, pp. 312-325.

Boyd, PJ, Cunliffe, VT, Roy, S & Wood, JD 2015, 'Sonic hedgehog functions upstream of disrupted-in-schizophrenia 1 (disc1): implications for mental illness', *Biol Open*, vol. 4, no. 10, Sep 24, pp. 1336-1343.

Brazelton, TR, Rossi, FM, Keshet, GI & Blau, HM 2000, 'From marrow to brain: expression of neuronal phenotypes in adult mice', *Science*, vol. 290, no. 5497, Dec 1, pp. 1775-1779.

Brickman, YG, Ford, MD, Gallagher, JT, Nurcombe, V, Bartlett, PF & Turnbull, JE 1998, 'Structural modification of fibroblast growth factor-binding heparan sulfate at a determinative stage of neural development', *Journal of Biological Chemistry*, vol. 273, no. 8, Feb 20, pp. 4350-4359.

Buecker, C, Chen, HH, Polo, JM, Daheron, L, Bu, L, Barakat, TS, Okwieka, P, Porter, A, Gribnau, J, Hochedlinger, K & Geijsen, N 2010, 'A murine ESC-like state facilitates transgenesis and homologous recombination in human pluripotent stem cells', *Cell Stem Cell*, vol. 6, no. 6, Jun 4, pp. 535-546.

Bursch, W, Hochegger, K, Torok, L, Marian, B, Ellinger, A & Hermann, RS 2000, 'Autophagic and apoptotic types of programmed cell death exhibit different fates of cytoskeletal filaments', *Journal of Cell Science*, vol. 113 (Pt 7), Apr, pp. 1189-1198.

Byers, S, Rozaklis, T, Brumfield, LK, Ranieri, E & Hopwood, JJ 1998, 'Glycosaminoglycan accumulation and excretion in the mucopolysaccharidoses: characterization and basis of a diagnostic test for MPS', *Molecular Genetics and Metabolism*, vol. 65, no. 4, Dec, pp. 282-290.

Cameron, HA, Woolley, CS, McEwen, BS & Gould, E 1993, 'Differentiation of newly born neurons and glia in the dentate gyrus of the adult rat', *Neuroscience*, vol. 56, no. 2, Sep, pp. 337-344.

Canals, I, Soriano, J, Orlandi, JG, Torrent, R, Richaud-Patin, Y, Jimenez-Delgado, S, Merlin, S, Follenzi, A, Consiglio, A, Vilageliu, L, Grinberg, D & Raya, A 2015, 'Activity and High-Order Effective Connectivity Alterations in Sanfilippo C Patient-Specific Neuronal Networks', *Stem Cell Reports*, vol. 5, no. 4, Oct 13, pp. 546-557.

Capurro, M, Martin, T, Shi, W & Filmus, J 2014, 'Glypican-3 binds to Frizzled and plays a direct role in the stimulation of canonical Wnt signaling', *Journal of Cell Science*, vol. 127, no. Pt 7, Apr 1, pp. 1565-1575.

Capurro, MI, Xiang, YY, Lobe, C & Filmus, J 2005, 'Glypican-3 promotes the growth of hepatocellular carcinoma by stimulating canonical Wnt signaling', *Cancer Research*, vol. 65, no. 14, Jul 15, pp. 6245-6254.

Cardin, AD & Weintraub, HJ 1989, 'Molecular modeling of protein-glycosaminoglycan interactions', *Arteriosclerosis*, vol. 9, no. 1, Jan-Feb, pp. 21-32.

Carpenter, DA & Ip, W 1996, 'Neurofilament triplet protein interactions: evidence for the preferred formation of NF-L-containing dimers and a putative function for the end domains', *Journal of Cell Science*, vol. 109 (Pt 10), Oct, pp. 2493-2498.

Carter, J, Gragerov, A, Konvicka, K, Elder, G, Weinstein, H & Lazzarini, RA 1998, 'Neurofilament (NF) assembly; divergent characteristics of human and rodent NF-L subunits', *Journal of Biological Chemistry*, vol. 273, no. 9, Feb 27, pp. 5101-5108.

Caviness, VS, Jr., Takahashi, T & Nowakowski, RS 1995, 'Numbers, time and neocortical neuronogenesis: a general developmental and evolutionary model', *Trends in Neurosciences*, vol. 18, no. 9, Sep, pp. 379-383.

Ceuterick, C, Martin, JJ, Libert, J & Farriaux, JP 1980, 'Sanfilippo A disease in the fetus--comparison with pre- and postnatal cases', *Neuropadiatrie*, vol. 11, no. 2, May, pp. 176-185.

Chang, SC, Mulloy, B, Magee, AI & Couchman, JR 2011, 'Two distinct sites in sonic Hedgehog combine for heparan sulfate interactions and cell signaling functions', *Journal of Biological Chemistry*, vol. 286, no. 52, Dec 30, pp. 44391-44402.

Chang, Z, Meyer, K, Rapraeger, AC & Friedl, A 2000, 'Differential ability of heparan sulfate proteoglycans to assemble the fibroblast growth factor receptor complex in situ', *FASEB Journal*, vol. 14, no. 1, Jan, pp. 137-144.

Charytoniuk, D, Porcel, B, Rodriguez Gomez, J, Faure, H, Ruat, M & Traiffort, E 2002, 'Sonic Hedgehog signalling in the developing and adult brain', *Journal of Physiology, Paris*, vol. 96, no. 1-2, Jan-Mar, pp. 9-16.

Chen, CW, Liu, CS, Chiu, IM, Shen, SC, Pan, HC, Lee, KH, Lin, SZ & Su, HL 2010, 'The signals of FGFs on the neurogenesis of embryonic stem cells', *Journal of Biomedical Science*, vol. 17, p. 33.

Chen, J & Long, F 2013, 'beta-catenin promotes bone formation and suppresses bone resorption in postnatal growing mice', *Journal of Bone and Mineral Research*, vol. 28, no. 5, May, pp. 1160-1169.

Chen, SJ, Li, YW, Wang, TR & Hsu, JC 1996, 'Bony changes in common mucopolysaccharidoses', *Zhonghua Min Guo Xiao Er Ke Yi Xue Hui Za Zhi*, vol. 37, no. 3, May-Jun, pp. 178-184.

Chen, X, Gu, Q, Wang, X, Ma, Q, Tang, H, Yan, X, Guo, X, Yan, H, Hao, J & Zeng, F 2013, 'Directed neuronal differentiation of mouse embryonic and induced pluripotent stem cells and their gene expression profiles', *International Journal of Molecular Medicine*, vol. 32, no. 1, Jul, pp. 25-34.

Chenn, A & Walsh, CA 2002, 'Regulation of cerebral cortical size by control of cell cycle exit in neural precursors', *Science*, vol. 297, no. 5580, Jul 19, pp. 365-369.

Chuang, CK, Lin, HY, Wang, TJ, Tsai, CC, Liu, HL & Lin, SP 2014, 'A modified liquid chromatography/tandem mass spectrometry method for predominant disaccharide units of urinary glycosaminoglycans in patients with mucopolysaccharidoses', *Orphanet Journal of Rare Diseases*, vol. 9, Sep 2, p. 135.

Chudickova, M, Bruza, P, Zajicova, A, Trosan, P, Svobodova, L, Javorkova, E, Kubinova, S & Holan, V 2015, 'Targeted neural differentiation of murine mesenchymal stem cells by a protocol simulating the inflammatory site of neural injury', *Journal of Tissue Engineering and Regenerative Medicine*, Jun 29.

Clarke, LA, Russell, CS, Pownall, S, Warrington, CL, Borowski, A, Dimmick, JE, Toone, J & Jirik, FR 1997, 'Murine mucopolysaccharidosis type I: targeted disruption of the murine alpha-L-iduronidase gene', *Human Molecular Genetics*, vol. 6, no. 4, Apr, pp. 503-511.

Constantopoulos, G & Dekaban, AS 1978, 'Neurochemistry of the mucopolysaccharidoses: brain lipids and lysosomal enzymes in patients with four types of mucopolysaccharidosis and in normal controls', *Journal of Neurochemistry*, vol. 30, no. 5, May, pp. 965-973.

Constantopoulos, G, McComb, RD & Dekaban, AS 1976, 'Neurochemistry of the mucopolysaccharidoses: brain glycosaminoglycans in normals and four types of mucopolysaccharidoses', *Journal of Neurochemistry*, vol. 26, no. 5, May, pp. 901-908.

Coppa, GV, Gabrielli, O, Zampini, L, Maccari, F, Mantovani, V, Galeazzi, T, Santoro, L, Padella, L, Marchesiello, RL, Galeotti, F & Volpi, N 2015, 'Mental retardation in mucopolysaccharidoses correlates with high molecular weight urinary heparan sulphate derived glucosamine', *Metabolic Brain Disease*, May 29.

Correa, D, Somoza, RA, Lin, P, Greenberg, S, Rom, E, Duesler, L, Welter, JF, Yayon, A & Caplan, AI 2015, 'Sequential exposure to fibroblast growth factors (FGF) 2, 9 and 18 enhances hMSC chondrogenic differentiation', *Osteoarthritis and Cartilage*, vol. 23, no. 3, Mar, pp. 443-453.

Coulson-Thomas, VJ, Caterson, B & Kao, WW 2013, 'Transplantation of human umbilical mesenchymal stem cells cures the corneal defects of mucopolysaccharidosis VII mice', *Stem Cells*, vol. 31, no. 10, Oct, pp. 2116-2126.

Crawley, AC, Gliddon, BL, Auclair, D, Brodie, SL, Hirte, C, King, BM, Fuller, M, Hemsley, KM & Hopwood, JJ 2006, 'Characterization of a C57BL/6 congenic mouse strain of mucopolysaccharidosis type IIIA', *Brain Research*, vol. 1104, no. 1, Aug 9, pp. 1-17.

da Silva, FH, Pereira, VG, Yasumura, EG, Tenorio, LZ, de Carvalho, LP, Lisboa, BC, Matsumoto, PK, Stilhano, RS, Samoto, VY, Calegare, BF, Brandao Lde, C, D'Almeida, V, Filippo, TR, Porcionatto, M, Toma, L, Nader, HB, Valero, VB, Camassola, M, Nardi, NB & Han, SW 2012, 'Treatment of adult MPSI mouse brains with IDUA-expressing mesenchymal stem cells decreases GAG deposition and improves exploratory behavior', *Genetic Vaccines and Therapy*, vol. 10, no. 1, p. 2.

Davidson, CD, Ali, NF, Micsenyi, MC, Stephney, G, Renault, S, Dobrenis, K, Ory, DS, Vanier, MT & Walkley, SU 2009, 'Chronic cyclodextrin treatment of murine Niemann-Pick C disease ameliorates neuronal cholesterol and glycosphingolipid storage and disease progression', *PloS One*, vol. 4, no. 9, Sep 11, p. e6951.

Day, TF, Guo, X, Garrett-Beal, L & Yang, Y 2005, 'Wnt/beta-catenin signaling in mesenchymal progenitors controls osteoblast and chondrocyte differentiation during vertebrate skeletogenesis', *Developmental Cell*, vol. 8, no. 5, May, pp. 739-750.

de Mara, CS, Duarte, AS, Sartori-Cintra, AR, Luzo, AC, Saad, ST & Coimbra, IB 2013, 'Chondrogenesis from umbilical cord blood cells stimulated with BMP-2 and BMP-6', *Rheumatology International*, vol. 33, no. 1, Jan, pp. 121-128.

De Pasquale, V, Sarogni, P, Pistorio, V, Cerulo, G, Paladino, S & Pavone, LM 2018, 'Targeting Heparan Sulfate Proteoglycans as a Novel Therapeutic Strategy for Mucopolysaccharidoses', *Mol Ther Methods Clin Dev*, vol. 10, Sep 21, pp. 8-16.

de Ruijter, J, Ijlst, L, Kulik, W, van Lenthe, H, Wagemans, T, van Vlies, N & Wijburg, FA 2013a, 'Heparan sulfate derived disaccharides in plasma and total urinary excretion of glycosaminoglycans correlate with disease severity in Sanfilippo disease', *Journal of Inherited Metabolic Disease*, vol. 36, no. 2, Mar, pp. 271-279.

de Ruijter, J, Maas, M, Janssen, A & Wijburg, FA 2013b, 'High prevalence of femoral head necrosis in Mucopolysaccharidosis type III (Sanfilippo disease): a national, observational, cross-sectional study', *Molecular Genetics and Metabolism*, vol. 109, no. 1, May, pp. 49-53.

de Ruijter, J, Valstar, MJ, Narajczyk, M, Wegrzyn, G, Kulik, W, Ijlst, L, Wagemans, T, van der Wal, WM & Wijburg, FA 2012, 'Genistein in Sanfilippo disease: a randomized controlled crossover trial', *Annals of Neurology*, vol. 71, no. 1, Jan, pp. 110-120.

Delgadillo, V, O'Callaghan Mdel, M, Artuch, R, Montero, R & Pineda, M 2011, 'Genistein supplementation in patients affected by Sanfilippo disease', *Journal of Inherited Metabolic Disease*, vol. 34, no. 5, Oct, pp. 1039-1044.

Deng, J, Petersen, BE, Steindler, DA, Jorgensen, ML & Laywell, ED 2006, 'Mesenchymal stem cells spontaneously express neural proteins in culture and are neurogenic after transplantation', *Stem Cells*, vol. 24, no. 4, Apr, pp. 1054-1064.

Deng, W, Obrocka, M, Fischer, I & Prockop, DJ 2001, 'In vitro differentiation of human marrow stromal cells into early progenitors of neural cells by conditions that increase intracellular cyclic AMP', *Biochemical and Biophysical Research Communications*, vol. 282, no. 1, Mar 23, pp. 148-152.

Denker, AE, Haas, AR, Nicoll, SB & Tuan, RS 1999, 'Chondrogenic differentiation of murine C3H10T1/2 multipotential mesenchymal cells: I. Stimulation by bone morphogenetic protein-2 in high-density micromass cultures', *Differentiation*, vol. 64, no. 2, Jan, pp. 67-76.

Di Natale, P, Villani, GR, Di Domenico, C, Daniele, A, Dionisi Vici, C & Bartuli, A 2003, 'Analysis of Sanfilippo A gene mutations in a large pedigree', *Clinical Genetics*, vol. 63, no. 4, Apr, pp. 314-318.

Di Nicola, M, Carlo-Stella, C, Magni, M, Milanesi, M, Longoni, PD, Matteucci, P, Grisanti, S & Gianni, AM 2002, 'Human bone marrow stromal cells suppress T-lymphocyte proliferation induced by cellular or nonspecific mitogenic stimuli', *Blood*, vol. 99, no. 10, May 15, pp. 3838-3843.

Dierker, T, Dreier, R, Petersen, A, Bordych, C & Grobe, K 2009, 'Heparan sulfate-modulated, metalloprotease-mediated sonic hedgehog release from producing cells', *Journal of Biological Chemistry*, vol. 284, no. 12, Mar 20, pp. 8013-8022.

Durak, O, de Anda, FC, Singh, KK, Leussis, MP, Petryshen, TL, Sklar, P & Tsai, LH 2015, 'Ankyrin-G regulates neurogenesis and Wnt signaling by altering the subcellular localization of beta-catenin', *Molecular Psychiatry*, vol. 20, no. 3, Mar, pp. 388-397.

Dwyer, CA, Scudder, SL, Lin, Y, Dozier, LE, Phan, D, Allen, NJ, Patrick, GN & Esko, JD 2017, 'Neurodevelopmental Changes in Excitatory Synaptic Structure and Function in the Cerebral Cortex of Sanfilippo Syndrome IIIA Mice', *Scientific Reports*, vol. 7, Apr 18, p. 46576.

Esko, J, Kimata, K & Lindahl, U 2009, 'Proteoglycans and Sulfated Glycosaminoglycans', in A Varki, R Cummings, J Esko, H Freeze, P Stanley, C Bertozzi, G Hart & M Etzler (eds), *Essentials of Glycobiology*, Cold Spring Harbor Laboratory Press, United States of America.

Esko, JD & Selleck, SB 2002, 'Order out of chaos: assembly of ligand binding sites in heparan sulfate', *Annual Review of Biochemistry*, vol. 71, pp. 435-471.

Espuny-Camacho, I, Michelsen, KA, Gall, D, Linaro, D, Hasche, A, Bonnefont, J, Bali, C, Orduz, D, Bilheu, A, Herpoel, A, Lambert, N, Gaspard, N, Peron, S, Schiffmann, SN, Giugliano, M, Gaillard, A & Vanderhaeghen, P 2013, 'Pyramidal neurons derived from human pluripotent stem cells integrate efficiently into mouse brain circuits in vivo', *Neuron*, vol. 77, no. 3, Feb 6, pp. 440-456.

Faissner, A, Clement, A, Lochter, A, Streit, A, Mandl, C & Schachner, M 1994, 'Isolation of a neural chondroitin sulfate proteoglycan with neurite outgrowth promoting properties', *Journal of Cell Biology*, vol. 126, no. 3, Aug, pp. 783-799.

Farzi-Molan, A, Babashah, S, Bakhshinejad, B, Atashi, A & Fakhr Taha, M 2018, 'Down-regulation of the non-coding RNA H19 and its derived miR-675 is concomitant with up-regulation of insulin-like growth factor receptor type 1 during neural-like differentiation of human bone marrow mesenchymal stem cells', *Cell Biology International*, Mar 7.

Faure, A, Verret, L, Bozon, B, El Tannir El Tayara, N, Ly, M, Kober, F, Dhenain, M, Rampon, C & Delatour, B 2011, 'Impaired neurogenesis, neuronal loss, and brain functional deficits in the APPxPS1-Ki mouse model of Alzheimer's disease', *Neurobiology of Aging*, vol. 32, no. 3, Mar, pp. 407-418.

Fedele, AO 2015, 'Sanfilippo syndrome: causes, consequences, and treatments', *Appl Clin Genet*, vol. 8, pp. 269-281.

Filges, I, Rothlisberger, B, Blattner, A, Boesch, N, Demougin, P, Wenzel, F, Huber, AR, Heinimann, K, Weber, P & Miny, P 2011, 'Deletion in Xp22.11: PTCHD1 is a candidate gene for X-linked intellectual disability with or without autism', *Clinical Genetics*, vol. 79, no. 1, Jan, pp. 79-85.

Filmus, J & Selleck, SB 2001, 'Glypicans: proteoglycans with a surprise', *Journal of Clinical Investigation*, vol. 108, no. 4, Aug, pp. 497-501.

Fischer, A, Carmichael, KP, Munnell, JF, Jhabvala, P, Thompson, JN, Matalon, R, Jezyk, PF, Wang, P & Giger, U 1998, 'Sulfamidase deficiency in a family of Dachshunds: a canine model of mucopolysaccharidosis IIIA (Sanfilippo A)', *Pediatric Research*, vol. 44, no. 1, Jul, pp. 74-82.

Fraichard, A, Chassande, O, Bilbaut, G, Dehay, C, Savatier, P & Samarut, J 1995, 'In vitro differentiation of embryonic stem cells into glial cells and functional neurons', *Journal of Cell Science*, vol. 108 (Pt 10), Oct, pp. 3181-3188.

Friedenstein, AJ 1980, 'Stromal mechanisms of bone marrow: cloning in vitro and retransplantation in vivo', *Haematology and Blood Transfusion*, vol. 25, pp. 19-29.

Friedenstein, AJ, Chailakhyan, RK, Latsinik, NV, Panasyuk, AF & Keiliss-Borok, IV 1974, 'Stromal cells responsible for transferring the microenvironment of the hemopoietic tissues. Cloning in vitro and retransplantation in vivo', *Transplantation*, vol. 17, no. 4, Apr, pp. 331-340.

Fuccillo, M, Rallu, M, McMahon, AP & Fishell, G 2004, 'Temporal requirement for hedgehog signaling in ventral telencephalic patterning', *Development*, vol. 131, no. 20, Oct, pp. 5031-5040.

Fuerer, C, Habib, SJ & Nusse, R 2010, 'A study on the interactions between heparan sulfate proteoglycans and Wnt proteins', *Developmental Dynamics*, vol. 239, no. 1, Jan, pp. 184-190.

Fujimura, J, Ogawa, R, Mizuno, H, Fukunaga, Y & Suzuki, H 2005, 'Neural differentiation of adipose-derived stem cells isolated from GFP transgenic mice', *Biochemical and Biophysical Research Communications*, vol. 333, no. 1, Jul 22, pp. 116-121.

Furuta, Y, Piston, DW & Hogan, BL 1997, 'Bone morphogenetic proteins (BMPs) as regulators of dorsal forebrain development', *Development*, vol. 124, no. 11, Jun, pp. 2203-2212.

Fusaki, N, Ban, H, Nishiyama, A, Saeki, K & Hasegawa, M 2009, 'Efficient induction of transgene-free human pluripotent stem cells using a vector based on Sendai virus, an RNA virus that does not integrate into the host genome', *Proceedings of the Japan Academy. Series B: Physical and Biological Sciences*, vol. 85, no. 8, pp. 348-362.

Fusar Poli, E, Zalfa, C, D'Avanzo, F, Tomanin, R, Carlessi, L, Bossi, M, Nodari, LR, Binda, E, Marmiroli, P, Scarpa, M, Delia, D, Vescovi, AL & De Filippis, L 2013, 'Murine neural stem cells model Hunter disease in vitro: glial cell-mediated neurodegeneration as a possible mechanism involved', *Cell Death & Disease*, vol. 4, Nov 7, p. e906.

Gallagher, JT & Turnbull, JE 1992, 'Heparan sulphate in the binding and activation of basic fibroblast growth factor', *Glycobiology*, vol. 2, no. 6, Dec, pp. 523-528.

Garcez, RC, Teixeira, BL, Schmitt Sdos, S, Alvarez-Silva, M & Trentin, AG 2009, 'Epidermal growth factor (EGF) promotes the in vitro differentiation of neural crest cells to neurons and melanocytes', *Cellular and Molecular Neurobiology*, vol. 29, no. 8, Dec, pp. 1087-1091.

Garcia-Verdugo, JM, Doetsch, F, Wichterle, H, Lim, DA & Alvarez-Buylla, A 1998, 'Architecture and cell types of the adult subventricular zone: in search of the stem cells', *Journal of Neurobiology*, vol. 36, no. 2, Aug, pp. 234-248.

Gaspard, N, Bouschet, T, Hourez, R, Dimidschstein, J, Naeije, G, van den Ameele, J, Espuny-Camacho, I, Herpoel, A, Passante, L, Schiffmann, SN, Gaillard, A & Vanderhaeghen, P 2008, 'An intrinsic mechanism of corticogenesis from embryonic stem cells', *Nature*, vol. 455, no. 7211, Sep 18, pp. 351-357.

Gatto, F, Redaelli, D, Salvade, A, Marzorati, S, Sacchetti, B, Ferina, C, Roobrouck, VD, Bertola, F, Romano, M, Villani, G, Antolini, L, Rovelli, A, Verfaillie, CM, Biondi, A, Riminucci, M, Bianco, P & Serafini, M 2012, 'Hurler disease bone marrow stromal cells exhibit altered ability to support osteoclast formation', *Stem Cells Dev*, vol. 21, no. 9, Jun 10, pp. 1466-1477.

Gazzerro, E, Smerdel-Ramoya, A, Zanotti, S, Stadmeyer, L, Durant, D, Economides, AN & Canalis, E 2007, 'Conditional deletion of gremlin causes a transient increase in bone formation and bone mass', *Journal of Biological Chemistry*, vol. 282, no. 43, Oct 26, pp. 31549-31557.

Gleitz, HF, Liao, AY, Cook, JR, Rowlston, SF, Forte, GM, D'Souza, Z, O'Leary, C, Holley, RJ & Bigger, BW 2018, 'Brain-targeted stem cell gene therapy corrects mucopolysaccharidosis type II via multiple mechanisms', *EMBO Molecular Medicine*, vol. 10, no. 7, Jul.

Goetz, R & Mohammadi, M 2013, 'Exploring mechanisms of FGF signalling through the lens of structural biology', *Nature Reviews: Molecular Cell Biology*, vol. 14, no. 3, Mar, pp. 166-180.

Gonmanee, T, Thonabulsombat, C, Vongsavan, K & Sritanaudomchai, H 2018, 'Differentiation of stem cells from human deciduous and permanent teeth into spiral ganglion neuron-like cells', *Archives of Oral Biology*, vol. 88, Apr, pp. 34-41.

Gordon, MD & Nusse, R 2006, 'Wnt signaling: multiple pathways, multiple receptors, and multiple transcription factors', *Journal of Biological Chemistry*, vol. 281, no. 32, Aug 11, pp. 22429-22433.

Gotz, M 2003, 'Glial cells generate neurons--master control within CNS regions: developmental perspectives on neural stem cells', *Neuroscientist*, vol. 9, no. 5, Oct, pp. 379-397.

Gotz, M & Huttner, WB 2005, 'The cell biology of neurogenesis', *Nature Reviews: Molecular Cell Biology*, vol. 6, no. 10, Oct, pp. 777-788.

Graham, A, Francis-West, P, Brickell, P & Lumsden, A 1994, 'The signalling molecule BMP4 mediates apoptosis in the rhombencephalic neural crest', *Nature*, vol. 372, no. 6507, Dec 15, pp. 684-686.

Greenwood, RS, Hillman, RE, Alcala, H & Sly, WS 1978, 'Sanfilippo A syndrome in the fetus', *Clinical Genetics*, vol. 13, no. 3, Mar, pp. 241-250.

Griffin, TA, Anderson, HC & Wolfe, JH 2015, 'Ex vivo gene therapy using patient iPSC-derived NSCs reverses pathology in the brain of a homologous mouse model', *Stem Cell Reports*, vol. 4, no. 5, May 12, pp. 835-846.

Gronthos, S, Mankani, M, Brahim, J, Robey, PG & Shi, S 2000, 'Postnatal human dental pulp stem cells (DPSCs) in vitro and in vivo', *Proceedings of the National Academy of Sciences of the United States of America*, vol. 97, no. 25, Dec 5, pp. 13625-13630.

Gronthos, S, Zannettino, AC, Hay, SJ, Shi, S, Graves, SE, Kortesidis, A & Simmons, PJ 2003, 'Molecular and cellular characterisation of highly purified stromal stem cells derived from human bone marrow', *Journal of Cell Science*, vol. 116, no. Pt 9, May 1, pp. 1827-1835.

Grumolato, L, Liu, G, Mong, P, Mudbhary, R, Biswas, R, Arroyave, R, Vijayakumar, S, Economides, AN & Aaronson, SA 2010, 'Canonical and noncanonical Wnts use a common mechanism to activate completely unrelated coreceptors', *Genes & Development*, vol. 24, no. 22, Nov 15, pp. 2517-2530.

Guan, F, Wang, X & He, F 2015, 'Promotion of cell migration by neural cell adhesion molecule (NCAM) is enhanced by PSA in a polysialyltransferase-specific manner', *PloS One*, vol. 10, no. 4, p. e0124237.

Guffon, N, Bertrand, Y, Forest, I, Fouilhoux, A & Froissart, R 2009, 'Bone marrow transplantation in children with Hunter syndrome: outcome after 7 to 17 years', *Journal of Pediatrics*, vol. 154, no. 5, May, pp. 733-737.

Guglier, S, Hricovini, M, Raman, R, Polito, L, Torri, G, Casu, B, Sasisekharan, R & Guerrini, M 2008, 'Minimum FGF2 binding structural requirements of heparin and heparan sulfate oligosaccharides as determined by NMR spectroscopy', *Biochemistry*, vol. 47, no. 52, Dec 30, pp. 13862-13869.

Guimaraes, ET, Cruz, GS, de Jesus, AA, Lacerda de Carvalho, AF, Rogatto, SR, Pereira Lda, V, Ribeiro-dos-Santos, R & Soares, MB 2011, 'Mesenchymal and embryonic characteristics of stem cells obtained from mouse dental pulp', *Archives of Oral Biology*, vol. 56, no. 11, Nov, pp. 1247-1255.

Gunhanlar, N, Shpak, G, van der Kroeg, M, Gouty-Colomer, LA, Munshi, ST, Lendemeijer, B, Ghazvini, M, Dupont, C, Hoogendijk, WJG, Gribnau, J, de Vrij, FMS & Kushner, SA 2018, 'A simplified protocol for differentiation of electrophysiologically mature neuronal networks from human induced pluripotent stem cells', *Molecular Psychiatry*, vol. 23, no. 5, May, pp. 1336-1344.

Guo, Z & Wang, Z 2009, 'The glypican Dally is required in the niche for the maintenance of germline stem cells and short-range BMP signaling in the Drosophila ovary', *Development*, vol. 136, no. 21, Nov, pp. 3627-3635.

Habuchi, H, Habuchi, O & Kimata, K 2004, 'Sulfation pattern in glycosaminoglycan: does it have a code?', *Glycoconjugate Journal*, vol. 21, no. 1-2, pp. 47-52.

Hacein-Bey-Abina, S, Garrigue, A, Wang, GP, Soulier, J, Lim, A, Morillon, E, Clappier, E, Caccavelli, L, Delabesse, E, Beldjord, K, Asnafi, V, MacIntyre, E, Dal Cortivo, L, Radford, I, Brousse, N, Sigaux, F, Moshous, D, Hauer, J, Borkhardt, A, Belohradsky, BH, Wintergerst, U, Velez, MC, Leiva, L, Sorensen, R, Wulffraat, N, Blanche, S, Bushman, FD, Fischer, A & Cavazzana-Calvo, M 2008, 'Insertional oncogenesis in 4 patients after retrovirus-mediated gene therapy of SCID-X1', *Journal of Clinical Investigation*, vol. 118, no. 9, Sep, pp. 3132-3142.

Hacein-Bey-Abina, S, Von Kalle, C, Schmidt, M, McCormack, MP, Wulffraat, N, Leboulch, P, Lim, A, Osborne, CS, Pawliuk, R, Morillon, E, Sorensen, R, Forster, A, Fraser, P, Cohen, JI, de Saint Basile, G, Alexander, I, Wintergerst, U, Frebourg, T, Aurias, A, Stoppa-Lyonnet, D, Romana, S, Radford-Weiss, I, Gross, F, Valensi, F, Delabesse, E, Macintyre, E, Sigaux, F, Soulier, J, Leiva, LE, Wissler, M, Prinz, C, Rabbitts, TH, Le Deist, F, Fischer, A & Cavazzana-Calvo, M 2003, 'LMO2-associated clonal T cell proliferation in two patients after gene therapy for SCID-X1', *Science*, vol. 302, no. 5644, Oct 17, pp. 415-419.

Hacker, U, Lin, X & Perrimon, N 1997, 'The Drosophila sugarless gene modulates Wingless signaling and encodes an enzyme involved in polysaccharide biosynthesis', *Development*, vol. 124, no. 18, Sep, pp. 3565-3573.

Hacker, U, Nybakken, K & Perrimon, N 2005, 'Heparan sulphate proteoglycans: the sweet side of development', *Nature Reviews: Molecular Cell Biology*, vol. 6, no. 7, Jul, pp. 530-541.

Harada, A, Teng, J, Takei, Y, Oguchi, K & Hirokawa, N 2002, 'MAP2 is required for dendrite elongation, PKA anchoring in dendrites, and proper PKA signal transduction', *Journal of Cell Biology*, vol. 158, no. 3, Aug 5, pp. 541-549.

Harper, PS, Laurence, KM, Parkes, A, Wusteman, FS, Kresse, H, von Figura, K, Ferguson-Smith, MA, Duncan, DM, Logan, RW, Hall, F & Whiteman, P 1974, 'Sanfilippo A disease in the fetus', *Journal of Medical Genetics*, vol. 11, no. 2, Jun, pp. 123-132.

Hassiotis, S, Jolly, RD & Hemsley, KM 2014, 'Development of cerebellar pathology in the canine model of mucopolysaccharidosis type IIIA (MPS IIIA)', *Molecular Genetics and Metabolism*, vol. 113, no. 4, Dec, pp. 283-293.

Haushalter, C, Asselin, L, Fraulob, V, Dolle, P & Rhinn, M 2017, 'Retinoic acid controls early neurogenesis in the developing mouse cerebral cortex', *Developmental Biology*, vol. 430, no. 1, Oct 1, pp. 129-141.

Hawley, SH, Wunnenberg-Stapleton, K, Hashimoto, C, Laurent, MN, Watabe, T, Blumberg, BW & Cho, KW 1995, 'Disruption of BMP signals in embryonic Xenopus ectoderm leads to direct neural induction', *Genes & Development*, vol. 9, no. 23, Dec 1, pp. 2923-2935.

Hemsley, KM, King, B & Hopwood, JJ 2007, 'Injection of recombinant human sulfamidase into the CSF via the cerebellomedullary cistern in MPS IIIA mice', *Molecular Genetics and Metabolism*, vol. 90, no. 3 SPEC. ISS., pp. 313-328.

Hemsley, KM, Luck, AJ, Crawley, AC, Hassiotis, S, Beard, H, King, B, Rozek, T, Rozaklis, T, Fuller, M & Hopwood, JJ 2009, 'Examination of intravenous and intra-CSF protein delivery for treatment of neurological disease', *European Journal of Neuroscience*, vol. 29, no. 6, Mar, pp. 1197-1214.

Hennemann, B, Chuo, JY, Schley, PD, Lambie, K, Humphries, RK & Eaves, CJ 2000, 'High-efficiency retroviral transduction of mammalian cells on positively charged surfaces', *Human Gene Therapy*, vol. 11, no. 1, Jan 1, pp. 43-51.

Hermann, A, Gastl, R, Liebau, S, Popa, MO, Fiedler, J, Boehm, BO, Maisel, M, Lerche, H, Schwarz, J, Brenner, R & Storch, A 2004, 'Efficient generation of neural stem cell-like cells from adult human bone marrow stromal cells', *Journal of Cell Science*, vol. 117, no. Pt 19, Sep 1, pp. 4411-4422.

Heuer, GG, Skorupa, AF, Prasad Alur, RK, Jiang, K & Wolfe, JH 2001, 'Accumulation of abnormal amounts of glycosaminoglycans in murine mucopolysaccharidosis type VII neural progenitor cells does not alter the growth rate or efficiency of differentiation into neurons', *Molecular and Cellular Neuroscience*, vol. 17, no. 1, Jan, pp. 167-178.

HGMD 2018, *The Human Gene Mutation Database - SGSH*, viewed 5/12/2018, <http://www.hgmd.org/>.

Hill, TP, Spater, D, Taketo, MM, Birchmeier, W & Hartmann, C 2005, 'Canonical Wnt/beta-catenin signaling prevents osteoblasts from differentiating into chondrocytes', *Developmental Cell*, vol. 8, no. 5, May, pp. 727-738.

Hinoi, E, Bialek, P, Chen, YT, Rached, MT, Groner, Y, Behringer, RR, Ornitz, DM & Karsenty, G 2006, 'Runx2 inhibits chondrocyte proliferation and hypertrophy through its expression in the perichondrium', *Genes & Development*, vol. 20, no. 21, Nov 1, pp. 2937-2942.

Hirabayashi, Y, Itoh, Y, Tabata, H, Nakajima, K, Akiyama, T, Masuyama, N & Gotoh, Y 2004, 'The Wnt/beta-catenin pathway directs neuronal differentiation of cortical neural precursor cells', *Development*, vol. 131, no. 12, Jun, pp. 2791-2801.

Hobbs, JR, Hugh-Jones, K, Barrett, AJ, Byrom, N, Chambers, D, Henry, K, James, DC, Lucas, CF, Rogers, TR, Benson, PF, Tansley, LR, Patrick, AD, Mossman, J & Young, EP 1981, 'Reversal of clinical features of Hurler's disease and biochemical improvement after treatment by bone-marrow transplantation', *Lancet*, vol. 2, no. 8249, Oct 3, pp. 709-712.

Hochuli, M, Wuthrich, K & Steinmann, B 2003, 'Two-dimensional NMR spectroscopy of urinary glycosaminoglycans from patients with different mucopolysaccharidoses', *NMR in Biomedicine*, vol. 16, no. 4, Jun, pp. 224-236.

Hoffman, PN 1989, 'Expression of GAP-43, a rapidly transported growth-associated protein, and class II beta tubulin, a slowly transported cytoskeletal protein, are coordinated in regenerating neurons', *Journal of Neuroscience*, vol. 9, no. 3, Mar, pp. 893-897.

Hoffman, PN, Cleveland, DW, Griffin, JW, Landes, PW, Cowan, NJ & Price, DL 1987, 'Neurofilament gene expression: a major determinant of axonal caliber', *Proceedings of the National Academy of Sciences of the United States of America*, vol. 84, no. 10, May, pp. 3472-3476.

Hoglinger, GU, Rizk, P, Muriel, MP, Duyckaerts, C, Oertel, WH, Caille, I & Hirsch, EC 2004, 'Dopamine depletion impairs precursor cell proliferation in Parkinson disease', *Nature Neuroscience*, vol. 7, no. 7, Jul, pp. 726-735.

Holley, RJ, Deligny, A, Wei, W, Watson, HA, Ninonuevo, MR, Dagalv, A, Leary, JA, Bigger, BW, Kjellen, L & Merry, CL 2011, 'Mucopolysaccharidosis type I, unique structure of accumulated heparan sulfate and increased N-sulfotransferase activity in mice lacking alpha-l-iduronidase', *Journal of Biological Chemistry*, vol. 286, no. 43, Oct 28, pp. 37515-37524.

Homan, CC, Pederson, S, To, TH, Tan, C, Piltz, S, Corbett, MA, Wolvetang, E, Thomas, PQ, Jolly, LA & Gecz, J 2018, 'PCDH19 regulation of neural progenitor cell differentiation suggests asynchrony of neurogenesis as a mechanism contributing to PCDH19 Girls Clustering Epilepsy', *Neurobiology of Disease*, vol. 116, Aug, pp. 106-119.

Hoogerbrugge, PM, Brouwer, OF, Bordigoni, P, Ringden, O, Kapaun, P, Ortega, JJ, O'Meara, A, Cornu, G, Souillet, G, Frappaz, D & et al. 1995, 'Allogeneic bone marrow transplantation for lysosomal storage diseases. The European Group for Bone Marrow Transplantation', *Lancet*, vol. 345, no. 8962, Jun 3, pp. 1398-1402.

Horvitz, HR & Herskowitz, I 1992, 'Mechanisms of asymmetric cell division: two Bs or not two Bs, that is the question', *Cell*, vol. 68, no. 2, Jan 24, pp. 237-255.

Howe, SJ, Mansour, MR, Schwarzwaelder, K, Bartholomae, C, Hubank, M, Kempski, H, Brugman, MH, Pike-Overzet, K, Chatters, SJ, de Ridder, D, Gilmour, KC, Adams, S, Thornhill, SI, Parsley, KL, Staal, FJ, Gale, RE, Linch, DC, Bayford, J, Brown, L, Quaye, M, Kinnon, C, Ancliff, P, Webb, DK, Schmidt, M, von Kalle, C, Gaspar, HB & Thrasher, AJ 2008, 'Insertional mutagenesis combined with acquired somatic mutations causes leukemogenesis following gene therapy of SCID-X1 patients', *Journal of Clinical Investigation*, vol. 118, no. 9, Sep, pp. 3143-3150.

Hu, B, Tai, A & Wang, P 2011, 'Immunization delivered by lentiviral vectors for cancer and infectious diseases', *Immunological Reviews*, vol. 239, no. 1, Jan, pp. 45-61.

Hu, H, Hilton, MJ, Tu, X, Yu, K, Ornitz, DM & Long, F 2005, 'Sequential roles of Hedgehog and Wnt signaling in osteoblast development', *Development*, vol. 132, no. 1, Jan, pp. 49-60.

Hu, Z, Wang, C, Xiao, Y, Sheng, N, Chen, Y, Xu, Y, Zhang, L, Mo, W, Jing, N & Hu, G 2009, 'NDST1-dependent heparan sulfate regulates BMP signaling and internalization in lung development', *Journal of Cell Science*, vol. 122, no. Pt 8, Apr 15, pp. 1145-1154.

Huang, JQ, Trasler, JM, Igdoura, S, Michaud, J, Hanal, N & Gravel, RA 1997, 'Apoptotic cell death in mouse models of GM2 gangliosidosis and observations on human Tay-Sachs and Sandhoff diseases', *Human Molecular Genetics*, vol. 6, no. 11, Oct, pp. 1879-1885.

Huang, X, Zhong, L, Hendriks, J, Post, JN & Karperien, M 2018, 'The Effects of the WNT-Signaling Modulators BIO and PKF118-310 on the Chondrogenic Differentiation of Human Mesenchymal Stem Cells', *International Journal of Molecular Sciences*, vol. 19, no. 2, Feb 13.

Hurtado, C & De Robertis, EM 2007, 'Neural induction in the absence of organizer in salamanders is mediated by MAPK', *Developmental Biology*, vol. 307, no. 2, Jul 15, pp. 282-289.

Huttner, WB & Brand, M 1997, 'Asymmetric division and polarity of neuroepithelial cells', *Current Opinion in Neurobiology*, vol. 7, no. 1, Feb, pp. 29-39.

Huttner, WB & Kosodo, Y 2005, 'Symmetric versus asymmetric cell division during neurogenesis in the developing vertebrate central nervous system', *Current Opinion in Cell Biology*, vol. 17, no. 6, Dec, pp. 648-657.

Hynes, K, Menicanin, D, Gronthos, S & Bartold, MP 2016, 'Differentiation of iPSC to Mesenchymal Stem-Like Cells and Their Characterization', *Methods in Molecular Biology*, vol. 1357, pp. 353-374.

Im, GI & Quan, Z 2010, 'The effects of Wnt inhibitors on the chondrogenesis of human mesenchymal stem cells', *Tissue Eng Part A*, vol. 16, no. 7, Jul, pp. 2405-2413.

Iozzo, RV 1998, 'Matrix proteoglycans: from molecular design to cellular function', *Annual Review of Biochemistry*, vol. 67, pp. 609-652.

Iozzo, RV & Schaefer, L 2015, 'Proteoglycan form and function: A comprehensive nomenclature of proteoglycans', *Matrix Biology*, vol. 42, March, pp. 11-55.

Irie, A, Habuchi, H, Kimata, K & Sanai, Y 2003, 'Heparan sulfate is required for bone morphogenetic protein-7 signaling', *Biochemical and Biophysical Research Communications*, vol. 308, no. 4, Sep 5, pp. 858-865.

Isgro, MA, Bottoni, P & Scatena, R 2015, 'Neuron-Specific Enolase as a Biomarker: Biochemical and Clinical Aspects', *Advances in Experimental Medicine and Biology*, vol. 867, pp. 125-143.

Ishii, M & Maeda, N 2008, 'Spatiotemporal expression of chondroitin sulfate sulfotransferases in the postnatal developing mouse cerebellum', *Glycobiology*, vol. 18, no. 8, Aug, pp. 602-614.

Israsena, N, Hu, M, Fu, W, Kan, L & Kessler, JA 2004, 'The presence of FGF2 signaling determines whether beta-catenin exerts effects on proliferation or neuronal differentiation of neural stem cells', *Developmental Biology*, vol. 268, no. 1, Apr 1, pp. 220-231.

Jackson, M, Derrick Roberts, A, Martin, E, Rout-Pitt, N, Gronthos, S & Byers, S 2015, 'Mucopolysaccharidosis enzyme production by bone marrow and dental pulp derived human mesenchymal stem cells', *Molecular Genetics and Metabolism*, vol. 114, no. 4, Apr, pp. 584-593.

Jacobs, S, Lie, DC, DeCicco, KL, Shi, Y, DeLuca, LM, Gage, FH & Evans, RM 2006, 'Retinoic acid is required early during adult neurogenesis in the dentate gyrus', *Proceedings of the National Academy of Sciences of the United States of America*, vol. 103, no. 10, Mar 7, pp. 3902-3907.

Jakobs, P, Exner, S, Schurmann, S, Pickhinke, U, Bandari, S, Ortmann, C, Kupich, S, Schulz, P, Hansen, U, Seidler, DG & Grobe, K 2014, 'Scube2 enhances proteolytic Shh processing from the surface of Shh-producing cells', *Journal of Cell Science*, vol. 127, no. Pt 8, Apr 15, pp. 1726-1737.

James, AW 2013, 'Review of Signaling Pathways Governing MSC Osteogenic and Adipogenic Differentiation', *Scientifica (Cairo)*, vol. 2013, p. 684736.

Jardim, LB, Villanueva, MM, de Souza, CF & Netto, CB 2010, 'Clinical aspects of neuropathic lysosomal storage disorders', *Journal of Inherited Metabolic Disease*, vol. 33, no. 4, Aug, pp. 315-329.

Jiang, P, Zhu, T, Xia, Z, Gao, F, Gu, W, Chen, X, Yuan, T & Yu, H 2015, 'Inhibition of MAPK/ERK signaling blocks hippocampal neurogenesis and impairs cognitive performance in prenatally infected neonatal rats', *European Archives of Psychiatry and Clinical Neuroscience*, vol. 265, no. 6, Sep, pp. 497-509.

Jing, Y, Machon, O, Hampl, A, Dvorak, P, Xing, Y & Krauss, S 2011, 'In vitro differentiation of mouse embryonic stem cells into neurons of the dorsal forebrain', *Cellular and Molecular Neurobiology*, vol. 31, no. 5, Jul, pp. 715-727.

Jolly, RD, Johnstone, AC, Norman, EJ, Hopwood, JJ & Walkley, SU 2007, 'Pathology of mucopolysaccharidosis IIIA in Huntaway dogs', *Veterinary Pathology*, vol. 44, no. 5, Sep, pp. 569-578.

Jones-Villeneuve, EM, McBurney, MW, Rogers, KA & Kalnins, VI 1982, 'Retinoic acid induces embryonal carcinoma cells to differentiate into neurons and glial cells', *Journal of Cell Biology*, vol. 94, no. 2, Aug, pp. 253-262.

Jones, SA, Breen, C, Heap, F, Rust, S, de Ruijter, J, Tump, E, Marchal, JP, Pan, L, Qiu, Y, Chung, JK, Nair, N, Haslett, PA, Barbier, AJ & Wijburg, FA 2016, 'A phase 1/2 study of intrathecal heparan-N-sulfatase in patients with mucopolysaccharidosis IIIA', *Molecular Genetics and Metabolism*, vol. 118, no. 3, Jul, pp. 198-205.

Junghans, U, Koops, A, Westmeyer, A, Kappler, J, Meyer, HE & Muller, HW 1995, 'Purification of a meningeal cell-derived chondroitin sulphate proteoglycan with neurotrophic activity for brain neurons and its identification as biglycan', *European Journal of Neuroscience*, vol. 7, no. 11, Nov 1, pp. 2341-2350.

Kaebisch, C, Schipper, D, Babczyk, P, Tobiasch, E 2015, 'The role of purinergic receptors in stem cell differentiation', *Computational and Structural Biotechnology Journal*, vol 13, pp. 75-84.

Kamata, M, Liu, S, Liang, M, Nagaoka, Y & Chen, IS 2010, 'Generation of human induced pluripotent stem cells bearing an anti-HIV transgene by a lentiviral vector carrying an internal murine leukemia virus promoter', *Human Gene Therapy*, vol. 21, no. 11, Nov, pp. 1555-1567.

Kappler, J, Junghans, U, Koops, A, Stichel, CC, Hausser, HJ, Kresse, H & Muller, HW 1997, 'Chondroitin/dermatan sulphate promotes the survival of neurons from rat embryonic neocortex', *European Journal of Neuroscience*, vol. 9, no. 2, Feb, pp. 306-318.

Karpova, EA, Voznyi Ya, V, Keulemans, JL, Hoogeveen, AT, Winchester, B, Tsvetkova, IV & van Diggelen, OP 1996, 'A fluorimetric enzyme assay for the diagnosis of Sanfilippo disease type A (MPS IIIA)', *Journal of Inherited Metabolic Disease*, vol. 19, no. 3, pp. 278-285.

Karten, B, Vance, DE, Campenot, RB & Vance, JE 2002, 'Cholesterol accumulates in cell bodies, but is decreased in distal axons, of Niemann-Pick C1-deficient neurons', *Journal of Neurochemistry*, vol. 83, no. 5, Dec, pp. 1154-1163.

Kawai, M, Mushiake, S, Bessho, K, Murakami, M, Namba, N, Kokubu, C, Michigami, T & Ozono, K 2007, 'Wnt/Lrp/beta-catenin signaling suppresses adipogenesis by inhibiting mutual activation of PPARgamma and C/EBPalpha', *Biochemical and Biophysical Research Communications*, vol. 363, no. 2, Nov 16, pp. 276-282.

Kelly, CM, Tyers, P, Borg, MT, Svendsen, CN, Dunnett, SB & Rosser, AE 2005, 'EGF and FGF-2 responsiveness of rat and mouse neural precursors derived from the embryonic CNS', *Brain Research Bulletin*, vol. 68, no. 1-2, Dec 15, pp. 83-94.

Khan, SA, Nelson, MS, Pan, C, Gaffney, PM & Gupta, P 2008, 'Endogenous heparan sulfate and heparin modulate bone morphogenetic protein-4 signaling and activity', *American Journal of Physiology: Cell Physiology*, vol. 294, no. 6, Jun, pp. C1387-1397.

Kim, G, Choe, Y, Park, J, Cho, S & Kim, K 2002, 'Activation of protein kinase A induces neuronal differentiation of HiB5 hippocampal progenitor cells', *Brain Research: Molecular Brain Research*, vol. 109, no. 1-2, Dec 30, pp. 134-145.

Kim, M, Habiba, A, Doherty, JM, Mills, JC, Mercer, RW & Huettner, JE 2009, 'Regulation of mouse embryonic stem cell neural differentiation by retinoic acid', *Developmental Biology*, vol. 328, no. 2, Apr 15, pp. 456-471.

Kim, MS, Saunders, AM, Hamaoka, BY, Beachy, PA & Leahy, DJ 2011, 'Structure of the protein core of the glypican Dally-like and localization of a region important for hedgehog signaling', *Proceedings of the National Academy of Sciences of the United States of America*, vol. 108, no. 32, Aug 9, pp. 13112-13117.

Kjellen, L & Lindahl, U 1991, 'Proteoglycans: structures and interactions', *Annual Review of Biochemistry*, vol. 60, pp. 443-475.

Kobayashi, H, Gao, Y, Ueta, C, Yamaguchi, A & Komori, T 2000, 'Multilineage differentiation of Cbfa1-deficient calvarial cells in vitro', *Biochemical and Biophysical Research Communications*, vol. 273, no. 2, Jul 5, pp. 630-636.

Kolkova, K, Novitskaya, V, Pedersen, N, Berezin, V & Bock, E 2000, 'Neural cell adhesion molecule-stimulated neurite outgrowth depends on activation of protein kinase C and the Ras-mitogen-activated protein kinase pathway', *Journal of Neuroscience*, vol. 20, no. 6, Mar 15, pp. 2238-2246.

Kolset, SO, Prydz, K & Pejler, G 2004, 'Intracellular Proteoglycans', *Biochemical Journal*, vol. 379, no. 2, April 15, pp. 217-227.

Komada, M, Saitsu, H, Kinboshi, M, Miura, T, Shiota, K & Ishibashi, M 2008, 'Hedgehog signaling is involved in development of the neocortex', *Development*, vol. 135, no. 16, Aug, pp. 2717-2727.

Koops, A, Kappler, J, Junghans, U, Kuhn, G, Kresse, H & Muller, HW 1996, 'Cultured astrocytes express biglycan, a chondroitin/dermatan sulfate proteoglycan supporting the survival of neocortical neurons', *Brain Research: Molecular Brain Research*, vol. 41, no. 1-2, Sep 5, pp. 65-73.

Kopen, GC, Prockop, DJ & Phinney, DG 1999, 'Marrow stromal cells migrate throughout forebrain and cerebellum, and they differentiate into astrocytes after injection into neonatal mouse brains', *Proceedings of the National Academy of Sciences of the United States of America*, vol. 96, no. 19, Sep 14, pp. 10711-10716.

Kramer, J, Hegert, C, Guan, K, Wobus, AM, Muller, PK & Rohwedel, J 2000, 'Embryonic stem cell-derived chondrogenic differentiation in vitro: activation by BMP-2 and BMP-4', *Mechanisms of Development*, vol. 92, no. 2, Apr, pp. 193-205.

Kraushaar, DC, Rai, S, Condac, E, Nairn, A, Zhang, S, Yamaguchi, Y, Moremen, K, Dalton, S & Wang, L 2012, 'Heparan sulfate facilitates FGF and BMP signaling to drive mesoderm differentiation of mouse embryonic stem cells', *Journal of Biological Chemistry*, vol. 287, no. 27, Jun 29, pp. 22691-22700.

Krencik, R & Zhang, SC 2011, 'Directed differentiation of functional astroglial subtypes from human pluripotent stem cells', *Nature Protocols*, vol. 6, no. 11, Oct 13, pp. 1710-1717.

Kretzschmar, M, Doody, J & Massague, J 1997, 'Opposing BMP and EGF signalling pathways converge on the TGF-beta family mediator Smad1', *Nature*, vol. 389, no. 6651, Oct 9, pp. 618-622.

Kreutz, F, dos Santos Petry, F, Camassola, M, Schein, V, Guma, FC, Nardi, NB & Trindade, VM 2013, 'Alterations of membrane lipids and in gene expression of ganglioside metabolism in different brain structures in a mouse model of mucopolysaccharidosis type I (MPS I)', *Gene*, vol. 527, no. 1, Sep 15, pp. 109-114.

Kriegstein, AR & Gotz, M 2003, 'Radial glia diversity: a matter of cell fate', *Glia*, vol. 43, no. 1, Jul, pp. 37-43.

Krivit, W, Pierpont, ME, Ayaz, K, Tsai, M, Ramsay, NK, Kersey, JH, Weisdorf, S, Sibley, R, Snover, D, McGovern, MM & et al. 1984, 'Bone-marrow transplantation in the Maroteaux-Lamy syndrome (mucopolysaccharidosis type VI). Biochemical and clinical status 24 months after transplantation', *New England Journal of Medicine*, vol. 311, no. 25, Dec 20, pp. 1606-1611.

Krivit, W, Sung, JH, Shapiro, EG & Lockman, LA 1995, 'Microglia: the effector cell for reconstitution of the central nervous system following bone marrow transplantation for lysosomal and peroxisomal storage diseases', *Cell Transplantation*, vol. 4, no. 4, Jul-Aug, pp. 385-392.

Krufka, A, Guimond, S & Rapraeger, AC 1996, 'Two hierarchies of FGF-2 signaling in heparin: mitogenic stimulation and high-affinity binding/receptor transphosphorylation', *Biochemistry*, vol. 35, no. 34, Aug 27, pp. 11131-11141.

Kuo, WJ, Digman, MA & Lander, AD 2010, 'Heparan sulfate acts as a bone morphogenetic protein coreceptor by facilitating ligand-induced receptor hetero-oligomerization', *Molecular Biology of the Cell*, vol. 21, no. 22, Nov 15, pp. 4028-4041.

Kuroda, H, Fuentealba, L, Ikeda, A, Reversade, B & De Robertis, EM 2005, 'Default neural induction: neuralization of dissociated Xenopus cells is mediated by Ras/MAPK activation', *Genes & Development*, vol. 19, no. 9, May 1, pp. 1022-1027.

Lamoureux, F, Baud'huin, M, Duplomb, L, Heymann, D & Redini, F 2007, 'Proteoglycans: key partners in bone cell biology', *Bioessays*, vol. 29, no. 8, Aug, pp. 758-771.

Lange, MC, Teive, HA, Troiano, AR, Bitencourt, M, Funke, VA, Setubal, DC, Zanis Neto, J, Medeiros, CR, Werneck, LC, Pasquini, R & Bonfim, CM 2006, 'Bone marrow transplantation in patients with storage diseases: a developing country experience', *Arquivos de Neuro-Psiquiatria*, vol. 64, no. 1, Mar, pp. 1-4.

Langereis, EJ, Wagemans, T, Kulik, W, Lefeber, DJ, van Lenthe, H, Oussoren, E, van der Ploeg, AT, Ruijter, GJ, Wevers, RA, Wijburg, FA & van Vlies, N 2015, 'A Multiplex Assay for the Diagnosis of Mucopolysaccharidoses and Mucolipidoses', *PloS One*, vol. 10, no. 9, p. e0138622.

Lau, AA, Hannouche, H, Rozaklis, T, Hassiotis, S, Hopwood, JJ & Hemsley, KM 2010, 'Allogeneic stem cell transplantation does not improve neurological deficits in mucopolysaccharidosis type IIIA mice', *Experimental Neurology*, vol. 225, no. 2, Oct, pp. 445-454.

Lee, MK, Tuttle, JB, Rebhun, LI, Cleveland, DW & Frankfurter, A 1990, 'The expression and posttranslational modification of a neuron-specific beta-tubulin isotype during chick embryogenesis', *Cell Motility and the Cytoskeleton*, vol. 17, no. 2, pp. 118-132.

Lee, TH, Song, SH, Kim, KL, Yi, JY, Shin, GH, Kim, JY, Kim, J, Han, YM, Lee, SH, Lee, SH, Shim, SH & Suh, W 2010, 'Functional recapitulation of smooth muscle cells via induced pluripotent stem cells from human aortic smooth muscle cells', *Circulation Research*, vol. 106, no. 1, Jan 8, pp. 120-128.

Lehman, TJ, Miller, N, Norquist, B, Underhill, L & Keutzer, J 2011, 'Diagnosis of the mucopolysaccharidoses', *Rheumatology (Oxford, England)*, vol. 50 Suppl 5, Dec, pp. v41-48.

Lemonnier, T, Blanchard, S, Toli, D, Roy, E, Bigou, S, Froissart, R, Rouvet, I, Vitry, S, Heard, JM & Bohl, D 2011, 'Modeling neuronal defects associated with a lysosomal disorder using patient-derived induced pluripotent stem cells', *Human Molecular Genetics*, vol. 20, no. 18, Sep 15, pp. 3653-3666.

Lendahl, U, Zimmerman, LB & McKay, RD 1990, 'CNS stem cells express a new class of intermediate filament protein', *Cell*, vol. 60, no. 4, Feb 23, pp. 585-595.

Lengner, CJ, Hassan, MQ, Serra, RW, Lepper, C, van Wijnen, AJ, Stein, JL, Lian, JB & Stein, GS 2005, 'Nkx3.2-mediated repression of Runx2 promotes chondrogenic differentiation', *Journal of Biological Chemistry*, vol. 280, no. 16, Apr 22, pp. 15872-15879.

Lepski, G, Jannes, CE, Maciaczyk, J, Papazoglou, A, Mehlhorn, AT, Kaiser, S, Teixeira, MJ, Marie, SK, Bischofberger, J & Nikkhah, G 2010, 'Limited Ca2+ and PKA-pathway dependent neurogenic differentiation of human adult mesenchymal stem cells as compared to fetal neuronal stem cells', *Experimental Cell Research*, vol. 316, no. 2, Jan 15, pp. 216-231.

Li, HH, Yu, WH, Rozengurt, N, Zhao, HZ, Lyons, KM, Anagnostaras, S, Fanselow, MS, Suzuki, K, Vanier, MT & Neufeld, EF 1999, 'Mouse model of Sanfilippo syndrome type B produced by targeted disruption of the gene encoding alpha-N-acetylglucosaminidase', *Proceedings of the National Academy of Sciences of the United States of America*, vol. 96, no. 25, Dec 7, pp. 14505-14510.

Li, HH, Zhao, HZ, Neufeld, EF, Cai, Y & Gomez-Pinilla, F 2002, 'Attenuated plasticity in neurons and astrocytes in the mouse model of Sanfilippo syndrome type B', *Journal of Neuroscience Research*, vol. 69, no. 1, Jul 1, pp. 30-38.

Li, XJ, Zhang, X, Johnson, MA, Wang, ZB, Lavaute, T & Zhang, SC 2009, 'Coordination of sonic hedgehog and Wnt signaling determines ventral and dorsal telencephalic neuron types from human embryonic stem cells', *Development*, vol. 136, no. 23, Dec, pp. 4055-4063.

Liao, J, Wu, Z, Wang, Y, Cheng, L, Cui, C, Gao, Y, Chen, T, Rao, L, Chen, S, Jia, N, Dai, H, Xin, S, Kang, J, Pei, G & Xiao, L 2008, 'Enhanced efficiency of generating induced pluripotent stem (iPS) cells from human somatic cells by a combination of six transcription factors', *Cell Research*, vol. 18, no. 5, May, pp. 600-603.

Lie, DC, Colamarino, SA, Song, HJ, Desire, L, Mira, H, Consiglio, A, Lein, ES, Jessberger, S, Lansford, H, Dearie, AR & Gage, FH 2005, 'Wnt signalling regulates adult hippocampal neurogenesis', *Nature*, vol. 437, no. 7063, Oct 27, pp. 1370-1375.

Lim, DA, Tramontin, AD, Trevejo, JM, Herrera, DG, Garcia-Verdugo, JM & Alvarez-Buylla, A 2000, 'Noggin antagonizes BMP signaling to create a niche for adult neurogenesis', *Neuron*, vol. 28, no. 3, Dec, pp. 713-726.

Lin, X 2004, 'Functions of heparan sulfate proteoglycans in cell signaling during development', *Development*, vol. 131, no. 24, Dec, pp. 6009-6021.

Lin, X, Buff, EM, Perrimon, N & Michelson, AM 1999, 'Heparan sulfate proteoglycans are essential for FGF receptor signaling during Drosophila embryonic development', *Development*, vol. 126, no. 17, Sep, pp. 3715-3723.

Liu, Z, Huang, D, Zhang, M, Chen, Z, Jin, J, Huang, S, Zhang, Z, Wang, Z, Chen, L, Chen, L & Xu, Y 2011, 'Cocaine- and amphetamine-regulated transcript promotes the differentiation of mouse bone marrow-derived mesenchymal stem cells into neural cells', *BMC Neuroscience*, vol. 12, Jul 14, p. 67.

Livak, KJ & Schmittgen, TD 2001, 'Analysis of relative gene expression data using real-time quantitative PCR and the 2(-Delta Delta C(T)) Method', *Methods*, vol. 25, no. 4, Dec, pp. 402-408.

Locatelli, F, Corti, S, Donadoni, C, Guglieri, M, Capra, F, Strazzer, S, Salani, S, Del Bo, R, Fortunato, F, Bordoni, A & Comi, GP 2003, 'Neuronal differentiation of murine bone marrow Thy-1- and Sca-1-positive cells', *Journal of Hematotherapy & Stem Cell Research*, vol. 12, no. 6, Dec, pp. 727-734.

Long, K, Moss, L, Laursen, L, Boulter, L & ffrench-Constant, C 2016, 'Integrin signalling regulates the expansion of neuroepithelial progenitors and neurogenesis via Wnt7a and Decorin', *Nat Commun*, vol. 7, Feb 3, p. 10354.

Loo, BM, Kreuger, J, Jalkanen, M, Lindahl, U & Salmivirta, M 2001, 'Binding of heparin/heparan sulfate to fibroblast growth factor receptor 4', *Journal of Biological Chemistry*, vol. 276, no. 20, May 18, pp. 16868-16876.

Lopes, RS, Cardoso, MM, Sampaio, AO, Barbosa, MS, Jr., Souza, CC, MC, DAS, Ferreira, EM, Freire, MA, Lima, RR & Gomes-Leal, W 2016, 'Indomethacin treatment reduces microglia activation and increases numbers of neuroblasts in the subventricular zone and ischaemic striatum after focal ischaemia', *Journal of Biosciences*, vol. 41, no. 3, Sep, pp. 381-394.

Lovestone, S, Killick, R, Di Forti, M & Murray, R 2007, 'Schizophrenia as a GSK-3 dysregulation disorder', *Trends in Neurosciences*, vol. 30, no. 4, Apr, pp. 142-149.

Lu, P, Blesch, A & Tuszynski, MH 2004, 'Induction of bone marrow stromal cells to neurons: differentiation, transdifferentiation, or artifact?', *Journal of Neuroscience Research*, vol. 77, no. 2, Jul 15, pp. 174-191.

Maccarana, M, Sakura, Y, Tawada, A, Yoshida, K & Lindahl, U 1996, 'Domain structure of heparan sulfates from bovine organs', *Journal of Biological Chemistry*, vol. 271, no. 30, Jul 26, pp. 17804-17810.

MacDonald, BT, Tamai, K & He, X 2009, 'Wnt/beta-catenin signaling: components, mechanisms, and diseases', *Developmental Cell*, vol. 17, no. 1, Jul, pp. 9-26.

Machold, R, Hayashi, S, Rutlin, M, Muzumdar, MD, Nery, S, Corbin, JG, Gritli-Linde, A, Dellovade, T, Porter, JA, Rubin, LL, Dudek, H, McMahon, AP & Fishell, G 2003, 'Sonic hedgehog is required for progenitor cell maintenance in telencephalic stem cell niches', *Neuron*, vol. 39, no. 6, Sep 11, pp. 937-950.

Maden, M 2007, 'Retinoic acid in the development, regeneration and maintenance of the nervous system', *Nature Reviews: Neuroscience*, vol. 8, no. 10, Oct, pp. 755-765.

Maherali, N, Ahfeldt, T, Rigamonti, A, Utikal, J, Cowan, C & Hochedlinger, K 2008, 'A high-efficiency system for the generation and study of human induced pluripotent stem cells', *Cell Stem Cell*, vol. 3, no. 3, Sep 11, pp. 340-345.

Majumdar, MK, Wang, E & Morris, EA 2001, 'BMP-2 and BMP-9 promotes chondrogenic differentiation of human multipotential mesenchymal cells and overcomes the inhibitory effect of IL-1', *Journal of Cellular Physiology*, vol. 189, no. 3, Dec, pp. 275-284.

Mangina, CA & Sokolov, EN 2006, 'Neuronal plasticity in memory and learning abilities: theoretical position and selective review', *International Journal of Psychophysiology*, vol. 60, no. 3, Jun, pp. 203-214.

Marco, S, Pujol, A, Roca, C, Motas, S, Ribera, A, Garcia, M, Molas, M, Villacampa, P, Melia, CS, Sanchez, V, Sanchez, X, Bertolin, J, Ruberte, J, Haurigot, V & Bosch, F 2016, 'Progressive neurologic and somatic disease in a novel mouse model of human mucopolysaccharidosis type IIIC', *Disease Models & Mechanisms*, vol. 9, no. 9, Sep 1, pp. 999-1013.

Martin, JJ & Ceuterick, C 1983, 'Prenatal pathology in mucopolysaccharidoses: a comparison with postnatal cases', *Clinical Neuropathology*, vol. 2, no. 3, pp. 122-127.

Martins, C, Hulkova, H, Dridi, L, Dormoy-Raclet, V, Grigoryeva, L, Choi, Y, Langford-Smith, A, Wilkinson, FL, Ohmi, K, DiCristo, G, Hamel, E, Ausseil, J, Cheillan, D, Moreau, A, Svobodova, E, Hajkova, Z, Tesarova, M, Hansikova, H, Bigger, BW, Hrebicek, M & Pshezhetsky, AV 2015, 'Neuroinflammation, mitochondrial defects and neurodegeneration in mucopolysaccharidosis III type C mouse model', *Brain*, vol. 138, no. Pt 2, Feb, pp. 336-355.

Martynoga, B, Drechsel, D & Guillemot, F 2012, 'Molecular control of neurogenesis: a view from the mammalian cerebral cortex', *Cold Spring Harbor Perspectives in Biology*, vol. 4, no. 10, Oct 1.

Mayr, B & Montminy, M 2001, 'Transcriptional regulation by the phosphorylation-dependent factor CREB', *Nature Reviews: Molecular Cell Biology*, vol. 2, no. 8, Aug, pp. 599-609.

McDowell, GA, Cowan, TM, Blitzer, MG & Greene, CL 1993, 'Intrafamilial variability in Hurler syndrome and Sanfilippo syndrome type A: implications for evaluation of new therapies', *American Journal of Medical Genetics*, vol. 47, no. 7, Nov 15, pp. 1092-1095.

McGlynn, R, Dobrenis, K & Walkley, SU 2004, 'Differential subcellular localization of cholesterol, gangliosides, and glycosaminoglycans in murine models of mucopolysaccharide storage disorders', *Journal of Comparative Neurology*, vol. 480, no. 4, Dec 20, pp. 415-426.

McGuiness, JA, Scheinert, RB, Asokan, A, Stadler, VC, Lee, CS, Rani, A, Kumar, A, Foster, TC & Ormerod, BK 2017, 'Indomethacin Increases Neurogenesis across Age Groups and Improves Delayed Probe Trial Difference Scores in Middle-Aged Rats', *Frontiers in Aging Neuroscience*, vol. 9, p. 280.

McIntyre, C, Byers, S & Anson, D 2010, 'Correction of mucopolysaccharidosis type IIIA somatic and central nervous system pathology by lentiviral-mediated gene transfer', *Journal of Gene Medicine*, vol. 12, no. 9, pp. 717-728.

McKinnis, EJ, Sulzbacher, S, Rutledge, JC, Sanders, J & Scott, CR 1996, 'Bone marrow transplantation in Hunter syndrome', *Journal of Pediatrics*, vol. 129, no. 1, Jul, pp. 145-148.

McMurray, CT 2000, 'Neurodegeneration: diseases of the cytoskeleton?', *Cell Death and Differentiation*, vol. 7, no. 10, Oct, pp. 861-865.

Meikle, PJ, Fietz, MJ & Hopwood, JJ 2004, 'Diagnosis of lysosomal storage disorders: current techniques and future directions', *Expert Review of Molecular Diagnostics*, vol. 4, no. 5, Sep, pp. 677-691.

Meikle, PJ, Hopwood, JJ, Clague, AE & Carey, WF 1999, 'Prevalence of lysosomal storage disorders', *JAMA*, vol. 281, no. 3, Jan 20, pp. 249-254.

Menezes, JR & Luskin, MB 1994, 'Expression of neuron-specific tubulin defines a novel population in the proliferative layers of the developing telencephalon', *Journal of Neuroscience*, vol. 14, no. 9, Sep, pp. 5399-5416.

Meng, XL, Shen, JS, Kawagoe, S, Ohashi, T, Brady, RO & Eto, Y 2010, 'Induced pluripotent stem cells derived from mouse models of lysosomal storage disorders', *Proceedings of the National Academy of Sciences of the United States of America*, vol. 107, no. 17, Apr 27, pp. 7886-7891.

Meyerrose, TE, Roberts, M, Ohlemiller, KK, Vogler, CA, Wirthlin, L, Nolta, JA & Sands, MS 2008, 'Lentiviral-transduced human mesenchymal stem cells persistently express therapeutic levels of enzyme in a xenotransplantation model of human disease', *Stem Cells*, vol. 26, no. 7, Jul, pp. 1713-1722.

Meyers, EA, Gobeske, KT, Bond, AM, Jarrett, JC, Peng, CY & Kessler, JA 2016, 'Increased bone morphogenetic protein signaling contributes to age-related declines in neurogenesis and cognition', *Neurobiology of Aging*, vol. 38, Feb, pp. 164-175.

Ming, GL & Song, H 2005, 'Adult neurogenesis in the mammalian central nervous system', *Annual Review of Neuroscience*, vol. 28, pp. 223-250.

Mishina, Y, Starbuck, MW, Gentile, MA, Fukuda, T, Kasparcova, V, Seedor, JG, Hanks, MC, Amling, M, Pinero, GJ, Harada, S & Behringer, RR 2004, 'Bone morphogenetic protein type IA receptor signaling regulates postnatal osteoblast function and bone remodeling', *Journal of Biological Chemistry*, vol. 279, no. 26, Jun 25, pp. 27560-27566.

Mitchell, N, Petralia, RS, Currier, DG, Wang, YX, Kim, A, Mattson, MP & Yao, PJ 2012, 'Sonic hedgehog regulates presynaptic terminal size, ultrastructure and function in hippocampal neurons', *Journal of Cell Science*, vol. 125, no. Pt 18, Sep 15, pp. 4207-4213.

Mitsunaga, C, Mikami, T, Mizumoto, S, Fukuda, J & Sugahara, K 2006, 'Chondroitin sulfate/dermatan sulfate hybrid chains in the development of cerebellum. Spatiotemporal regulation of the expression of critical disulfated disaccharides by specific sulfotransferases', *Journal of Biological Chemistry*, vol. 281, no. 28, Jul 14, pp. 18942-18952.

Mizuguchi, S, Uyama, T, Kitagawa, H, Nomura, KH, Dejima, K, Gengyo-Ando, K, Mitani, S, Sugahara, K & Nomura, K 2003, 'Chondroitin proteoglycans are involved in cell division of Caenorhabditis elegans', *Nature*, vol. 423, no. 6938, May 22, pp. 443-448.

Mohamad, O, Yu, SP, Chen, D, Ogle, M, Song, M & Wei, L 2013, 'Efficient neuronal differentiation of mouse ES and iPS cells using a rotary cell culture protocol', *Differentiation*, vol. 86, no. 4-5, Nov-Dec, pp. 149-158.

Mohammad, MH, Al-Shammari, AM, Al-Juboory, AA & Yaseen, NY 2016, 'Characterization of neural stemness status through the neurogenesis process for bone marrow mesenchymal stem cells', *Stem Cells Cloning*, vol. 9, pp. 1-15.

Montero, A, Okada, Y, Tomita, M, Ito, M, Tsurukami, H, Nakamura, T, Doetschman, T, Coffin, JD & Hurley, MM 2000, 'Disruption of the fibroblast growth factor-2 gene results in decreased bone mass and bone formation', *Journal of Clinical Investigation*, vol. 105, no. 8, Apr, pp. 1085-1093.

Muenzer, J 2011, 'Overview of the mucopolysaccharidoses', *Rheumatology (Oxford, England)*, vol. 50 Suppl 5, Dec, pp. v4-12.

Muenzer, J, Lamsa, JC, Garcia, A, Dacosta, J, Garcia, J & Treco, DA 2002, 'Enzyme replacement therapy in mucopolysaccharidosis type II (Hunter syndrome): a preliminary report', *Acta Paediatrica. Supplement*, vol. 91, no. 439, pp. 98-99.

Mukai, T, Nagamura-Inoue, T, Shimazu, T, Mori, Y, Takahashi, A, Tsunoda, H, Yamaguchi, S & Tojo, A 2016, 'Neurosphere formation enhances the neurogenic differentiation potential and migratory ability of umbilical cord-mesenchymal stromal cells', *Cytotherapy*, vol. 18, no. 2, Feb, pp. 229-241.

Mundy, C, Bello, A, Sgariglia, F, Koyama, E & Pacifici, M 2016, 'HhAntag, a Hedgehog Signaling Antagonist, Suppresses Chondrogenesis and Modulates Canonical and Non-Canonical BMP Signaling', *Journal of Cellular Physiology*, vol. 231, no. 5, May, pp. 1033-1044.

Munji, RN, Choe, Y, Li, G, Siegenthaler, JA & Pleasure, SJ 2011, 'Wnt signaling regulates neuronal differentiation of cortical intermediate progenitors', *Journal of Neuroscience*, vol. 31, no. 5, Feb 2, pp. 1676-1687.

Murali, S, Rai, B, Dombrowski, C, Lee, JL, Lim, ZX, Bramono, DS, Ling, L, Bell, T, Hinkley, S, Nathan, SS, Hui, JH, Wong, HK, Nurcombe, V & Cool, SM 2013, 'Affinity-selected heparan sulfate for bone repair', *Biomaterials*, vol. 34, no. 22, Jul, pp. 5594-5605.

Murphy, KJ, Merry, CL, Lyon, M, Thompson, JE, Roberts, IS & Gallagher, JT 2004, 'A new model for the domain structure of heparan sulfate based on the novel specificity of K5 lyase', *Journal of Biological Chemistry*, vol. 279, no. 26, Jun 25, pp. 27239-27245.

Murphy, M, Reid, K, Ford, M, Furness, JB & Bartlett, PF 1994, 'FGF2 regulates proliferation of neural crest cells, with subsequent neuronal differentiation regulated by LIF or related factors', *Development*, vol. 120, no. 12, Dec, pp. 3519-3528.

Mutch, CA, Schulte, JD, Olson, E & Chenn, A 2010, 'Beta-catenin signaling negatively regulates intermediate progenitor population numbers in the developing cortex', *PloS One*, vol. 5, no. 8, p. e12376.

Nakato, H & Kimata, K 2002, 'Heparan sulfate fine structure and specificity of proteoglycan functions', *Biochimica et Biophysica Acta (BBA) - Bioenergetics*, vol. 1573, no. 3, Dec 19, pp. 312-318.

Neufeld, E & Muenzer, J 2001, 'The Mucopolysaccharidoses', in C Scriver, A Beaudet, W SLY & D Valle (eds), *The metabolic and molecular bases of inherited disease*, McGraw Hill, United States of America, pp. 3421-3452.

Neuhuber, B, Gallo, G, Howard, L, Kostura, L, Mackay, A & Fischer, I 2004, 'Reevaluation of in vitro differentiation protocols for bone marrow stromal cells: disruption of actin cytoskeleton induces rapid morphological changes and mimics neuronal phenotype', *Journal of Neuroscience Research*, vol. 77, no. 2, Jul 15, pp. 192-204.

New, SE, Alvarez-Gonzalez, C, Vagaska, B, Gomez, SG, Bulstrode, NW, Madrigal, A & Ferretti, P 2015, 'A matter of identity - Phenotype and differentiation potential of human somatic stem cells', *Stem Cell Res*, vol. 15, no. 1, Jul, pp. 1-13.

Nixon, RA & Logvinenko, KB 1986, 'Multiple fates of newly synthesized neurofilament proteins: evidence for a stationary neurofilament network distributed nonuniformly along axons of retinal ganglion cell neurons', *Journal of Cell Biology*, vol. 102, no. 2, Feb, pp. 647-659.

Nur, BG, Nur, H & Mihci, E 2016, 'Bone mineral density in patients with mucopolysaccharidosis type III', *Journal of Bone and Mineral Metabolism*, May 18.

Ohkubo, Y, Uchida, AO, Shin, D, Partanen, J & Vaccarino, FM 2004, 'Fibroblast growth factor receptor 1 is required for the proliferation of hippocampal progenitor cells and for hippocampal growth in mouse', *Journal of Neuroscience*, vol. 24, no. 27, Jul 7, pp. 6057-6069.

Ohlig, S, Farshi, P, Pickhinke, U, van den Boom, J, Hoing, S, Jakuschev, S, Hoffmann, D, Dreier, R, Scholer, HR, Dierker, T, Bordych, C & Grobe, K 2011, 'Sonic hedgehog shedding results in functional activation of the solubilized protein', *Developmental Cell*, vol. 20, no. 6, Jun 14, pp. 764-774.

Ohmi, K, Zhao, HZ & Neufeld, EF 2011, 'Defects in the medial entorhinal cortex and dentate gyrus in the mouse model of Sanfilippo syndrome type B', *PloS One*, vol. 6, no. 11, p. e27461.

Okada, Y, Shimazaki, T, Sobue, G & Okano, H 2004, 'Retinoic-acid-concentration-dependent acquisition of neural cell identity during in vitro differentiation of mouse embryonic stem cells', *Developmental Biology*, vol. 275, no. 1, Nov 1, pp. 124-142.

Okamoto, M, Murai, J, Yoshikawa, H & Tsumaki, N 2006, 'Bone morphogenetic proteins in bone stimulate osteoclasts and osteoblasts during bone development', *Journal of Bone and Mineral Research*, vol. 21, no. 7, Jul, pp. 1022-1033.

Okolicsanyi, RK, Griffiths, LR & Haupt, LM 2014, 'Mesenchymal stem cells, neural lineage potential, heparan sulfate proteoglycans and the matrix', *Developmental Biology*, vol. 388, no. 1, Apr 1, pp. 1-10.

Ono, M, Hamada, Y, Horiuchi, Y, Matsuo-Takasaki, M, Imoto, Y, Satomi, K, Arinami, T, Hasegawa, M, Fujioka, T, Nakamura, Y & Noguchi, E 2012, 'Generation of induced pluripotent stem cells from human nasal epithelial cells using a Sendai virus vector', *PloS One*, vol. 7, no. 8, p. e42855.

Ortmann, C, Pickhinke, U, Exner, S, Ohlig, S, Lawrence, R, Jboor, H, Dreier, R & Grobe, K 2015, 'Sonic hedgehog processing and release are regulated by glypican heparan sulfate proteoglycans', *Journal of Cell Science*, vol. 128, no. 23, Dec 01, p. 4462.

Osterholm, C, Barczyk, MM, Busse, M, Gronning, M, Reed, RK & Kusche-Gullberg, M 2009, 'Mutation in the heparan sulfate biosynthesis enzyme EXT1 influences growth factor signaling and fibroblast interactions with the extracellular matrix', *Journal of Biological Chemistry*, vol. 284, no. 50, Dec 11, pp. 34935-34943.

Palmer, TD, Markakis, EA, Willhoite, AR, Safar, F & Gage, FH 1999, 'Fibroblast growth factor-2 activates a latent neurogenic program in neural stem cells from diverse regions of the adult CNS', *Journal of Neuroscience*, vol. 19, no. 19, Oct 1, pp. 8487-8497.

Pan, C, Nelson, MS, Reyes, M, Koodie, L, Brazil, JJ, Stephenson, EJ, Zhao, RC, Peters, C, Selleck, SB, Stringer, SE & Gupta, P 2005, 'Functional abnormalities of heparan sulfate in mucopolysaccharidosis-I are associated with defective biologic activity of FGF-2 on human multipotent progenitor cells', *Blood*, vol. 106, no. 6, Sep 15, pp. 1956-1964.

Panakova, D, Sprong, H, Marois, E, Thiele, C & Eaton, S 2005, 'Lipoprotein particles are required for Hedgehog and Wingless signalling', *Nature*, vol. 435, no. 7038, May 05, pp. 58-65.

Panchision, DM & McKay, RD 2002, 'The control of neural stem cells by morphogenic signals', *Current Opinion in Genetics & Development*, vol. 12, no. 4, Aug, pp. 478-487.

Paris, I, Perez-Pastene, C, Cardenas, S, Iturriaga-Vasquez, P, Munoz, P, Couve, E, Caviedes, P & Segura-Aguilar, J 2010, 'Aminochrome induces disruption of actin, alpha-, and beta-tubulin cytoskeleton networks in substantia-nigra-derived cell line', *Neurotoxicity Research*, vol. 18, no. 1, Jul, pp. 82-92.

Parivar, K, Baharara, J & Sheikholeslami, A 2015, 'Neural differentiation of mouse bone marrow-derived mesenchymal stem cells treated with sex steroid hormones and basic fibroblast growth factor', *Cell J*, vol. 17, no. 1, Spring, pp. 27-36.

Park, SY, Shin, JH & Kee, SH 2017, 'E-cadherin expression increases cell proliferation by regulating energy metabolism through nuclear factor-kappaB in AGS cells', *Cancer Science*, vol. 108, no. 9, Sep, pp. 1769-1777.

Pei, JJ, Braak, E, Braak, H, Grundke-Iqbal, I, Iqbal, K, Winblad, B & Cowburn, RF 1999, 'Distribution of active glycogen synthase kinase 3beta (GSK-3beta) in brains staged for Alzheimer disease neurofibrillary changes', *Journal of Neuropathology & Experimental Neurology*, vol. 58, no. 9, Sep, pp. 1010-1019.

Penc, SF, Pomahac, B, Winkler, T, Dorschner, RA, Eriksson, E, Herndon, M & Gallo, RL 1998, 'Dermatan sulfate released after injury is a potent promoter of fibroblast growth factor-2 function', *Journal of Biological Chemistry*, vol. 273, no. 43, Oct 23, pp. 28116-28121.

Pera, EM, Ikeda, A, Eivers, E & De Robertis, EM 2003, 'Integration of IGF, FGF, and anti-BMP signals via Smad1 phosphorylation in neural induction', *Genes & Development*, vol. 17, no. 24, Dec 15, pp. 3023-3028.

Pereira, RF, Halford, KW, O'Hara, MD, Leeper, DB, Sokolov, BP, Pollard, MD, Bagasra, O & Prockop, DJ 1995, 'Cultured adherent cells from marrow can serve as long-lasting precursor cells for bone, cartilage, and lung in irradiated mice', *Proceedings of the National Academy of Sciences of the United States of America*, vol. 92, no. 11, May 23, pp. 4857-4861.

Pereira, RF, O'Hara, MD, Laptev, AV, Halford, KW, Pollard, MD, Class, R, Simon, D, Livezey, K & Prockop, DJ 1998, 'Marrow stromal cells as a source of progenitor cells for nonhematopoietic tissues in transgenic mice with a phenotype of osteogenesis imperfecta', *Proceedings of the National Academy of Sciences of the United States of America*, vol. 95, no. 3, Feb 3, pp. 1142-1147.

Perkins, KJ, Muller, V, Weber, B & Hopwood, JJ 2001, 'Prediction of Sanfilippo phenotype severity from immunoquantification of heparan-N-sulfamidase in cultured fibroblasts from mucopolysaccharidosis type IIIA patients', *Molecular Genetics and Metabolism*, vol. 73, no. 4, Aug, pp. 306-312.

Perrimon, N & Bernfield, M 2000, 'Specificities of heparan sulphate proteoglycans in developmental processes', *Nature*, vol. 404, no. 6779, Apr 13, pp. 725-728.

Pfaffl, MW 2001, 'A new mathematical model for relative quantification in real-time RT-PCR', *Nucleic Acids Research*, vol. 29, no. 9, May 1, p. e45.

Pfeiffer, S, Ricardo, S, Manneville, JB, Alexandre, C & Vincent, JP 2002, 'Producing cells retain and recycle Wingless in Drosophila embryos', *Current Biology*, vol. 12, no. 11, Jun 04, pp. 957-962.

Pimentel, B, de la Rosa, EJ & de Pablo, F 1996, 'Insulin acts as an embryonic growth factor for Drosophila neural cells', *Biochemical and Biophysical Research Communications*, vol. 226, no. 3, Sep 24, pp. 855-861.

Piotrowska, E, Jakobkiewicz-Banecka, J, Tylki-Szymanska, A, Czartoryska, B, Wegrzyn, A & Wegrzyn, G 2009, 'Correlation between severity of mucopolysaccharidoses and combination of the residual enzyme activity and efficiency of glycosaminoglycan synthesis', *Acta Paediatrica*, vol. 98, no. 4, Apr, pp. 743-749.

Pittenger, MF, Mackay, AM, Beck, SC, Jaiswal, RK, Douglas, R, Mosca, JD, Moorman, MA, Simonetti, DW, Craig, S & Marshak, DR 1999, 'Multilineage potential of adult human mesenchymal stem cells', *Science*, vol. 284, no. 5411, Apr 2, pp. 143-147.

Plaisant, M, Giorgetti-Peraldi, S, Gabrielson, M, Loubat, A, Dani, C & Peraldi, P 2011, 'Inhibition of hedgehog signaling decreases proliferation and clonogenicity of human mesenchymal stem cells', *PloS One*, vol. 6, no. 2, Feb 3, p. e16798.

Powell, PP, Finklestein, SP, Dionne, CA, Jaye, M & Klagsbrun, M 1991, 'Temporal, differential and regional expression of mRNA for basic fibroblast growth factor in the developing and adult rat brain', *Brain Research: Molecular Brain Research*, vol. 11, no. 1, Aug, pp. 71-77.

Prud'homme, B, Lartillot, N, Balavoine, G, Adoutte, A & Vervoort, M 2002, 'Phylogenetic analysis of the Wnt gene family. Insights from lophotrochozoan members', *Current Biology*, vol. 12, no. 16, Aug 20, p. 1395.

Purpura, DP & Suzuki, K 1976, 'Distortion of neuronal geometry and formation of aberrant synapses in neuronal storage disease', *Brain Research*, vol. 116, no. 1, Oct 29, pp. 1-21.

Pye, DA, Vives, RR, Hyde, P & Gallagher, JT 2000, 'Regulation of FGF-1 mitogenic activity by heparan sulfate oligosaccharides is dependent on specific structural features: differential requirements for the modulation of FGF-1 and FGF-2', *Glycobiology*, vol. 10, no. 11, Nov, pp. 1183-1192.

Pye, DA, Vives, RR, Turnbull, JE, Hyde, P & Gallagher, JT 1998, 'Heparan sulfate oligosaccharides require 6-O-sulfation for promotion of basic fibroblast growth factor mitogenic activity', *Journal of Biological Chemistry*, vol. 273, no. 36, Sep 4, pp. 22936-22942.

Qian, X, Davis, AA, Goderie, SK & Temple, S 1997, 'FGF2 concentration regulates the generation of neurons and glia from multipotent cortical stem cells', *Neuron*, vol. 18, no. 1, Jan, pp. 81-93.

Qu, Q, Sun, G, Murai, K, Ye, P, Li, W, Asuelime, G, Cheung, YT & Shi, Y 2013, 'Wnt7a regulates multiple steps of neurogenesis', *Molecular and Cellular Biology*, vol. 33, no. 13, Jul, pp. 2551-2559.

Quartu, M, Serra, MP, Boi, M, Ibba, V, Melis, T & Del Fiacco, M 2008, 'Polysialylated-neural cell adhesion molecule (PSA-NCAM) in the human trigeminal ganglion and brainstem at prenatal and adult ages', *BMC Neuroscience*, vol. 9, Nov 6, p. 108.

Raballo, R, Rhee, J, Lyn-Cook, R, Leckman, JF, Schwartz, ML & Vaccarino, FM 2000, 'Basic fibroblast growth factor (Fgf2) is necessary for cell proliferation and neurogenesis in the developing cerebral cortex', *Journal of Neuroscience*, vol. 20, no. 13, Jul 1, pp. 5012-5023.

Rai, KS, Hattiangady, B & Shetty, AK 2007, 'Enhanced production and dendritic growth of new dentate granule cells in the middle-aged hippocampus following intracerebroventricular FGF-2 infusions', *European Journal of Neuroscience*, vol. 26, no. 7, Oct, pp. 1765-1779.

Rakic, P 1995, 'A small step for the cell, a giant leap for mankind: a hypothesis of neocortical expansion during evolution', *Trends in Neurosciences*, vol. 18, no. 9, Sep, pp. 383-388.

Raman, R, Venkataraman, G, Ernst, S, Sasisekharan, V & Sasisekharan, R 2003, 'Structural specificity of heparin binding in the fibroblast growth factor family of proteins', *Proceedings of the National Academy of Sciences of the United States of America*, vol. 100, no. 5, Mar 4, pp. 2357-2362.

Rash, BG, Lim, HD, Breunig, JJ & Vaccarino, FM 2011, 'FGF signaling expands embryonic cortical surface area by regulating Notch-dependent neurogenesis', *Journal of Neuroscience*, vol. 31, no. 43, Oct 26, pp. 15604-15617.

Reichert, R, Campos, LG, Vairo, F, de Souza, CF, Perez, JA, Duarte, JA, Leiria, FA, Anes, M & Vedolin, LM 2016, 'Neuroimaging Findings in Patients with Mucopolysaccharidosis: What You Really Need to Know', *Radiographics*, vol. 36, no. 5, Sep-Oct, pp. 1448-1462.

Reynolds, BA, Tetzlaff, W & Weiss, S 1992, 'A multipotent EGF-responsive striatal embryonic progenitor cell produces neurons and astrocytes', *Journal of Neuroscience*, vol. 12, no. 11, Nov, pp. 4565-4574.

Rezaei, M, Karbalaie, K, Tanjaoe, S, Madano, H, Hossein Nasar Esfahani, M & Baharvand, H 2011, 'Bone morphogenetic protein-4 influences neural differentiation of induced mouse mesenchymal stem cells', *Cell Journal*, vol. 12, no. 4, Winter, pp. 511-516.

Rigante, D & Caradonna, P 2004, 'Secondary skeletal involvement in Sanfilippo syndrome', *QJM*, vol. 97, no. 4, Apr, pp. 205-209.

Roberts, AL, Howarth, GS, Liaw, WC, Moretta, S, Kritas, S, Lymn, KA, Yazbeck, R, Tran, C, Fletcher, JM, Butler, RN & Byers, S 2009, 'Gastrointestinal pathology in a mouse model of mucopolysaccharidosis type IIIA', *Journal of Cellular Physiology*, vol. 219, no. 2, May, pp. 259-264.

Roberts, AL, Rees, MH, Klebe, S, Fletcher, JM & Byers, S 2007, 'Improvement in behaviour after substrate deprivation therapy with rhodamine B in a mouse model of MPS IIIA', *Molecular Genetics and Metabolism*, vol. 92, no. 1-2, Sep-Oct, pp. 115-121.

Roberts, AL, Thomas, BJ, Wilkinson, AS, Fletcher, JM & Byers, S 2006, 'Inhibition of glycosaminoglycan synthesis using rhodamine B in a mouse model of mucopolysaccharidosis type IIIA', *Pediatric Research*, vol. 60, no. 3, Sep, pp. 309-314.

Roca, C, Motas, S, Marco, S, Ribera, A, Sanchez, V, Sanchez, X, Bertolin, J, Leon, X, Perez, J, Garcia, M, Villacampa, P, Ruberte, J, Pujol, A, Haurigot, V & Bosch, F 2017, 'Disease correction by AAV-mediated gene therapy in a new mouse model of mucopolysaccharidosis type IIID', *Human Molecular Genetics*, vol. 26, no. 8, Apr 15, pp. 1535-1551.

Rodda, SJ & McMahon, AP 2006, 'Distinct roles for Hedgehog and canonical Wnt signaling in specification, differentiation and maintenance of osteoblast progenitors', *Development*, vol. 133, no. 16, Aug, pp. 3231-3244.

Rogers, CD, Ferzli, GS & Casey, ES 2011, 'The response of early neural genes to FGF signaling or inhibition of BMP indicate the absence of a conserved neural induction module', *BMC Developmental Biology*, vol. 11, Dec 15, p. 74.

Rong, J, Habuchi, H, Kimata, K, Lindahl, U & Kusche-Gullberg, M 2001, 'Substrate specificity of the heparan sulfate hexuronic acid 2-O-sulfotransferase', *Biochemistry*, vol. 40, no. 18, May 8, pp. 5548-5555.

Roper, RJ, Baxter, LL, Saran, NG, Klinedinst, DK, Beachy, PA & Reeves, RH 2006, 'Defective cerebellar response to mitogenic Hedgehog signaling in Down [corrected] syndrome mice', *Proceedings of the National Academy of Sciences of the United States of America*, vol. 103, no. 5, Jan 31, pp. 1452-1456.

Rossignol, J, Fink, K, Davis, K, Clerc, S, Crane, A, Matchynski, J, Lowrance, S, Bombard, M, Dekorver, N, Lescaudron, L & Dunbar, GL 2014, 'Transplants of adult mesenchymal and neural stem cells provide neuroprotection and behavioral sparing in a transgenic rat model of Huntington's disease', *Stem Cells*, vol. 32, no. 2, Feb, pp. 500-509.

Rostovskaya, M & Anastassiadis, K 2012, 'Differential expression of surface markers in mouse bone marrow mesenchymal stromal cell subpopulations with distinct lineage commitment', *PloS One*, vol. 7, no. 12, p. e51221.

Rozaklis, T, Beard, H, Hassiotis, S, Garcia, AR, Tonini, M, Luck, A, Pan, J, Lamsa, JC, Hopwood, JJ & Hemsley, KM 2011, 'Impact of high-dose, chemically modified sulfamidase on pathology in a murine model of MPS IIIA', *Experimental Neurology*, vol. 230, no. 1, Jul, pp. 123-130.

Rusnati, M, Coltrini, D, Caccia, P, Dell'Era, P, Zoppetti, G, Oreste, P, Valsasina, B & Presta, M 1994, 'Distinct role of 2-O-, N-, and 6-O-sulfate groups of heparin in the formation of the ternary complex with basic fibroblast growth factor and soluble FGF receptor-1', *Biochemical and Biophysical Research Communications*, vol. 203, no. 1, Aug 30, pp. 450-458.

Rybova, J, Ledvinova, J, Sikora, J, Kuchar, L & Dobrovolny, R 2018, 'Neural cells generated from human induced pluripotent stem cells as a model of CNS involvement in mucopolysaccharidosis type II', *Journal of Inherited Metabolic Disease*, vol. 41, no. 2, Mar, pp. 221-229.

Safford, KM, Hicok, KC, Safford, SD, Halvorsen, YD, Wilkison, WO, Gimble, JM & Rice, HE 2002, 'Neurogenic differentiation of murine and human adipose-derived stromal cells', *Biochemical and Biophysical Research Communications*, vol. 294, no. 2, Jun 7, pp. 371-379.

Sahara, S & O'Leary, DD 2009, 'Fgf10 regulates transition period of cortical stem cell differentiation to radial glia controlling generation of neurons and basal progenitors', *Neuron*, vol. 63, no. 1, Jul 16, pp. 48-62.

Saito, K, Kawaguchi, A, Kashiwagi, S, Yasugi, S, Ogawa, M & Miyata, T 2003, 'Morphological asymmetry in dividing retinal progenitor cells', *Development Growth & Differentiation*, vol. 45, no. 3, Jun, pp. 219-229.

Samsonraj, RM, Rai, B, Sathiyanathan, P, Puan, KJ, Rotzschke, O, Hui, JH, Raghunath, M, Stanton, LW, Nurcombe, V & Cool, SM 2015, 'Establishing criteria for human mesenchymal stem cell potency', *Stem Cells*, vol. 33, no. 6, Jun, pp. 1878-1891.

Sanchez-Ramos, J, Song, S, Cardozo-Pelaez, F, Hazzi, C, Stedeford, T, Willing, A, Freeman, TB, Saporta, S, Janssen, W, Patel, N, Cooper, DR & Sanberg, PR 2000, 'Adult bone marrow stromal cells differentiate into neural cells in vitro', *Experimental Neurology*, vol. 164, no. 2, Aug, pp. 247-256.

Scaramuzzo, L, Perisano, C, Leone, A, Graci, C, Spinelli, MS, Di Giacomo, G, Venanzi, E, Schiavone Panni, A & Maccauro, G 2012, 'Skeletal modifications in mucopolysaccharidoses: an overview', *Journal of Biological Regulators and Homeostatic Agents*, vol. 26, no. 1, Jan-Mar, pp. 139-144.

Schmidt-Hieber, C, Jonas, P & Bischofberger, J 2004, 'Enhanced synaptic plasticity in newly generated granule cells of the adult hippocampus', *Nature*, vol. 429, no. 6988, May 13, pp. 184-187.

Schmidt, L, Taiyab, A, Melvin, VS, Jones, KL & Williams, T 2018, 'Increased FGF8 signaling promotes chondrogenic rather than osteogenic development in the embryonic skull', *Disease Models & Mechanisms*, vol. 11, no. 6, Jun 15.

Seki, T, Yuasa, S & Fukuda, K 2012, 'Generation of induced pluripotent stem cells from a small amount of human peripheral blood using a combination of activated T cells and Sendai virus', *Nature Protocols*, vol. 7, no. 4, Apr, pp. 718-728.

Shapiro, EG, Lockman, LA, Balthazor, M & Krivit, W 1995, 'Neuropsychological outcomes of several storage diseases with and without bone marrow transplantation', *Journal of Inherited Metabolic Disease*, vol. 18, no. 4, pp. 413-429.

Shapiro, EG, Nestrasil, I, Delaney, KA, Rudser, K, Kovac, V, Nair, N, Richard, CW, 3rd, Haslett, P & Whitley, CB 2016, 'A Prospective Natural History Study of Mucopolysaccharidosis Type IIIA', *Journal of Pediatrics*, vol. 170, Mar, pp. 278-287.e271-274.

Shi, Y, Kirwan, P & Livesey, FJ 2012a, 'Directed differentiation of human pluripotent stem cells to cerebral cortex neurons and neural networks', *Nature Protocols*, vol. 7, no. 10, Oct, pp. 1836-1846.

Shi, Y, Kirwan, P, Smith, J, Robinson, HP & Livesey, FJ 2012b, 'Human cerebral cortex development from pluripotent stem cells to functional excitatory synapses', *Nature Neuroscience*, vol. 15, no. 3, Feb 5, pp. 477-486, s471.

Shimazaki, Y, Nagata, I, Ishii, M, Tanaka, M, Marunouchi, T, Hata, T & Maeda, N 2005, 'Developmental change and function of chondroitin sulfate deposited around cerebellar Purkinje cells', *Journal of Neuroscience Research*, vol. 82, no. 2, Oct 15, pp. 172-183.

Shou, J, Rim, PC & Calof, AL 1999, 'BMPs inhibit neurogenesis by a mechanism involving degradation of a transcription factor', *Nature Neuroscience*, vol. 2, no. 4, Apr, pp. 339-345.

Siegel, DA & Walkley, SU 1994, 'Growth of ectopic dendrites on cortical pyramidal neurons in neuronal storage diseases correlates with abnormal accumulation of GM2 ganglioside', *Journal of Neurochemistry*, vol. 62, no. 5, May, pp. 1852-1862.

Sivakumur, P & Wraith, JE 1999, 'Bone marrow transplantation in mucopolysaccharidosis type IIIA: a comparison of an early treated patient with his untreated sibling', *Journal of Inherited Metabolic Disease*, vol. 22, no. 7, Oct, pp. 849-850.

Song, HH, Shi, W, Xiang, YY & Filmus, J 2005, 'The loss of glypican-3 induces alterations in Wnt signaling', *Journal of Biological Chemistry*, vol. 280, no. 3, Jan 21, pp. 2116-2125.

Steinert, AF, Weissenberger, M, Kunz, M, Gilbert, F, Ghivizzani, SC, Gobel, S, Jakob, F, Noth, U & Rudert, M 2012, 'Indian hedgehog gene transfer is a chondrogenic inducer of human mesenchymal stem cells', *Arthritis Research & Therapy*, vol. 14, no. 4, Jul 20, p. R168.

Stockinger, A, Eger, A, Wolf, J, Beug, H & Foisner, R 2001, 'E-cadherin regulates cell growth by modulating proliferation-dependent beta-catenin transcriptional activity', *Journal of Cell Biology*, vol. 154, no. 6, Sep 17, pp. 1185-1196.

Strubing, C, Ahnert-Hilger, G, Shan, J, Wiedenmann, B, Hescheler, J & Wobus, AM 1995, 'Differentiation of pluripotent embryonic stem cells into the neuronal lineage in vitro gives rise to mature inhibitory and excitatory neurons', *Mechanisms of Development*, vol. 53, no. 2, Oct, pp. 275-287.

Suh, JM, Gao, X, McKay, J, McKay, R, Salo, Z & Graff, JM 2006, 'Hedgehog signaling plays a conserved role in inhibiting fat formation', *Cell Metabolism*, vol. 3, no. 1, Jan, pp. 25-34.

Swaroop, M, Brooks, MJ, Gieser, L, Swaroop, A & Zheng, W 2018, 'Patient iPSC-derived neural stem cells exhibit phenotypes in concordance with the clinical severity of mucopolysaccharidosis I', *Human Molecular Genetics*, vol. 27, no. 20, Oct 15, pp. 3612-3626.

Taha, MF & Hedayati, V 2010, 'Isolation, identification and multipotential differentiation of mouse adipose tissue-derived stem cells', *Tissue & Cell*, vol. 42, no. 4, Aug, pp. 211-216.

Takahashi, K, Tanabe, K, Ohnuki, M, Narita, M, Ichisaka, T, Tomoda, K & Yamanaka, S 2007, 'Induction of pluripotent stem cells from adult human fibroblasts by defined factors', *Cell*, vol. 131, no. 5, Nov 30, pp. 861-872.

Takahashi, K & Yamanaka, S 2006, 'Induction of pluripotent stem cells from mouse embryonic and adult fibroblast cultures by defined factors', *Cell*, vol. 126, no. 4, Aug 25, pp. 663-676.

Takahashi, T, Nowakowski, RS & Caviness, VS, Jr. 1996, 'The leaving or Q fraction of the murine cerebral proliferative epithelium: a general model of neocortical neuronogenesis', *Journal of Neuroscience*, vol. 16, no. 19, Oct 1, pp. 6183-6196.

Tan, BT, Wang, L, Li, S, Long, ZY, Wu, YM & Liu, Y 2015, 'Retinoic acid induced the differentiation of neural stem cells from embryonic spinal cord into functional neurons in vitro', *International Journal of Clinical and Experimental Pathology*, vol. 8, no. 7, pp. 8129-8135.

Tang, QQ, Otto, TC & Lane, MD 2003, 'CCAAT/enhancer-binding protein beta is required for mitotic clonal expansion during adipogenesis', *Proceedings of the National Academy of Sciences of the United States of America*, vol. 100, no. 3, Feb 4, pp. 850-855.

Tang, QQ, Otto, TC & Lane, MD 2004, 'Commitment of C3H10T1/2 pluripotent stem cells to the adipocyte lineage', *Proceedings of the National Academy of Sciences of the United States of America*, vol. 101, no. 26, Jun 29, pp. 9607-9611.

Tardieu, M, Zerah, M, Husson, B, de Bournonville, S, Deiva, K, Adamsbaum, C, Vincent, F, Hocquemiller, M, Broissand, C, Furlan, V, Ballabio, A, Fraldi, A, Crystal, RG, Baugnon, T, Roujeau, T, Heard, JM & Danos, O 2014, 'Intracerebral administration of adeno-associated viral vector serotype rh.10 carrying human SGSH and SUMF1 cDNAs in children with mucopolysaccharidosis type IIIA disease: results of a phase I/II trial', *Human Gene Therapy*, vol. 25, no. 6, Jun, pp. 506-516.

Taylor, KR & Gallo, RL 2006, 'Glycosaminoglycans and their proteoglycans: host-associated molecular patterns for initiation and modulation of inflammation', *FASEB Journal*, vol. 20, no. 1, Jan, pp. 9-22.

Taylor, KR, Rudisill, JA & Gallo, RL 2005, 'Structural and sequence motifs in dermatan sulfate for promoting fibroblast growth factor-2 (FGF-2) and FGF-7 activity', *Journal of Biological Chemistry*, vol. 280, no. 7, Feb 18, pp. 5300-5306.

Thakurela, S, Tiwari, N, Schick, S, Garding, A, Ivanek, R, Berninger, B & Tiwari, VK 2016, 'Mapping gene regulatory circuitry of Pax6 during neurogenesis', *Cell Discov*, vol. 2, p. 15045.

Tkachenko, E, Rhodes, JM & Simons, M 2005, 'Syndecans: new kids on the signaling block', *Circulation Research*, vol. 96, no. 5, Mar 18, pp. 488-500.

Toda, T & Gage, FH 2018, 'Review: adult neurogenesis contributes to hippocampal plasticity', *Cell and Tissue Research*, vol. 373, no. 3, Sep, pp. 693-709.

Tolar, J, Park, IH, Xia, L, Lees, CJ, Peacock, B, Webber, B, McElmurry, RT, Eide, CR, Orchard, PJ, Kyba, M, Osborn, MJ, Lund, TC, Wagner, JE, Daley, GQ & Blazar, BR 2011, 'Hematopoietic differentiation of induced pluripotent stem cells from patients with mucopolysaccharidosis type I (Hurler syndrome)', *Blood*, vol. 117, no. 3, Jan 20, pp. 839-847.

Tomatsu, S, Gutierrez, MA, Ishimaru, T, Pena, OM, Montano, AM, Maeda, H, Velez-Castrillon, S, Nishioka, T, Fachel, AA, Cooper, A, Thornley, M, Wraith, E, Barrera, LA, Laybauer, LS, Giugliani, R, Schwartz, IV, Frenking, GS, Beck, M, Kircher, SG, Paschke, E, Yamaguchi, S, Ullrich, K, Isogai, K, Suzuki, Y, Orii, T & Noguchi, A 2005, 'Heparan sulfate levels in mucopolysaccharidoses and mucolipidoses', *Journal of Inherited Metabolic Disease*, vol. 28, no. 5, pp. 743-757.

Tomatsu, S, Orii, KO, Vogler, C, Grubb, JH, Snella, EM, Gutierrez, MA, Dieter, T, Sukegawa, K, Orii, T, Kondo, N & Sly, WS 2002, 'Missense models [Gustm(E536A)Sly, Gustm(E536Q)Sly, and Gustm(L175F)Sly] of murine mucopolysaccharidosis type VII produced by targeted mutagenesis', *Proceedings of the National Academy of Sciences of the United States of America*, vol. 99, no. 23, Nov 12, pp. 14982-14987.

Tondreau, T, Lagneaux, L, Dejeneffe, M, Massy, M, Mortier, C, Delforge, A & Bron, D 2004, 'Bone marrow-derived mesenchymal stem cells already express specific neural proteins before any differentiation', *Differentiation*, vol. 72, no. 7, Sep, pp. 319-326.

Topczewski, J, Sepich, DS, Myers, DC, Walker, C, Amores, A, Lele, Z, Hammerschmidt, M, Postlethwait, J & Solnica-Krezel, L 2001, 'The zebrafish glypican knypek controls cell polarity during gastrulation movements of convergent extension', *Developmental Cell*, vol. 1, no. 2, Aug, pp. 251-264.

Tran, TH, Shi, X, Zaia, J & Ai, X 2012, 'Heparan sulfate 6-O-endosulfatases (Sulfs) coordinate the Wnt signaling pathways to regulate myoblast fusion during skeletal muscle regeneration', *Journal of Biological Chemistry*, vol. 287, no. 39, Sep 21, pp. 32651-32664.

Tropel, P, Platet, N, Platel, JC, Noel, D, Albrieux, M, Benabid, AL & Berger, F 2006, 'Functional neuronal differentiation of bone marrow-derived mesenchymal stem cells', *Stem Cells*, vol. 24, no. 12, Dec, pp. 2868-2876.

Truxal, KV, Fu, H, McCarty, DM, McNally, KA, Kunkler, KL, Zumberge, NA, Martin, L, Aylward, SC, Alfano, LN, Berry, KM, Lowes, LP, Corridore, M, McKee, C, McBride, KL & Flanigan, KM 2016, 'A prospective one-year natural history study of mucopolysaccharidosis types IIIA and IIIB: Implications for clinical trial design', *Molecular Genetics and Metabolism*, vol. 119, no. 3, Nov, pp. 239-248.

Tukachinsky, H, Kuzmickas, RP, Jao, CY, Liu, J & Salic, A 2012, 'Dispatched and scube mediate the efficient secretion of the cholesterol-modified hedgehog ligand', *Cell Rep*, vol. 2, no. 2, Aug 30, pp. 308-320.

Turnbull, JE, Fernig, DG, Ke, Y, Wilkinson, MC & Gallagher, JT 1992, 'Identification of the basic fibroblast growth factor binding sequence in fibroblast heparan sulfate', *Journal of Biological Chemistry*, vol. 267, no. 15, May 25, pp. 10337-10341.

Uccelli, A, Moretta, L & Pistoia, V 2008, 'Mesenchymal stem cells in health and disease', *Nature Reviews: Immunology*, vol. 8, no. 9, Sep, pp. 726-736.

Urban, N & Guillemot, F 2014, 'Neurogenesis in the embryonic and adult brain: same regulators, different roles', *Frontiers in Cellular Neuroscience*, vol. 8, p. 396.

Vallejo-Diez, S, Fleischer, A, Martin-Fernandez, JM, Sanchez-Gilabert, A & Bachiller, D 2018, 'Generation of two induced pluripotent stem cells lines from a Mucopolysaccharydosis IIIB (MPSIIIB) patient', *Stem Cell Res*, vol. 33, Nov 1, pp. 180-184.

Valstar, MJ, Neijs, S, Bruggenwirth, HT, Olmer, R, Ruijter, GJ, Wevers, RA, van Diggelen, OP, Poorthuis, BJ, Halley, DJ & Wijburg, FA 2010, 'Mucopolysaccharidosis type IIIA: clinical spectrum and genotype-phenotype correlations', *Annals of Neurology*, vol. 68, no. 6, Dec, pp. 876-887.

Varga, E, Nemes, C, Bock, I, Varga, N, Feher, A, Dinnyes, A & Kobolak, J 2016a, 'Generation of Mucopolysaccharidosis type II (MPS II) human induced pluripotent stem cell (iPSC) line from a 1-year-old male with pathogenic IDS mutation', *Stem Cell Res*, vol. 17, no. 3, Nov, pp. 482-484.

Varga, E, Nemes, C, Bock, I, Varga, N, Feher, A, Kobolak, J & Dinnyes, A 2016b, 'Generation of Mucopolysaccharidosis type II (MPS II) human induced pluripotent stem cell (iPSC) line from a 3-year-old male with pathogenic IDS mutation', *Stem Cell Res*, vol. 17, no. 3, Nov, pp. 479-481.

Varga, E, Nemes, C, Bock, I, Varga, N, Feher, A, Kobolak, J & Dinnyes, A 2016c, 'Generation of Mucopolysaccharidosis type II (MPS II) human induced pluripotent stem cell (iPSC) line from a 7-year-old male with pathogenic IDS mutation', *Stem Cell Res*, vol. 17, no. 3, Nov, pp. 463-465.

Varga, E, Nemes, C, Kovacs, E, Bock, I, Varga, N, Feher, A, Dinnyes, A & Kobolak, J 2016d, 'Generation of human induced pluripotent stem cell (iPSC) line from an unaffected female carrier of Mucopolysaccharidosis type II (MPS II) disorder', *Stem Cell Res*, vol. 17, no. 3, Nov, pp. 514-516.

Vellodi, A, Young, E, Cooper, A, Lidchi, V, Winchester, B & Wraith, JE 1999, 'Long-term follow-up following bone marrow transplantation for Hunter disease', *Journal of Inherited Metabolic Disease*, vol. 22, no. 5, Jun, pp. 638-648.

Venere, M, Han, YG, Bell, R, Song, JS, Alvarez-Buylla, A & Blelloch, R 2012, 'Sox1 marks an activated neural stem/progenitor cell in the hippocampus', *Development*, vol. 139, no. 21, Nov, pp. 3938-3949.

Venero Galanternik, M, Kramer, KL & Piotrowski, T 2015, 'Heparan Sulfate Proteoglycans Regulate Fgf Signaling and Cell Polarity during Collective Cell Migration', *Cell Rep*, Jan 15.

Vescovi, AL, Parati, EA, Gritti, A, Poulin, P, Ferrario, M, Wanke, E, Frolichsthal-Schoeller, P, Cova, L, Arcellana-Panlilio, M, Colombo, A & Galli, R 1999, 'Isolation and cloning of multipotential stem cells from the embryonic human CNS and establishment of transplantable human neural stem cell lines by epigenetic stimulation', *Experimental Neurology*, vol. 156, no. 1, Mar, pp. 71-83.

Veugelers, M, De Cat, B, Ceulemans, H, Bruystens, AM, Coomans, C, Durr, J, Vermeesch, J, Marynen, P & David, G 1999, 'Glypican-6, a new member of the glypican family of cell surface heparan sulfate proteoglycans', *Journal of Biological Chemistry*, vol. 274, no. 38, Sep 17, pp. 26968-26977.

Vicente, CP, Zancan, P, Peixoto, LL, Alves-Sa, R, Araujo, FS, Mourao, PA & Pavao, MS 2001, 'Unbalanced effects of dermatan sulfates with different sulfation patterns on coagulation, thrombosis and bleeding', *Thrombosis and Haemostasis*, vol. 86, no. 5, Nov, pp. 1215-1220.

Vlodavsky, I, Ilan, N, Naggi, A & Casu, B 2007, 'Heparanase: structure, biological functions, and inhibition by heparin-derived mimetics of heparan sulfate', *Current Pharmaceutical Design*, vol. 13, no. 20, pp. 2057-2073.

Voleti, B & Duman, RS 2012, 'The roles of neurotrophic factor and Wnt signaling in depression', *Clinical Pharmacology and Therapeutics*, vol. 91, no. 2, Feb, pp. 333-338.

Wada, R, Tifft, CJ & Proia, RL 2000, 'Microglial activation precedes acute neurodegeneration in Sandhoff disease and is suppressed by bone marrow transplantation', *Proceedings of the National Academy of Sciences of the United States of America*, vol. 97, no. 20, Sep 26, pp. 10954-10959.

Walkley, SU 2004, 'Secondary accumulation of gangliosides in lysosomal storage disorders', *Seminars in Cell & Developmental Biology*, vol. 15, no. 4, Aug, pp. 433-444.

Walton, RM & Wolfe, JH 2007, 'Abnormalities in neural progenitor cells in a dog model of lysosomal storage disease', *Journal of Neuropathology & Experimental Neurology*, vol. 66, no. 8, Aug, pp. 760-769.

Wang, J, Luan, Z, Jiang, H, Fang, J, Qin, M, Lee, V & Chen, J 2016, 'Allogeneic Hematopoietic Stem Cell Transplantation in Thirty-Four Pediatric Cases of Mucopolysaccharidosis-A Ten-Year Report from the China Children Transplant Group', *Biology of Blood and Marrow Transplantation*, vol. 22, no. 11, Nov, pp. 2104-2108.

Wang, L, Fuster, M, Sriramarao, P & Esko, JD 2005, 'Endothelial heparan sulfate deficiency impairs L-selectin- and chemokine-mediated neutrophil trafficking during inflammatory responses', *Nature Immunology*, vol. 6, no. 9, Sep, pp. 902-910.

Wang, RN, Green, J, Wang, Z, Deng, Y, Qiao, M, Peabody, M, Zhang, Q, Ye, J, Yan, Z, Denduluri, S, Idowu, O, Li, M, Shen, C, Hu, A, Haydon, RC, Kang, R, Mok, J, Lee, MJ, Luu, HL & Shi, LL 2014, 'Bone Morphogenetic Protein (BMP) signaling in development and human diseases', *Genes Dis*, vol. 1, no. 1, Sep, pp. 87-105.

Wang, S, Ai, X, Freeman, SD, Pownall, ME, Lu, Q, Kessler, DS & Emerson, CP, Jr. 2004, 'QSulf1, a heparan sulfate 6-O-endosulfatase, inhibits fibroblast growth factor signaling in mesoderm induction and angiogenesis', *Proceedings of the National Academy of Sciences of the United States of America*, vol. 101, no. 14, Apr 6, pp. 4833-4838.

Wang, S, Bates, J, Li, X, Schanz, S, Chandler-Militello, D, Levine, C, Maherali, N, Studer, L, Hochedlinger, K, Windrem, M & Goldman, SA 2013, 'Human iPSC-derived oligodendrocyte progenitor cells can myelinate and rescue a mouse model of congenital hypomyelination', *Cell Stem Cell*, vol. 12, no. 2, Feb 7, pp. 252-264.

Wang, TT, Tio, M, Lee, W, Beerheide, W & Udolph, G 2007, 'Neural differentiation of mesenchymal-like stem cells from cord blood is mediated by PKA', *Biochemical and Biophysical Research Communications*, vol. 357, no. 4, Jun 15, pp. 1021-1027.

Watson, HA, Holley, RJ, Langford-Smith, KJ, Wilkinson, FL, van Kuppevelt, TH, Wynn, RF, Wraith, JE, Merry, CL & Bigger, BW 2014, 'Heparan sulfate inhibits hematopoietic stem and progenitor cell migration and engraftment in mucopolysaccharidosis I', *Journal of Biological Chemistry*, vol. 289, no. 52, Dec 26, pp. 36194-36203.

Werner, S, Unsicker, K & von Bohlen und Halbach, O 2011, 'Fibroblast growth factor-2 deficiency causes defects in adult hippocampal neurogenesis, which are not rescued by exogenous fibroblast growth factor-2', *Journal of Neuroscience Research*, vol. 89, no. 10, Oct, pp. 1605-1617.

White, KK, Karol, LA, White, DR & Hale, S 2011, 'Musculoskeletal manifestations of Sanfilippo Syndrome (mucopolysaccharidosis type III)', *Journal of Pediatric Orthopedics*, vol. 31, no. 5, Jul-Aug, pp. 594-598.

Wilkinson, FL, Holley, RJ, Langford-Smith, KJ, Badrinath, S, Liao, A, Langford-Smith, A, Cooper, JD, Jones, SA, Wraith, JE, Wynn, RF, Merry, CL & Bigger, BW 2012, 'Neuropathology in mouse models of mucopolysaccharidosis type I, IIIA and IIIB', *PloS One*, vol. 7, no. 4, p. e35787.

Wirths, O 2017, 'Altered neurogenesis in mouse models of Alzheimer disease', *Neurogenesis (Austin)*, vol. 4, no. 1, p. e1327002.

Woodbury, D, Schwarz, EJ, Prockop, DJ & Black, IB 2000, 'Adult rat and human bone marrow stromal cells differentiate into neurons', *Journal of Neuroscience Research*, vol. 61, no. 4, Aug 15, pp. 364-370.

Wrobel, CN, Mutch, CA, Swaminathan, S, Taketo, MM & Chenn, A 2007, 'Persistent expression of stabilized beta-catenin delays maturation of radial glial cells into intermediate progenitors', *Developmental Biology*, vol. 309, no. 2, Sep 15, pp. 285-297.

Xian, X, Whiteford, J & Couchman, J 2012, 'Syndecans as Receptors for Pericellular Molecules', in N Karamanos (ed.), *Extracellular Matrix: Pathobiology and Signalling*, Walter de Gruyter Gmbh & Co, Germany.

Xiao, L, Sobue, T, Esliger, A, Kronenberg, MS, Coffin, JD, Doetschman, T & Hurley, MM 2010, 'Disruption of the Fgf2 gene activates the adipogenic and suppresses the osteogenic program in mesenchymal marrow stromal stem cells', *Bone*, vol. 47, no. 2, Aug, pp. 360-370.

Xie, N & Tang, B 2016, 'The Application of Human iPSCs in Neurological Diseases: From Bench to Bedside', *Stem Cells Int*, vol. 2016, p. 6484713.

Yamada, J, Nadanaka, S, Kitagawa, H, Takeuchi, K & Jinno, S 2018, 'Increased Synthesis of Chondroitin Sulfate Proteoglycan Promotes Adult Hippocampal Neurogenesis in Response to Enriched Environment', *Journal of Neuroscience*, vol. 38, no. 39, Sep 26, pp. 8496-8513.

Yamada, Y, Kato, K, Sukegawa, K, Tomatsu, S, Fukuda, S, Emura, S, Kojima, S, Matsuyama, T, Sly, WS, Kondo, N & Orii, T 1998, 'Treatment of MPS VII (Sly disease) by allogeneic BMT in a female with homozygous A619V mutation', *Bone Marrow Transplantation*, vol. 21, no. 6, Mar, pp. 629-634.

Yamaguchi, Y 2001, 'Heparan sulfate proteoglycans in the nervous system: their diverse roles in neurogenesis, axon guidance, and synaptogenesis', *Seminars in Cell & Developmental Biology*, vol. 12, no. 2, Apr, pp. 99-106.

Yan, D & Lin, X 2007, 'Drosophila glypican Dally-like acts in FGF-receiving cells to modulate FGF signaling during tracheal morphogenesis', *Developmental Biology*, vol. 312, no. 1, Dec 1, pp. 203-216.

Yao, PJ, Petralia, RS & Mattson, MP 2016, 'Sonic Hedgehog Signaling and Hippocampal Neuroplasticity', *Trends in Neurosciences*, vol. 39, no. 12, Dec, pp. 840-850.

Yao, PJ, Petralia, RS, Ott, C, Wang, YX, Lippincott-Schwartz, J & Mattson, MP 2015, 'Dendrosomatic Sonic Hedgehog Signaling in Hippocampal Neurons Regulates Axon Elongation', *Journal of Neuroscience*, vol. 35, no. 49, Dec 9, pp. 16126-16141.

Yogalingam, G & Hopwood, JJ 2001, 'Molecular genetics of mucopolysaccharidosis type IIIA and IIIB: Diagnostic, clinical, and biological implications', *Human Mutation*, vol. 18, no. 4, Oct, pp. 264-281.

Yousef, H, Morgenthaler, A, Schlesinger, C, Bugaj, L, Conboy, IM & Schaffer, DV 2015, 'Age-Associated Increase in BMP Signaling Inhibits Hippocampal Neurogenesis', *Stem Cells*, vol. 33, no. 5, May, pp. 1577-1588.

Yu, J, Vodyanik, MA, Smuga-Otto, K, Antosiewicz-Bourget, J, Frane, JL, Tian, S, Nie, J, Jonsdottir, GA, Ruotti, V, Stewart, R, Slukvin, II & Thomson, JA 2007, 'Induced pluripotent stem cell lines derived from human somatic cells', *Science*, vol. 318, no. 5858, Dec 21, pp. 1917-1920.

Zehentner, BK, Leser, U & Burtscher, H 2000, 'BMP-2 and sonic hedgehog have contrary effects on adipocyte-like differentiation of C3H10T1/2 cells', *DNA and Cell Biology*, vol. 19, no. 5, May, pp. 275-281.

Zeng, X, Goetz, JA, Suber, LM, Scott, WJ, Jr., Schreiner, CM & Robbins, DJ 2001, 'A freely diffusible form of Sonic hedgehog mediates long-range signalling', *Nature*, vol. 411, no. 6838, Jun 07, pp. 716-720.

Zhang, B, Zhang, J, Shi, H, Mao, F, Wang, J, Yan, Y, Zhang, X, Qian, H & Xu, W 2018, 'A novel method to isolate mesenchymal stem cells from mouse umbilical cord', *Mol Med Rep*, vol. 17, no. 1, Jan, pp. 861-869.

Zhang, X, Huang, CT, Chen, J, Pankratz, MT, Xi, J, Li, J, Yang, Y, Lavaute, TM, Li, XJ, Ayala, M, Bondarenko, GI, Du, ZW, Jin, Y, Golos, TG & Zhang, SC 2010, 'Pax6 is a human neuroectoderm cell fate determinant', *Cell Stem Cell*, vol. 7, no. 1, Jul 2, pp. 90-100.

Zhang, Z, Casey, DM, Julien, JP & Xu, Z 2002, 'Normal dendritic arborization in spinal motoneurons requires neurofilament subunit L', *Journal of Comparative Neurology*, vol. 450, no. 2, Aug 19, pp. 144-152.

Zhao, B, Katagiri, T, Toyoda, H, Takada, T, Yanai, T, Fukuda, T, Chung, UI, Koike, T, Takaoka, K & Kamijo, R 2006, 'Heparin potentiates the in vivo ectopic bone formation induced by bone morphogenetic protein-2', *Journal of Biological Chemistry*, vol. 281, no. 32, Aug 11, pp. 23246-23253.

Zhao, XL, Yang, B, Ma, LN & Dong, YH 2016, 'MicroRNA-1 effectively induces differentiation of myocardial cells from mouse bone marrow mesenchymal stem cells', *Artif Cells Nanomed Biotechnol*, vol. 44, no. 7, Nov, pp. 1665-1670.

Zhu, H, Guo, ZK, Jiang, XX, Li, H, Wang, XY, Yao, HY, Zhang, Y & Mao, N 2010, 'A protocol for isolation and culture of mesenchymal stem cells from mouse compact bone', *Nature Protocols*, vol. 5, no. 3, Mar, pp. 550-560.

Zimmermann, P & David, G 1999, 'The syndecans, tuners of transmembrane signaling', *FASEB Journal*, vol. 13 Suppl, pp. S91-s100.

zur Nieden, NI, Kempka, G, Rancourt, DE & Ahr, HJ 2005, 'Induction of chondro-, osteo- and adipogenesis in embryonic stem cells by bone morphogenetic protein-2: effect of cofactors on differentiating lineages', *BMC Developmental Biology*, vol. 5, Jan 26, p. 1.